

**THE ROLE OF CaMKII δ IN
MODULATION OF NF- κ B SIGNALLING
IN NORMAL AND HYPERTROPHIED
MOUSE HEARTS**

A thesis presented by

TAMARA PATRICIA MARTIN

In fulfilment of the requirements for the degree of
Doctor of Philosophy

October 2011

UNIVERSITY OF STRATHCLYDE, GLASGOW

STRATHCLYDE INSTITUTE OF PHARMACY
AND BIOMEDICAL SCIENCES

The copyright of this thesis belongs to the author under the terms of the United Kingdom Copyright Acts as qualified by University of Strathclyde Regulation 3.49. Due acknowledgement must always be made of the use of any material contained in, or derived from, this thesis.

ACKNOWLEDGEMENTS

First and foremost, I would like to offer my sincere gratitude to my supervisors, Drs Susan Currie and Andrew Paul, for their assistance, support and encouragement throughout. Thank you for all the guidance and advice offered, and for spending a significant amount of time with me discussing the significance of my work as well as stimulating ideas for further investigation.

Special thanks also to Dr. James Beattie (University of Leeds) for allowing me to visit his laboratory to perform Surface Plasmon Resonance experiments, and for all his help and guidance throughout.

My sincere gratitude is also extended to Margaret MacDonald for her help and support throughout my project, but most importantly for her expert technical assistance with the development of the animal model of hypertrophy.

I extend my thanks and appreciation to all of the research fellows and technical staff with whom I have had the pleasure of working and socialising with over the past 3 years. I thank everyone for helping make my work easier and more understandable.

I would also like to thank all of my fellow colleagues, in particular members of the Cardiovascular and Cell Biology groups within the department of Strathclyde Institute for Pharmacy and Biomedical Sciences, for their generous support and encouragement throughout.

Lastly and most importantly, I owe my deepest gratitude to my parents, brothers and sister for their encouragement, love and support throughout my studies.

PUBLICATIONS

Martin T.P., Beattie J., Paul A., Currie S. (2011) CaMKII δ interacts directly with IKK β and modulates NF- κ B signalling in adult mouse heart, *Biochem J.* (In preparation)

Martin T.P., Lawan A., Plevin R., Paul A., Currie S. (2011) Adult cardiac fibroblast proliferation is modulated by calcium/calmodulin dependent protein kinase II in normal and hypertrophied hearts, *J Mol Cell Cardiol.* (In Preparation)

Martin T.P., Robinson E., Grieve D.J., MacDonald M., Paul A., Currie, S. (2011) Optimisation of a minimally invasive aortic banding procedure to induce cardiac hypertrophy in mice, *Exptl. Physiol.* (In Preparation)

Martin T.P., Lawan A., Plevin R., Paul A., Currie S., (2011). Altered cardiac fibroblast proliferation during cardiac hypertrophy is modulated by calcium/calmodulin-dependent protein kinase II δ . *Proc Physiol Soc* **23**, PC24

Martin T.P., Chong T.S.Y., MacDonald M., Currie S., (2011). IP3R expression is increased in a minimally invasive surgical mouse model of cardiac hypertrophy. *Proc Physiol Soc* **23**, PC25

Poster communications

Biophysics Society Annual Meeting, Baltimore, Maryland, 5-9 March 2011. Martin T.P., Lawan A., Plevin R., Paul A., Currie S., (2011). Altered cardiac fibroblast proliferation during cardiac hypertrophy is modulated by calcium/calmodulin-dependent protein kinase II δ .

Mammalian Myocardium Meeting, University of Manchester, 28-29 June 2010. Martin T.P., Beattie J., Paul A., Currie S., (2010). Selective interaction of CaMKII δ with IKK β : a novel target for CaMKII in the heart.

Integrative Mammalian Biology, University of Glasgow, 31 March 2010. Martin T.P., Paul A., Currie S., (2010). Development of a minimally invasive aortic banding mouse model of pressure-overload cardiac hypertrophy.

Scottish Cardiovascular Forum, University of Glasgow, 5 February 2010 and Young Physiological Society Symposium, University of Leicester, 23-24 September 2009. Martin T.P., Beattie J., Paul A., Currie S., (2010). Investigation of a direct interaction between CaMKII δ and NF- κ B signalling: a role for CaMKII δ in cardiac inflammation?

Oral communications

Young Physiological Society Symposium, University of Leicester, 23-24 September 2009. Martin T.P., Beattie J., Paul A., Currie S., (2009). Investigation of a direct interaction between CaMKII δ and NF- κ B signalling: a role for CaMKII δ in cardiac inflammation?

TABLE OF CONTENTS

Acknowledgements	i
Publications	ii
Table of Contents	iv
List of Figures	xi
List of Tables	xiv
Abbreviations	xv
Abstract	xix
Chapter 1: Introduction	1
1.1 Physiology of the heart	2
1.2 Pathophysiology of the heart	3
1.2.1 Arrhythmia	4
1.2.2 Coronary artery disease	4
1.2.3 Myocarditis	4
1.2.4 Hypertrophy and heart failure	5
1.3 Animal models of cardiac disease	6
1.3.1 Models of cardiac hypertrophy	8
1.3.1.1 Pressure-overload via aortic banding	8
1.3.2 Models of heart failure	9
1.4 Key cell types of the heart	10
1.4.1 Myocytes	10
1.4.1.1 Normal excitation-contraction coupling	11
1.4.1.2 Alterations in EC-coupling in hypertrophy and heart failure	13
1.4.2 Cardiac fibroblasts	13
1.4.2.1 Physiological role of cardiac fibroblasts in the heart	13
1.4.2.2 Role of cardiac fibroblasts in the diseased heart	14
1.4.3 Cardiac fibroblast – myocyte interaction	15
1.4.3.1 In the healthy heart	15
1.4.3.2 In the pathological heart	18
1.4.3.2.1 Growth factors	18

1.4.3.2.2	Vasoactive peptides and neurohumoral agonists	19
1.4.3.2.3	Electrophysiology	19
1.4.3.2.4	Cytokines	20
1.5	Therapeutic targets in the treatment of cardiovascular disease	21
1.5.1	Current therapies	21
1.5.2	Novel approaches	22
1.5.3	Targeting Ca ²⁺ -handling and myocardial contractility	22
1.5.4	Targeting remodelling of the ECM	23
1.5.5	Targeting inflammation	23
1.5.6	Ca ²⁺ /calmodulin-dependent kinase II	24
1.6	Introduction to CaMKII	25
1.6.1	Isoforms of CaMKII present in the heart	25
1.6.2	Structure and activity regulation	26
1.6.3	CaMKII substrate targets in the heart	31
1.6.3.1	EC-coupling proteins and ion channels	31
1.6.3.2	Gene transcription	33
1.6.3.3	Cardiac fibroblast activation	34
1.6.3.4	Inflammatory signalling	35
1.7	Involvement of CaMKII in cardiac hypertrophy and heart failure	36
1.7.1	Human studies	36
1.7.2	In vitro experiments	37
1.7.3	Animal models	37
1.7.3.1	Transgenic/over-expression and knock-out studies	38
1.8	CaMKII inhibition as a therapeutic target	40
1.9	Introduction to the nuclear factor kappa B pathway	41
1.9.1	The NF-κB family	42
1.9.2	NF-κB pathway activation	43
1.9.3	Regulation of NF-κB activity	45
1.9.4	Regulation of transcription by NF-κB	46
1.10	Involvement of NF-κB in cardiac hypertrophy and heart failure	48
1.10.1	Human studies	48
1.10.2	In vitro studies	49
1.10.3	Animal studies	49
1.10.3.1	Transgenic/over-expression and knock-out studies	50

1.11	NF- κ B inhibition as a therapeutic target	52
1.12	Modulation of the NF- κ B pathway by CaMKII δ	54
1.13	Hypothesis	56
1.14	Thesis aims and objectives	56
Chapter 2: Materials and Methods		57
2.1	Materials	58
2.2	Minimally invasive transverse aortic banding (MTAB)	62
2.3	Transthoracic echocardiography	63
2.4	Measurement of mean arterial blood pressure	63
2.5	Termination of experiment	64
2.6	Post-mortem measurements	64
2.7	Preparation of tissue samples	65
2.7.1	Mouse ventricular whole homogenates	65
2.8	Histology	65
2.8.1	Processing, embedding and sectioning	65
2.8.2	Picro-sirius red staining	66
2.8.3	Quantification of staining	66
2.9	Cell isolation and culture	66
2.9.1	Adult cardiac fibroblasts	66
2.9.2	Adult cardiac myocytes	67
2.10	Characterization of cardiac fibroblasts by immunofluorescence	68
2.11	Preparation of cell samples	69
2.11.1	Cardiac fibroblast cell extracts	69
2.11.2	Cardiac myocyte cell extracts	69
2.12	Stimulation of cardiac fibroblasts	69
2.13	Proliferation of cardiac fibroblasts	70
2.14	Protein quantification	70
2.15	Quantitative immunoblotting and densitometry	71
2.16	Immunoprecipitation	76
2.17	Autoradiography	78
2.18	Surface Plasmon Resonance	79
2.18.1	Introduction to the Biacore technology	79

2.18.2	Experimental protocol	82
2.19	CaMKII activity assay	83
2.20	Electrophoretic Mobility Shift Assay (EMSA)	83
2.20.1	Nuclear Protein Extraction from Tissue	83
2.20.2	Nuclear protein extraction from cardiac fibroblasts	84
2.20.3	Labelling of consensus oligonucleotides	85
2.20.4	DNA binding reaction	85
2.21	Enzyme-linked immunosorbent assay (ELISA)	86
2.22	Data analysis	87

Chapter 3: CaMKII interaction with and modulation of NF- κ B signalling **88**

3.1	Introduction	89
3.2	Characterisation of cardiac fibroblasts by immunofluorescence	93
3.3	Characterising antibody specificity for CaMKII δ and NF- κ B signalling proteins in mouse cardiac preparations	95
3.3.1	CaMKII δ	95
3.3.2	IKK α	97
3.3.3	IKK β	97
3.3.4	IKK γ	100
3.3.5	I κ B α	100
3.4	A functional role for CaMKII in NF- κ B signalling – effect of CaMKII inhibition on I κ B α degradation in stimulated cardiac fibroblasts	103
3.5	Investigation of CaMKII δ interaction with specific components of the NF- κ B signalling pathway using immunoprecipitation	106
3.5.1	Introduction to immunoprecipitation	106
3.5.1.1	Factors that determine the success of immunoprecipitating a protein	106
3.5.1.1.1	Lysis buffer composition	106
3.5.1.1.2	Precipitation of immune complexes	107
3.5.1.1.3	Method for immunoprecipitation	107
3.5.2	Immunoprecipitation using a variety of mouse heart preparations	108

3.6	Investigation of CaMKII δ phosphorylation of specific components of the NF- κ B signalling pathway	112
3.7	Surface Plasmon Resonance	114
3.7.1	Ligand immobilisation	114
3.7.2	Determination of CaMKII δ Immobilisation and Reactivity	115
3.8	Investigation of CaMKII δ interaction with IKKs using surface plasmon resonance	118
3.8.1	Assessment of conditions for CaMKII δ -IKK β interaction	122
3.9	Discussion	126
3.9.1	Characterisation of adult cardiac fibroblasts	126
3.9.2	Functional role for CaMKII δ in NF- κ B signalling in adult cardiac fibroblasts	127
3.9.3	Analysis of the CaMKII-NF- κ B interaction	129
3.9.3.1	CaMKII δ selectively phosphorylates and directly interacts with IKK β	129
3.10	Conclusions	132

Chapter 4: Development and characterisation of a minimally invasive aortic banding mouse model of pressure-overload mediated cardiac hypertrophy

4.1	Introduction	134
4.2	Assessment of growth rate of in-house bred C57BL/6J animals	137
4.3	Assessment of anaesthesia	137
4.4	Minimally invasive transverse aortic banding (MTAB)	141
4.5	Assessment of mean arterial pressure (MAP) at 1 week in sham and MTAB animals	144
4.6	Echocardiographic assessment of left ventricular function	146
4.7	Post-mortem assessment of hypertrophy after 4 weeks sham or MTAB surgery	147
4.8	Assessment of cardiac fibrosis at 4 weeks in sham and MTAB animals	153
4.9	Assessment of cardiac remodelling and cytokine expression 48 h, 1 week and 4 weeks after sham and MTAB surgery	153

4.10	Discussion	158
4.10.1	Characterising the MTAB protocol	158
4.10.1.1	Anaesthesia	158
4.10.1.2	Animals and sex-specific differences	160
4.10.1.3	Post-surgery remodelling period	161
4.10.2	In-vivo and post-mortem analysis of model	162
4.10.2.1	Pressure measurements	162
4.10.2.2	Echocardiography	163
4.10.2.3	Organ weight to body weights ratios	165
4.10.2.4	Cardiac fibrosis	165
4.10.2.5	Inflammation	166
4.11	Conclusions	169

Chapter 5: Alterations in CaMKII and NF- κ B signalling

following cardiac hypertrophy 170

5.1	Introduction	171
5.2	Altered CaMKII δ protein expression and activity in cardiac preparations following hypertrophy	173
5.3	Pro-inflammatory signalling following cardiac hypertrophy	176
5.4	Cardiac fibroblast proliferation following cardiac hypertrophy and effect of CaMKII inhibition	180
5.5	Discussion	184
5.5.1	Altered NF- κ B expression and activity during cardiac hypertrophy	184
5.5.2	Altered CF function during cardiac hypertrophy and the role of CaMKII	185
5.6	Conclusions	186

Chapter 6: General Discussion	188
6.1 CaMKII δ - NF- κ B signalling interaction	189
6.2 Characterisation of MTAB model	190
6.3 CaMKII δ and pro-inflammatory signalling following cardiac hypertrophy	191
6.4 Altered CF function following cardiac hypertrophy	192
6.5 CaMKII δ as a target for therapeutic intervention in cardiac hypertrophy	194
References	196

LIST OF FIGURES

CHAPTER 1

Figure 1.1	Types of cardiac hypertrophy.	7
Figure 1.2	Cardiac excitation-contraction coupling in ventricular myocytes.	12
Figure 1.3	Alterations in cardiac fibroblast function associated with myocardial remodelling.	16
Figure 1.4	Schematic representation of CaMKII δ structure.	27
Figure 1.5	Activation of CaMKII.	29
Figure 1.6	The NF- κ B signalling pathway.	44

CHAPTER 2

Figure 2.1	BSA standard calibration curve.	73
Figure 2.2	CM5 sensor chip.	80
Figure 2.3	Principle of Surface Plasmon Resonance phenomenon.	81

CHAPTER 3

Figure 3.1	Potential modulation of the NF- κ B signalling pathway by CaMKII δ .	91
Figure 3.2	IKK α and IKK β subunit composition.	92
Figure 3.3	Characterization of cardiac fibroblasts by immunofluorescence.	94
Figure 3.4	Specificity of commercially available anti-CaMKII δ antibodies.	96
Figure 3.5	Specificity of commercially available anti-IKK α antibodies.	98
Figure 3.6	Specificity of commercially available anti-IKK β antibodies.	99
Figure 3.7	Specificity of commercially available anti-IKK γ antibodies.	101
Figure 3.8	Specificity of commercially available anti-I κ B α antibodies.	102
Figure 3.9	Agonist-induced I κ B α degradation in adult cardiac fibroblasts.	104
Figure 3.10	LPS-induced I κ B α degradation in cardiac fibroblasts is reversed following CaMKII inhibition.	105
Figure 3.11	Immunoprecipitation of IKK γ from solubilised whole heart tissue.	111

Figure 3.12	CaMKII δ shows preferential phosphorylation of IKK β over IKK α .	113
Figure 3.13	Immobilisation profile of CaMKII δ .	116
Figure 3.14	Calmodulin interaction with CaMKII δ .	117
Figure 3.15	IKK γ does not interact with CaMKII δ .	119
Figure 3.16	IKK α does not interact with CaMKII δ .	120
Figure 3.17	IKK β interaction with CaMKII δ .	121
Figure 3.18	IKK β interaction with CaMKII δ in the presence of imidazole.	123
Figure 3.19	IKK β interaction with CaMKII δ in the presence of ATP.	124
Figure 3.20	IKK β interaction with CaMKII δ in the absence of Ca ²⁺ .	125

CHAPTER 4

Figure 4.1	Comparison of the dimensions of the intact heart between different species.	136
Figure 4.2	Growth curve of in-house bred C57BL/6J mice.	137
Figure 4.3	Design of the inhalation anaesthesia cone mask.	140
Figure 4.4	Representative images of MTAB mouse surgery.	142
Figure 4.5	Suture detail around the transverse aortic arch.	143
Figure 4.6	Representative echocardiography of Sham and MTAB animals.	148
Figure 4.7	Echocardiography wall measurements after two and four weeks aortic banding.	149
Figure 4.8 %	Fractional Shortening after 2 and 4 weeks aortic banding.	150
Figure 4.9	Heart weight to body weight measurements from sham and MTAB animals.	151
Figure 4.10	Picro-sirius red collagen quantification of sham-operated and MTAB heart sections.	155

CHAPTER 5

Figure 5.1	CaMKII δ expression in sham and MTAB whole heart homogenates	174
Figure 5.2	CaMKII δ activity in sham and MTAB whole heart homogenates	175
Figure 5.3	IKK α expression in sham and MTAB whole heart homogenates	177

Figure 5.4	NF- κ B p65 expression in sham and MTAB whole heart homogenates	178
Figure 5.5	NF- κ B activity in sham and MTAB whole heart nuclear extracts	179
Figure 5.6	Proliferation of cardiac fibroblasts is increased in cells isolated from MTAB hearts compared with those isolated from sham-operated hearts	181
Figure 5.7	Proliferation of cardiac fibroblasts from sham-operated hearts is reduced following CaMKII inhibition	182
Figure 5.8	Proliferation of cardiac fibroblasts from sham-operated hearts is reduced following CaMKII inhibition	183

LIST OF TABLES

CHAPTER 1

Table 1.1	Transgenic/over-expression studies implicating a role for CaMKII in cardiac hypertrophy and heart failure.	39
-----------	--	----

CHAPTER 2

Table 2.1	Optimised quantitative immunoblotting conditions for each protein of interest.	74
Table 2.2	Types of primary and secondary antibodies used for each protein of interest.	75

CHAPTER 3

Table 3.1	Immunoprecipitation of IKK γ from a variety of mouse heart preparations.	110
-----------	---	-----

CHAPTER 4

Table 4.1	Summary of anaesthesia tested during optimisation of the MTAB procedure.	139
Table 4.2	Haemodynamic parameters in MTAB and sham-operated mice (data courtesy of Dr. Grieve, Queens University Belfast).	145
Table 4.3	Summary of echocardiographic and post-mortem measurements in sham-operated and MTAB mice.	152
Table 4.4	Summary of echocardiographic measurements in sham-operated and MTAB mice 48 hours post-surgery.	156
Table 4.5	Summary of post-mortem and cytokine measurements in sham and MTAB mice 48 hours, 1 week and 4 weeks post-surgery.	157

ABBREVIATIONS

[Ca ²⁺]	- Calcium concentration
32P	- Phosphorus-32
α-SMA	- Alpha smooth muscle actin
ACE	- Angiotensin-converting enzyme
AEBSF	- 4-(2-aminoethyl)benzenesulfonyl fluoride hydrochloride
AIP	- Autocamide II-related inhibitory peptide, myristoylated
AKAP	-A kinase anchoring protein
Ang II	- Angiotensin II
ANF	- Atrial natriuretic factor
AP	- Action potential
AP-1	- Activating protein-1
ASK1	- Apoptosis signal-regulating kinase 1
ATP	- Adenosine 5'-triphosphate
AT ₁ R	- Angiotensin II type 1 receptor
AV	- Atrioventricular
AW	- Anterior wall
BMS	- Bristol-Myers Squibb
BSA	- Bovine serum albumin
Ca ²⁺	- Calcium ion
CaCl ₂	- Calcium chloride
CAD	- Coronary artery disease
CAL	- Coronary artery ligation
CaM	- Calmodulin
CaMKII	- Calcium/calmodulin-dependent protein kinase II
cAMP	- Cyclic adenosine monophosphate
CREB	- cAMP response element-binding
CF	- Cardiac fibroblasts
CICR	- Calcium induced calcium release
CT-1	- Cardiotrophin-1
CVD	- Cardiovascular disease
DAPI	- 4',6-diamidino-2-phenylindole
ddH ₂ O	- Double distilled water

DDR2	- Discoidin domain receptor 2
DTT	- Dithiothreitol
EC-coupling	- Excitation-contraction coupling
ECL	- Enhanced chemiluminescence
ECM	- Extracellular matrix
EDC	- 1-ethyl-3-[3-dimethylamino-propyl]carbodiimide hydrochloride
EDTA	- Ethylenediaminetetra-acetic acid
EF	- Ejection fraction
EGTA	- Ethyleneglycol-bis-(β -aminoethylether)-N, N, N'-tetraacetic acid
EPAC	- Exchange protein directly activated by cAMP
ET-1	- Endothelin-1
FCS	- Foetal calf serum
FITC	- Fluorescein isothiocyanate
FKBP12.6	- FK506 binding protein 12.6
FRET	- Fluorescence Resonance Energy Transfer
FS	- Fractional shortening
GAPDH	- Glyceraldehyde-3-phosphate dehydrogenase
HDAC	- Histone deacetylases
HEPES	- 4-(2-hydroxyethyl)-1-piperazineethanesulfonic acid
HF	- Heart failure
HRP	- Horseradish peroxidase
I_{Ca}	- Inward calcium current
I_{K1}	- Inward rectifying K^+ current
$I_{\kappa B}$	- Inhibitory kappa B ($I_{\kappa B}$)
IKK	- Inhibitory- κB kinase
I_{Na}	- Sodium current
InP_3R_2	- Type 2 inositol 1,4,5-trisphosphate receptor
IP_3	- Inositol 1,4,5-trisphosphate
I/R	- Ischemia/reperfusion
I_{to}	- Transient outward K^+ current
IgG	- Immunoglobulin
IL-1 β	- Interleukin-1 beta
IL-6	- Interleukin-6
K^+	- Potassium ion

KCl	- Potassium chloride
KH ₂ PO ₄	- Potassium dihydrogen orthophosphate
LDS	- Lithium dodecyl sulfate
LIF	- Leukemia inhibitor factor
LPS	- Lipopolysaccharide
LTCC	- Voltage-gated L-type calcium channel
LV	- Left ventricle
LVEDD	- Left ventricular end diastolic dimension
LVESD	- Left ventricular end systolic dimension
MAP	- Mean arterial pressure
MES	- 2-(N-morpholino)ethanesulfonic acid
MET	- Methionine
MgCl ₂ .6H ₂ O	- Magnesium chloride hexahydrate
MgSO ₄ .7H ₂ O	- Magnesium sulphate heptahydrate
MI	- Myocardial infarction
MMP	- Matrix metalloproteinases
MOPS	- 3-(N-Morpholino)propanesulfonic acid
mRNA	- Messenger ribonucleic acid
MTAB	- Minimally invasive transverse aortic banding
Myo-CF	- Cardiac myofibroblast
Na ⁺	- Sodium ion
Na ₂ HPO ₄	- Disodium hydrogen orthophosphate
Na ₃ VO ₄	- Sodium orthovanadate
NaCl	- Sodium chloride
NaH ₂ PO ₄	- Sodium dihydrogen orthophosphate
NaTT	- Sodium and Tris buffer containing Tween 20
NCX	- Sodium-calcium exchanger
NEMO	- Nuclear factor kappa B essential modulator
NF-κB	- Nuclear factor kappa B
NHS	- N-hydroxysuccinimide
NIK	- Nuclear factor kappa B inducing kinase
NLS	- Nuclear localisation signal
PAGE	- Polyacrylamide gel electrophoresis
PBS	- Phosphate buffered solution

PDTC	- Pyrrolidine dithiocarbamate
pI	- Isoelectric point
PKA	- Protein kinase A
PKC	- Protein kinase C
PKD	- Protein kinase D
PLB	- Phospholamban
PMSF	- Phenylmethylsulphonylfluoride
PW	- Posterior wall
RAAS	- Renin-angiotensin- aldosterone system
RHD	- Rel-homology domain
ROS	- Reactive oxygen species
RU	- Response unit
RWT	- Relative wall thickness
RyR ₂	- Ryanodine receptor 2
SA	- Sinoatrial
SDS	- Sodium dodecyl sulphate
Ser	- Serine
SERCA2a	- Sacro-endoplasmic reticulum calcium-ATPase enzyme
SHR	- Spontaneously hypertensive rat
SR	- Sarcoplasmic reticulum
TAC	- Transverse aortic constriction
TAD	- Transcription activation domain
TBST	- Tris buffered solution containing Tween 20
TGF- β	- Transforming growth factor- β
Thr	- Threonine
TIMPs	- Tissue inhibitor of metalloproteinases
TAK1	- TGF- β -activated kinase
TNF- α	- Tumour necrosis factor alpha
TRAFs	- TNF-receptor-associated factors
TRITC	- Tetramethylrhodamine isothiocyanate
T-tubule	- Transverse tubule
Tyr	- Tyrosine
WH	- Whole heart homogenate
WT	- Wild type

ABSTRACT

Calcium/calmodulin-dependent protein kinase II δ (CaMKII δ) has been identified as a central regulatory molecule in the heart, important not only in modulating normal cardiac function, but also in promoting cardiac hypertrophy and heart failure. The focus for CaMKII δ action in the myocardium has been placed upon the cardiac myocytes due to the fundamental role these cells play in cardiac contractility. However, the non-contractile cells of the heart, predominantly cardiac fibroblasts (CFs), are now emerging as equally important candidates for modulating cardiac function. CaMKII δ is well established as a key modulator of excitation-contraction coupling in normal and diseased myocardium, however additional roles for this enzyme in other areas of cardiac function and dysfunction are less well understood. Cardiac inflammation and fibrosis are two key features of various cardiomyopathies. The role of CaMKII δ in either or both has yet to be established. CFs, through their proliferative capacity and potential to secrete various growth factors and pro-inflammatory cytokines are pivotal in regulating both fibrosis and inflammation within the myocardium. However, the regulatory mechanisms underlying these features remain poorly understood.

This study has focused on (i) identifying a link between CaMKII and Nuclear Factor kappa B (NF- κ B) pro-inflammatory signalling in the heart, (ii) development and characterisation of a novel minimally invasive (MTAB) model of cardiac hypertrophy in mice, and (iii) assessing alterations in both CaMKII and NF- κ B signalling following hypertrophy. Importantly there has been a focus on CFs in this work, providing new information about the role of CaMKII in these cells in both normal and hypertrophied hearts, including for the first time evidence for CaMKII modulation of pro-inflammatory NF- κ B signalling in normal adult murine CFs. A direct interaction between CaMKII δ and NF- κ B signalling has been demonstrated at the level of inhibitory- κ B kinase β (IKK β) using Surface Plasmon Resonance (SPR). Successful development of the MTAB model has allowed assessment of hypertrophic development and progression. One week following surgery, there is evidence for both systolic and diastolic dysfunction. Characteristic features of significant cardiac hypertrophy are evident four weeks following surgery. These include an increase in heart size, cardiac contractile dysfunction and increased cardiac fibrosis.

Elevated CaMKII δ and NF- κ B expression and activity correlate with impaired cardiac contractile function following hypertrophy. In parallel with increased fibrosis, evidence has been provided for increased proliferation of CFs isolated from MTAB hearts in response to agonist stimulation. Using selective inhibition of CaMKII, proliferation is reduced in CFs isolated from both sham and MTAB hearts. For the first time, this has highlighted an important role for CaMKII at the level of the CF.

Findings from this study provide evidence for two novel modes of action of CaMKII in the adult heart, one at the level of pro-inflammatory signalling and the other at the level of cardiac fibrosis. Both actions highlight additional mechanisms by which increased levels of CaMKII may exert deleterious effects on cardiac function during hypertrophic adaptation and cardiac remodelling.

Chapter 1: Introduction

1.1 Physiology of the heart

The human heart is a large muscular organ responsible for pumping blood to various areas of the body. The mammalian heart consists of two halves divided into four chambers; two upper chambers on either side referred to as the right and left atria, and two lower chambers referred to as the right and left ventricles. The right side of the heart receives deoxygenated blood from the body via the vena cava. This blood enters the right atrium, passes to the right ventricle and is ejected into the pulmonary system via the pulmonary artery, which delivers it to the lungs. The left side of the heart receives the oxygenated blood returning from the lungs. The oxygen-rich blood enters the left atrium via the pulmonary veins, passes into the left ventricle, and is then ejected into the systemic circulation via the aorta.

The periodic contraction and relaxation of these muscle chambers is responsible for the mechanical events of the cardiac cycle, which ultimately controls the function of the heart. Highly coordinated and efficient cardiac contraction is achieved by a specialised conducting system arising from the sinoatrial (SA) node, and is essential to ensure sufficient cardiac output. From the SA node a wave of electrical impulses (or action potentials, APs) are conducted through the atria causing them to contract simultaneously and force blood into the ventricles. Subsequent conduction of impulses to the atrioventricular (AV) node and propagation to the Purkinje fibres cause the ventricles to contract and forcibly eject blood into the aorta and the pulmonary artery. The set of events that occur between depolarisation of the AV node to the trigger of ventricular contraction is called systole. During systole, a subset of events called excitation-contraction (EC) coupling takes place that regulates cardiac calcium (Ca^{2+}) cycling within each muscle cell. At the end of systole, the heart enters into diastole when the ventricles relax. This allows the chambers to fill with blood again before the trigger of another AP (Vander et al., 1998).

The myocardium is a 'syncytium' of electrically excitable muscle cells, called cardiomyocytes or myocytes, which are interconnected by continuous cytoplasmic bridges to allow APs to propagate readily to neighbouring cells. This is essential for synchronised and efficient contraction of the myocardium. Myocytes exhibit electrophysiological properties that distinguish them from other excitable tissues, such as an intrinsic rhythm generated in the SA node and the fact that Ca^{2+} currents

determine the initiation, propagation and duration of the AP rather than Na^+ and K^+ currents, as is the case in other excitable cells. As mentioned, Ca^{2+} cycling regulated by EC-coupling is a key feature of cardiac performance and this will be discussed further in Section 1.4.1.1.

Contractile myocytes occupy the bulk volume of the myocardium although myocardial tissue comprises other non-contractile cell types, including cardiac fibroblasts (CFs), endothelial cells and mast cells (Baudino et al., 2006). In fact, up to 70% of the myocardium is comprised of non-myocyte cells, of which CFs account for a large proportion (in terms of cell numbers), although this number can vary between species (Ottaviano and Yee, 2011). The degree and duration of mechanical, chemical, and electrical signalling in the heart determines the dynamic interactions between these cells and the extracellular matrix (ECM) of the heart (Baudino et al., 2006). Fibrillar collagen, a major stress-bearing constituent of the ECM, forms a three-dimensional structure around bundles of myocytes to generate a stress tolerant network that transmits myocyte shortening into ventricular contractility (Manabe et al., 2002). CFs serve as the main source of collagen, particularly types I, III and VI and hence, CFs contribute to the mechanical and electrical properties of the myocardium (Camelliti et al., 2005, Chen et al., 2010). Thus, normal cardiac function is regulated by coordinated and dynamic interactions of these two major cell types (myocytes and CFs) and highlights that the importance of CFs extends beyond simple regulation of ECM, as was previously assumed (Porter and Turner, 2009).

1.2 Pathophysiology of the heart

Cardiovascular diseases (CVDs) constitute the largest single cause of morbidity and mortality globally, with an estimated 17.1 million people dying from CVD in 2004 (World Health Organisation, 2011). In the U.K. in 2009, there were ~750,000 people living with heart failure (HF) and one in three of all deaths was CVD related (British Heart Foundation, 2011). There are various types of CVD, with some arising from abnormal EC-coupling and heart rhythm such as cardiac arrhythmia, whilst others involve mainly the vasculature such as coronary artery disease (CAD).

1.2.1 Arrhythmia

Cardiac arrhythmia occurs when the heart rhythm, set by the SA node, becomes too fast (tachycardia) or too slow (bradycardia), or the frequency of atrial and ventricular beating are different and out of synchronicity. A common cause of arrhythmia is myocardial ischaemia or infarction, with altered impulse conduction associated with complete or partial block of electrical conduction within the heart. Ventricular tachycardia is a serious condition that can progress to ventricular fibrillation and results in HF and death (Klabunde, 2005).

1.2.2 Coronary artery disease

CAD is the result of damage to the intima of large and medium sized arteries, causing a chronic inflammatory response and accumulation of cholesterol, leading to formation of an atherosclerotic plaque. CAD can eventually result in ischaemia and myocardial infarction (MI) due to the atherosclerotic plaque gradually decreasing the luminal space of the artery, or via rupture of unstable plaques and subsequent blockage of blood flow through the artery. MI occurs when the myocardium is starved of oxygen, leading to irreversible death and damage (or infarction) of the heart, eventually resulting in HF (Rang et al., 2003).

1.2.3 Myocarditis

Myocarditis or inflammation of the myocardium with consequent myocardial injury is a leading cause of HF (Leuschner et al., 2009). Inflammation of the heart can occur due to immune activation by viral infection, cardiac injury, and cytokine release by cardiac cells in response to haemodynamic stress (Celis et al., 2008).

Immune activation by viral infection occurs when a virus infects cardiac cells and triggers a variety of immune responses that include mononuclear B and T cell infiltration, and the subsequent release of pro-inflammatory cytokines and reactive oxygen species (ROS) that may alter cardiac function (Papageorgiou and Heymans, 2011). Inflammatory cell infiltration into the myocardium may also be stimulated by myocyte necrosis due to cardiac injury. Damage-associated molecular patterns are

released from dying cells into the cytosol and provoke an inflammatory response via activation of the innate immune system and production of auto-antibodies (Shah and Mann, 2011). Mechanical overload and haemodynamic stress can also promote myocardial inflammation via cytokine release from myocytes and non-myocytes including CFs, with secondary activation of the pro-inflammatory transcription factor Nuclear Factor kappa B (NF- κ B) (Frangogiannis, 2008). To date there is still not a lot understood about the cellular and molecular mechanisms involved.

1.2.4 Hypertrophy and heart failure

Congestive or chronic HF is the final consequence of many of the disease etiologies described above. The heart initially adapts to changes in mechanical, chemical and electrical signalling via remodelling of the myocardium, such as undergoing hypertrophy and under physiological conditions this is initially an adaptive response, helping to maintain a balance between cardiac demand and the capacity for contractile force (Frey and Olson, 2003). Persistent (pathological) hypertrophy however, leads to cardiac dysfunction as a result of myocyte apoptosis and the progression of interstitial and perivascular fibrosis. Cardiac hypertrophy is recognised as an independent risk factor for cardiac-related morbidity and mortality and is therefore an accurate predictor of HF.

Pathological hypertrophy can result from various cardiomyopathies, genetic abnormalities and as a result of CAD. The key characteristic features of cardiac hypertrophy include (i) an increase in size of individual myocytes, (ii) changes in the spatial relationship among myocytes and CFs and, (iii) reprogramming of adult gene expression as well as re-expression of foetal genes. These factors act together to alter the contractile properties of myocytes (Olson and Williams, 2000). CFs also play a key role in the development of hypertrophy as their proliferation and migration increases dramatically, as well as exerting changes in the extent and composition of the ECM, thus initiating remodelling of the heart (Camelliti et al., 2005).

Generally it is considered that there are three patterns of LV hypertrophy; (i) concentric hypertrophy characterised by an increase in LV mass and relative wall thickness (RWT), (ii) eccentric hypertrophy characterised by an increase in LV mass with normal RWT (i.e. dilation of the ventricle), and (iii) concentric remodelling

characterised by normal LV mass with increased RWT (Figure 1.1) (Barrick et al., 2007). Concentric hypertrophy is caused by chronic pressure overload, which increases the afterload on the heart, whilst eccentric hypertrophy is caused by volume overload and increased preload on the heart. Mechanistically, concentric hypertrophy occurs by the addition of new sarcomeres in parallel to existing ones whilst eccentric hypertrophy occurs by addition of new sarcomeres in series causing cell elongation (Barry et al., 2008). In the case of concentric hypertrophy, the increase in RWT is capable of generating greater force at higher pressures and therefore maintains normal wall stress, however reduced compliance of the ventricle can lead to diastolic dysfunction. Progressive concentric remodelling promotes LV dilatation resulting in impaired contractility, decreasing cardiac output until it is insufficient and eventually resulting in HF (Klabunde, 2005). LV function and the geometric pattern of LV hypertrophy have been found to be closely related (Barrick et al., 2007).

1.3 Animal models of cardiac disease

Due to the impracticalities in examining human subjects for long periods of time, or in some cases throughout their lifetimes, and the associated ethical issues, *in vivo* animal models have been used extensively to study various CVDs. Factors such as how closely the model mimics human patho-physiology, the reproducibility of the technique, ethics, and the cost of animal housing and care, all determine the choice of animal model employed. Furthermore, the species, strain and gender can all affect the patho-physiology of the manipulated heart and therefore must be considered when establishing an animal model (Klocke et al., 2007).

Rodents are widely used in cardiac research as they are small, breed rapidly and have relatively low maintenance costs. Importantly, many of the systems implicated in human HF are also affected in rodents, including activation of the renin-angiotensin-aldosterone system (RAAS), natriuretic peptides and the inflammatory response (Lygate, 2006). The rodent genome is very similar to that of human, with every human gene having an exact homolog in mouse. Transgenic animals, with over-expression or knockout of specific genes, are proving vital to the study of the pathogenesis of HF and to the discovery and development of novel therapeutic targets for treatment (Robbins, 2004).

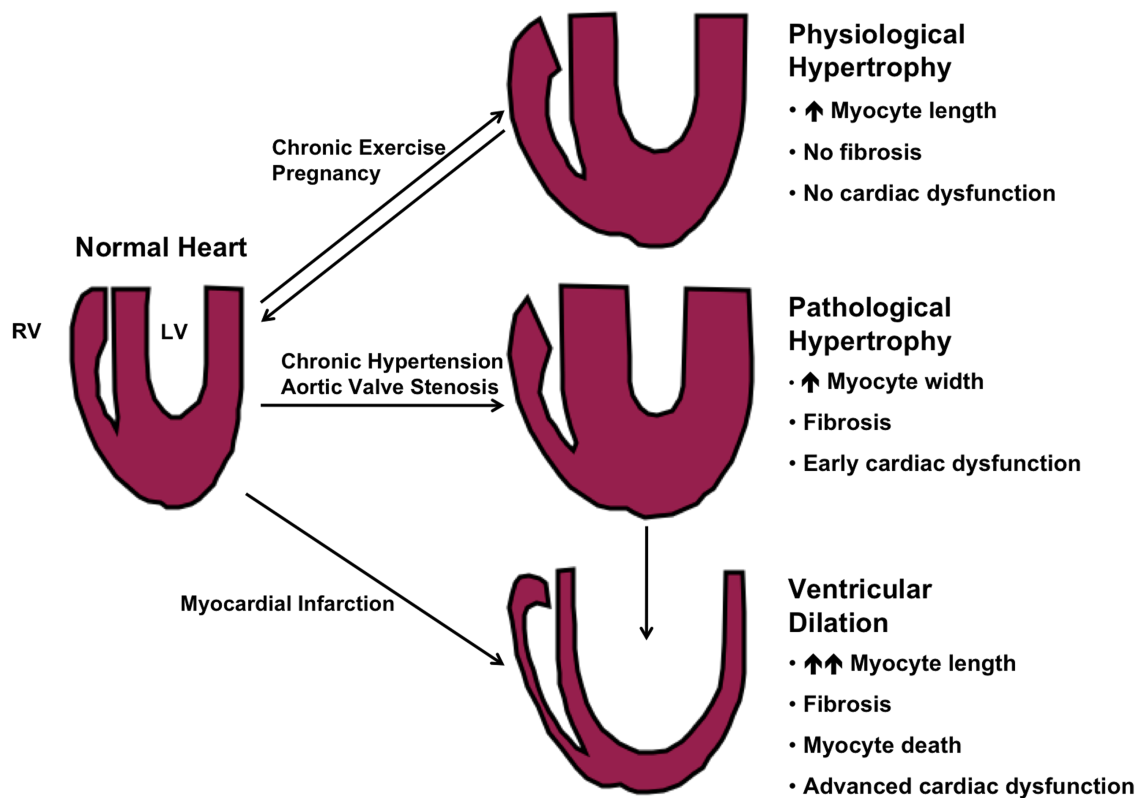


Figure 1.1 Types of cardiac hypertrophy.

Pathological cardiac hypertrophy is associated with ventricular remodelling through fibrosis, altered ECM turnover, an increase in myocyte size and myocyte death through apoptosis and necrosis, all of which eventually impact on cardiac function. Pathological or concentric hypertrophy is characterised by an increase in relative wall thickness (RWT) of the ventricle with a net decrease in ventricular chamber dimensions thus comprising cardiac function. Although not technically hypertrophy, ventricular dilation can follow due to concentric remodelling, with characteristic features including myocyte death and severe cardiac dysfunction. However, not all forms of cardiac hypertrophy are detrimental to cardiac function, for example athletic endurance training induces a state of ‘physiological’ hypertrophy characterised by an increase in RWT of the ventricle and an increase in chamber dilation. This type of hypertrophy is referred to as eccentric hypertrophy and is adaptive in the long term. Abbreviations: RV, right ventricle; LV, left ventricle.

1.3.1 Models of cardiac hypertrophy

In vivo models of haemodynamic stress to induce cardiac hypertrophy include development of pressure-overload hypertrophy via banding the aortic arch or volume overload via aortocaval fistula shunt. The generation of these animal models, along with the ability to transgenically over-express or knockout specific proteins in mice have lead to a number of important findings that have implications for the clinical management of cardiac disease.

1.3.1.1 Pressure-overload via aortic banding

Stenosis of the aorta by placement of a constricting band around this vessel has proved invaluable for assessing the patho-physiology of LV hypertrophy (Nakamura et al., 2001, Gao et al., 2005), including identification of diagnostic markers (Ogawa et al., 1996) and the role of specific genes (Backs et al., 2009). Aortic banding-induced pressure-overload models of LV hypertrophy have equally been important for testing therapeutic agents (Ago et al., 2010) as well as gene therapy approaches (del Monte et al., 2001). Furthermore, cardiac hypertrophy is a dynamic and progressive disease, with a subset of aortic-banded animals progressing to HF after several months (Patten and Hall-Porter, 2009). Thus, the induction of hypertension and ventricular hypertrophy should be considered when assessing new HF treatments *in vivo*.

Various animal species have been used to assess hypertrophy following aortic banding including large animals such as sheep, pig and dog, as well as smaller animal models including rabbit, guinea-pig, rat and mouse (Hasenfuss, 1998). The constricting band can be placed at the level of the ascending (Liao et al., 2002a), abdominal (Hara et al., 2002) or more commonly the transverse aorta (Rockman et al., 1991) to induce pressure-overload. Constriction of the aorta increases the pressure against which the heart has to pump during systole (i.e. increases the afterload on the heart), causing the LV to undergo hypertrophic remodelling to compensate. Transverse aortic constriction (TAC), pioneered by Rockman and colleagues (Rockman et al., 1991), has been used extensively over the past two decades to evaluate the cellular and molecular development of LV hypertrophy in response to

haemodynamic stress. TAC is a well-characterised, reproducible and potent method for inducing pressure-overload LV remodelling, with low mortality rates (~15-25%).

While the TAC procedure is performed routinely by a number of groups, the procedure is technically difficult, requiring tracheal intubation and mechanical ventilation once the thorax is entered, increasing the time and expense associated with these procedures. Moreover, subsequent inflammatory reactions within the chest cavity may impede the analysis of cardiac function and pathology. Development of a minimally invasive model of aortic banding has proved a significant refinement on previous TAC models (Hu et al., 2003). The minimally invasive transverse aortic banding (MTAB) procedure circumvents the need for mechanical ventilation as the pleural space is not entered, and therefore can be performed rapidly. Although very few groups have employed this method of aortic banding due to the expertise required, those that have, report consistent and sustained increases in LV pressure and prominent cardiac hypertrophy after 2-4 weeks aortic banding (Hu et al., 2003). More recently, this model was used to assess the development and regression of LV hypertrophy by MTAB for 4 weeks followed by de-banding (Stansfield et al., 2007).

1.3.2 Models of heart failure

With the improvement of medical diagnostics and therapies, more patients survive after acute coronary syndrome and MI, however most cases progress to HF. Animal models that closely mimic human HF with respect to structural and functional characteristics are imperative for the understanding of the patho-physiological mechanisms underlying the disorder as well as aiding the identification of novel therapeutic approaches (Klocke et al., 2007). As the clinical symptoms of HF are complex and include changes in gene expression, cell populations, ECM composition and LV geometry, development of an animal model to mimic all of these symptoms has proved challenging, thus no model system has superiority over another.

Methods to induce HF include left anterior descending coronary artery ligation (CAL) to induce myocardial ischaemia and infarction, aortic banding and chronic rapid pacing, with each technique having unique advantages and disadvantages. Genetic models have also been employed, such as the Dahl salt-sensitive rat that develops systemic hypertension when fed on a high salt diet, and the spontaneously

hypertensive rat (SHR) that develops progressive hypertension, eventually resulting in cardiac failure. Many different animal species have been used to study HF progression including large animal models such as sheep, pig and dog, as well as small rodent models (Hasenfuss, 1998). Smaller animal models are vast becoming the model of choice due to the advent of transgenic mouse strains coupled with the availability of micro-surgical equipment for the performance and assessment of HF. In addition, the lower costs of rodents compared to larger animals means that more animals can be assessed in a given study, increasing the statistical power (Patten and Hall-Porter, 2009).

CAL is the most widely used method for inducing HF, and has been used to explore the relationship between infarct size and LV chamber dilatation (Pfeffer et al., 1979) as well as to assess several drugs including vasodilators, angiotensin-converting enzyme (ACE) inhibitors and angiotensin II type 1 receptor (AT₁R) antagonists (Patten and Hall-Porter, 2009). As eluded to earlier, aortic banding to induce pressure-overload is another important model of HF as pathological remodelling develops gradually with progression from compensated hypertrophy to HF, making it potentially more clinically relevant to human HF (Patten and Hall-Porter, 2009).

1.4 Key cell types of the heart

1.4.1 Myocytes

The cardiac myocyte is a specialised muscle cell that is composed of bundles of myofibrils that contain myofilaments. Each myofibril contains repeating sarcomere contractile units, composed of thick myosin and thin actin filaments. Chemical and physical interactions between myosin and actin cause the sarcomere to shorten and lengthen during EC-coupling, causing myocardial contraction and relaxation, respectively (Klabunde, 2005). Cardiac Ca²⁺ cycling within each muscle cell during EC-coupling is essential for myocardial contraction during systole and relaxation during diastole. In the normal heart, free intracellular cytosolic Ca²⁺ concentrations ([Ca²⁺]) are tightly regulated despite considerable changes during the cardiac AP. In diseased myocardium however, intracellular Ca²⁺ regulation is severely impaired.

1.4.1.1 Normal excitation-contraction coupling

EC-coupling is the phrase used to describe the coupling of the cardiac AP with ventricular contraction (Figure 1.2). EC-coupling starts with myocyte depolarisation, causing an influx of Ca^{2+} via voltage-sensitive L-type Ca^{2+} channels (LTCC) present on the sarcolemmal membrane in structures known as transverse tubules (T-tubules). These are invaginations of the sarcolemmal membrane that are in close proximity to the intracellular Ca^{2+} store, the sarcoplasmic reticulum (SR) (Wehrens and Marks, 2004). This influx of extracellular Ca^{2+} is known as inward Ca^{2+} current (I_{Ca}). This I_{Ca} promotes a relatively larger release of Ca^{2+} from the SR via the activation and opening of ryanodine receptors (RyR_2 s) located on the SR membrane that are functionally coupled to the channels in the plasma membrane (Currie, 2008). This process is termed Ca^{2+} -induced calcium release (CICR) and raises the cytosolic $[\text{Ca}^{2+}]$ from 100 nM to $\sim 1 \mu\text{M}$ (Maier and Bers, 2002). Synchronous activation of these channels causes a transient increase in cytosolic $[\text{Ca}^{2+}]$, promoting Ca^{2+} binding to the Ca^{2+} sensitive myofilament subunit, troponin C. The Ca^{2+} -troponin C complex initiates myocardial contraction during systole, with the amplitude of the Ca^{2+} transient determining the force of contraction (Wehrens et al., 2004).

Following myocardial contraction, the heart must relax (diastole) to allow time for the heart to fill with blood. Relaxation of the cell is brought about by lowering cytosolic $[\text{Ca}^{2+}]$. This is achieved primarily due to RyR_2 inactivation, Ca^{2+} re-uptake into the SR via the SR Ca^{2+} -ATPase (SERCA2a), which is regulated/modulated by an accessory protein called phospholamban, and removal of Ca^{2+} from the cell via the $\text{Na}^+/\text{Ca}^{2+}$ exchanger (NCX), thus allowing Ca^{2+} dissociation from troponin C (Figure 1.2) (Maier and Bers, 2002). SERCA2a is the predominant method of Ca^{2+} extrusion from the cytosol and contributes $\sim 70\%$ to removal of cytosolic Ca^{2+} in human and rabbit and $\sim 90\%$ in rat and mouse. Other pathways contribute to cytosolic $[\text{Ca}^{2+}]$ decline such as via the sarcolemmal Ca^{2+} -ATPase and a small amount of Ca^{2+} is transported into the mitochondrion via the mitochondrial Ca^{2+} uniport (Bers, 2002).

Notably, all of the key Ca^{2+} -handling proteins have been shown to be regulated via phosphorylation, predominately by protein kinase A (PKA) and Ca^{2+} /calmodulin-dependent protein kinase II (CaMKII).

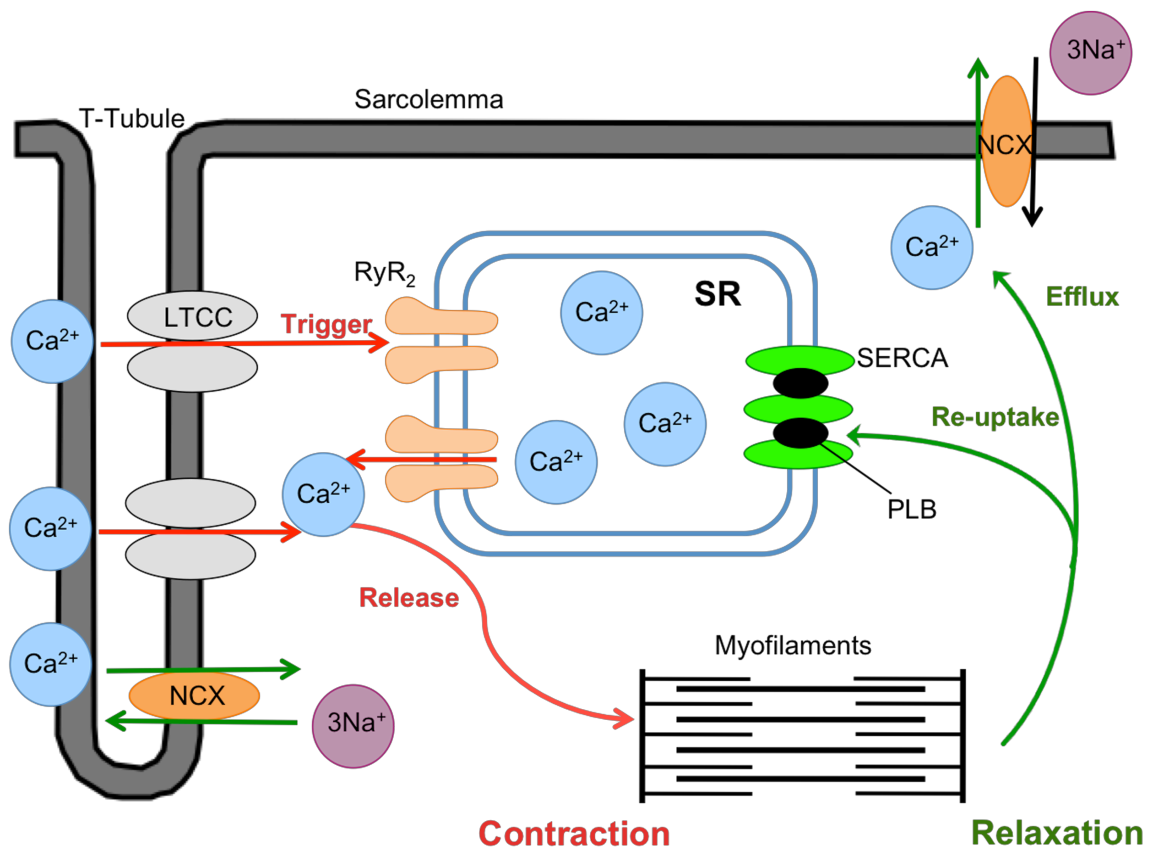


Figure 1.2 Cardiac excitation-contraction coupling in ventricular myocytes.

During systole (red arrows), myocyte depolarisation activates L-type Ca²⁺ channels (LTCC) triggering Ca²⁺ release from the sarcoplasmic reticulum (SR) via the ryanodine receptors (RyR₂s). This causes a transient increase in intracellular Ca²⁺ concentration, accompanied by myofilament activation and contraction. For relaxation to occur during diastole (green arrows), cytosolic Ca²⁺ levels must decline and dissociate from the myofilament complex. This is achieved primarily via RyR₂ inactivation, Ca²⁺ uptake into the SR by the SR Ca²⁺-ATPase (SERCA) and by removal of Ca²⁺ from the cell via the Na⁺/Ca²⁺ exchanger (NCX). Note for clarity only major Ca²⁺-handling proteins are shown. Abbreviations: PLB, phospholamban.

1.4.1.2 Alterations in EC-coupling in hypertrophy and heart failure

A key feature of cardiac hypertrophy is altered Ca^{2+} homeostasis with a resultant increase in the force of contraction. On the other hand, progression from hypertrophy to HF results in contractile dysfunction and development of arrhythmias.

The majority of clinical and animal studies published to date suggest that all of the four key Ca^{2+} -handling proteins (LTCC, RyR₂, SERCA2a and NCX) have altered expression and function in cardiac hypertrophy and HF. Many studies have reported a down-regulation of SERCA2a messenger ribonucleic acid (mRNA) and protein (Currie and Smith, 1999b, Prasad et al., 2007), an up-regulation of NCX protein expression and activity (Wang et al., 2001, Mork et al., 2007) and an increase in RyR₂ phosphorylation, particularly by CaMKII (Currie et al., 2004, Curran et al., 2007), in hypertrophic and HF hearts. Thus, the observed decrease in myocardial contraction and relaxation in HF is a consequence of (i) altered SR function due to reduced SR Ca^{2+} content as a result of an imbalance between Ca^{2+} uptake via SERCA2a and SR Ca^{2+} release via RyR₂, and (ii) altered NCX activity. Collectively these processes decrease the SR Ca^{2+} available for release during subsequent EC-coupling, ultimately leading to diastolic dysfunction.

1.4.2 Cardiac fibroblasts

1.4.2.1 Physiological role of cardiac fibroblasts in the heart

During cardiac development, CFs develop from multipotent progenitor cells or mesenchymal stem cells (Baum and Duffy, 2011), with cell numbers increasing with normal development and aging (Camelliti et al., 2005). In comparison to the usual flattened stellate shape of fibroblasts, CFs are elongated cells with a highly elaborated endoplasmic reticulum and an elliptical shaped nucleus containing one or two nucleoli and no basement membrane (Baum and Duffy, 2011). The cells form a network, connected by long filopodia, responding to both mechanical and chemical signalling (Baum and Duffy, 2011). CFs play an important role in maintaining ECM homeostasis via production of factors, such as cytokines (e.g. interleukin-6 (IL-6)), growth factors (e.g. transforming growth factor- β (TGF- β)), matrix

metalloproteinases (MMPs) and proteases, that are involved in maintaining a balance between synthesis and degradation of connective tissue such that collagen levels remain stable in the normal/healthy heart (Brown et al., 2005a).

CFs have been gaining attention since the discovery that cardiac fibrosis is a significant feature of various forms of cardiac disease, including hypertension, MI and HF. The observation that CF express angiotensin receptors on their surface directly links the RAAS system with pathological myocardial and ECM remodelling (Villarreal et al., 1993, Crabos et al., 1994). Traditionally CFs have been associated with cardiac pathophysiology, however accumulating evidence now suggests that they also play a key role in normal cardiac function. Numerous studies have demonstrated that CFs can not only modulate the activity of adjacent CFs but can also influence myocyte function via paracrine signalling (e.g. via TGF- β and endothelin-1, (ET-1)) (Gray et al., 1998, Fredj et al., 2005b, Pedrotty et al., 2009) and via direct cell-cell gap junctions. The electrophysiological cross talk between CFs and myocytes occurs via connexon gap junctions, namely Cx43 and Cx45 (Gaudesius et al., 2003).

1.4.2.2 Role of cardiac fibroblasts in the diseased heart

CFs are significant participants in the response to pathological cardiac remodelling. These cells exhibit an increase in migration and proliferation as well as exerting significant changes in the extent and composition of the ECM (Figure 1.3). The augmented deposition of collagen by CFs provides increased contacts between myocytes and CFs, the CFs themselves and with the ECM; contacts which can be both beneficial and detrimental to cardiac function (Porter and Turner, 2009).

It is generally considered that there are two types of fibrosis; (i) reparative fibrosis which is dispersed throughout the myocardium and takes place as a result of tissue injury, and (ii) reactive fibrosis which occurs due to the direct stimulation of CFs and is associated with capillaries (Creemers and Pinto, 2011). Excessive CF proliferation and disproportionate accumulation of fibrillar collagen results in disruption of myocyte coupling and myocardial stiffening, reducing ventricular compliance leading to diastolic dysfunction and eventually HF (Manabe et al., 2002).

Following cardiac injury or stress, CFs release various growth factors and pro-inflammatory cytokines, which signal to other CFs and to myocytes to induce their

hypertrophic growth (Manabe et al., 2002, Baudino et al., 2006). This is achieved via the activation of intracellular signalling pathways and various transcription factors (e.g. activating protein-1 (AP-1) and NF- κ B) which ultimately leads to changes in gene expression (Manabe et al., 2002). The remodelling process is associated with augmented release of these hormonal factors from CFs, with subsequent changes in gene expression promoting the differentiation of CFs into a myo-CF phenotype that actively participates in the inflammatory response to injury (Figure 1.3) (Baum and Duffy, 2011). Myo-CFs are only present in the diseased or injured heart. These 'activated' cells express higher levels of α -smooth muscle actin (α -SMA) making them more motile and allowing them to migrate readily to the site of injury (Rohr, 2009). Myo-CFs are more responsive to chemokines and cytokines released at the site of injury and produce a number of cytokines and growth factors themselves (Baum and Duffy, 2011). Increases in mechanical force can regulate myo-CF differentiation by increasing α -SMA expression (Wang et al., 2003).

1.4.3 Cardiac fibroblast – myocyte interaction

1.4.3.1 In the healthy heart

The ability of CFs to modulate myocyte activity via homogeneous and heterogeneous gap junctions *in vitro* has been demonstrated by a number of electrophysiological experiments, with co-cultured CFs and myocytes readily forming functional gap junctions (Kohl et al., 1994). A study using strands of neonatal myocytes interrupted with neonatal CFs demonstrated that electrical impulses could be conducted over distances of 300 μ m. Mechanical stretch was not involved but rather electrotonic interactions via Cx43 and Cx45, (Gaudesius et al., 2003). Although CFs are considered non-electrically excitable cells and on their own cannot maintain impulse propagation, this study highlights that they can readily conduct electrical signals, possibly via multiple Na⁺ and K⁺ channels (Baum and Duffy, 2011).

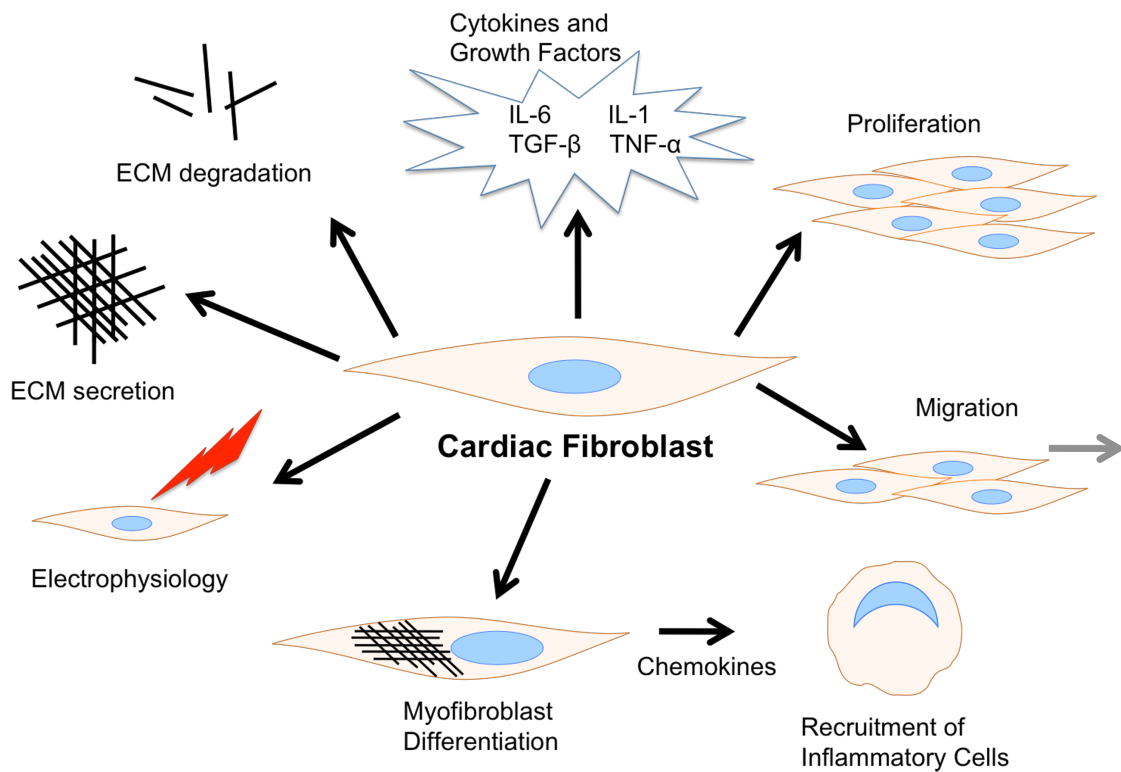


Figure 1.3 Alterations in cardiac fibroblast function associated with myocardial remodelling.

The cardiac fibroblast responds to environmental stimuli in various ways, including secretion of cytokines and growth factors, proliferation and migration, transformation to a myofibroblast phenotype expressing α -smooth muscle actin, and altering extracellular matrix (ECM) generation and degradation. These changes in fibroblast function are initially adaptive to increases in mechanical stress, however they can become maladaptive leading to pathological remodelling and fibrosis.

As mentioned previously, CFs can alter myocyte phenotype via paracrine signalling, although it is also likely that myocytes alter CF function via the same mechanism. Recently a study using myocytes cultured in CF-conditioned media highlighted the effect of these paracrine interactions, whereby various cytokines present in the CF-conditioned media induced changes in myocytes including hypertrophy, intracellular expression of vimentin and diminished contractile capacity (LaFramboise et al., 2007). These results established that factors produced by CFs could induce phenotypic plasticity in myocytes distinct from the dedifferentiation program normally seen *in vitro* (LaFramboise et al., 2007).

The first suggestion that CFs and myocytes interact within the intact heart came from *ex vivo* electrophysiology studies using spontaneously beating rat atrium with double-barrelled floating microelectrodes inserted into the sub-endocardial layers of the atria. These studies demonstrated that changes in the CF membrane potential were similar to the AP in adjacent myocytes (Kohl et al., 1994). Functional studies have been impeded by the fact that CFs have a very high membrane resistance, which although providing an obvious advantage for electrotonic impulse conduction, it means that CFs mimic the intracellular membrane potential of well coupled myocytes, thus making it difficult to electrophysiologically separate these cells *in situ* (Kohl, 2003). Another limiting factor for imaging CF *in vivo* is the lack of a truly specific marker, although staining for vimentin is commonly used. Goldsmith et al. (2004) proposed that the discoidin domain receptor 2 (DDR2) was specific for CFs. By using DDR2 as a marker for CFs and various types of microscopy, including laser scanning confocal microscopy, they reported that CFs are interconnected via gap junctions composed of Cx43 and Cx45, and form a three-dimensional network directly associated with myocytes (Goldsmith et al., 2004).

In rabbit SA node, CFs were shown to express Cx43 in CF-rich areas devoid of myocytes and Cx45 when intermingled with myocytes, suggesting that there are two spatially distinct populations of CFs in nodal tissue (Camelliti et al., 2004b). The functional significance of homogeneous and heterogeneous cell coupling in the SA node was confirmed using transfer of Lucifer yellow, a gap junction permeable dye. Dye transfer was predominately along threads of interconnected CFs, and occasionally between neighbouring CFs and myocytes, highlighting that CFs form a wide coupled network of cells which may also be functionally linked to myocytes (Camelliti et al., 2004b). Similar heterogeneous cell coupling may also occur in

ventricular tissue, with supporting evidence from the identification of Cx43 and Cx45 expressing CF in sheep whole heart sections (Camelliti et al., 2004a).

Collectively these data suggest that in the normal heart CFs actively modulate myocyte function and ultimately myocardial function via electrical connections and via paracrine signalling factors. Due to the potential role of CFs in the regulation of global cardiac function and the fact that many CVDs are frequently associated with myocardial remodelling involving fibrosis, it is important not to underestimate the importance of bi-directional signalling between CFs and myocytes in the development of CVD.

1.4.3.2 In the pathological heart

Remodelling of the myocardium is associated with enhanced autocrine/paracrine signalling (via growth factors and cytokines) between CFs and myocytes as well as altered electrophysiological CF-myocyte interactions.

1.4.3.2.1 Growth factors

TGF- β plays an important role in myocardial remodelling and is both released and expressed by neonatal and adult myocytes and CFs, although CFs have been reported to be the primary source of TGF- β (Bujak and Frangogiannis, 2007). TGF- β is released by myocytes following pressure-overload (Takahashi et al., 1994), mechanical stretch (van Wamel et al., 2002) and MI (Bujak and Frangogiannis, 2007). TGF- β receptors are found on ventricular myocytes and CFs (Santiago et al., 2010), and can elicit myo-CF transformation by increasing α -SMA expression (Tomasek et al., 2002). TGF- β also mediates non-myocyte cell proliferation and fibrosis *in vivo* (Teekakirikul et al., 2010). An inducible dominant-negative mutation of TGF- β prevented non-myocyte cell proliferation and collagen deposition in response to pressure-overload, however it did not protect against ventricular dilatation or diastolic dysfunction (Lucas et al., 2010). Similarly, an anti-TGF- β neutralising antibody prevented CF activation and subsequent collagen production and fibrosis in response to pressure overload, however it did not reverse myocyte hypertrophy (Kuwahara et al., 2002). Other research has suggested that TGF- β may actually protect against

ischaemic myocardial remodelling during the early phase (24 h), however the beneficial effects may be lost with sustained expression, thereby leading to LV remodelling and failure (Ikeuchi et al., 2004).

1.4.3.2.2 Vasoactive peptides and neurohumoral agonists

Studies have highlighted that in the heart, Ang II is a key mediator of collagen synthesis and gene expression, and inhibits MMPs preventing collagen degradation (Zannad et al., 2001). Similarly ET-1 has been shown to induce myocyte hypertrophy, stimulate collagen synthesis and induce proliferation of neonatal and adult CFs (Piacentini et al., 2000). More recently ET-1 has been shown to induce CF to myo-CF differentiation with increased expression of α -SMA (Nishida et al., 2007). These vasoactive peptides appear to elicit their action via bi-directional signalling between CFs and myocytes, with research demonstrating that myocytes regulate CF adhesion and/or proliferation *in vitro* (Fredj et al., 2005b). Ang II does this by acting through the AT₁R present on CFs, promoting the release of TGF- β and ET-1 from CFs which induce the hypertrophic growth of myocytes (Gray et al., 1998).

1.4.3.2.3 Electrophysiology

Structural remodelling of the myocardium promotes excessive secretion of ECM proteins, resulting in collagenous septa that can contribute to arrhythmogenesis due to slow conduction. The differentiation of CFs into a myo-CF phenotype can induce ectopic activity in myocardial tissue, as evidenced by myo-CFs inducing synchronised spontaneous activity in co-cultured myocytes (Miragoli et al., 2007). Research suggests that activated myo-CFs communicate with myocytes via expression of Cx43 (Asazuma-Nakamura et al., 2009), with normal CFs expressing Cx45 and only weakly coupling to myocytes without significant depolarisation of cardiac resting potential (McSpadden et al., 2009). A recent study demonstrated that the cardiac AP conduction velocity and duration were significantly decreased in neonatal rat myocyte monolayers when treated with either conditioned media from CFs isolated from infarcted hearts (MI-CFs) or when co-cultured with MI-CFs compared to normal CFs. Intercellular coupling was higher between myocytes and

MI-CFs compared with CFs, due to increased expression of Cx43 (Vasquez et al., 2010), suggesting that enhanced CF-myocyte interactions following cardiac injury are partially responsible for the increased incidence of arrhythmia observed in the fibrotic heart. Signalling from CFs to myocytes may be bi-directional as stimulation of rabbit myocytes influenced the intracellular $[Ca^{2+}]$ of the linked myo-CF via Cx43 (Chilton et al., 2007). Other research has suggested that mechanical myo-CF-myocyte interactions and activation of mechanosensitive channels may alter myocyte electrophysiology (Thompson et al., 2011) as well as paracrine factors produced by CFs (Pedrotty et al., 2009).

1.4.3.2.4 Cytokines

MMPs regulate ECM turnover as they act to degrade interstitial collagen. Disruption of the collagen ECM network enhances inflammation within the myocardium, including inflammatory cell infiltration (e.g. leukocytes and neutrophils) and release of cytokines, which lead to CF migration and proliferation (Camelliti et al., 2005). Members of the IL-6 family of cytokines, leukemia inhibitor factor (LIF) and cardiotrophin-1 (CT-1), have been shown to be involved in myocyte-CF crosstalk. For example in neonatal rat cultures, Ang II increased expression of IL-6, LIF and CT-1 in CFs, which contributed to Ang II induced hypertrophy in myocytes (Sano et al., 2000). Addition of an anti-IL-6 antibody to myocyte-CF co-cultures decreased myocyte hypertrophy and decreased CF proliferation (Fredj et al., 2005a).

IL-1 β and TNF- α also play a role in remodelling of the heart. For example, IL-1 β and TNF- α are involved in post-MI remodelling via the upregulation of the AT₁R on CFs, thus enhancing CF responses to Ang II, favouring ECM turnover (Cowling et al., 2002). In adult and neonatal rat CF cultures, IL-1 β and TNF- α independently decreased fibrillar collagen deposition and increased MMP-2 and MMP-13 expression and activity (Siwik et al., 2000). Accordingly, a TNF- α -blocking protein prevented the increased MMP expression and activity in chronically paced dog hearts (Bradham et al., 2002). The actions of these pro-inflammatory cytokines were found to be additive in rat neonatal CFs (Gurantz et al., 2005) and adult CFs (Brown et al., 2007). TNF- α and IL-1 β also increase the expression of tissue inhibitor of metalloproteinases (TIMPs) (Peng et al., 2002, Brown et al., 2007). TIMPs are important regulators of

ECM composition by inhibiting the activity of MMPs, and therefore play a key role in the remodelling heart (Porter and Turner, 2009). IL-1 β may actually play a role in preventing cardiac fibrosis by inhibiting myo-CF differentiation via decreasing α -SMA expression and inducing myo-CF apoptosis via the activation of nitric oxide synthase (Baum and Duffy, 2011). Accordingly, compensated LV hypertrophy during pressure-overload was attenuated in IL-1 β ^{-/-} mice (Honsho et al., 2009).

Overall these data illustrate that various cytokines and growth factors, produced by CFs and myocytes, act independently or coordinately via autocrine and/or paracrine signalling to induce myocardial remodelling. Normalising the expression and activity of these factors is therefore a potential therapeutic target for modulating remodelling after cardiac insult (Nian et al., 2004, Brown et al., 2005a, Leask, 2010).

1.5 Therapeutic targets in the treatment of cardiovascular disease

Despite the advancement in medical technology and pharmacological therapy, the prevalence and incidence of chronic HF is rising and the disease imposes substantial economic costs as well as being a major cause of disability and death. Due to the fact that many current cardiovascular drugs lack selectivity and have serious side effects (McMurray and Pfeffer, 2002a, 2002b), it is clear that a deeper understanding of the cellular and molecular mechanisms involved in the complex remodelling process during CVD is required with the aim of identifying novel targets.

1.5.1 Current therapies

Pharmacological therapies have been the mainstay of treatment for cardiac dysfunction for the last century and has rapidly shifted from diuretics and digoxin to inotropes and vasodilators (e.g. isosorbide-dinitrate and hydralazine) to a focus on RAAS inhibitors (i.e. ACE inhibitors, angiotensin-receptor blockers and aldosterone inhibitors) and sympathetic nervous system inhibitors (e.g. β -adrenoreceptor antagonists, also named β -blockers) (Krum and Teerlink, 2011). The current 'gold-standard' treatment for chronic HF recommended by the European Society of Cardiology include a combination of an ACE inhibitor, a β -blocker and a diuretic (Currie et al., 2011). Although these drugs have been shown to substantially improve

morbidity and mortality in chronic HF patients, each drug is associated with serious adverse effects. For example, the aldosterone inhibitor eplerenone and the ACE inhibitor enalapril are associated with hyperkalaemia (which can lead to arrhythmia), hypotension and worsened renal function (Krum and Teerlink, 2011). β -blockers are often not prescribed at the clinically optimum dose because of hypotension and bradycardia (Krum and Teerlink, 2011). In addition, these drugs are not effective in treating patients with HF with preserved ejection fraction, thus new therapeutic approaches are required.

1.5.2 Novel approaches

1.5.3 Targeting Ca^{2+} -handling and myocardial contractility

Intracellular Ca^{2+} is an extremely important second messenger in the heart as it regulates both acute physiological functions, such as myocardial contraction and relaxation, as well as activation of signal transduction pathways responsible for chronic cellular responses (Frey et al., 2000, Zhang et al., 2004). At the centre of cardiac dysfunction lies impaired contractility of individual myocytes regulated by EC-coupling. Reduced SR content as a result of reduced SERCA2a activity and 'leaky' RyR_2 function is a key determinant of contractile dysfunction and therapeutic targeting of these Ca^{2+} -handling proteins is an attractive approach. Approaches to increase SR Ca^{2+} uptake include enhancement of SERCA2a activity and PLB inhibition. Pharmacological targeting of SERCA2a has not yielded drugs with high specificity thus enhancement of SERCA2a activity by gene transfer of the SERCA2a gene, ATP2a2, is the current approach (Lompre et al., 2010). Phase 1 clinical trials have recently been completed, although larger Phase 2 trials are required to determine the beneficial effect (Jaski et al., 2009, Lompre et al., 2010). Findings from animal models with PLB inhibition via various strategies including over-expression of dominant-negative PLB mutants and genetic ablation, have shown improved SR function and myocardial contractility (Lompre et al., 2010). Stabilisation of the RyR_2 to inhibit Ca^{2+} leak, for example by PKA or CaMKII inhibitors, is another potential strategy to reduce arrhythmias (Shah and Mann, 2011). A benzothiazepine derivative, K201 also named JTV-519, has been studied extensively in animal models of HF and has been shown to improve cardiac function by stabilising the closed state of the

RyR₂, possibly by increasing the affinity of FKBP12.6 for the PKA-hyperphosphorylated channel (Currie et al., 2011).

1.5.4 Targeting remodelling of the ECM

Changes in the ECM and CF proliferation and migration are key features of the remodelling heart, leading to fibrosis and dilatation. However clinical trials aimed at reducing LV remodelling with an MMP inhibitor (PG-116800) following MI were unsuccessful, with no improvement in clinical outcome despite beneficial findings when used in animal models of MI and HF (Hudson et al., 2006). Potential new therapies aimed at targeting altered CF function, either via inhibition of proliferation/migration or by inhibiting CF to myo-CF differentiation, are desirable given the extensive paracrine signalling between CFs and myocytes and deposition of collagen in the remodelling heart. Indeed, some of the ‘off-target’ properties of current therapeutic agents for the treatment of chronic HF, including ACE inhibitors, angiotensin-receptor blockers and β -blockers, have been shown to exert beneficial effects on CF function (Porter and Turner, 2009). For example, ACE inhibitors and angiotensin-receptor blockers have been shown to exhibit anti-proliferative effects on CFs as well as reducing CF to myo-CF differentiation (Yu et al., 2001). Similar findings have been shown with β -blockers (Porter and Turner, 2009) however specific CF-targeting agents may prove more beneficial.

1.5.5 Targeting inflammation

As alluded to already, inflammation, cytokine release and inflammatory cell influx within the myocardium play an important role in remodelling following MI, myocarditis as well as the haemodynamically overloaded heart. A highly specific anti-inflammatory therapeutic approach would be to directly target particular cytokines released by cardiac cells, such as TNF- α or IL-6. Etanercept, a recombinant human TNF- α receptor that binds to circulating TNF- α and functionally inactivates it by preventing it from binding to its receptors on cell surface membranes, has been shown to improve clinical symptoms of rheumatoid arthritis and psoriasis. However, two well designed clinical trials with etanercept failed to show any benefit on the rate

of death or hospitalisation due to chronic HF (Mann et al., 2004). A separate clinical trial using a monoclonal antibody against TNF- α , infliximab, actually increased mortality (Leuschner et al., 2009). These results may be attributed to the presence of other inflammatory mediators maintaining inflammatory signalling in the absence of TNF- α , and therefore broad-spectrum immuno-modulatory strategies may prove more beneficial. Intravenous gamma-globulin and immunoadsorption and immune-modulation therapy are currently under investigation. Removal of circulating immunoglobins (IgGs) from the plasma of dilated cardiomyopathy patients has been shown to improve LV ejection fraction and the clinical symptoms of HF (Leuschner et al., 2009, Celis et al., 2008).

It is clear that a better understanding of the activation of the innate immune response following cardiac injury as well as alterations in myocyte and non-myocyte function and the paracrine cross-talk between these cell types within the myocardium may yield novel treatments. Again, the CF appears an attractive therapeutic target to inhibit cytokine/chemokine signalling and prevent the recruitment of inflammatory cells into the remodelling myocardium.

1.5.6 Ca^{2+} /calmodulin-dependent kinase II

One strong candidate for therapeutic targeting is CaMKII. There is significant evidence for CaMKII playing a multifunctional role in the heart and for augmented CaMKII activity in structural heart disease. CaMKII plays an important role in myocardial function by translating and coordinating Ca^{2+} signals into appropriate cellular responses via phosphorylation events. CaMKII has a well established role in modulation of cardiac contractility (Anderson et al., 2011) and may have possible roles in hypertrophic gene transcription (Ramirez et al., 1997, Backs et al., 2006), fibrosis (Zhang et al., 2010c) and inflammation (Singh and Anderson, 2011) (Section 1.6.3). As a result, CaMKII may act as a point of convergence of hypertrophic signalling cross talk and is therefore an attractive novel therapeutic target.

1.6 Introduction to CaMKII

There are three types of CaMK serine/threonine kinases; I, II, and IV. Following binding to $\text{Ca}^{2+}/\text{CaM}$, the monomeric enzymes, CaMKI and CaMKIV, are activated through phosphorylation by an upstream CaMK kinase (CaMKK) (Zhang and Brown, 2004). CaMKI is a ubiquitously expressed cytoplasmic enzyme, and although present in the heart, it does not seem to be involved in structural heart disease as expression levels do not increase during the development of hypertrophy (Colomer et al., 2003). In contrast, CaMKIV's expression is restricted to neuronal tissues, T lymphocytes and testis (Zhang and Brown, 2004). Unlike CaMKI and CaMKIV, CaMKII is a multifunctional protein ubiquitously expressed in the cytoplasm and nucleus of a diverse range of cell types, and is the most prominent CaMK expressed in cardiac myocytes (Colbran, 2004). $\text{Ca}^{2+}/\text{CaM}$ binding alone produces maximal activation of CaMKII, without the requirement of additional phosphorylation by CaMKK (Hudmon and Schulman, 2002).

1.6.1 Isoforms of CaMKII present in the heart

CaMKII is a multimeric kinase of about 50-60 kDa that is involved in modulating a variety of intracellular Ca^{2+} -dependent signalling processes such as neuronal plasticity, learning and memory, muscle contraction, cell secretion and gene expression (Colbran, 2004). There are four CaMKII isoforms encoded by one of four distinct genes; α , β , δ , γ . Whereas the expression of α and β subunits is normally restricted to neuronal tissue, the δ and γ subunits are present in a variety of tissues, including the heart (Anderson, 2005). The δ isoform is the prominent form expressed in the heart (Edman and Schulman, 1994), with expression levels varying throughout cardiac development (Hagemann et al., 2001) and disease (Hempel et al., 2002). Although much of the primary sequence between CaMKII isoforms is conserved, the δ_B isoform has a nuclear localisation signal (NLS) present between the regulatory and association domains, therefore localising it to the nucleus in both CF and myocytes (Edman and Schulman, 1994, Ramirez et al., 1997, Zhang et al., 2002a). The δ_C isoform lacks this NLS and therefore localises to the cytosol, particularly to the SR in myocytes (Zhang et al., 2004).

1.6.2 Structure and activity regulation

All CaMKII isoforms are capable of forming a holoenzyme of homo- or hetero-multimers containing between 6-12 kinase subunits, arranged in a circular-shaped structure (Figure 1.4) (Colbran, 2004). Each CaMKII subunit contains a highly conserved N-terminus catalytic domain (approx. 280 amino acids) and a C-terminus association domain (150-220 amino acids) that flank a regulatory domain (approx. 40 amino acids) (Anderson, 2005). The regulatory domain contains a pseudo-substrate and a calmodulin (CaM)-binding region that cooperate to integrate CaMKII activity responses to changes in cytoplasmic $[Ca^{2+}]$ i.e. the frequency, amplitude, and duration of Ca^{2+} transients (Zhang and Brown, 2004, Anderson, 2007).

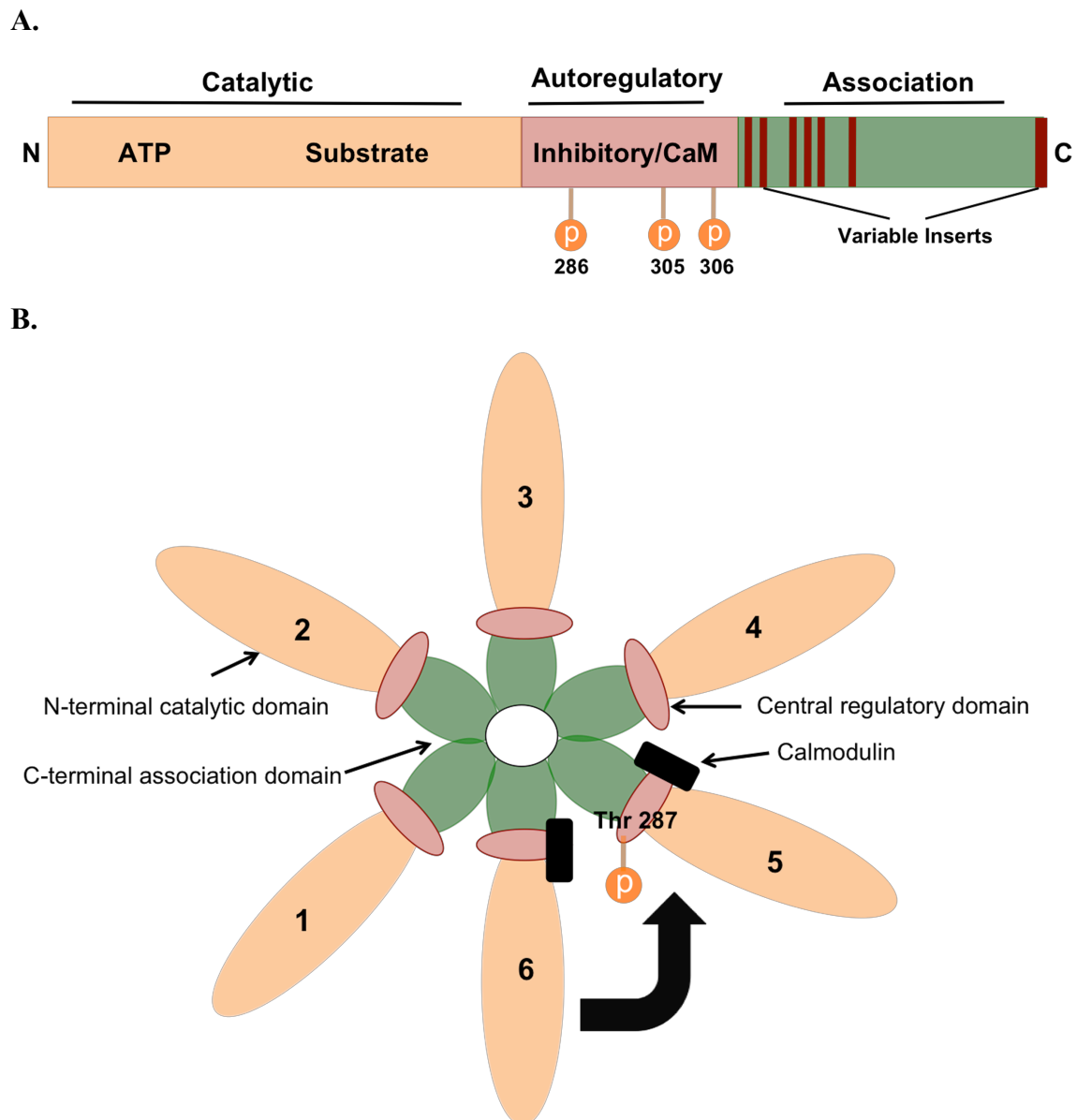


Figure 1.4 Schematic representation of CaMKII δ structure.

A. CaMKII isoforms consists of three domains; (i) an N-terminus catalytic domain containing ATP binding and substrate binding areas, (ii) a regulatory domain containing an autoinhibitory domain and a calmodulin (CaM) binding domain and, (iii) a C-terminus association domain with four main variable regions. B. Diagram shows a single ring from the CaMKII holoenzyme, which exist as a stacked pair of hexameric rings. Autophosphorylation at Thr 287 (δ isoform) requires simultaneous binding of Ca^{2+} /CaM to adjacent subunits in the holoenzyme, one of which serves as the catalytic unit and the other as the substrate. In this example, Ca^{2+} /CaM bound in subunit 5 will be autophosphorylated and subunit 6 will not i.e. it is the catalytic unit. (Figure adapted from Colbran, 2004)

In the absence of Ca^{2+} bound CaM ($\text{Ca}^{2+}/\text{CaM}$), substrates are inhibited from binding to the catalytic domain by interaction with the regulatory domain at threonine 286/287 (Thr 287 in δ isoform) (Anderson, 2007, Zhang and Brown, 2004). This inhibitory interaction is disrupted by the binding of $\text{Ca}^{2+}/\text{CaM}$ causing activation of CaMKII (Colbran, 2004). In this activated state, ATP and CaMKII substrates have access to the catalytic domain of the kinase for subsequent enzymatic catalytic activities (Hudmon and Schulman, 2002). Once the kinase has been activated by $\text{Ca}^{2+}/\text{CaM}$ and under sustained $\text{Ca}^{2+}/\text{CaM}$, the enzyme can lock itself in the activated state by autophosphorylation at Thr 287 and Thr 306/307 (δ isoform) within the regulatory domain (Figure 1.5) (Anderson, 2007, Zhang and Brown, 2004). Autophosphorylation is associated with a 1,000-fold increase in affinity for $\text{Ca}^{2+}/\text{CaM}$, which prolongs the $\text{Ca}^{2+}/\text{CaM}$ stimulated activity of CaMKII because CaM is slower to dissociate from the enzyme once the intracellular $[\text{Ca}^{2+}]$ has returned to basal (Skelding and Rostas, 2009). CaMKII phosphorylation at Thr 287 also results in autonomous Ca^{2+} -independent activity, i.e. the enzymatic activity of CaMKII is retained even in the absence of bound $\text{Ca}^{2+}/\text{CaM}$ (Hudmon and Schulman, 2002, Anderson, 2007, Zhang and Brown, 2004). This complex autoregulatory behaviour may potentially underlie CaMKII's ability to become differentially activated with a transient Ca^{2+} stimulus and thus, CaMKII may act as a 'molecular switch' capable of rapidly responding to changes in cytosolic $[\text{Ca}^{2+}]$ within microenvironments of the cell and coordinating localised modulation/phosphorylation of Ca^{2+} handling proteins and other yet unknown targets (Hudmon and Schulman, 2002, Currie, 2008). Complete inactivation of the kinase can occur following dephosphorylation by protein phosphatases PP1, PP2A and PP2C (Anderson, 2007, Zhang and Brown, 2004).

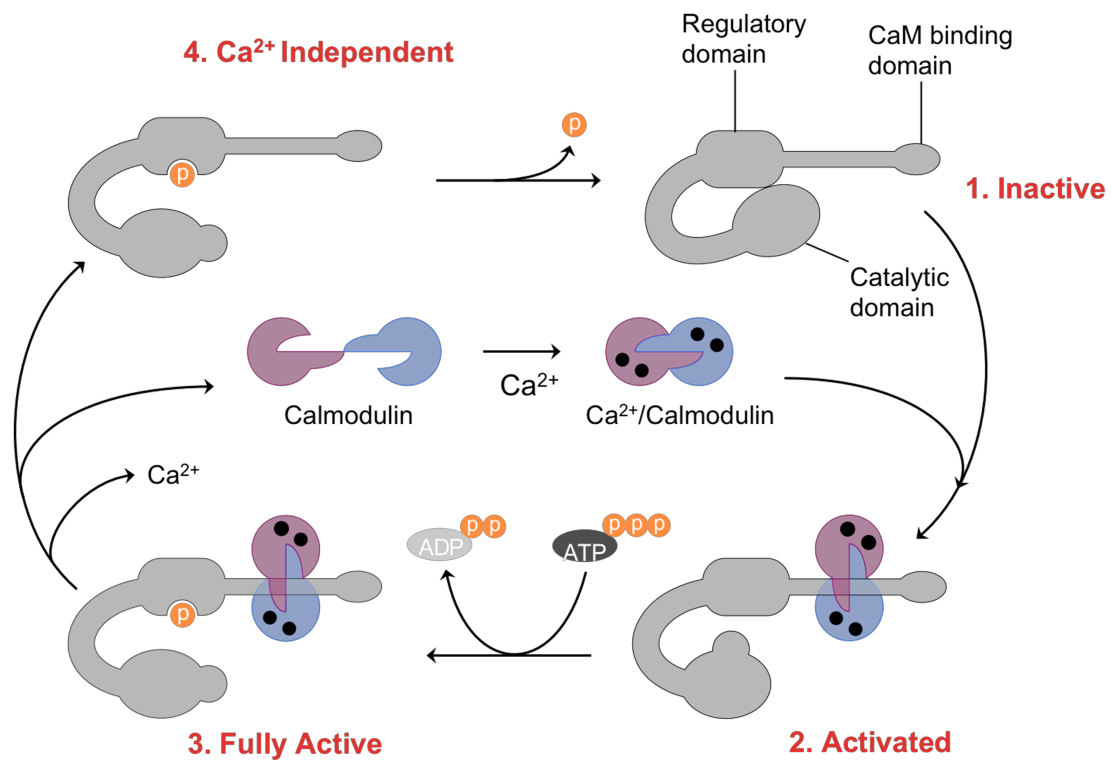


Figure 1.5 Activation of CaMKII.

CaMKII is inactive in the absence of Ca^{2+} bound CaM (Ca^{2+} /CaM) and substrates are inhibited from binding to the catalytic domain by interaction with the regulatory domain (1). Binding of Ca^{2+} /CaM disrupts this interaction, causing activation of CaMKII (2) and subsequent autophosphorylation at Thr 286/287 within the regulatory domain (3). Phosphorylation at Thr 286/287 results in autonomous Ca^{2+} -independent activity (4).

As mentioned, a distinguishing feature of CaMKII regulation is autophosphorylation at Thr 287 that renders the kinase autonomously active. Although this autonomous activity is $\text{Ca}^{2+}/\text{CaM}$ independent, a recent study has suggested that it is substrate and ATP dependent, with the latter varying significantly during pathological conditions (Coultrap et al., 2010). Thus, under normal physiological conditions autonomous activity is low and complete independence from $\text{Ca}^{2+}/\text{CaM}$ is unusual (Currie et al., 2011). The suggestion that autonomous activity of CaMKII increases under pathological conditions had been supported by a recent finding that the enzyme may be modulated by methionine oxidation of paired residues present in the regulatory domain (Met 281/282) (Erickson et al., 2008, Erickson et al., 2011). Increased oxidation can shift the Ca^{2+} dependence of CaMKII activation to low levels and therefore promote CaMKII activation even under low intracellular Ca^{2+} activity (Anderson et al., 2011). Autophosphorylation at Thr 287 and Met 281/282 oxidation appear to be interactive processes as Thr 287 phosphorylation is enhanced under circumstances of increased ROS (Anderson et al., 2011). This Ca^{2+} -independent route of CaMKII activation may therefore be important in disease states where oxidative stress is increased, such as MI and ischemia/reperfusion injury (Perrelli et al., 2011), and thus adds additional regulation to this kinase under pathological conditions.

Recent work has provided evidence for additional regulation of CaMKII function by phosphorylation at Thr 253 in the regulatory domain (Skelding et al., 2010). Phosphorylation at Thr 253 does not alter CaMKII activity but rather alters its interaction with binding protein partners (Skelding et al., 2010). CaMKII α binding profiles, examined in neuronal tissue and cell extracts, varied with cell type and differed according to phosphorylation status of the protein at Thr 253 (Skelding et al., 2010). This highlights the idea that the intracellular microenvironment in which CaMKII is found in any particular cell type and physiological situation can influence kinase function (Skelding and Rostas, 2009). This study suggested that different 'pools' of CaMKII may be selectively phosphorylated at either one or both Thr 286 and Thr 253 sites depending on the local environment in which the enzyme resides (Skelding et al., 2010). Although this still needs to be demonstrated for the cardiac δ isoform, it may explain how CaMKII can be selectively targeted to particular substrates within the cell (Currie et al., 2011).

Interaction of CaMKII with a variety of neuronal and cardiac (see below) proteins has been demonstrated, with evidence that CaMKII can bind directly to proteins at sequences that are identical to the autoinhibitory domain of CaMKII (Skelding and Rostas, 2009). Indirect interactions with substrates has also been proposed via interaction with an anchoring protein termed α -KAP (Currie et al., 2011). α -KAP has been shown to form heteromultimers with CaMKII and targets it to the SR membrane in rat skeletal muscle (Bayer et al., 1998). The expression of α -KAP in the heart has recently been demonstrated. Specifically, α -KAP binds to SERC2a to recruit CaMKII δ_C to enable the enzyme to phosphorylate both SERC2a and PLB (Singh et al., 2009b). Importantly this study highlights that CaMKII does not interact directly with SERCA2a and indicates that α -KAP is a key regulatory protein of CaMKII function. It is intriguing to speculate that α -KAP may complex with other CaMKII targets in the heart, though this has yet to be demonstrated.

Other non-canonical pathways of CaMKII activation have been identified. A recent study has shown that β -arrestin scaffolds CaMKII and exchange protein directly activated by cAMP (EPAC) and triggers translocation of this multimeric complex to agonist stimulated β -adrenergic receptors (β -AR) i.e. β -AR are capable of activating CaMKII independent of cAMP-dependent protein kinase or elevated $[Ca^{2+}]$ (Mangmool et al., 2010). Collectively these findings add new complexity to CaMKII regulation and signalling.

1.6.3 CaMKII substrate targets in the heart

The number of CaMKII substrate targets in the heart is continually growing with wide diversity, thus emphasising the capacity of this enzyme to modulate physiological and pathological cardiac function. The major ‘groups’ of CaMKII targets are discussed below.

1.6.3.1 EC-coupling proteins and ion channels

It is well recognised that CaMKII, in particular the δ_C isoform, is involved in maintaining Ca^{2+} homeostasis by phosphorylating many Ca^{2+} -handling proteins, such as RyR₂, PLB, and LTCCs (Maier and Bers, 2007, Anderson et al., 2011). In general,

CaMKII tends to increase inward Ca^{2+} current that acts to prolong the cardiac AP duration. CaMKII is also a mediator of Ca^{2+} -dependent I_{Ca} facilitation by interacting directly with LTCCs (Grueter et al., 2006), phosphorylating the carboxyl terminal of the α -subunit and Thr 498 in β subunit (Maier and Bers, 2007). I_{Ca} facilitation occurs when the amplitude increases and inactivation slows over a series of several APs. Thus, CaMKII modulation of I_{Ca} may contribute to arrhythmias, brought about by inappropriate reactivation of I_{Ca} during long APs (Anderson et al., 2011).

CaMKII has also been shown to phosphorylate PLB at Thr 17 with a resultant increase in SERCA2a activity. This leads to increased Ca^{2+} uptake, increased speed of relaxation, increased SR Ca^{2+} content and hence increased myocardial contractility (Mattiuzzi et al., 2005). Although some studies have shown that CaMKII can directly phosphorylate SERCA2a on Ser 38 (Xu et al., 1993, Toyofuku et al., 1994), the majority of studies suggest that CaMKII does not directly phosphorylate SERCA2a (Reddy et al., 1996, Singh et al., 2009b, Maier and Bers, 2007).

CaMKII can also enhance Ca^{2+} release from the SR by directly associating with RyR_2 (Currie et al., 2004). CaMKII phosphorylates RyR_2 at Ser 2815 and although there is some discrepancy (Lokuta et al., 1995, Maier and Bers, 2007) in the literature, the vast majority of studies suggest that this interaction increases the open probability of the channel, increasing fractional SR Ca^{2+} release during EC-coupling as well as increasing the susceptibility to Ca^{2+} spark activity (Wehrens et al., 2004, Ai et al., 2005, Maier and Bers, 2007). CaMKII δ phosphorylation of RyR_2 has been shown to play an important role in mediating positive force frequency relationship in the normal mouse heart (Kushnir et al., 2010). Other studies have reported that RyR_2 can be hyperphosphorylated by CaMKII, a process which promotes increased diastolic SR Ca^{2+} leak and plays a key role in arrhythmogenesis and the development of HF (Bers, 2006a). It follows that in HF, there is an increase in CaMKII expression with more of this CaMKII associated with the RyR_2 as well as increased phosphorylation of the RyR_2 (Ai et al., 2005). Thus, CaMKII plays a key role in HF via enhancing SR Ca^{2+} leak and diminishing SR Ca^{2+} content characteristic of the disease (Maier and Bers, 2007). CaMKII may also affect membrane excitability via effect on Na^+ current and the NCX (Maier, 2011).

In addition to Ca^{2+} -handling proteins, CaMKII can modulate a variety of other ion channels namely voltage gated Na^+ and K^+ channels. CaMKII can modulate the cardiac Na^+ current (I_{Na}) and has been shown to co-immunoprecipitate with Nav1.5

channels (Wagner et al., 2006)). This alters I_{Na} gating to enhance accumulation of Na^+ channels in the inactivated state at high heart rates while enhancing late I_{Na} which could prolong AP duration and increase the chance of arrhythmia (Wagner et al., 2006). This occurs on both normal and failing myocytes (Maltsev et al., 2008). CaMKII also modulates the transient outward K^+ current (I_{to}) that is responsible for early cardiac AP repolarisation. A recent study demonstrated that acute and chronic over-expression of CaMKII δ_C increases $I_{to,slow}$ amplitude as well as the expression of the channel protein Kv1.4, whereas chronic over-expression downregulates $I_{to,fast}$ and Kv4.3 protein (Wagner et al., 2009), as seen in HF. These effects would shorten the AP duration and narrow the membrane potential window for I_{Ca} , potentially leading to arrhythmogenesis. CaMKII has also been shown to bind to Kv4.3 channels in myocytes (El-Haou et al., 2009). Over-expression of CaMKII δ_C decreased the inward rectifying K^+ current (I_{K1}) and channel protein, Kir2.1 (Wagner et al., 2009). I_{K1} is responsible for stabilising the resting membrane potential and is decreased in HF, leading to prolonged AP duration and hence susceptibility to ventricular arrhythmias. Overall, many Ca^{2+} -handling proteins and ion channels are subject to modulation by CaMKII, which may affect depolarisation, membrane excitability and repolarisation of myocytes.

1.6.3.2 Gene transcription

In addition to the vast array of cytosolic targets, CaMKII can also regulate various nuclear substrates to modulate gene transcription; a process referred to as excitation-transcription (ET) coupling. One key Ca^{2+} -dependent ET-coupling pathway that involves CaMKII phosphorylation is that of class II Histone Deacetylases (HDACs).

In myocytes, CaMKII δ_C and δ_B isoforms signal specifically to HDAC4 by binding to and phosphorylating a unique kinase-docking site that is absent in other class IIa HDAC. This promotes nuclear export of HDAC4 and de-repression of HDAC target genes (for example myocyte enhancer factor 2), ultimately resulting in hypertrophic growth (Backs et al., 2006, Little et al., 2007, Zhang et al., 2007). A recent study demonstrated that nifedipine (an LTCC blocker) was able to inhibit pathological hypertrophy induced by pressure overload by suppressing

phosphorylation of CaMKII and nuclear export of HDAC4 (Ago et al., 2010). Other research has shown that HDAC5 can become responsive to phosphorylation by CaMKII through direct phosphorylation and association with HDAC4 (Backs et al., 2008). Correspondingly, inhibition of CaMKII δ_B activity by AIP targeted specifically to the nucleus decreased HDAC5 translocation from the nucleus to the cytoplasm (Li et al., 2006) and CaMKII $\delta^{-/-}$ mice did not undergo myocardial remodelling due to diminished kinase activity against HDAC4 but not HDAC5 (Backs et al., 2009). A more recent study has also suggested a role for HDAC6 (a member of the class IIb HDAC) in cardiac disease whereby HDAC6 catalytic activity was increased in pathological, but not in physiological, hypertrophy (Lemon et al., 2011). Whether this involves CaMKII still needs to be determined.

CaMKII phosphorylation of HDAC may be modulated via inositol 1,4,5-trisphosphate (IP₃)-mediated Ca²⁺ release as research has demonstrated that CaMKII, specifically the δ_B isoform, associates with and phosphorylates the type 2 IP₃ receptor (InP₃R₂) located at the nuclear envelope (Bare et al., 2005). Evidence for InP₃R₂-CaMKII modulation of HDAC export has been shown whereby ET-1 stimulation or surgically induced HF promoted IP₃ production and elicited local nuclear Ca²⁺ release which activated CaMKII δ_B , triggering HDAC5 phosphorylation and nuclear export (Wu et al., 2006, Bossuyt et al., 2008). Interestingly, global Ca²⁺ transients throughout the cell did not induce HDAC5 export, thus highlighting how the myocyte can utilise different local Ca²⁺ signalling for EC-coupling and ET-coupling.

CaMKII may also function as an anti-hypertrophic signal by inhibiting gene transcription via phosphorylation of the transcription factor cAMP response element binding protein (CREB) at Ser 142, thus preventing CREB dimerisation and recruitment of CREB-binding protein (Anderson, 2007). Another transcription factor regulated by CaMKII is activating transcription factor-1 (ATF-1) (Maier and Bers, 2002).

1.6.3.3 Cardiac fibroblast activation

As mentioned in Section 1.4.2.1, CFs play an important role in cardiac development, structure and electro-mechanical function. However, very little is known of the functional role CaMKII may play in these cells. Recent work has

suggested that CaMKII may be involved in the proliferative response in neonatal rat CFs, as well as ECM secretion (Zhang et al., 2010c). Other work has suggested that CaMKII can phosphorylate, and thus modulate the activity of, the connexin gap junction Cx43 (Huang et al., 2010b) which is important for CF-myocyte electrical communication. Importantly these studies highlight the possibility that CaMKII may be involved in modulating adult CF function however this still needs to be confirmed. Given the vast amount of research suggesting that CFs can alter myocyte function under physiological and pathological conditions (see Sections 1.4.2.1 and 1.4.3.2, respectively) it seems possible that CaMKII signalling in both cell types may be important in the development of cardiac disease, however this still remains to be determined.

1.6.3.4 Inflammatory signalling

There is growing evidence that CaMKII mediates pro-inflammatory signalling in the heart. One key mediator in the regulation of immediate early genes and genes involved in the inflammatory response is the transcription factor NF- κ B. There is evidence for increased NF- κ B signalling following injury to the myocardium, and that this is involved in the pathophysiology of ischemia pre-conditioning, dilated cardiomyopathy, and unstable angina (Purcell and Molkentin, 2003, Gupta and Sen, 2005). Studies suggest that the NF- κ B pathway is also involved in the development of cardiac hypertrophy (Purcell et al., 2001, Li et al., 2004, Gupta et al., 2005), as discussed in Section 1.9.4. Research has suggested that CaMKII can positively regulate the NF- κ B signalling pathway in neurons (Meffert et al., 2003). More importantly, CaMKII has been shown to activate NF- κ B signalling in neonatal rat myocytes over-expressing CaMKII δ_B with resultant myocyte hypertrophy (Kashiwase et al., 2005). More recent *in vivo* work using targeted myocyte CaMKII inhibition with an inhibitory peptide (AC3-I), demonstrated that following MI, a number of pro-inflammatory genes were upregulated and that this upregulation was abolished with CaMKII inhibition (Singh et al., 2009a). Crucially, CaMKII inhibition reduced NF- κ B signalling and complement factor B expression *in vitro* (in response to bacterial endotoxin, LPS) and *in vivo* (Singh et al., 2009a). This study highlights several important findings, namely (i) new targets for CaMKII in the heart, (ii) that myocytes

themselves express pro-inflammatory genes and, (iii) that CaMKII regulates Toll-like receptor-mediated NF- κ B signalling (Singh and Anderson, 2011). There is the possibility that CaMKII may interact directly with components of the NF- κ B pathway, although this needs to be examined. CaMKII involvement in inflammatory signalling via modulation of NF- κ B signalling will be discussed in Section 1.12.

1.7 Involvement of CaMKII in cardiac hypertrophy and heart failure

There is a strong link between disordered Ca²⁺ regulation and increased CaMKII (autonomous) activity and expression. These acute changes are initially beneficial for EC-coupling as they lead to increased myocardial contractility. Chronic up-regulation of CaMKII activity however correlates with myocyte hypertrophy and apoptosis, fibrosis and arrhythmias, that together can lead to insufficient myocardial contraction with progression to cardiac failure (Bers, 2006b).

1.7.1 Human studies

Due to ethical issues and difficulties in obtaining human tissue biopsies, most research into CaMKII's involvement in hypertrophy have focused on studies *in vitro* using isolated myocytes and studies *in vivo* using a selection of animal models of cardiac hypertrophy and HF, as discussed in Section 1.3. Some research however has demonstrated that CaMKII activity and expression are increased in cardiac tissue from failing human hearts compared to non-failing hearts, and the level of CaMKII activity was closely correlated with cardiac performance (Kirchhefer et al., 1999, Hoch et al., 1999). Specifically, transcript levels of CaMKII δ_B were increased, whilst other isoforms remained unchanged in patients with dilated cardiomyopathy (Kirchhefer et al., 1999). A more recent study demonstrated that both CaMKII δ_C and δ_B were significantly increased in ventricles from patients with dilated or ischaemic cardiomyopathy, with CaMKII inhibition (by KN-93 and AIP) improving contractility by increasing SR Ca²⁺ loading and reducing diastolic Ca²⁺ leak by reducing RyR₂ phosphorylation (Sossalla et al., 2010). These studies highlight the importance of

CaMKII signalling in human cardiac disease and the potential for CaMKII inhibition as a potential therapeutic strategy (discussed in section 1.8).

1.7.2 *In vitro* experiments

In vitro studies using pharmacological inhibitors have indicated a role for CaMKII in the development of hypertrophy induced by various agonists. The α_1 -adrenergic agonist, phenylephrine, stimulated the expression of embryonic atrial natriuretic factor (ANF) (a well documented hypertrophic marker) in neonatal rat ventricular myocytes, with a correlation between the expression of ANF and the activation of CaMKII δ_B but not δ_C , and this could be blocked by the CaMKII inhibitor KN-93 (Ramirez et al., 1997). Similarly in cultured neonatal rat ventricular myocytes the vasoconstrictor peptide, ET-1, increased the activity of CaMKII, which could be suppressed by pre-treatment with the CaMK inhibitor, KN-62 (Zhu et al., 2007). Cultured rat myocytes with hypertrophy induced by phenylephrine, Ang-II and ET-1 displayed elevated CaMKII activity and increased phosphorylation of PLB (Lu et al., 2007). Collectively these studies imply that CaMKII is involved in the development of cardiac hypertrophy *in vitro*.

1.7.3 *Animal models*

Increased CaMKII expression and activity have been reported in genetic and surgical animal models of cardiac hypertrophy and HF. For example, studies using SHR revealed increased CaMKII expression and activity in the hypertrophied myocardium (Boknik et al., 2001, Hagemann et al., 2001). Increased CaMKII activity as well as increased protein expression of the CaMKII δ isoform was reported in isolated SR preparations from rabbit myocardium in which pressure-overload hypertrophy was induced by coronary artery ligation (Currie and Smith, 1999a). Similarly, CaMKII expression and activity was found to be upregulated in isolated myocytes from TAC-induced HF rabbits (Ai et al., 2005). TAC induced pressure overload in mice up-regulated CaMKII activity (Zhang et al., 2003b, Colomer et al., 2003, Saito et al., 2003), with increased expression of γ and δ genes (Colomer et al., 2003). In fact both δ_C and δ_B isoforms were up-regulated resulting in constitutive

Ca²⁺/CaM-independent activity of CaMKII in the myocardium (Colomer et al., 2003). Likewise, cats with TAC-induced hypertrophy displayed reduced myocardial contractility to isoprenaline with increased PLB phosphorylation at the CaMKII-specific site (Thr 17) but not at the PKA-specific site (Ser 16), thus indicating increased CaMKII activity (Mills et al., 2006). Other studies have demonstrated that mice with TAC mediated hypertrophy demonstrated increased I_{Ca} and slowed I_{Ca} inactivation with 2-3 fold increased CaMKII activity. Inhibition of CaMKII with AIP reduced I_{Ca} and inactivation time course, thus demonstrating that activation of CaMKII contributes to I_{Ca} remodelling in pressure overload-mediated hypertrophy (Wang et al., 2008). In addition, pressure overload induced by increased rate of perfusion in Langendorff-perfused rat hearts also increased CaMKII activity and protein expression; an increase in protein synthesis that could be prevented by KN-62 (Saito et al., 2003). A more recent study demonstrated that nifedipine attenuated TAC induced hypertrophy in mice, partially attributed to decreased autonomous CaMKII activity (measured by Thr 286 phosphorylation) (Ago et al., 2010).

1.7.3.1 Transgenic/over-expression and knock-out studies

Genetically altered animals have further confirmed a role for CaMKII in the development of cardiac hypertrophy, as illustrated in Table 1.1. Recently two groups reported the development of cardiac-restricted CaMKII δ knockout (CaMKII δ ^{-/-}) mice that ameliorated hypertrophy in response to TAC, however there were some differences between their results (Backs et al., 2009, Ling et al., 2009). Both groups showed that CaMKII δ expression was effectively abolished and that under normal physiological conditions, CaMKII δ ^{-/-} mice displayed no gross baseline changes in ventricular structure or function. One group found that wild-type (WT) and CaMKII δ ^{-/-} mice displayed similar myocardial hypertrophy responses after 2 weeks TAC, but only WT mice developed LV dilatation and HF after prolonged TAC (6 weeks), suggesting that CaMKII δ is not involved in early/adaptive hypertrophy but is involved in the progression to HF (Ling et al., 2009). In contrast, the other group suggest that CaMKII δ is involved in the early stages of hypertrophy as CaMKII δ ^{-/-} mice were resistant to myocardial remodelling after 3 weeks TAC compared to WT animals (Backs et al., 2009).

Transgene	Species	Preparation	Effect	Reference
Over-expression of Calmodulin	Mouse	Ventricular myocytes	Increased autonomous CaMKII activity and expression of ANF.	(Colomer and Means, 2000)
Over-expression of CaMKIV	Mouse	Whole animal and myocytes	Increased CaMKII activity, resulting in increased arrhythmias at baseline and in response to isoproterenol. Inhibition of CaMKII by AC3-I in myocytes reduced the frequency of arrhythmia.	(Wu et al., 2002)
Over-expression of AC3-I	Mouse	Whole animal and myocytes	CaMKII inhibition maintained ventricular contractility and prevented maladaptive remodeling in response to excessive β -AR stimulation.	(Zhang et al., 2005)
Over-expression of CaMKII δ_B	Mouse	Whole animal and myocytes	Cardiac hypertrophy with upregulation of embryonic and contractile protein genes, and decreased cardiac function with ventricular dilation.	(Zhang et al., 2002b)
Over-expression of renin and angiotensinogen genes and SHR	Rat	Whole animal and myocytes	Animals developed cardiac hypertrophy and exhibited increased CaMKII activity and CaMKII δ expression. The ACE inhibitor, cilazapril, completely regressed myocardial hypertrophy in SHR rats with a parallel decrease in CaMKII δ protein.	(Hempel et al., 2002, Hagemann et al., 2001)
Over-expression of CaMKII δ_C	Mouse	Whole animal and myocytes	Animals displayed reduced cardiac contractility, arrhythmias, dilated cardiomyopathy and HF. Inhibition of CaMKII by AIP both <i>in vitro</i> and <i>in vivo</i> reduced afterdepolarisations and spontaneous AP.	(Maier et al., 2003, Zhang et al., 2003b, Sag et al., 2009)
Over-expression of CaMKII δ_C	Mouse	Whole animal and myocytes	Animals exhibited proteome changes similar to that observed in failing myocytes, such as alterations in metabolic proteins, cell-protecting proteins including antioxidants, and proteins involved in protein synthesis.	(Schott et al., 2011)
Over-expression of CaMKII δ_C and CaMKII δ_B	Mouse	Whole animal and myocytes	CaMKII δ_C and CaMKII δ_B have disparate effects on Ca^{2+} handling but similar effects on gene expression as δ_C but not δ_B mice increase both RyR ₂ and PLB phosphorylation leading to increased SR Ca^{2+} spark activity and decreased SR Ca^{2+} content, whereas both isoforms induce transactivation of MEF2 and up-regulate a variety of hypertrophic genes including ANF	(Zhang et al., 2007)

Table 1.1 Transgenic/over-expression studies implicating a role for CaMKII in cardiac hypertrophy and heart failure.

Although it is not clear why different results are reported for CaMKII $\delta^{-/-}$ studies, one hypothesis may be that other CaMKII isoforms (γ and β) are upregulated to compensate for the loss of the δ isoform. Supporting this theory, one study did report that CaMKII γ was upregulated and therefore in the shorter term may maintain hypertrophic responses in CaMKII $\delta^{-/-}$ animals. In addition, after 2 weeks TAC, protein kinase D (PKD) expression and activity was increased in both WT and CaMKII $\delta^{-/-}$ mice (Ling et al., 2009). PKD shares phosphorylation consensus sites with CaMKII and can induce hypertrophic signalling via HDAC phosphorylation and MEF2-mediated gene transcription (Fielitz et al., 2008), therefore it is feasible that PKD acts to compensate for the loss of CaMKII, although this needs to be examined. A separate study using isolated ventricular myocytes from CaMKII $\delta^{-/-}$ mice demonstrated increased basal cardiac contractility, but a decrease in heart rate following increased β -AR stimulation. At the cellular level there was an increase in LTCC channel expression and a decrease in β -AR expression, which the authors suggest is a compensatory mechanism to chronic CaMKII inhibition (Xu et al., 2010).

1.8 CaMKII inhibition as a therapeutic target

From the evidence presented above, it is clear that CaMKII plays an important role in the development of cardiac hypertrophy, thus pharmacological modulation of CaMKII activity seems like a valid therapeutic strategy for the treatment of structural heart disease. Studies in transgenic mouse myocytes with chronic CaMKII inhibition however have shown that myocardial contractility is compromised (Grimm et al., 2007), thus the level of CaMKII inhibition is crucial. An important consideration when targeting CaMKII is that the δ isoform exists as two splice variants and these may have differing effects on pathological remodelling. Although initial studies suggested that both δ_C and δ_B are up-regulated in cardiac hypertrophy (Zhang et al., 2002b, Maier et al., 2003), more recent work *in vivo* has suggested that δ_B is down-regulated in a rat model of ischemia/reperfusion (I/R). Over-expression of δ_B but not δ_C protected against apoptosis in cultured cardiac myocytes, possibly via phosphorylation of heat shock factor 1 (Peng et al., 2010). Other research has demonstrated similar findings, whereby a persistent level of CaMKII δ_B is required for myocyte integrity and survival, as siRNA mediated depletion of CaMKII δ_B in primary

neonatal rat myocytes resulted in abnormal sarcomere organisation and severe loss of the anti-apoptotic protein Bcl-2 (Little et al., 2009).

Targeting downstream substrates involved in the development of the hypertrophic response may prove to be more beneficial. For example, targeted inhibition of the transcription factors and signalling cascades that are substrates of CaMKII may help to control alterations in new gene expression, fibrosis and myocyte apoptosis. CaMKII regulation of cytosolic Ca²⁺-handling is fairly well understood and although SR-targeted CaMKII inhibition in mice over-expressing CaMKII δ_C lead to reduced diastolic Ca²⁺ leak and overall better myocyte Ca²⁺-handling, cardiac remodelling was exacerbated and animals displayed depressed cardiac function (Huke et al., 2010). A similar study with PLB ablation in CaMKII δ_C over-expressing mice demonstrated that SR Ca²⁺ content was restored with PLB ablation and contractile function was improved in isolated myocytes, however *in vivo* HF was exacerbated with a concomitant decrease in contractile function (Zhang et al., 2010b). The authors proposed that interventions that increased SR Ca²⁺ content when there is enhanced diastolic leak (due to CaMKII phosphorylation of RyR₂) predisposes myocytes to apoptosis, possibly due to mitochondrial Ca²⁺ loading (Zhang et al., 2010b). These findings demonstrate that CaMKII signalling to non-SR CaMKII targets contributes to hypertrophic dysfunction and increased global Ca²⁺ transients may enhance this CaMKII signalling. Potential new substrate targets of CaMKII involved in other areas of cellular function during hypertrophic growth have yet to be identified. As mentioned previously, inflammation plays a key role in structural remodelling of the heart and a role for CaMKII in cardiac inflammation has been suggested. Some studies have shown a possible link between elevated CaMKII activity and NF- κ B activation (Meffert et al., 2003, Singh et al., 2009a, Singh and Anderson, 2011). Involvement of the NF- κ B pathway in myocyte hypertrophy is a novel and interesting topic of research given the fact that inflammatory cytokines (such as TNF- α and IL-1 β) are mediators of CVD (Purcell and Molkenin, 2003).

1.9 Introduction to the nuclear factor kappa B pathway

NF- κ B was identified in B lymphocytes as a nuclear factor that regulates Immunoglobulin G (IgG) gene expression by binding to the κ light chain enhancer

DNA sequence. Thought to be B cell specific, it was called Nuclear Factor bound to the kappa site of B cells (Sen and Baltimore, 1986). Since these early observations and the subsequent realisation of the ubiquitous nature of this transcription factor, NF- κ B has become one of the most intensively studied signalling pathways (Gamble et al., 2011). The NF- κ B signalling pathway is activated by numerous stimuli, such as a variety of pro-inflammatory cytokines, growth factors, ROS and viral proteins (Chen and Grenne, 2004). NF- κ B regulates various inflammatory genes involved in the innate and adaptive immune response (Valen et al., 2001a) as well as genes involved in cell survival and apoptosis (Li et al., 2004). Recent research has suggested that NF- κ B is also involved in the development of cardiac hypertrophy (Gupta et al., 2005), which may have an inflammatory basis.

1.9.1 The NF- κ B family

The NF- κ B family consists of five Rel protein members; p65 (RelA), RelB, c-Rel, p105/p50 (NF κ B1) and p100/p52 (NF κ B2). These proteins form homo- or heterodimers, with the prototypical NF- κ B complex consisting of a heterodimer of p50 and p65 (Chen and Grenne, 2004). NF- κ B dimers bind to κ B sites with the promoters of a variety of genes that contain the consensus motif 5'-GGRNN(WYYCC)-3' (where R is any purine, N is any nucleotide, W is adenine or thymidine and Y is any pyrimidine) and regulate transcription through the recruitment of co-activators and co-repressors (Basak and Hoffmann, 2008). Each NF- κ B protein contains a highly conserved N-terminal Rel-homology domain (RHD), responsible for nuclear localisation, DNA binding, subunit dimerisation and association with the inhibitory kappa B (I κ B) family of cytoplasmic inhibitory proteins (Ghosh and Karin, 2002). The p65, RelB and c-Rel subunits also contain C-terminal transcription activation domains (TAD1 and TAD2), which are necessary for transcriptional activation of target genes (Van der Heiden et al., 2010). As p50 and p52 lack TADs, they may repress transcription unless associated with an NF- κ B family member that contains a TAD or associated with other proteins capable of recruiting co-activators (Hayden and Ghosh, 2008).

1.9.2 *NF-κB pathway activation*

Under basal conditions, the NF-κB dimers are predominantly sequestered to the cytosol by masking of their nuclear localisation signal (NLS). Eight proteins have been identified that can inhibit NF-κB activity. These include five IκBs (IκBα, β, γ, ε, ζ), Bcl-3 and two NF-κB precursor proteins (p100 and p105) (Basak and Hoffmann, 2008, Hayden and Ghosh, 2008). All of these inhibitory proteins contain an ankyrin repeat domain (ARD), which masks NF-κB DNA binding and NLS (Van der Heiden et al., 2010). NF-κB is activated by stimulus-induced proteolysis of the inhibitors via two major signalling pathways; the classical or canonical pathway and the non-canonical or alternative pathway (Figure 1.6).

The canonical pathway utilises an inhibitory-κB kinase (IKK) complex comprising two catalytic subunits, IKKα and IKKβ, in complex with two essential regulatory subunits termed NF-κB essential modulator (NEMO) or IKKγ (Poyet et al., 2000, Solt et al., 2009). The canonical pathway is activated by pro-inflammatory stimuli such as TNF-α, IL-1, and lipopolysaccharide (LPS), as well as ROS, hypoxia and mechanical stress (Van der Heiden et al., 2010). Following stimulation, various adaptor molecules are recruited, including TNF-receptor-associated factors (TRAFs) (Gamble et al., 2011). This facilitates the recruitment of key enzymes such as TGF-β-activated kinase (TAK1) and ERK kinase kinase 3 (MEKK3), which phosphorylate and activate inhibitory-κB kinase (IKK) β at Ser 177 and Ser 181 (Schmidt et al., 2003). Activated IKKβ phosphorylates IκBα at Ser 32 and Ser 36 (or Ser 19 and Ser 23 of IκBβ) targeting it for polyubiquitination and subsequent proteolytic degradation by the proteasome (Hayden and Ghosh, 2008). IκBα may also be subject to phosphorylation at tyrosine (Tyr) 42 in response to certain stimuli, such as TNF-α (Bui et al., 2001). The now activated NF-κB complex translocates to the nucleus where it binds specific NF-κB-response sequences, promoting the transcription and translation of a large and diverse array of target genes that modulate various physiological and pathological processes (Hall et al., 2006). It is important to note that there is some evidence for NF-κB:IκBα shuttling as IκBα only masks the NLS of p65 and not p50, thus the exposed NLS of p50 coupled with the nuclear export sequence in IκBα and p65 leads to constant shuttling between the nucleus and the cytosol (Bergqvist et al., 2006, Bergqvist et al., 2008).

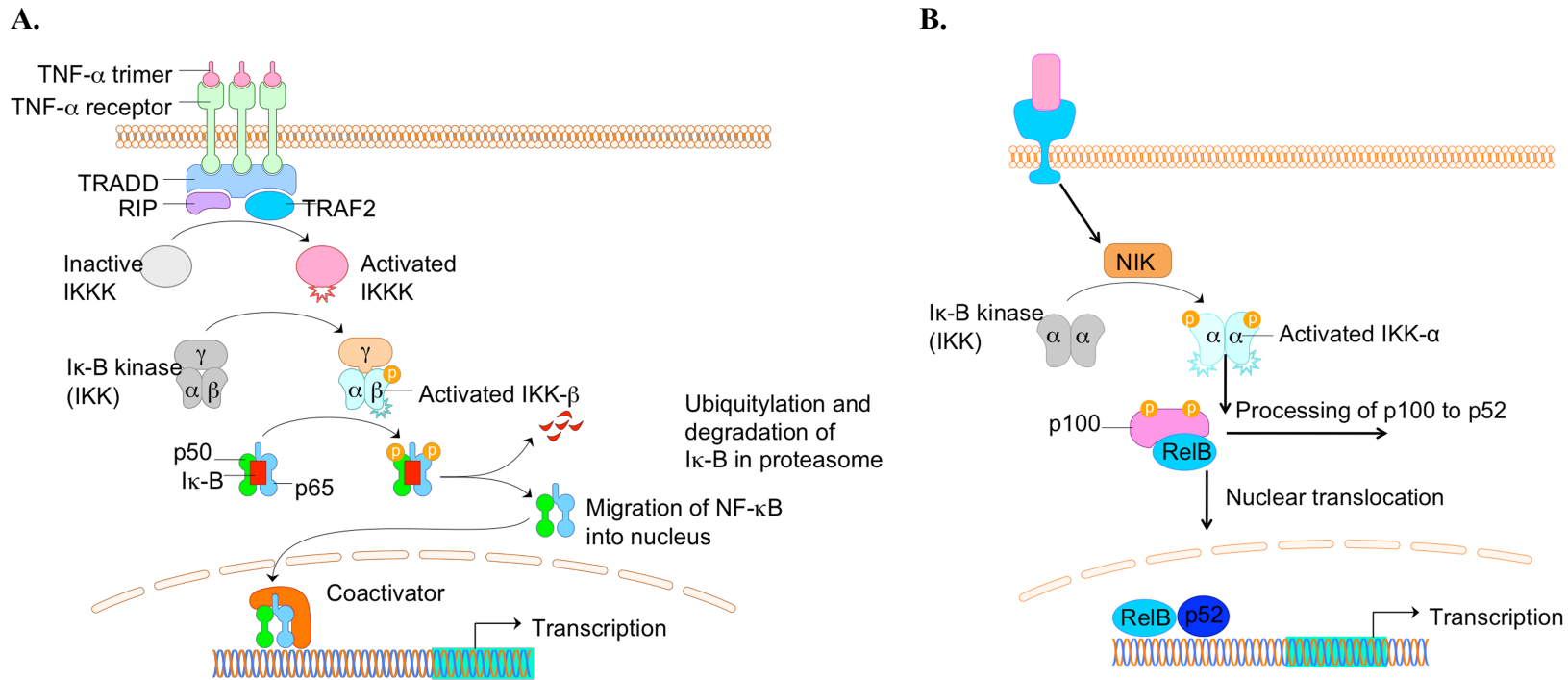


Figure 1.6 The NF- κ B signalling pathway.

Canonical NF- κ B signalling (A) utilises the I κ B kinase (IKK) complex comprised typically of IKK α , IKK β and IKK γ subunits. Activation of the IKK complex leads to phosphorylation and degradation of the I κ B inhibitor and subsequent NF- κ B activation. The non-canonical pathway (B) utilizes an IKK complex comprised of two IKK α subunits, but not IKK γ . Activation of NF- κ B-inducing kinase (NIK) phosphorylates and activates the IKK complex, which in turn phosphorylates p100 leading to the processing and liberation of the p52/RelB active heterodimer.

Research has demonstrated that IKK β can directly phosphorylate p65 at Ser 536, leading to nuclear localisation and transcriptional activation (Sakurai et al., 1999). Studies using IKK $\beta^{-/-}$ mice and dominant-negative mutants of IKK β have demonstrated that IKK β is both necessary and sufficient for canonical pathway activation (Tanaka et al., 1999, Li et al., 1999b). Subsequent research has identified IKK β as key regulator of cell survival and protecting against apoptosis (Mustapha et al., 2000), with IKK $\beta^{-/-}$ mice dying at embryonic day ~14.5 due to apoptotic liver degeneration (Li et al., 1999a). IKK $\alpha^{-/-}$ studies have demonstrated that there is no positive regulatory role in I κ B α phosphorylation/degradation after TNF- α stimulation, suggesting that IKK α is not necessary for canonical NF- κ B activation (Takeda et al., 1999). Further investigations identified IKK α as a key component of the non-canonical pathway however IKK α may participate in the canonical pathway via a novel nuclear mechanism as discussed in Section 1.9.4.

In the non-canonical pathway, NF- κ B precursors of higher molecular weight (p100 or p105) are processed to generate other lower molecular isoforms (p52 and p50, respectively) which then translocate to the nucleus to regulate a specific subset of target genes (Figure 1.6) (Gamble et al., 2011). This pathway utilises an IKK complex comprising of two IKK α subunits (Van der Heiden et al., 2010). Ligand induced activation, by a variety of stimuli including lymphotoxin- β and B cell activating factor (BAFF), results in the activation of NF- κ B-inducing kinase (NIK), which in turn phosphorylates IKK α at Ser 176 and Ser 180 (Ling et al., 1998, Hayden and Ghosh, 2008). Activated IKK α in turn phosphorylates p100 at multiple sites (Ser 99, 108, 115, 123 and 872) (Xiao et al., 2004) leading to ubiquitination and proteolytical processing to p52. Nuclear translocation of the active p52/RelB heterodimer results in transcription of genes involved in B cell maturation and lymphoid organogenesis (Gamble et al., 2011). In contrast to p100, p105 undergoes constitutive cleavage to produce p50 (Hayden and Ghosh, 2004).

1.9.3 Regulation of NF- κ B activity

The activity of NF- κ B and the amount of new gene product is determined by the composition of the NF- κ B complex, its regulatory proteins and the nature of the stimulus (Valen et al., 2001b). Although most NF- κ B dimers promote transcription,

the p50/p50 and p52/p52 homodimers act to repress transcription (Ghosh and Karin, 2002). In addition, activated NF- κ B promotes the transcription of the I κ B α gene, thus replenishing the cytoplasmic stores that were proteolytically degraded in the activation of NF- κ B. This newly synthesised I κ B α can bind to and export the NF- κ B complex associated with DNA, allowing the NF- κ B complex to facilitate its own inactivation (Hall et al., 2006). NF- κ B activity is also controlled by a signalling accessory protein, A20, which functions to suppress NF- κ B by interfering with the upstream signalling events that normally promote its activation (Wertz et al., 2004). The NF- κ B complex actually regulates the expression of A20 and so in this way facilitates its own inactivation (Purcell and Molkentin, 2003). Similarly ABIN-2, an A20-binding inhibitor of NF- κ B, plays a critical role in terminating NF- κ B responses. ABIN-2 interferes with NF- κ B activation upstream of the IKK complex as it inhibits TNF- α induced NF- κ B activation but does not inhibit NF- κ B activation due to over-expression of IKK β (Van Huffel et al., 2001). In the nucleus, gene expression is negatively regulated via interaction of p65 with HDAC1 and HDAC2 (Ghosh and Karin, 2002). Another protein involved in regulating NF- κ B activity is NIBP, a NIK and IKK β binding protein. NIBP potentiates TNF- α induced NF- κ B activation through increased phosphorylation of the IKK complex and subsequent I κ B α and p65 phosphorylation (Hu et al., 2005).

1.9.4 Regulation of transcription by NF- κ B

The primary level of regulation of NF- κ B activity starts in the cytoplasm with its liberation, however to allow maximal NF- κ B transcriptional activity, the transcription factor and surrounding chromatin structure must undergo post-translational modifications, such as phosphorylation and acetylation (Vermeulen et al., 2002). The p65 subunit is the principal target for phosphorylation in response to a variety of pro-inflammatory factors as it contains a C-terminal TAD with many phosphorylation sites that can be modified in a cell-type and stimulus-specific manner (Hall et al., 2005, Hall et al., 2006). Phosphorylation has been found in both the TAD and in the RHD domains of p65, thus enhancing the trans-activation potential of the NF- κ B complex (Vermeulen et al., 2002). Transcriptional activity of NF- κ B is also

greatly increased when it becomes phosphorylated as it can more effectively remove transcriptionally repressive HDAC complexes (Chen and Grenne, 2004).

Phosphorylation of p65 can occur via the action of various kinases, such as PKA and mitogen/stress-activated kinase 1 and 2 (MSK1 and MSK2) at Ser 276, 311, 468, 529, 535 and 536; a modification that results in the binding of histone acetylases (Chen and Grenne, 2004, Hall et al., 2006, Dhingra et al., 2010). Research suggests that IKK β but not IKK α regulates LPS-induced TNF- α production through modulation of p65 subunit phosphorylation at Ser 536 in TAD1 (Sakurai et al., 1999). Other research has demonstrated that IKK β but not IKK α can also phosphorylate p65 at Ser 468 in TAD2 whilst in complex with I κ B α (Schwabe and Sakurai, 2005). Additionally CaMKIV is able to directly associate with and phosphorylate p65 at Ser 535 of TAD1 both *in vitro* and *in vivo* (Jang et al., 2001, Hall et al., 2006). It remains to be elucidated whether other CaMK isoforms can interact with and modify the NF- κ B signalling pathway. Phosphorylated p65 recruits the transcriptional co-activator CREB-binding protein (CBP) with concomitant release of co-repressors, thus enhancing the trans-activation potential of the NF- κ B complex (Jang et al., 2001). Other kinases reported to phosphorylate p65 include protein kinase C (PKC ζ) at Ser 311, glycogen-synthase kinase-3 β (GSK3 β) at Ser 468, and casein kinase at Ser 529 (Schwabe and Sakurai, 2005). Other kinases involved in controlling the activity of NF- κ B include AKT/phosphatidylinositol 3-kinase (PI3K) and NF- κ B-activating kinase (NAK) (Chen and Grenne, 2004).

Acetylation is another post-translational modification that is important for NF- κ B signalling as it regulates subunit subcellular localisation, assembly with DNA, interaction with co-factors and trans-activation potential (Chen and Grenne, 2004). Three NF- κ B subunits are targets of histone acetylation; p65, p50, and p52 (Hall et al., 2006). The p65 subunit has been best characterised with acetylation sites at lysines (Lys) 218, 221 and 310, leading to enhanced DNA binding and decreased affinity for I κ B α , thus increasing NF- κ B transcriptional activity (Chen and Grenne, 2004). IKK α may also promote Lys 310 acetylation by translocating to the nucleus and phosphorylating and de-repressing silencing mediator for retinoic acid and thyroid hormone receptor (SMRT) (Hoberg et al., 2004). IKK α can also regulate NF- κ B gene expression via phosphorylation of Histone H3 (Anest et al., 2003, Yamamoto et al., 2003), regulating cell-cycle progression through phosphorylation of Aurora A (Prajapati et al., 2006) as well as being involved in the modulation of angiogenesis

(Agarwal et al., 2005). Interestingly, research has demonstrated that the catalytic activity of both IKK α and IKK β is not always essential for NF- κ B gene expression (Massa et al., 2005). For example, IKK β ^{-/-} endothelial cells displayed increased permeability and decreased migration, which could be reversed equally well by wild-type IKK β or kinase-inactive IKK β (Ashida et al., 2011). Similarly, IKK γ is required for canonical signalling despite a lack of catalytic activity (Hayden and Ghosh, 2008).

1.10 Involvement of NF- κ B in cardiac hypertrophy and heart failure

Various genes of cardiovascular relevance are regulated by NF- κ B including those that function in nitric oxide production, Ca²⁺ handling, myocyte function, cell death and/or survival, cell adhesion, stress responses, growth factors and natriuretic factors (Brown et al., 2005a). Stimuli such as ROS, TNF- α , as well as β AR stimulation have been shown to activate NF- κ B in the heart (Dhingra et al., 2010). Furthermore, NF- κ B signalling has been linked to several cardiac pathologies including atherosclerosis, MI and reperfusion injury, ischaemic preconditioning, as well as hypertrophy and HF, as discussed below. Although NF- κ B proteins are ubiquitously expressed, only p65, p50, p52 and RelB have been identified in cardiac myocytes (Hall et al., 2006) and only recently has NF- κ B signalling been identified in adult CF (Sangeetha et al., 2011).

1.10.1 Human studies

Several studies have shown that increased NF- κ B activity correlates with the development of heart disease. Patients with suspected myocarditis exhibited increased activation of NF- κ B, with increased levels correlating with decreased LV function (Alter et al., 2006). Increased NF- κ B activity, IKK β activity and I κ B α phosphorylation were observed in human failing hearts compared to non-failing hearts (Gupta and Sen, 2005). Likewise, increased expression of NF- κ B was observed in myocardial tissue samples from patients with end-stage HF compared to tissue samples from healthy hearts (Wong et al., 1998, Frantz et al., 2003). Correspondingly, LV assist device support in patients with end-stage HF decreased the extent of NF- κ B activation, as evidenced by a decrease in the number of NF- κ B

positive myocytes, decreased myocyte hypertrophy and decreased NF- κ B DNA-binding activity (Grabellus et al., 2002). Recently, a polymorphism in the promoter of the NF κ B1 gene was identified as a risk factor for dilated cardiomyopathy (Zhou et al., 2009).

1.10.2 In vitro studies

In vitro studies using pharmacological inhibitors have indicated a role for NF- κ B in the development of hypertrophy induced by various agonists. Studies using isolated neonatal rat ventricular myocytes illustrated that a variety of hypertrophic agonists (phenylephrine, ET-1, Ang-II and TNF- α) could stimulate NF- κ B translocation and transcriptional activity (Hirotani et al., 2002), as well as stimulating expression of ANF (Purcell et al., 2001). Both NF- κ B activity and ANF expression could be inhibited by expression of a ‘super-suppressor’ I κ B α mutant that is resistant to degradation (due to Ser 32/36 to alanine mutations), and by a dominant-negative IKK β mutant that can no longer be activated (due to Ser 177/181 to alanine mutations) (Purcell et al., 2001, Higuchi et al., 2002). Importantly, expression of the super-suppressor I κ B α mutant also inhibited all CaMKII δ_B -induced hypertrophic responses (Kashiwase et al., 2005). In addition hypertrophic agonists, for example ET-1 and Ang-II, activated a protein kinase upstream of the IKK complex known as apoptosis signal-regulating kinase 1 (ASK1), and over-expression of a constitutively active mutant of ASK1 led to NF- κ B activation (Hirotani et al., 2002, Kashiwase et al., 2005). Other studies have shown that liver X receptor expression is increased following TAC, with liver X signalling acting to reduce Ang II mediated hypertrophy in rat myocytes. Inhibition of hypertrophy by liver X signalling was via inhibition of NF- κ B and subsequent reduction of pro-inflammatory cytokine expression, including IL-6 and TNF- α (Wu et al., 2009).

1.10.3 Animal studies

Surgical and genetic animal models of cardiac hypertrophy have confirmed a role for NF- κ B in the development of the hypertrophic response. For example, NF- κ B activation was increased in rats with TAC induced cardiac hypertrophy, that could

be attenuated by transfection of an I κ B α dominant-negative mutant with concomitant regression of hypertrophy (Li et al., 2004). Similarly, the antioxidant pyrrolidine dithiocarbamate (PDTC) known to inhibit NF- κ B activity reduced heart weight/body weight ratio in both TAC mediated hypertrophic mice (Ha et al., 2005a) and SHR (Gupta et al., 2005). Another study demonstrated that only high dose Ang II infusion (2.5 mg/kg per min) for 6 days increased NF- κ B activity compared to low dose Ang II (0.5 mg/kg per min), with PDTC able to abolish Ang II-induced increases in LV/body weight ratio, LV wall thickness, myocyte hypertrophy and apoptosis, as well as fibrosis and collagen type 1 expression (Sármán et al., 2007). Inhibition of IKK β (with the drug IMD-0354) improved mortality in rats with CAL mediated HF by improving LV function and decreasing remodelling (Onai et al., 2007). IKK β inhibition also reduced the accumulation of inflammatory cells in the infarct area, suppressed the expression of pro-inflammatory cytokines and chemokines, and decreased MMP activity (Onai et al., 2007, Onai et al., 2004). Other studies have indirectly shown the involvement of NF- κ B in cardiac hypertrophy, for example, administration of the anti-malarial drug, Artemisinin, protected against pressure-overload hypertrophy (as assessed by LV function and ANF expression) in rats via inhibition of NF- κ B signalling (Xiong et al., 2010).

1.10.3.1 Transgenic/over-expression and knock-out studies

Transgenic animals have further confirmed a role for NF- κ B in the development of cardiac hypertrophy. For example, hypertrophy in response to chronic infusion of Ang-II was attenuated in NF- κ B p50^{-/-} mice, without causing a deterioration in cardiac function (Kawano et al., 2005). Other research has shown that targeted disruption of NF- κ B p50 reduced early mortality and ventricular dilatation following MI (Frantz et al., 2006). On the other hand, a recent study has suggested that deletion of NF- κ B p50 markedly enhances LV remodelling and functional deterioration following CAL (Timmers et al., 2009). These differences may be due to the time point chosen to observe remodelling after MI (8 weeks versus 28 days), or simply due to the method used to measure changes in LV function (echocardiography versus magnetic resonance imaging). Thus, more experiments are required to determine whether NF- κ B p50^{-/-} in the heart is beneficial or detrimental. Other studies have

shown that NF- κ B p65^{-/-} leads to embryonic lethality at 15-16 days gestation, due to hepatocyte apoptosis (Beg et al., 1995).

Transgenic over-expression of a myocyte-restricted I κ B α dominant-negative mutant improved survival, decreased ventricular remodelling, improved systolic function, decreased fibrosis and decreased apoptosis in response to CAL mediated HF (Hamid et al., 2010). In the control HF mice, p65 homodimers were identified as the major dimer responsible for NF- κ B activation, with negligible p50 activity (Hamid et al., 2010). Other studies using the hypertrophic agonists Ang-II and isoproterenol demonstrated that hypertrophy in mice was attenuated by targeted inhibition of NF- κ B by an I κ B α mutant (Freund et al., 2005). Myotrophin, a ubiquitously expressed 12 kDa soluble ankyrin repeat domain protein related to I κ B α , is able to activate NF- κ B and has been found in SHR hearts and cardiomyopathic human hearts (Young et al., 2008). Transgenic over-expression of myotrophin (Myo-TG) in mice promoted the development of cardiac hypertrophy and HF with a concomitant increase in NF- κ B activity (Young et al., 2008, Gupta et al., 2008). NF- κ B p65 gene knockdown, using an RNA interference-based inhibitor complementary to p65 delivered directly to Myo-TG mice using a lentiviral vector, caused significant regression of hypertrophy associated with a decrease in NF- κ B activity and ANF expression (Gupta et al., 2008). Similar results with Myo-TG mice with an I κ B α triple mutant (Ser 32/36 and Tyr 42 mutated; Myo-3M mice) displayed improved cardiac function and reduced ANF expression (Young et al., 2008). Recent evidence suggests that myotrophin stimulates protein synthesis and myocyte growth by co-localising with p65. Initially myotrophin and p65 co-localise in the cytosol before co-translocation to the nucleus where they initiate new gene expression and myocyte growth (Das et al., 2008). Collectively these studies indicate that activation of the NF- κ B pathway is required for myotrophin induced cardiac hypertrophy *in vivo*.

Increased NF- κ B activity (evidenced by increased NF- κ B:DNA binding) has also been documented in studies of ischemia/reperfusion (I/R) injury. For example, transgenic mice with an I κ B α double mutant displayed reduced infarct size after I/R, however an I κ B α triple mutant could reduce infarct size further (Brown et al., 2005a). This indicates that two NF- κ B pathways are activated during I/R; one via Ser 32 and Ser 36 phosphorylation and, the other via Tyr 42 phosphorylation (Brown et al., 2005a). Other studies have shown that IKK β inhibition in mice that underwent CAL displayed a significant reduction in infarct size, preserved cardiac function and

decreased expression of phospho-I κ B α and phospho-p65 following I/R (Moss et al., 2007, Moss et al., 2008).

Results however are disparate as to whether NF- κ B activation is detrimental or beneficial; for example, NF- κ B signalling appears to underlie the cytoprotective effects of ischemia pre-conditioning (Zhang et al., 2003a, Misra et al., 2003). Several studies have suggested this, for example, blockade of NF- κ B with PDTC in rabbit myocardium increases infarct size (Morgan et al., 1999) and mice with transgenic expression of dominant-negative I κ B α protein display increased infarct size following ischemia (Misra et al., 2003). These conflicting results may be due to the fact that phosphorylation of I κ B α at Tyr 42 involves other kinases such as protein kinase C (PKC) and protein tyrosine kinases (Brown et al., 2005a), thus the kinetics of NF- κ B activation may be different from that activated by the IKK complex, and therefore there may be differences in gene expression. Research has shown that the pro-apoptotic transcription factor AP-1 is up-regulated during I/R injury whereas the anti-apoptotic protein Bcl-2 is activated during ischemia pre-conditioning (Maulik et al., 1999). Disparate results may also be explained by IKK isoform specific responses, for example IKK β appears to drive cell apoptosis (Purcell et al., 2001) whilst the cytoprotective effects of NF- κ B signalling in ischemia pre-conditioning may be due to IKK α as activation of IKK α was reportedly higher than IKK β in the hearts of conscious rabbits subjected to ischemia pre-conditioning (Zhang et al., 2003a). NF- κ B's regulation of myocyte apoptosis is discussed below.

1.11 NF- κ B inhibition as a therapeutic target

As discussed, a large amount of research has implicated a role for NF- κ B in the development of cardiac hypertrophy and therefore NF- κ B represents an attractive therapeutic target for treating heart disease. Like CaMKII, the nature of NF- κ B inhibition is crucial as either inhibition or activation can lead to myocyte apoptosis. This can depend upon the nature of the stimulus of activation and the activated effector pathways that link to the NF- κ B signalling system (Brown et al., 2005a). NF- κ B directly regulates a variety of anti-apoptotic genes including cellular inhibitor of apoptosis (c-IAPs), members of the Bcl-2 family (A1, Bcl-x1) and X-linked inhibitor of apoptosis protein (XIAP) genes. NF- κ B however also directly regulates pro-

apoptotic genes such as Fas receptor, Fas ligand, caspase's 8 and 11 and TNF- α (Purcell and Molkenin, 2003).

In support of NF- κ B inhibition as a therapeutic target in heart disease (in addition to the studies described above in Section 1.10), research has shown that the NF- κ B inhibitory protein, A20, can effectively inhibit the NF- κ B cascade without inducing myocyte apoptosis (Cook et al., 2003) and cardiac-specific over-expression of A20 improved cardiac function and inhibited cardiac remodelling, inflammation, apoptosis and fibrosis after MI (Li et al., 2007). Further investigation *in vitro* using cultured neonatal rat myocytes revealed that A20 acted to suppress TGF- β -induced collagen synthesis and TAK1 signalling (Huang et al., 2010a). Other studies have shown that complete inhibition of NF- κ B (Myo-3M mice) increased cardiac function but did not promote any changes in apoptotic gene expression (Young et al., 2008). In contrast, a recent study suggested that NF- κ B signalling may only be important in the early stages of compensatory remodelling of the heart as a cardiac-specific mutant of I κ B α attenuated cardiac hypertrophy after 4 weeks but not 8 weeks TAC (Zelarayan et al., 2009).

Other studies suggest that complete therapeutic inhibition of the NF- κ B signalling pathway may actually predispose myocytes to apoptosis (Brown et al., 2005a). A more recent study using adult CFs demonstrated that hypoxia activated NF- κ B signalling, and under these conditions this was found to be important for cell survival and viability as a super-repressor I κ B α mutant compromised cell viability under hypoxic but not normoxic conditions (Sangeetha et al., 2011). Likewise, myocyte-specific IKK β -deficient mice developed HF characteristics including LV dilation and cardiac dysfunction in response to 1 week TAC, whereas wild-type animals displayed compensated hypertrophy. Oxidative stress was elevated in IKK β deficient mice, thus IKK β /NF- κ B signalling may play a protective role in myocytes via attenuation of oxidative stress in response to pressure-overload (Hikoso et al., 2009). Similar results have been observed in myocyte-specific IKK γ ^{-/-} mice, whereby TAC induced rapid transition to ventricular dilation and HF compared to wild-type animals, with antioxidant intervention partially alleviating this pathological remodelling (Kratsios et al., 2010). These studies suggest that, under certain conditions, NF- κ B plays a pro-survival/cardioprotective role by inhibiting apoptosis inducing signals.

It is clear that the effect of NF- κ B on myocyte apoptosis may be dependent on activating stimuli, for example hypertrophic agonist stimulation, haemodynamic stress or hypoxia. Disparate results with respect to apoptosis may be due to IKK isoform specific responses in relation to cytoprotection and apoptosis. In support of this idea, research has shown that the anti-apoptotic protein Bcl-2 activates NF- κ B via IKK β , but not IKK α (Regula et al., 2002). The exact role of NF- κ B signalling in the heart and cell types other than myocytes, such as CFs, remains to be elucidated. Key questions that need to be addressed include whether NF- κ B signalling plays a cardioprotective role or whether it contributes to pathological remodelling via cytokine gene transcription.

1.12 Modulation of the NF- κ B pathway by CaMKII δ

Early observations that inhibition of calmodulin and CaMK could prevent degradation of I κ B α (Hughes et al., 1998, Howe et al., 2002) and that CaMKIV could associate with and phosphorylate p65 (Jang et al., 2001), prompted speculation that CaMKII may be involved in NF- κ B modulation. Subsequent research has illustrated that expression of a constitutively active form of CaMKII resulted in NF- κ B activation, and inhibition of CaMKII resulted in decreased IKK phosphorylation (Hughes et al., 2001). Furthermore, CaMKII activated NF- κ B in T-lymphocytes indirectly by phosphorylating CARMA1, a kinase involved in NF- κ B activation (Ishiguro et al., 2006). Another study demonstrated that NF- κ B translocation and activation in synaptic neurons was dependent upon CaMKII (Meffert et al., 2003). Other studies have shown similar results, for example Ca²⁺/CaM can interact directly with and inhibit the nuclear import of c-Rel whereas Ca²⁺/CaM interacts with and allows translocation of p65 in to the nucleus (Antonsson et al., 2003). Stimulation of CaMKII in T-lymphocytes resulted in up-regulation of the transcriptional potential of p65 (Lilienbaum and Israel, 2003). Although these studies are not in the setting of cardiac hypertrophy, they do provide unequivocal evidence for CaMKII modulation of NF- κ B signalling. It seems feasible therefore that CaMKII could possibly modulate NF- κ B signalling in cardiac cells and in cardiac disease.

In support of this idea, a recent study demonstrated the ability of CaMKII to modulate NF- κ B signalling in the heart, whereby inhibition of CaMKII suppressed

NF- κ B activity both *in vitro* and *in vivo* (Singh et al., 2009a). Indeed, infection of neonatal rat myocytes with an adenovirus vector expressing CaMKII δ_B (Ad-CaMKII δ_B) induced features of hypertrophy *in vitro*, stimulated activation of ASK1 and induced I κ B α degradation (Kashiwase et al., 2005). It seems likely therefore that CaMKII can modulate NF- κ B activity either (i) in the cytoplasm via modulation of the IKK complex and/or (ii) in the nucleus via phosphorylation of the NF- κ B heterodimer. As CaMKII δ_B can signal to HDACs to remove transcriptional repression, and that NF- κ B's transcriptional activity is increased by removal of HDACs, it seems feasible that CaMKII may potentially modulate NF- κ B activity via HDACs. The mechanism of how CaMKII regulates NF- κ B signalling however is still to be elucidated. In neuronal cells, activation of Ca²⁺ was sufficient to activate NF- κ B, whereas CaMKII inhibition completely blocked NF- κ B signalling (Meffert et al., 2003). CaMKII inhibition in T-cells abolished phorbol 12-myristate 13-acetate (PMA)-induced I κ B phosphorylation and degradation but did not interfere with TNF- α -induced I κ B degradation (Hughes et al., 2001). These findings suggest that there could be a pathway-specific role for CaMKII. The potential for a direct protein-protein interaction between CaMKII and NF- κ B remains to be elucidated.

Cardiac stress/injury results in a number of key characteristic features including dysfunctional Ca²⁺ homeostasis, fibrosis, stimulation of cell apoptosis and inflammation, resulting from the activation of a plethora of distinct but possibly interrelated signalling pathways. Therapeutically targeting one specific signalling pathway may therefore be unsuccessful in treating cardiac disease. As discussed previously, targeting multifunctional CaMKII may allow modulation of various aspects of cardiac disease, including inflammation possibly via modulation of NF- κ B signalling. Selectively targeting CaMKII or specific CaMKII protein-protein interactions may improve on current broad-spectrum CVD therapies.

1.13 Hypothesis

The overall hypothesis is that CaMKII δ regulates gene expression during hypertrophic growth through its effects on the NF- κ B signalling pathway. Specifically I have tested the hypothesis that this regulation occurs at the level of the IKK complex whereby CaMKII causes degradation of I κ B α and translocation of NF- κ B by modulation of IKK activity

1.14 Thesis aims and objectives

A definite role for CaMKII in cardiac inflammation requires further evidence. Given that CaMKII and NF- κ B signalling are both causally linked to hypertrophic growth of the myocardium, and that inflammation plays a key role in structural remodelling of the heart, this study will investigate potential CaMKII interaction with and modulation of NF- κ B signalling in the heart. If modulation of NF- κ B signalling by CaMKII is demonstrated, the role of this interaction will be studied further in both normal and hypertrophied hearts. Experiments will focus on examining adult CF as this is a relatively novel and less-well understood area in cardiovascular research. Specifically, this study will focus on a number of goals as described below.

1. Investigation of the potential for CaMKII to modulate NF- κ B activity through the interaction of the δ isoform indirectly or directly with the IKK complex. This will be assessed using both cardiac preparations (tissue and cells) and recombinant proteins.
2. Establishment and characterisation of a minimally invasive mouse model of cardiac hypertrophy using aortic constriction. Characterisation of this model will include assessment of haemodynamic parameters, LV contractility and extent of hypertrophy following banding. Evidence for altered fibrosis and inflammation following banding will also be assessed.
3. Altered CaMKII δ and NF- κ B activities following cardiac hypertrophy will be assessed. Changes in CF function following cardiac hypertrophy will also be monitored and related to CaMKII activity.

Chapter 2: Materials and Methods

2.1 Materials

Abcam

Anti-Glyceraldehyde-3-phosphate dehydrogenase (GAPDH) mouse monoclonal immunoglobulin G (IgG) 1 antibody.

Abgent

Anti-CaMKII δ rabbit polyclonal antibody.

Alstoe Lt. Animal Health

Buprenorphine (Vertergesic).

AnalaR

Formaldehyde.

Biacore AB

CM5 sensor chip, N-hydroxysuccinimide (NHS) and 1-ethyl-3-[3-dimethylaminopropyl]carbodiimide hydrochloride (EDC) solutions, 10 mM Sodium acetate pH 4.5 buffer, 1 M Ethanolamine pH 8.5, Surfactant P20.

BioRad Laboratories

Pre-stained SDS-PAGE molecular weight markers, Tween 20.

Boehringer Mannheim

Bovine Serum Albumin (BSA; Fraction V).

Cell Signaling

Anti-I κ B α mouse monoclonal IgG1 antibody.

Concord Pharmaceuticals Ltd

Isoflurane.

Corning Costar

All tissue culture plastics including graduated pipettes, flasks and plates.

Dunlop's Veterinary Supplies

5-0 Vicryl sutures.

Eurogentec

Custom made anti-CaMKII δ rabbit polyclonal antibody.

Fisher Scientific

Anti-phospho-threonine-286 CaMKII mouse monoclonal IgG1 antibody, Restore stripping buffer.

GE Healthcare

Enhanced chemiluminescence (ECL) reagents, Anti-mouse immunoglobulin G (IgG)-horseradish peroxidase (HRP)-linked whole antibody.

Gibco Life Technologies Ltd.

Dulbecco's Modified Eagle Medium (DMEM), Penicillin/Streptomycin antibiotics, Foetal calf serum (FCS), L-Glutamate.

Invitrogen Corporation

NuPAGE Lithium dodecyl sulphate (LDS) sample buffer, NuPAGE gels (Bis-tris and Tris-acetate), Running buffers (MOPS, MES and Tris-acetate), Pre-stained protein markers (See blue plus2 and HiMark), Nitrocellulose membrane.

Jackson ImmunoResearch Laboratories Inc.

Donkey anti-mouse immunoglobulin G (IgG)-horseradish peroxidase (HRP)-linked whole antibody.

Leo Laboratories Ltd.

Heparin (5000 IU/ml).

Merck Biosciences

Protein inhibitor cocktail set V EDTA-free, Calmodulin, Anti-IKK α mouse monoclonal IgG1 antibody, Anti- IKK β mouse monoclonal IgG1 antibody, Autocamtide II related inhibitory protein (AIP).

Merial

Euthatal

Millipore (Upstate Technology)

Purified CaMKII δ enzyme, purified IKK α enzyme, purified IKK β enzyme, P81 phosphocellulose squares, Autocamtide II substrate, PKA inhibitor peptide, PKC inhibitor peptide.

MIUS

Ultrasound transmission gel.

National Diagnostics

Histoclear, Histomount.

Perkin Elmer

[γ -³²P]ATP [3000 Ci/mmol].

Pierce Biotechnology

Coomassie Plus Reagent, Albumin standards (2mg/ml).

Promega

NF- κ B Consensus oligonucleotide, T4 Polynucleotide, 10X T4 Polynucleotide kinase buffer, 5X Gel-shift binding buffer.

Reckitt Benckiser

Veet (topical depilatory cream).

Roche

Quick Spin Columns (Sephadex G-25, fine) for radiolabeled DNA purification.

Santa Cruz

Anti-CaMKII δ goat polyclonal IgG antibody, Anti-IKK α rabbit polyclonal IgG antibody, Anti-IKK β goat polyclonal IgG antibody, Anti-IKK α/β rabbit polyclonal IgG antibody, UltraCruz autoradiography film.

Sigma-Aldrich Co. Ltd.

ATP, Ethyleneglycol-bis-(β -aminoethylether)-N, N, N'-tetraacetic acid (EGTA), Ethylenediaminetetra-acetic acid (EDTA), 4-(2-Hydroxyethyl)piperazine-1-ethanesulfonic acid (HEPES), Taurine, Creatine, Minimum 98% bovine serum albumin (BSA) for electrophoresis, Potassium chloride (KCl), Sodium dihydrogen orthophosphate (NaH_2PO_4), Magnesium chloride hexahydrate ($\text{MgCl}_2 \cdot 6\text{H}_2\text{O}$), Glucose anhydrous, 1 M Calcium chloride (CaCl_2), Disodium hydrogen orthophosphate (Na_2HPO_4), Direct red 80 dye, Saturated aqueous solution of picric acid, Dithiothreitol (DTT), Potassium dihydrogen orthophosphate (KH_2PO_4), Disodium hydrogen orthophosphate ($\text{Na}_2\text{HPO}_4 \cdot 12\text{H}_2\text{O}$), Sodium orthovanadate (Na_3VO_4), Triton-X 100, Thimerosal, Sodium Dodecyl Sulphate (SDS), Sodium Chloride, Glycine, Acrylamide, bis-Acrylamide, Tris-base, Sigmacote, TEMED, Hydrochloric acid (HCl), anti-rabbit IgG-peroxidase conjugate whole molecule antibody, phenylmethylsulphonyl fluoride (PMSF), glycerol, NP-40, Endothelin-1, Angiotensin II, Calyculin A, Protein G sepharose beads, Protein A sepharose beads, Mowiol, Anti-nucleolin rabbit polyclonal IgG antibody.

Special Diet Services

Rat and Mouse Chow.

SurgiPath

Haematoxylin.

Worthington Ltd.

Collagenase type II (351 u/mg).

Vector Laboratories

Vectashield[®] mounting medium containing 4',6-diamidino-2-phenylindole (DAPI).

Vetasept

Betadine (Povidone-iodine antiseptic solution)

Recombinant proteins

IKK γ produced in lab from Baculovirus expression system provided by Dr Carly Gamble, University of Strathclyde, Sorcin produced in lab from bacterial swabs kindly supplied by Dr Marian Meyers, University of New York.

2.2 Minimally invasive transverse aortic banding (MTAB)

All experiments were carried out under licence from the British Home Office and conformed with the Animals (Scientific Procedures) Act, 1986. Animals were bred in-house or purchased from Harlan (UK). Animals were group housed in conditions of a 12-hour light-dark cycle with ad-lib feeding (Rat and Mouse Chow) and water.

Adult male C57BL/6J mice weighing between 25-30g were used for these experiments. Surgical protocol was an adaptation of an MTAB technique described previously (Hu et al., 2003). Briefly, animals were anaesthetised in a Perspex chamber with 3% Isoflurane in the presence of 100% Oxygen at a flow rate of 2 l/min. After 2 to 3 minutes mice were placed supine under an operating microscope (Zeiss, U.K.) on a face-mask and were maintained with 1.5 - 2% Isoflurane in the presence of 0.5 - 1L/min oxygen. Animals were given 60 μ g/kg Buprenorphine intramuscularly and body temperature was maintained within physiological limits ($37.0^{\circ}\text{C} \pm 0.5^{\circ}\text{C}$) using a homeothermic blanket or heat lamp. A topical depilatory cream was used to remove fur from the neck and upper chest area, and the area was wiped with Betadine to prevent opportunistic infection. Thereafter a small horizontal skin incision \sim 0.5 - 1.0 cm in length was made at the level of the suprasternal notch. Once the trachea was located and the pre-tracheal muscle divided in the midline, a 2-3 mm longitudinal cut was made down the sternum and the thymus was retracted to allow visualisation of the aortic arch, left carotid artery and the innominate artery. A 5-0 silk suture was snared with a wire and was passed under the arch and the suture tied between the origin of the right innominate and left common carotid arteries using

a bent 27-gauge needle to control the tightness of the suture. After ligation of the arch, the skin was sutured and the mice were allowed to recover until fully awake. Sham-operated animals went through the same procedure except the aortic arch was not tied. Immediately after surgery 0.5 ml saline and another dose of Buprenorphine was given subcutaneously. Animals were housed in heated cages for 24 h following surgery and were left for 2 or 4 weeks to allow cardiac remodelling to occur.

2.3 Transthoracic echocardiography

Echocardiography of left ventricular function was assessed 2 and 4 weeks after MTAB or sham surgery. Animals were anaesthetised and fur removed as described above in Section 2.2. Two-dimensional short axis views and M-mode images were recorded at the level of the papillary muscle with the use of MIUS HDI 3000CV echocardiography system, a 13 MHz linear array transducer and ultrasound transmission gel. Systolic and diastolic LV wall measurements, including anterior (AW) and posterior wall (PW) measurements, LV end systolic dimension (LVESDD), LV end diastolic dimension (LVEDD) and fractional shortening (% FS) were assessed from M-mode traces. Fractional shortening is expressed as $[(\text{end diastolic dimension} - \text{end systolic dimension}) / \text{end diastolic dimension}] \times 100$. An average of three measurements of each variable was used for each animal.

2.4 Measurement of mean arterial blood pressure

To ensure that the band placed around the aortic arch was in fact producing pressure-overload, mean arterial blood pressure (MAP) was measured 4 weeks after MTAB or sham surgery. Briefly, the arterial cannula was fashioned from a 450-mm segment of polyethylene tube (ID: 0.28 mm, OD: 0.61 mm) with a tip that was tapered to ~0.1 mm in diameter over hot air. Animals were anaesthetised with Isoflurane in 100% oxygen and body temperature maintained within physiological limits ($37.0^{\circ}\text{C} \pm 0.5^{\circ}\text{C}$), as described in Section 2.2. The right carotid artery was exposed and ligated with a 5.0 silk suture at both anterior and posterior ends before a small incision was made in the arterial wall. The tip of the cannula was introduced

through the incision and advanced by ~10 mm before being tied securely into place. To avoid blood clotting around the tip of the cannula it was filled with heparin-treated saline (0.9% (w/v) NaCl containing 15 i.u. ml/heparin). MAP was measured through the arterial cannula connected to a Bell and Howell type 4-422 transducer, which was linked to a Gould 6615-30 DC bridge amplifier. The amplified arterial blood pressure signal was recorded at a sampling rate of 250 Hz by a Ponemah data acquisition system. After a stabilisation period of 10 min, MAP was continuously recorded for 10-15 min. Values were averaged to give one representative value per animal.

2.5 Termination of experiment

After the assigned period of cardiac remodelling each animal was euthanized with an intravenous injection of pentobarbital sodium (10 µl/g weight of animal; Euthatal) and Heparin (0.1 µl/g weight of animal; 5,000 units/ml). Terminal anaesthesia was confirmed by testing the loss of the animal's pedal reflex. The heart was rapidly excised and washed thoroughly in ice-cold Ca²⁺-free Krebs solution (120 mM NaCl, 5.4 mM KCl, 0.52 mM NaH₂PO₄, 20 mM HEPES, 11.1 mM glucose, 3.5 mM MgCl₂, 20 mM Taurine, 10 mM Creatine; pH 7.4) to clear the heart of blood. Tissue was then processed appropriately for a series of quantitative experiments.

2.6 Post-mortem measurements

After 4 weeks of cardiac remodelling, the mice were weighed and euthanized as described in Section 2.5. The hearts were rapidly excised and washed in Ca²⁺-free Krebs, trimmed of fat and vessels and any clots removed. Hearts were gently blotted dry and weighed. Liver and lungs weights were also recorded from sham-operated and banded animals.

2.7 Preparation of tissue samples

2.7.1 Mouse ventricular whole homogenates

Whole ventricular tissue homogenates were prepared from control, sham-operated and MTAB mice and were used for a series of quantitative experiments. Animals were euthanized, the hearts were removed rapidly and washed thoroughly in ice-cold Ca^{2+} -free Krebs solution as described in Section 2.5. All subsequent steps were performed on ice. The atria, vessels and any clots were removed, the heart was weighed and the ventricles were cut into small pieces in ten volumes of homogenisation buffer (20 mM Tris-base buffer, pH 7.4, 1 mM DTT, 1X protease inhibitor cocktail (500 μM AEBSF, 150 nM Aprotinin, 1 μM E-64, and 1 μM Leupeptin) and 1X phosphatase inhibitor cocktail (0.5 mM calyculin A and 20 μM Na_3VO_4) before homogenisation using an Ultra-Turrax T8 (IKA®, U.K.) hand-held homogeniser. The tissue samples were then assayed for total protein content (Section 2.14) and stored at $-80\text{ }^\circ\text{C}$ until use.

2.8 Histology

Hearts were rapidly excised from euthanized animals as described previously (Section 2.5). Hearts were trimmed of fat and vessels and fixed for 48 h hours in 10% (v/v) formaldehyde. Before tissue processing, samples were rehydrated in running tap water for 24 h.

2.8.1 Processing, embedding and sectioning

Tissue was processed (dehydrated) in increasing concentration of ethanol ranging from 70 – 100% (v/v), followed by ‘clearing’ of the tissue by incubation in solution containing 50% ethanol: 50% histoclear using a Thermo tissue processor. Clearing was continued by incubated in 100% histoclear before incubation with paraffin. Immediately after processing samples were embedded in paraffin and tissue sectioned at 5 μm .

2.8.2 *Picro-sirius red staining*

Sectioned tissue was de-waxed by heating at 60 °C for 1 h followed by rehydration through 100% histoclear, 100% ethanol and tap water using a Thermo autostainer. Slides were stained for 1 h in Picro-Sirius Red solution containing 0.1% (w/v) direct red 80 dye in a saturated aqueous solution of 1.3% (v/v) picric acid. Slides were washed in 2 changes of 0.5% (v/v) acidified water before dehydration in 2 changes of 100% ethanol and 5 changes of 100% histoclear. Excess histoclear was removed and slides mounted with histomount.

2.8.3 *Quantification of staining*

Five random sections per heart (5 µm sections with a distance of 200 µm between section), and 10 areas of interest per section were photographed at 10X magnification using non-polarised light with a Leica DM LB2 microscope and a Leica DFC 320 camera (Leica Microsystems, Germany). Quantification of Picro-Sirius red staining used ImageProPlus software (version 5.0; MediaCybernetics, U.S.A), with stained area expressed as a percentage of the total area of interest. Values were averaged to give one representative value per heart.

2.9 *Cell isolation and culture*

2.9.1 *Adult cardiac fibroblasts*

Adult male mice (C57BL/6J) and adult male rats (Sprague-Dawley) were used in these experiments. Although cardiac fibroblasts can be isolated along with myocytes via the Langendorff perfusion method (as described Takahashi et al., 1994)), this procedure is not sterile and therefore there is the potential for infection in cultures. To avoid infection and associated up-regulation of inflammatory signalling pathways, a chunk-digestion method was used with all procedures being performed under sterile conditions.

Briefly, hearts were rapidly removed from 2-3 mice following terminal overdose with pentobarbital sodium as described previously (Section 2.5). The hearts

were washed in warmed Ca^{2+} -free Krebs solution containing 1 mM EGTA and Penicillin/Streptomycin, and the atria, vessels and any clots removed. The ventricles were pooled together, cut into small pieces and fibroblasts were dissociated from the tissue via digestion in Ca^{2+} -free Krebs solution containing 0.8 mg/ml collagenase Type 2 and 0.03 mg/ml protease XIV. The digestion steps were repeated 3-4 times until the tissue was completely digested. After each digestion step, the solution was centrifuged at 462 g for 3 min and the supernatant containing the isolated cells collected. After complete digestion, the supernatants containing the cells were combined and centrifuged for 10 min at 5,143 g. Once the supernatant was discarded the cell pellet was re-suspended in culture media consisting of Dulbecco's Modified Eagle Medium supplemented with 20% (v/v) foetal calf serum (heat-inactivated), 1% (v/v) L-glutamine and 2% (v/v) Penicillin/Streptomycin. The resulting cell mixture was plated in T25 flasks and incubated at 37°C in an atmosphere of 5% CO_2 for 4-5 h. After this time remaining myocytes were removed by replacement with fresh culture medium. Medium was then changed every second day. Cells were cultured for 5 -7 days or until grown to 70-90% confluency before subsequent assay. All experiments were performed with cells from passage 1. For experiments that used adult rat cardiac fibroblasts, only one heart was used and cells were isolated using exactly the same protocol except that the resulting cell mixture was plated into T75 flasks. Rat cardiac fibroblasts were used from passages 1-3.

2.9.2 *Adult cardiac myocytes*

A good yield of viable cardiac myocytes is heavily dependent on such parameters as enzyme activity and enzyme digestion time, the quality of water used, cleanliness of the Langendorff system, Ca^{2+} concentration and general handling of the isolated cells. Thus the Langendorff perfusion system was washed with 2 L of double distilled water (ddH_2O) prior to every isolation procedure and with 2 L boiled ddH_2O , 1 L of 70% (v/v) ethanol and a further 2 L of ddH_2O following the isolation. The Langendorff system was then primed with Ca^{2+} - free Krebs containing 1 mM EGTA (hereafter referred to as Krebs/EGTA) followed by Ca^{2+} - free Krebs (without EGTA).

Healthy adult male C57BL/6J mice weighing between 25-30 g were used for these experiments. Animals were euthanized (as described in Section 2.5) and hearts

removed rapidly and washed in warmed Krebs containing a few drops of Heparin to remove excess blood. With use of a dissection microscope, the heart was cannulated via the aorta using a blunted 23 G needle attached to a flexible tube and clamped in place using a small finely serrated crocodile clip. The cannulated heart was mounted onto the Langendorff system and perfused at a constant flow rate of 4 ml/min at 37 °C with Ca²⁺- free Krebs to remove excess blood. To minimise stress to the cells, enzyme was introduced gradually to the heart by dilution of the stock enzyme cocktail (0.8 mg/ml collagenase Type II and 0.03 mg/ml protease XIV prepared in Ca²⁺- free Krebs solution). Digestion/perfusion was initiated with dilute enzyme (0.3 mg/ml collagenase Type II and 0.01 mg/ml protease XIV) prepared in Ca²⁺- free Krebs solution. Once this had run through (~ 4 min) the remainder of the stock enzyme cocktail was perfused and re-circulated for ~12 min or until the heart appeared paler and slightly swollen. Enzymatic digestion was terminated with perfusion of Krebs/EGTA solution for ~ 5 min, followed by removal of the heart from the perfusion system. Atria were removed and ventricular tissue was finely chopped in Krebs/EGTA solution. Cells were retrieved by collection of the supernatant once the tissue chunks had settled to the bottom of a collecting tube. Cells were allowed to settle by gravity at room temperature and were used immediately.

2.10 Characterization of cardiac fibroblasts by immunofluorescence

Cardiac fibroblasts and smooth muscle cells were grown on plain cover slips until confluent. Cells were fixed by aspirating the culture medium and applying 4% (v/v) paraformaldehyde for 10 min, followed by a 10 min exposure to cold methanol. Cover slips were washed once with sterile phosphate buffered solution (PBS) and then permeabilised using 0.01% triton X-100 (prepared in PBS) for 10 min. Non-specific binding was blocked using 1% (w/v) BSA in PBS for 1 h at room temperature followed by direct addition and incubation of either vimentin or α -smooth muscle actin antibody overnight at 4°C. Both primary antibodies were prepared with 1% (w/v) BSA in PBS at a concentration of 1:100. Cover slips were then washed 3 times with PBS followed by incubation with secondary antibody (anti-rabbit IgG TRITC conjugate and anti-mouse IgG FITC conjugate, respectively) at room temperature for 1 hour. Both secondary antibodies were prepared to a concentration of 1:100 in

sterile PBS. Controls were performed in the absence of primary antibody. After washing 3 times with PBS, cover slips were mounted using Vectashield® mounting medium containing DAPI and stored at 4°C in the dark until they were viewed and photographed. The DAPI counter-stain in the mounting medium stained the cells' nucleus blue. Pictures were taken using Nikon Eclipse™ E600 Oil Immersion microscope connected to a photometrics (CoolSnap™ Fx) digital camera managed by MetaMorph™ software (Universal Imaging Corporation, West Chester, PA).

2.11 Preparation of cell samples

2.11.1 Cardiac fibroblast cell extracts

Cardiac fibroblasts grown on a 6 or 12-well plate 48h prior to assay were solubilised by addition of 150 µl 1X Invitrogen NuPAGE® LDS sample buffer containing 75 mM dithiothreitol (DTT). Cells were scraped from the bottom of wells and DNA disrupted by passing through a syringe and a 23 G needle several times.

2.11.2 Cardiac myocyte cell extracts

Freshly isolated cardiomyocytes were solubilised by the addition of 1X Invitrogen NuPAGE® LDS sample buffer containing 75 mM DTT to give a final cell concentration of 1×10^6 cells/ml. Samples were passed through a syringe and a 23 G needle several times to disrupt DNA.

2.12 Stimulation of cardiac fibroblasts

Confluent healthy mouse or rat cardiac fibroblasts grown in a 25 or 75 cm³ flask, respectively, were trypsinised, re-suspended in growth media and plated into a 12-well plate 48 h prior to assay. Once cells were 90-100% confluent they were serum starved with serum-free medium for 24 h. Cells (mouse at p1 and rat at p1-3) were treated with agonist (1 µM Ang II, 100 nM ET-1, 5 µg/ml LPS or 20 ng/ml TNF-α) over a variable time course from 0 – 120 min, respectively. For experiments including inhibitor, cells were pre-treated with either 5 µM AIP or 5 µM KN-93 for 1

h before agonist treatment. After specified time, reactions were terminated on ice via aspiration of medium and addition of 150 μ l 1X Invitrogen NuPAGE® LDS sample buffer and 75 mM DTT. Cells were scraped from the bottom of wells and DNA disrupted by syringing using a 23 G needle. Samples were analysed using SDS-PAGE and scanned autoradiographs were quantified by densitometry as described previously (Section 2.15).

2.13 Proliferation of cardiac fibroblasts

Mouse cardiac fibroblasts isolated from sham-operated and MTAB hearts were plated onto sterile cover slips in 12-well culture plates at 5,000 cells per well and allowed to attach for 24 h before serum starvation for a further 24 h. Cells were then stimulated with 1 μ M Ang II and proliferation assessed by cell counting over a variable time course from 0 – 72 h, with each point performed in triplicate. At the appropriate time, cells were washed twice with sterile PBS and fixed with 70% (v/v) methanol for 30 min. After washing with PBS (2 x 5 min washes) cells were stained with haematoxylin for 20 min, followed by thorough washing with tap water. Excess water was removed and cover slips were mounted onto slides using mowiol mounting medium. Photographs of the cells were taken (10 images per point, 5X objective) with use of a Leica DFC 320 digital camera (Leica Microsystems, Germany) connected to a Leica DM LB2 microscope (Leica Microsystems, Germany) and Adobe Photoshop.

2.14 Protein quantification

Total protein concentration of tissue or cell preparations was quantified using a Bradford assay (Bradford, 1976). Bovine serum albumin (BSA) was used to generate a standard curve with concentrations ranging from 0.1-1.0 mg/ml. Samples were prepared at appropriate dilutions that fell within the linear range of the protein BSA standard curve (Figure 2.1). A total volume of 10 μ l of each BSA standard and tissue/cell sample was loaded onto a 96-well plate in triplicate with one row of distilled water as a blank background. Coomassie Plus Protein Reagent (200 μ l) was then added to each well and the plate was read using a microplate reader (Model 680,

BioRad) set at 595 nm absorbance. Standards were plotted using a sigmoidal fit and only samples with absorbance readings falling in the linear area of the curve were quantified. When quantifying total protein in samples containing detergents, the solubilisation buffer was used as a background as some detergents react with the acidic Coomassie dye reagent and can cause a colour change in the assay.

2.15 Quantitative immunoblotting and densitometry

Samples were prepared in 1X Invitrogen NuPAGE® LDS sample buffer that contained 75 mM DTT as a reducing agent. Samples were heated to 100 °C for 5 min prior to loading onto denaturing gels and analysed by SDS-polyacrylamide gel electrophoresis (PAGE) using the Invitrogen NuPAGE® system. To reduce inter-gel variations, comparisons between sham-operated and MTAB homogenate samples were made by loading a range of protein amounts onto the same gel. Amounts of protein to be loaded were optimised for subsequent densitometry analysis, taking into account the signal strength and linear limitations of the equipment. For comparisons between control and stimulated cell lysates, one protein sample from each treatment group was loaded onto the same gel. In addition, optimisation involved being able to resolve both the protein of interest and an internal standard, GAPDH, in the same gel. Thus, running conditions including the type of gel used, running buffer and running time as well as protein loads were optimised for each protein of interest as shown in Table 2.1.

Electrophoresis was performed at a constant voltage of 200 V for 45-60 min (Table 2.1), followed by transfer onto a nitrocellulose membrane using Towbin's transfer buffer (25 mM Tris-base, 192 mM glycine, 20% (v/v) methanol) for 1 h at 25 V. Subsequently, non-specific binding sites on the membranes were blocked with 5% (w/v) non-fat dry milk diluted in Tris buffered saline solution containing Tween 20 (TBST) buffer (20 mM Tris-base, 137 mM NaCl and 0.1 % (v/v) Tween 20, pH 7.6) for 1 h at room temperature, then membrane were incubated overnight at 4 °C with the appropriate primary antibody (Table 2.2) prepared in 5% (w/v) non-fat milk in TBST buffer. Following this, membranes were washed for 3 x 5 min washes with TBST buffer then incubated for 2 h at room temperature with either horseradish peroxidase conjugated anti-mouse or anti-rabbit IgG prepared in 5% (w/v) non-fat milk in TBST.

Finally, blots were washed for 3 x 5 min washes with TBST buffer and signals developed by enhanced chemiluminescence (ECL) and visualised on autoradiography film. After ECL development, signals of the scanned autoradiographs were quantified by densitometry using a GS-800 densitometer and Quantity One Image software (version 4.5.2, BioRad). All proteins investigated were normalised to GAPDH and scatter plot graphs of normalised protein loads were plotted, using the gradient values of this plots to generate histogram data.

During the optimisation of antibodies, different blocking buffers, antibody dilution buffers and wash buffers were tested in addition to the TBST protocol. Buffer protocols tested were, 1) Swiss buffer and 2) Sodium and Tris solution containing Tween 20 (NaTT) buffer. Buffer conditions are specified in the appropriate experiments throughout this thesis.

1) With the Swiss buffer protocol, nitrocellulose membranes were blocked in Swiss buffer (100 mM Tris-base pH 7.5, 100 mM MgCl₂, 1% (v/v) Tween 20, 1% (v/v) Triton X 100, 1% (w/v) BSA, 5% (v/v) FCS and 0.01% (w/v) Thimersol) containing 3% BSA (4% BSA, final concentration) for 1 h at room temperature, then incubated overnight at 4 °C with primary antibodies prepared in Swiss buffer containing 3% BSA. Membranes were washed with 1 x 5 min rinse buffer (7.6 mM Tris-base pH 7.5, 150 mM NaCl, 0.1% (v/v) Triton X 100, 1 mM ethylenediaminetetraacetate (EDTA)), 1 x 5 min high salt rinse buffer (7.6 mM Tris-base pH 7.5, 600 mM NaCl, 0.1% (v/v) Triton X 100, 1 mM EDTA), 1 x 5 min rinse buffer followed by incubation with secondary antibodies prepared in Swiss buffer containing 3% BSA for 2 h at room temperature. Blots were then washed, developed and quantified as described above.

2) With the NaTT protocol, membranes were blocked in 3% (w/v) BSA diluted in NaTT buffer (20 mM Tris-base pH 7.4, 20 mM NaCl and 0.2 % (v/v) Tween 20) for 2 h at room temperature, then incubated overnight at 4 °C with primary antibodies prepared in 0.2% (w/v) BSA in NaTT. Membranes were then washed for 6 x15 min washes with NaTT buffer followed by incubation with secondary antibodies prepared in 0.2% (w/v) BSA in NaTT for 2 h at room temperature. The blots were then washed, developed and quantified as described above.

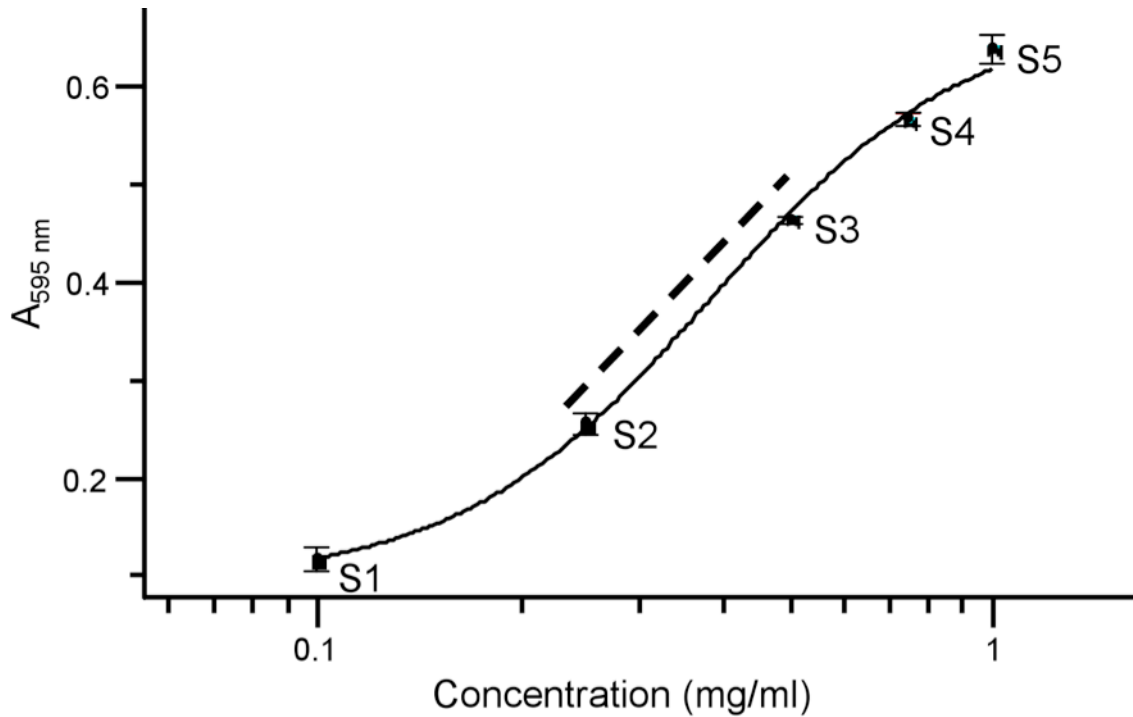


Figure 2.1 BSA standard calibration curve.

Graph showing absorbance reading at a wavelength of 595 nm versus concentrations of BSA standards (S1-S5). Concentration readings of unknown protein samples are only taken when the absorbance readings fall within the linear range of the calibration curve, as indicated by the dashed line, as readings above or below this linear range are considered inaccurate due to the sigmoidal nature of the curve.

	Protein Size (kDa)	NuPAGE Gel	Running Buffer (20x)	Running Time (Min)	Protein Loads (μg)
CaMKIIδ	56	10% Bis-Tris	MOPS	60	8-12
Phosphorylated CaMKIIδ	56	10% Bis-Tris	MOPS	60	8-12
IKKα	85	7% Tris-Acetate	Tris-Acetate	50	14-18
IKKβ	87	7% Tris-Acetate	Tris-Acetate	50	14-18
IKKγ	48	10% Bis-Tris	MOPS	60	8-12
p65 NF-κB	65	10% Bis-Tris	MOPS	60	8-12
IκBα	39	10% Bis-Tris	MES	60	~ 5

Table 2.1 Optimised quantitative immunoblotting conditions for each protein of interest.

Primary Antibody	Company	Dilution	Secondary Antibody	Company	Dilution
CaMKIIδ	Eurogentec, custom made	1:1,000	Anti-rabbit IgG-HRP	Sigma-Aldrich, Cat. # A6154	1:10,000
Phospho CaMKIIδ	Fisher Scientific, Cat. # MAI-047	1:500	Anti-mouse IgG-HRP	Jackson Immuno- Research Cat. # 715-035-150	1:5,000
IKKα	Calbiochem, Cat. # OP133	1:500	Anti-mouse IgG-HRP	Jackson Immuno- Research Cat. # 715-035-150	1:5,000
IKKβ	Calbiochem, Cat. # OP134	1:500	Anti-mouse IgG-HRP	Jackson Immuno- Research, Cat. # 715-035-150	1:5,000
IKKγ	Santa Cruz Cat. # sc-8330	1:7,500	Anti-rabbit IgG-HRP	Sigma-Aldrich, Cat. # A6154	1:10,000
p65 NF-κB	Santa Cruz Cat. # sc-372	1:7,500	Anti-rabbit IgG-HRP	Sigma-Aldrich, Cat. # A6154	1:10,000
IκBα	Cell Signaling, Cat. # 4814	1:1000	Anti-mouse IgG-HRP antibody	Jackson Immuno- Research, Cat. # 715-035-150	1:1,000
GAPDH	Abcam, Cat. # ab8245	1:80,000	Anti-mouse IgG-HRP	GE Healthcare, Cat. # NA931	1:60,000
Nucleolin	Sigma- Aldrich, Cat. # N2662	1:3,000	Anti-rabbit IgG-HRP	Sigma-Aldrich, Cat. # A6154	1:10,000

Table 2.2 Types of primary and secondary antibodies used for each protein of interest.

2.16 Immunoprecipitation

Immunoprecipitation (IP) was performed using both homogenised tissue and cell preparations (myocytes and fibroblasts) to isolate CaMKII δ , IKK α , IKK β and IKK γ .

For IP from cardiac tissue, two protocols were used as described below. The latter protocol was used only with the peptide-affinity purified custom anti-CaMKII δ antibody and was based on a published protocol that used this particular antibody (Huke and Bers, 2007). Adult male mice (C57BL/6J) weighing 25 - 30g were used in these experiments. The heart was rapidly removed following terminal overdose as described in Section 2.3. The ventricles were cut into small pieces in 4 volumes ice-cold homogenisation buffer (50 mM Tris-base pH 7.5, 1% Glycerol, 1 mM EDTA, 1 mM DTT and protease inhibitors) and homogenised on ice as described previously (section 2.7.1).

In the first protocol, which was based on a previously published protocol (Currie et al., 2004), homogenates were centrifuged at 16,060 g for 10 min and the resulting pellet was re-suspended in 4 volumes ice-cold solubilisation buffer (50 mM Tris-base pH 7.5, 50 mM NaCl, 1% (v/v) glycerol, 1 mM EDTA, 1 mM DTT, 1% (v/v) Triton X 100 and protease inhibitors). Preparations were left to mix end-over-end for 20 min at 4 °C before centrifugation at 16,060 g for 10 min. Recovered solubilised supernatants were assayed for total protein content. A total of 500 μ g of solubilised supernatant (diluted in 500 μ l homogenisation buffer) was incubated with 1- 3 μ g antibody (anti-IKK α , anti-IKK β or anti-IKK γ) and left to mix end-over-end overnight at 4 °C. Negative control samples without solubilised supernatant or without antibody were included. To separate protein-antibody complexes from the samples, samples were incubated with 50 μ l Protein G sepharose beads (50% (v/v) slurry) and left to mix end-over-end for 1 h at 4 °C. Following incubation, tubes were pulse-centrifuged and beads washed (2 x 500 μ l solubilisation buffer, 2 x 500 μ l homogenisation buffer and 2 x 500 μ l PBS) before re-suspension in 4X Invitrogen NuPAGE® LDS sample buffer containing 75 mM DTT. Beads were well mixed in sample buffer and left to extract at room temperature for 30 min prior to heating at 100 °C for 5 min. Immunoprecipitated proteins were identified using SDS-PAGE

analysis and proteins visualised using ECL as described previously (section 2.15). Antibodies used for immunoblotting of CaMKII δ and IKKs are outlined in Table 2.2.

For the second protocol, homogenates were centrifuged at 16,060 g for 10 min and the resulting pellet was re-suspended in 3 volumes ice-cold solubilisation buffer (8% (v/v) Triton X-100, 9 mM EGTA, 5 mM NaF and protease inhibitors). Preparations were left to mix end-over-end for 20 min at 4 °C before centrifugation at 45,000 g for 10 min. Recovered solubilised supernatants were assayed for total protein content. Samples were diluted to 500 μ g total protein per tube with RIPA-buffer (1% NP-40, 150 mM NaCl, 10 mM Tris-base pH 7.2, 2 mM EGTA, 50 mM NaF, 1 mM Na₂H₂P₂O₇ and protease inhibitors). Tubes were rotated end-over-end overnight at 4 °C with 5-10 μ g of anti-CaMKII δ antibody. Negative control samples without solubilised supernatant or without antibody were included. To separate protein-antibody complexes from the samples, samples were incubated with 50 μ l Protein A sepharose beads (50% (v/v) slurry) and left to mix end-over-end for 1 h at 4 °C. Tubes were pulse-centrifuged and beads washed (3 x 500 μ l RIPA-buffer) before re-suspension in 4X Invitrogen NuPAGE® LDS sample buffer containing 75 mM DTT. Samples were analysed by SDS-PAGE as described for the previous protocol.

For experiments using cell preparations a slightly different protocol was used and was again based on a published protocol (MacKenzie et al., 2007). Briefly, once mouse cardiac fibroblasts grown on a 25 cm³ flask reached 90-100% confluency they were washed twice with ice-cold PBS and lysed using 300 μ l ice-cold solubilisation buffer (20 mM Tris-HCl pH 7.6, 1 mM EDTA, 0.5 mM EGTA, 10% (v/v) glycerol, 1% (w/v) Triton X-100, 0.1% Brij 35, 150 mM NaCl, 20 mM NaF, 20 mM β -glycerophosphate, 0.5 mM sodium orthovanadate, 1 mM PMSF and protease inhibitors (10 μ g/ml each of leupeptin, aprotinin and pepstatin A)). Cells were scraped and the cell lysates were incubated on ice for 30 min. Lysates were then centrifuged at 16,060 g for 5 min and the insoluble material removed. Solubilised cell extracts (50 μ l per tube) were incubated and left to mix end-over-end overnight at 4 °C with Protein G sepharose beads (50% slurry) that had been pre-coupled to 3 μ g primary antibody on a shaker at 4 °C for 1 hour. Samples without solubilised cell extract or without antibody were included as negative controls. The beads were washed 3 x 500 μ l solubilisation buffer, proteins eluted from the beads and boiled,

and immunoprecipitated proteins analysed by SDS-PAGE as described above (Section 2.15).

For cardiac myocyte preparations, cells isolated from one mouse heart were lysed in solubilisation buffer immediately after the isolation procedure and were prepared to 500 µg protein per tube (diluted in 500 µl solubilisation buffer). IP was carried out as described above for cardiac fibroblasts.

For co-immunoprecipitation experiments, where interaction between two proteins was investigated, one protein was immunoprecipitated and an antibody against the second protein was used to probe these IP's in immunoblots. Antibodies used for immunoblotting of CaMKIIδ and IKKs are outlined in Table 2.2.

2.17 Autoradiography

Assay components consisted of either (i) substrate (50 µM autocamtide II (control substrate for CaMKIIδ), or 1 µg IκBα (control substrate for IKKs)) (ii) enzyme (100 ng IKKα, 100 ng IKKβ, or 30 ng CaMKIIδ), (iii) inhibitor (5 µM AIP or 10 µM BMS) and (iv) 50 µM/5 µCi [γ -³²P]ATP (final concentration). Components were mixed with 40 µg/ml calmodulin, 1.5 mM CaCl₂ (final concentration) and prepared to a final volume of 50 µl with assay dilution buffer before incubation on a shaker at 30 °C for 30 min. Assay dilution buffer consisted of 20 mM HEPES (pH 7.6), 25 mM MgCl₂, 2 mM DTT, 20 mM β-glycerophosphate and 0.5 mM sodium orthovanadate. Reactions were terminated on ice by addition of 4X LDS sample buffer containing 300 mM DTT (to give 1X sample buffer containing 75 mM DTT, final concentration). Samples were analysed by SDS-PAGE on a 4-12% (w/v) Bis-Tris acrylamide gel (as described in section 2.15) followed by incubation fixer solution (40% (v/v) methanol and 10% (v/v) acetic acid) for ~30 min. The gel was then vacuum-dried and protein phosphorylation assessed by exposure of the dried gel to X-ray film overnight at -20 °C.

2.18 Surface Plasmon Resonance

2.18.1 Introduction to the Biacore technology

Surface Plasmon Resonance (SPR) was used to establish whether there was a direct protein-protein interaction between CaMKII δ and the IKKs. All SPR experiments were conducted using a Biacore 3000 biosensor that works on the principle of Surface Plasmon Resonance. This is a novel technique used to investigate direct protein-protein interactions between two proteins of interest, where one protein, referred to as the ligand, is immobilised via covalent coupling to the dextran matrix of a sensor chip; Figure 2.2. The other protein or analyte in solution is injected over the sensor chip surface in contact with the flow cells of the system. Any interaction between the two proteins is viewed in real time using computer software.

The Biacore system works on the principle of measurements of changes in refractive index, which is equated to a change in mass or surface concentration. Briefly, the SPR phenomenon depends on the generation of a wedged polarised light from the light source (Figure 2.3 (a)) hitting the glass:gold interface of the sensor chip surface (Figure 2.3 (b)) thus resulting in the occurrence of SPR and the subsequent generation of an ‘evanescent’ wave’. This wave propagates beyond the glass:gold surface into the flow channel. Any interaction between proteins passing through the flow channel in solution with proteins immobilised onto the sensor chip surface (Figure 2.3 (c)) causes a change in refractive index, which interacts with the ‘evanescent wave’ and results in alteration of the angle of incidence required to generate SPR. This ultimately results in a change in the resonance angle that will be detected (Figure 2.3 (d)) and displayed on a sensogram as an increase or decrease in response unit (RU) or mass change upon proteins association and dissociation. As an approximation one change in RU corresponds to a change in surface concentration of about 1 pg/mm². (The information found in this subsection is courtesy of Biacore, U.K., Biacore Sensor Surface Handbook, 2003).

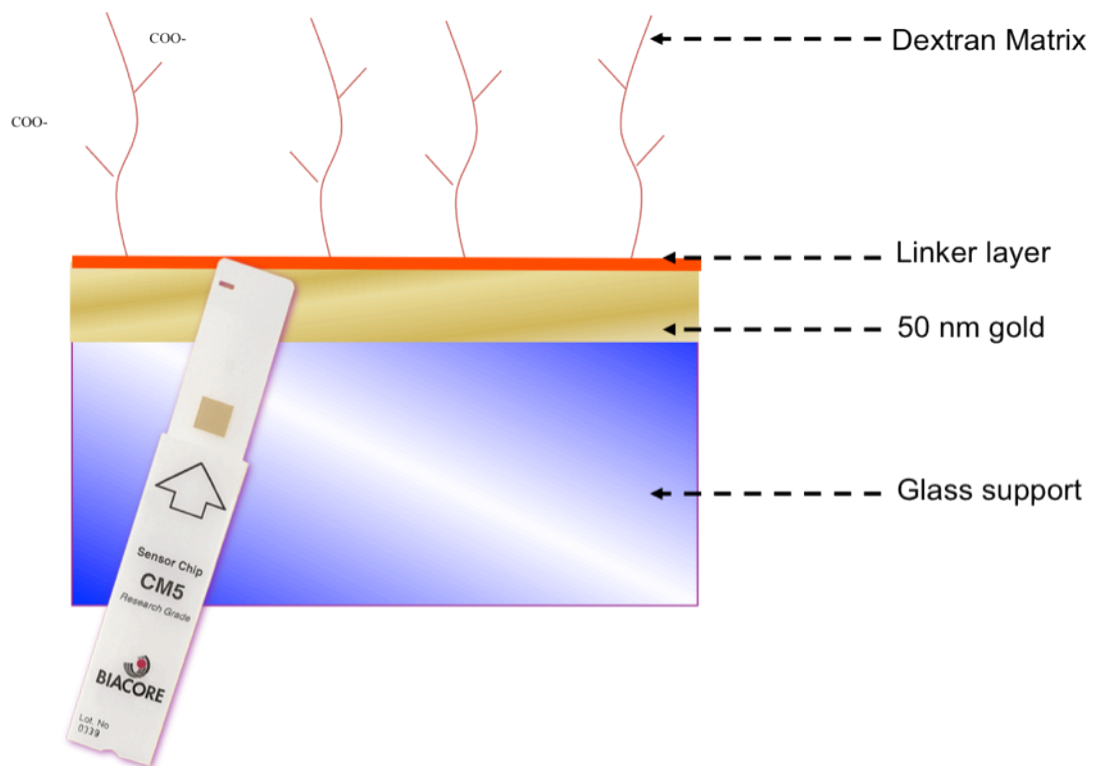


Figure 2.2 CM5 sensor chip.

A schematic representation of a CM5 sensor chip showing the hydrophilic carboxymethylated dextran matrix required for the immobilisation of a ligand. Also depicted is a glass slide coated with a layer of gold, required for the generation of SPR. Diagram courtesy of Biacore U.K.

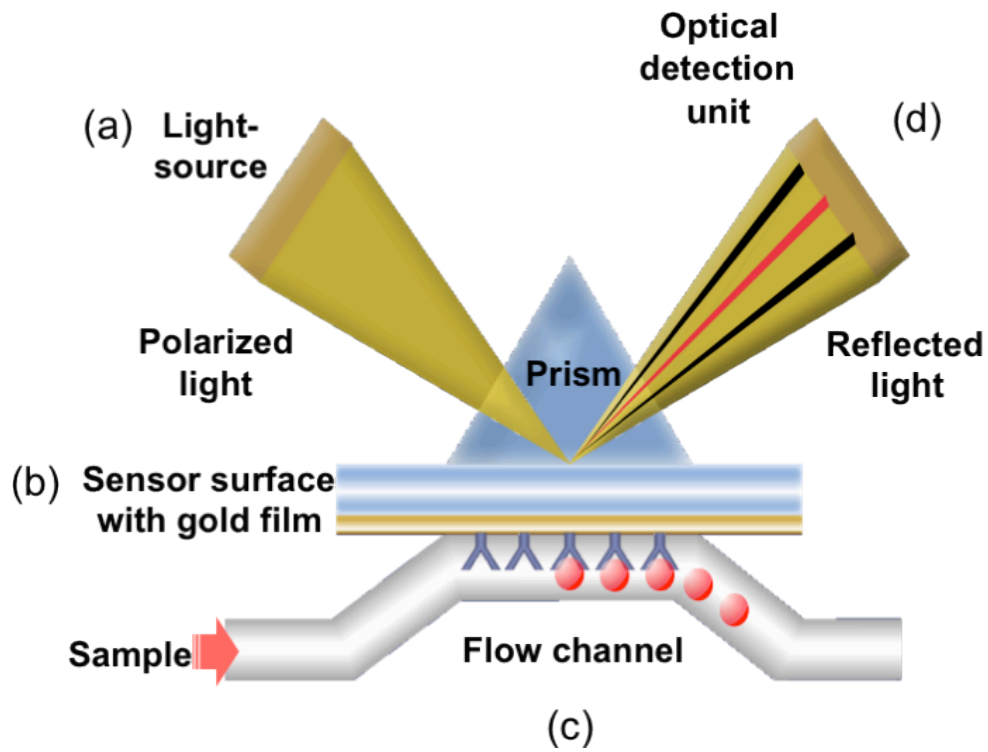


Figure 2.3 Principle of Surface Plasmon Resonance phenomenon.

A schematic diagram illustrating the key elements of Biacore Biosensor technology. Generation of SPR takes place on the sensor chip surface at the glass:gold interface. Diagram adapted from Biacore U.K.

In Biacore systems, interactions occur in flow cells on the sensor chip surface. These flow cells are in contact with the gold surface of the sensor chip and together they form a microfluidic system, allowing a continuous flow of solution over the course of analysis. The sensor chip surfaces used in this study have two flow cells, with serial flow direction. This is advantageous as it enables the use of one flow cell as an internal negative or positive control, depending upon the protein immobilised or to allow binding to two different and independent ligands at the same time.

2.18.2 Experimental protocol

Studies were based on a previously published protocol (Anthony et al., 2007). Recombinant CaMKII δ was immobilised onto a CM5 sensor chip to a density of approximately 3000 - 4000 response units (RU), equating to 3 - 4 pg/mm² of immobilised protein. Further experiments used immobilisation levels of 7000 - 8000 RU, which equates to 7 - 8 pg/mm². Prior to immobilisation the sensor chip surface was activated using a mixture of 1:1 NHS:EDC (N-hydroxysuccinimide 1-ethyl-3-(3-dimethylaminopropyl)-carbodiimide hydrochloride). CaMKII δ (100 μ g/ml stock) was prepared to 7 μ g/ml with 10 mM sodium acetate buffer pH 4.5 for immobilisation. Immobilisation was performed at 25 °C at a flow rate of 5 μ l/min using SPR running buffer (20 mM HEPES pH 7.4, 150 mM NaCl, 0.005% (v/v) surfactant P20, 5 mM MgCl₂, 1.5 mM CaCl₂ and 2 mM DTT). After immobilisation the sensor chip surface was inactivated using 1 M ethanolamine pH 8.5. The system was left to stabilise overnight at 25 °C in the running buffer. All experiments used BSA as a negative control with equivalent amounts of protein immobilised under exactly the same conditions as for CaMKII δ .

Before starting any experiments the system was primed with the running buffer. Calmodulin (CaM), recombinant IKK α , IKK β and recombinant IKK γ were used as analytes and were prepared at final concentrations of 0.0125 - 0.2 μ M in running buffer and were injected in random sequence for 3 min into the flow cell at a rate of 30 μ l/min with a 15 min dissociation period. In experiments investigating the effect of Ca²⁺, imidazole and ATP on analyte-ligand interactions, SPR running buffer did not have Ca²⁺ added or contained 100 mM imidazole or 1 mM ATP, respectively. The interaction was followed in real time on a sensorgram. After each measuring

cycle, the sensor chip surface was regenerated with 2 x 30 s pulse of regeneration buffer containing 2 mM EDTA and 1 M NaCl, followed by a 2 min stabilisation period before another injection. Data analysis was carried out using the BIA evaluation version 3.2 (Biacore).

2.19 CaMKII activity assay

CaMKII δ activity was measured in immunoprecipitated IKK γ samples using a CaMKII kinase assay as previously described (Anthony et al., 2007). The assay measures the phosphotransferase activity of CaMKII in purified or crude preparations and is based on phosphorylation of a specific substrate peptide (autocamtide; KKALRRQETVDAL) by the transfer of [γ - 32 P]ATP. Assay components consisting of CaMKII substrate cocktail (500 μ M autocamtide II and 40 μ g/ml calmodulin), PKA/PKC inhibitor cocktail (2 μ M PKA peptide inhibitor and 2 μ M PKC peptide inhibitor) and enzyme preparation (10 μ g whole ventricular homogenates) were prepared in assay dilution buffer (20 mM MOPS, pH 7.2, 25 mM β -glycerol phosphate, 1 mM sodium orthovanadate, 1 mM dithiothreitol, 75 mM MgCl₂, 1 mM CaCl₂) and were mixed on ice before reactions started by the addition of 500 μ M/ 0.2 μ Ci [γ - 32 P]ATP (final concentration). Samples were incubated at 30 °C for 10 min and reactions stopped by transferring to P81 phosphocellulose paper. Phosphocellulose paper was washed 3 x 2 min washes with 0.75% (v/v) phosphoric acid containing 0.1% (v/v) Tween 20 followed by a single 2 min wash with acetone. Papers were allowed to air dry before transfer to vials and associated radioactivity measured using liquid scintillation counting. All samples in each experiment were assayed in triplicate.

2.20 Electrophoretic Mobility Shift Assay (EMSA)

2.20.1 Nuclear Protein Extraction from Tissue

Tissues were minced and incubated on ice for 30 min in 0.5 ml of ice-cold buffer 1 (10 mM HEPES pH 7.9, 1.5 mM KCl, 10 mM MgCl₂, 0.5 mM DTT, 0.1% (v/v) NP-40, and 0.5 mM phenylmethylsulfonyl fluoride (PMSF), and a protease

inhibitor cocktail containing 10 µg/ml each of leupeptin, aprotinin and pepstatin A). The minced tissue was homogenised using a hand-held glass homogeniser followed by centrifuging at 5000 X g for 10 min at 4°C. The crude nuclear pellet was re-suspended in 200 µl of buffer 2 (20 mM HEPES pH 7.9, 25% (v/v) glycerol, 1.5 mM MgCl₂, 420 mM NaCl, 0.5 mM DTT, 0.2 mM EDTA, 0.5 mM PMSF, and protease inhibitors) and incubated on ice for 30 min. After the specified time, the suspension was centrifuged at 16,000 X g for 30 min at 4°C. The supernatant (nuclear proteins) was collected and kept at -80°C until use. Protein concentrations were determined using the Bradford assay as described in Section 2.14.

2.20.2 Nuclear protein extraction from cardiac fibroblasts

Cells were grown to confluency in 6-well plates and rendered quiescent after 24 h in serum free medium. Following stimulation with LPS (5 µg/ml) and inhibitor (Bristol-Myers Squibb-345541, BMS, 10 µM; autocamtide 2-related inhibitory peptide, AIP, 5 µM; KN-93, 5 µM), cells were disrupted in ice-cold PBS and were harvested by centrifugation at 13,000 x g for 2 min. The cell pellet was re-suspended in 400 µl of buffer 1 (10 mM HEPES pH 7.9, 10 mM KCl, 0.1 mM EDTA, 0.1 mM EGTA, 1 mM DTT, 0.5 mM PMSF, and a protease inhibitor cocktail containing 10 µg/ml of each of leupeptin, aprotinin and pepstatin A) and incubated at 4°C for 15 min, followed by addition of 25 µl of 10% (v/v) NP-40. Suspensions were vortexed at full speed for 10 s and cells pelleted by centrifugation at 13,000 x g for 1 min, before resuspension in 50 µl of buffer 2 (20 mM HEPES pH 7.9, 25% (v/v) glycerol, 400 mM NaCl, 1 mM EDTA, 1 mM EGTA, 1 mM DTT, 0.5 mM PMSF, and protease inhibitors). Following incubation on a shaker for 15 min at 4°C, suspensions were sonicated in a bath-type sonicator for 2 x 30 s. Extracted nuclear proteins were then recovered by centrifugation at 13,000 x g for 15 min at 4°C, and stored at -80°C until use. Protein concentrations were determined using Coomassie Plus Protein Reagent as described in Section 2.14.

2.20.3 Labelling of consensus oligonucleotides

Oligonucleotide containing the consensus binding sequence for the NF- κ B transcription factor (5'-AGTTGAGGGGACTTTCCCAGGC-3') was labelled with γ -³²P-labelled ATP at its 5'-end by incubation with T4 polynucleotide kinase at 37 °C for 30 min. The reaction system consisted of 2 μ l oligonucleotide probe; 1 μ l 10X T4 polynucleotide kinase buffer (700 mM Tris-HCL pH 7.6, 100 mM MgCl₂ and 50 mM DTT); 1 μ l [γ -³²P] ATP (3,000 Ci/mmol at 10 mCi/ml); 5 μ l nuclease-free water; 1 μ l T4 polynucleotide kinase (5-10 u/ μ l). The reaction was stopped by addition of 1 μ l 0.5 M EDTA and 89 μ l TE buffer (10 mM Tris-base pH 8.0, 1 mM EDTA, 0.5 M Na₂HPO₄). Quick spin columns (G-25 Sephadex) were used to purify radiolabelled DNA by removal of unincorporated [γ -³²P] ATP. Briefly, columns were prepared by centrifugation at 1100 x g for 2 min and eluted buffer discarded. Keeping the column in the upright position, 50 μ l of the DNA sample was loaded into the centre of the column bed and purified [γ -³²P]-labelled NF- κ B oligonucleotide was collected by centrifugation at 1100 x g for 4 min. Labelled nucleotide was stored at 4 °C until use.

2.20.4 DNA binding reaction

Nuclear protein (10-20 μ g from tissue or 2-10 μ g from cells) was incubated with gel-shift binding buffer (containing 10 mM Tris-HCL pH 7.5, 4% (v/v) glycerol, 1 mM MgCl₂, 0.5 mM EDTA, 50 mM NaCl, 50 μ g/ml poly (dI-dC) (dI-dC); final concentration) for 20 min at room temperature. The transcription factor binding reaction was then initiated by addition of [γ -³²P]-labelled NF- κ B oligonucleotide (approx. 50,000 cpm) for 20 min at room temperature. In the supershift assay, antibody (1 μ g) reactive to p65, RelB, c-Rel, p50 and p52 was added to the reaction mixture 20 min after addition of the radiolabelled NF- κ B probe, and assay components were incubated for a further 20 min. Reactions were stopped by addition of 1 μ l 10X gel loading buffer (250 mM Tris-HCL pH 7.5, 0.2% (w/v) bromophenol blue, 40% (v/v) glycerol) and samples were subjected to non-denaturing PAGE in 0.5% (w/v) Tris-borate/EDTA buffer (45 mM Tris-base pH 8.3, 1 mM EDTA, 45 mM boric acid) buffer. The gel was then vacuum-dried and exposed to X-ray film.

2.21 Enzyme-linked immunosorbent assay (ELISA)

Whole ventricular tissue homogenates from sham-operated and MTAB animals after banding for 48h, 1 week and 4 weeks were assayed for levels of interleukin-6 (IL-6) and tumour necrosis factor α (TNF- α) protein using commercially available ELISA kits (ELISA Ready-SET-Go![®] kit, eBioscience). Animals were euthanized as described in Section 2.5. The heart was immediately removed, weighed and was snap-frozen in liquid nitrogen before homogenisation in 10 volumes of homogenisation buffer as described previously (Section 2.7.1). The tissue samples were then assayed for total protein content (as described in Section 2.14) and prepared to a final concentration of 5 mg/ml. IL-6 and TNF- α ELISAs were performed according to manufacture's instructions. Briefly, ELISA plates were coated with 50 μ l/well of capture antibody (purified antibody) and incubated overnight at 4°C. Coating solution was then removed and wells washed 5 times with 250 μ l/well wash buffer (PBS containing 0.05% (v/v) Tween-20), with any residual buffer removed by blotting the plate on absorbent paper. To block any non-specific protein binding, plates were incubated with 200 μ l/well 1X assay diluent for 1 h at room temperature, which was followed by washing plates 5 times with wash buffer as described above. The appropriate protein standards (IL-6 and TNF- α recombinant protein) were prepared to generate a standard curve with a top concentration of 2000 pg/ml. A total volume of 50 μ l/well of standard or sample were then added to the appropriate wells, plates were sealed with adhesive plastic and incubated overnight at 4°C. Following washing as described previously, 50 μ l/well of detection antibody (biotin-conjugated antibody) diluted in 1X assay diluent was added to each well and was incubated at room temperature for 1 h. Detection antibody was then removed and plates were washed as described, followed by addition of 50 μ l/well of avidin-HRP diluted in 1X assay diluent and incubation at room temperature for 30 min. Wells were then thoroughly washed 7 times with 250 μ l/well wash buffer before 15 min incubation with 100 μ l/well of 3,3',5,5'-tetramethylbenzidine (TMB) substrate solution (at room temperature). Finally, 50 μ l of stop solution (2M H₂SO₄) was added to each well and the plate was read at 450 nm using 570 nm as a reference using, a BioTeK EPOCH plate reader and Gen5 software. Standards were plotted using a log-log linear fit and only samples with absorbance readings falling in the linear area of the curve were quantified.

2.22 Data analysis

All data and associated statistics were analysed within GraphPad Prism® (version 5.0) with resultant graphical data and values in text as mean \pm standard error of the mean (s.e.m) of the number of experiments (n). All statistical analysis was performed using either unpaired or paired Student's t-tests or two-ANOVA analysis with a Bonferroni post-test. Correlation analysis was performed using Spearman correlation. $P < 0.05$ was set as a threshold for statistical significance, and where no P value is shown, $P > 0.05$.

**Chapter 3: CaMKII interaction
with and modulation of NF- κ B
signalling**

3.1 Introduction

Cardiac inflammation is a key feature of the stressed/injured myocardium, with augmented inflammatory signalling correlating with adverse patient outcome (Singh and Anderson, 2011). NF- κ B signalling has been implicated in modulating cardiac inflammation and fibrosis, although information on activation of this pathway in CFs is limited. Previous studies have highlighted a possible link between CaMKII and NF- κ B, however there is only very limited evidence for this link in the heart (Singh et al., 2009a). Cardiac-specific studies suggest that CaMKII may modulate NF- κ B signalling, however this has not been confirmed in adult cardiac cells nor has the underlying mechanism of modulation been explored. The possibility that this modulation may occur in cardiac cells other than myocytes has not been examined, even though ~70% of the cells in the myocardium are non-contractile CFs that contribute to pro-inflammatory signalling during cardiac disease (Manabe et al., 2002).

Based on findings from previous studies (Chapter 1, Section 1.12), it is possible that CaMKII may interact directly with specific components of the NF- κ B pathway. As illustrated in Figure 3.1, CaMKII δ could potentially interact with specific proteins and modulate the canonical NF- κ B pathway at one or more of four key areas. This could be at the level of (i) the upstream inhibitory κ B kinase kinase (IKKK), (ii) the IKK complex, interacting with IKK α , IKK β and/or IKK γ , (iii) the inactive cytosolic NF- κ B complex or, (iv) the transcriptionally active NF- κ B complex located within the nucleus. The most critical step in the activation of NF- κ B signalling is translocation of the NF- κ B dimers into the nucleus to regulate transcription. This is a highly regulated process involving many proteins that, with the exception of the IKKs, are either constitutively active or lack catalytic activity (Ghosh and Karin, 2002). Gene-targeting experiments have demonstrated that IKK β and IKK γ are absolutely required for pro-inflammatory induced NF- κ B activation (Ghosh and Karin, 2002), thus it could be argued that the major regulator of NF- κ B signalling is the activity of the tightly regulated IKK complex.

Activation of the catalytically active α and β subunits of the IKK complex requires association with a regulatory γ subunit (Ghosh and Karin, 2002). Although devoid of catalytic activity, IKK γ recognises Lys 63-linked polyubiquitin chains and

becomes itself ubiquitinated, and this is absolutely required for IKK activity and hence NF- κ B activation (Israel, 2010). Therefore, experiments outlined in this chapter will examine the potential interaction of CaMKII δ with all three subunits of the IKK complex. As illustrated in Figure 3.2, IKK α and IKK β have very similar structures and perhaps may therefore have overlapping function in the heart. To date, the possibility that CaMKII δ directly interacts with the IKK complex of the NF- κ B signalling pathway has not been explored.

Experiments presented in the current chapter explore CaMKII modulation of NF- κ B signalling at the level of the adult CF. The possibility that CaMKII may directly interact with specific components of NF- κ B signalling has been explored. Using purified proteins of the IKK complex, autoradiography and Surface Plasmon Resonance (SPR) analysis has highlighted the potential for specific and direct protein-protein interaction between CaMKII δ and NF- κ B signalling.

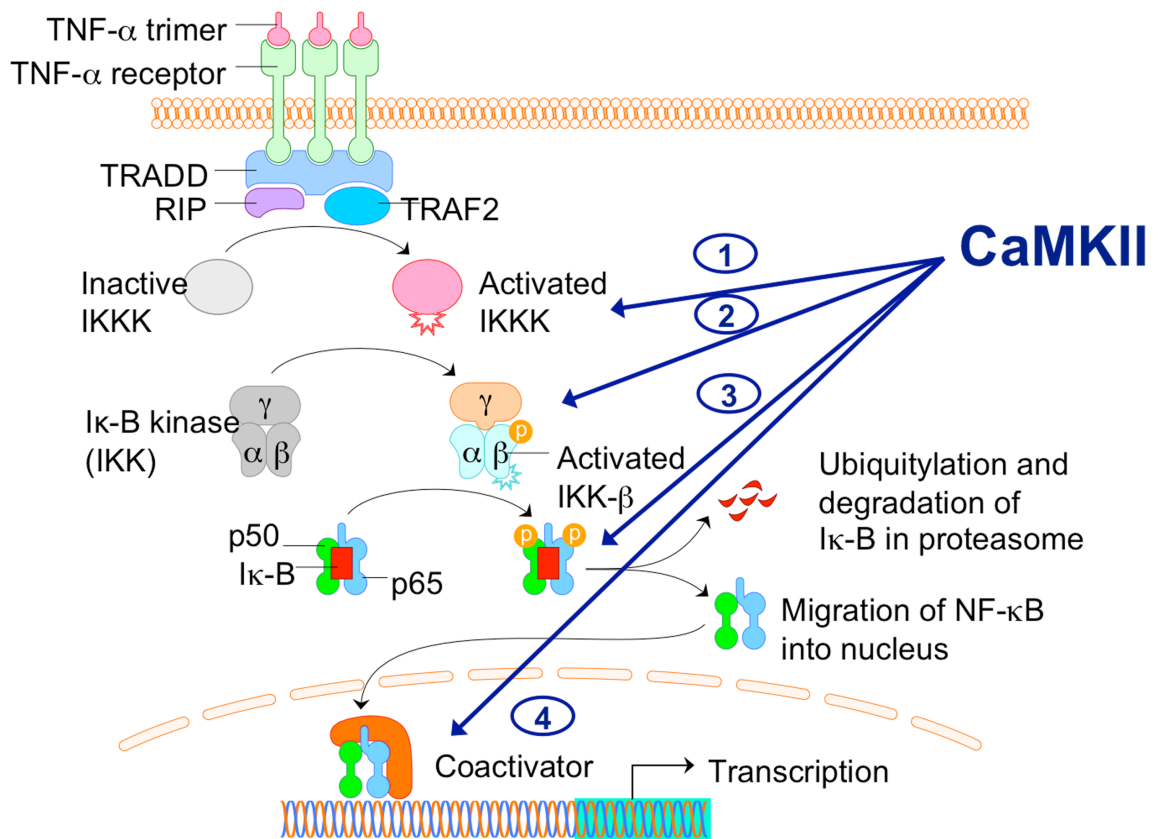


Figure 3.1 Potential modulation of the NF-κB signalling pathway by CaMKIIδ.

Schematic of the canonical NF-κB signalling pathway highlighting potential areas of interaction and modulation by CaMKIIδ. This could be at the level of (1) the upstream inhibitory κ B kinase kinase (IKKK), (2) the IKK complex consisting of the catalytically active subunits IKKα and IKKβ and the regulatory subunit IKKγ, (3) the inactive cytosolic NF-κB complex or (4) the activated NF-κB complex in the nucleus.

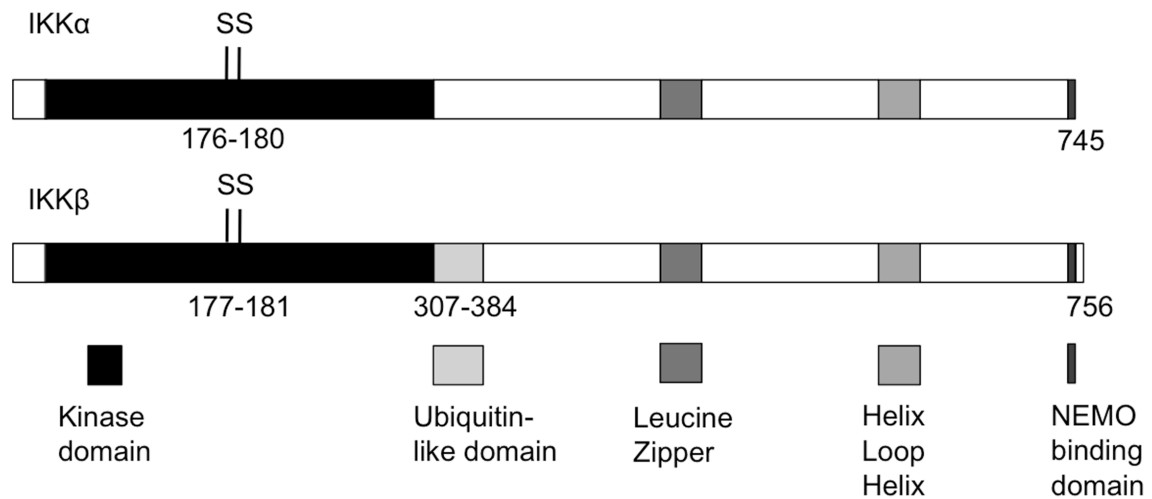


Figure 3.2 IKK α and IKK β subunit composition.

Schematic depicting the α and β subunits of the IKK complex highlighting the similarities between the kinase subunits. As illustrated, the kinase domains of IKK α and IKK β are located at the amino-terminus, followed by an activation loop (amino acids 176-180 in IKK α and 171-181 in IKK β). IKK β , but not IKK α , contains an ubiquitin-like structure (amino acids 307-384) located carboxy-terminal to the kinase domain, thought to be involved in the catalytic activity of kinase. A leucine zipper domain and a helix-loop-helix domain are present in both kinases to allow homo-or hetero-dimerisation of the kinases and modulation of kinase activity, respectively. At the extreme carboxyl-terminus of both kinases a \sim 40 amino acid region allows interaction with IKK γ /NEMO, referred to as the NEMO binding domain (NBD). Adapted from Israel, 2010).

3.2 Characterisation of cardiac fibroblasts by immunofluorescence

Adult CFs were isolated under sterile conditions using a chunk dissociation method and cultured at 37 °C in 5% CO₂ as described in the Chapter 2, Section 1.9.1. A typical fibroblast preparation is shown in Figure 3.3A. Immunofluorescence staining for anti-vimentin and α -smooth muscle actin (α -SMA) was used to verify that the isolated cells were indeed predominately CFs and cultures were free from contamination by smooth muscle cells or myo-CFs, respectively. Vimentin is an intermediate filament protein expressed in mesenchymal cell types (including fibroblasts) but replaced by desmin in non-vascular smooth muscle and striated muscle cells. Anti-vimentin antibodies react only with the abundant intermediate filaments of CFs and therefore can reliably identify cultures of CFs (Camelliti et al., 2005). Normal or ‘un-activated’ CFs do not express α -SMA, therefore staining for α -SMA will identify potentially contaminating smooth muscle cells. Colonic smooth muscle cells, isolated and cultured in parallel, were used as a positive control for α -SMA staining.

As illustrated in Figure 3.3B, CFs in culture express vimentin and there is no background staining of the CFs with α -SMA (Figure 3.3C), compared to control staining of colonic smooth muscle cells (Figure 3.3D), indicating that there is no contamination with smooth muscle cells. Note the DAPI counter-stain in the mounting medium stained the cells’ nucleus blue. Cells were kept in culture for up to two weeks with only one passage (subsequent passages show phenotypic changes and myo-CF appearance) before use for protein analysis or cell stimulation.

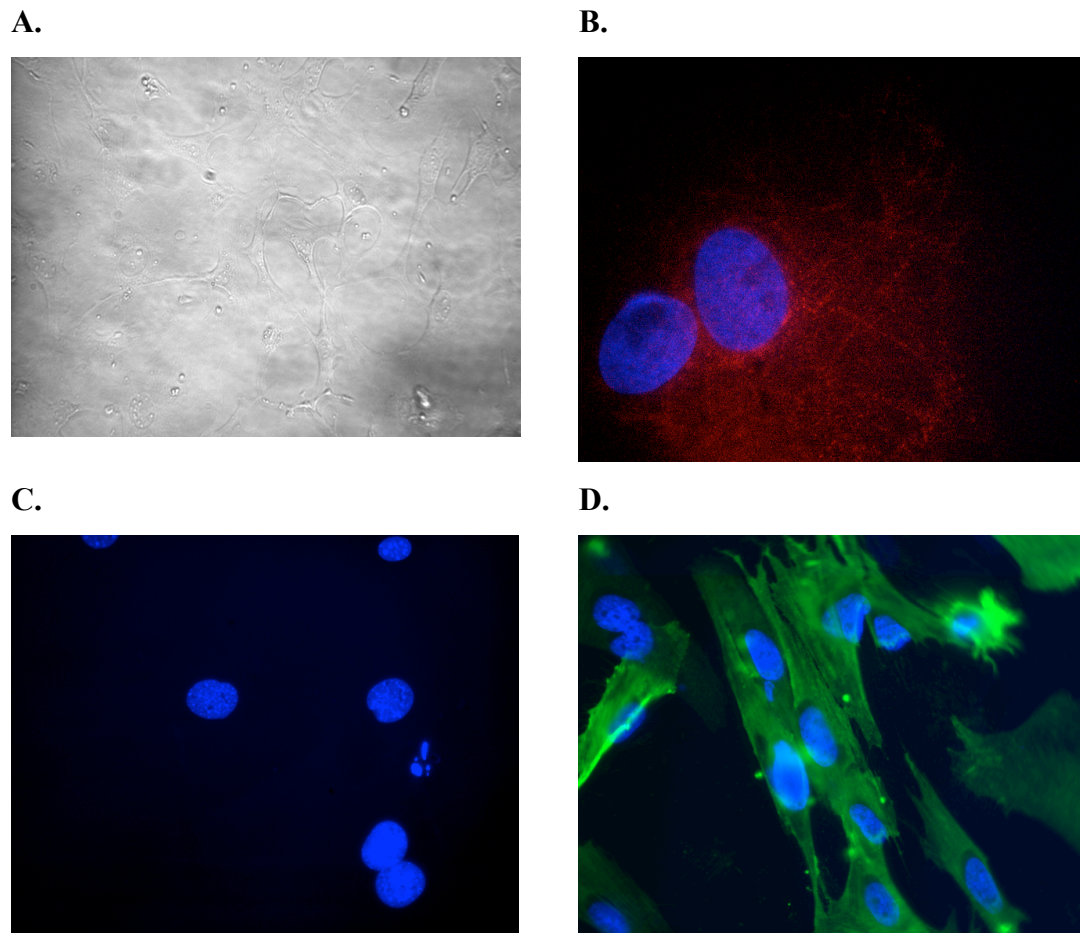


Figure 3.3 Characterization of cardiac fibroblasts by immunofluorescence.

Adult murine CFs were maintained in culture at 37 °C, 5% O₂ until cells were 80-100% confluent (A. magnification X 200). Cells were fixed to plain cover slips, permeabilised with Triton X 100 and incubated with anti-vimentin (B) or α -smooth muscle actin antibody overnight at 4°C (C). Panels C. and D. show fibroblasts and colonic smooth muscle cells, respectively, stained for α -smooth muscle actin (green). The DAPI counter-stain in the mounting medium stained the cells' nucleus blue. Data from an individual experiment, typical of two others.

3.3 Characterising antibody specificity for CaMKII δ and NF- κ B signalling proteins in mouse cardiac preparations

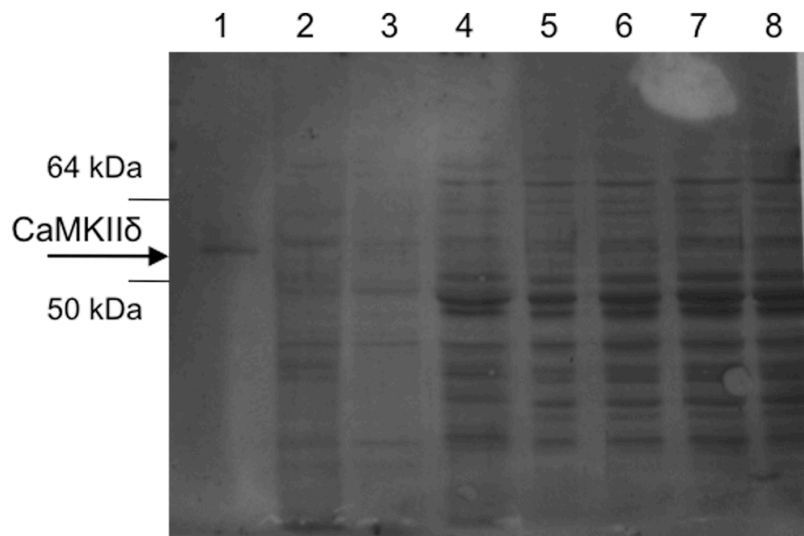
Protein detection, interaction and quantification require the use of highly specific antibodies. For this study, it was important at the outset to verify the selectivity of antibodies directed against CaMKII δ and components of the NF- κ B signalling pathway. As some future experiments would use CF preparations, it was essential to establish the detection of these proteins in CFs as well as in whole heart homogenate (WH) preparations. Importantly, to our knowledge, this is the first time these proteins have been examined in CFs.

3.3.1 CaMKII δ

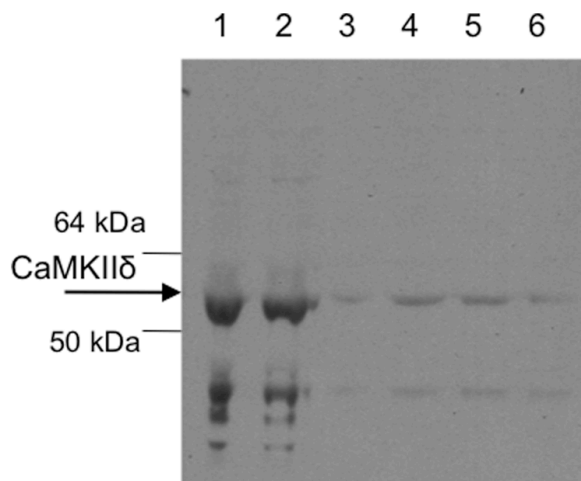
To enable detection (and future quantification, see Chapter 5) of CaMKII δ expression in heart preparations, an antibody raised to an epitope specific to CaMKII δ was sought. Various antibodies from different companies were tested on a range of preparations including WH and isolated CFs and myocytes. All antibodies were tested at a variety of recommended concentrations and under different buffer conditions as described in Chapter 2, Section 2.15.

Commercially available CaMKII δ antibodies tested included, i) Abgent rabbit polyclonal (U.S.A. Cat. # AP7209a) diluted 1:2000, ii) R & D Systems mouse monoclonal (U.K; Cat. # MAB4176) diluted between 1:500 -1:1000, and iii) Santa Cruz (U.S.A.; Cat. # sc-5392) goat polyclonal diluted between 1:500-1:1000. All antibodies displayed low specificity for CaMKII δ in mouse heart preparations, with a typical immunoblot shown in Figure 3.4A. The final antibody tested was a custom made rabbit polyclonal (Eurogentec, U.K.) diluted 1:500 (Huke and Bers, 2007). The high specificity of this antibody is exemplified in Figure 3.4B. This antibody detects three bands very close together in WH preparations representing three of the four splice variants of the δ isoform of CaMKII expressed in the heart; namely the cytosolic δ_C , the nuclear δ_B , δ_D and δ_I isoforms. The custom made CaMKII δ was used at a concentration of 1:500 for all subsequent immunoblot experiments.

A.



B. (i)



(ii)

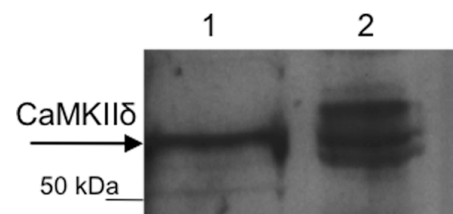


Figure 3.4 Specificity of commercially available anti-CaMKIIδ antibodies.

Panel A. Typical immunoblot probed with an anti-CaMKIIδ produced by Santa Cruz. Samples tested include: lane 1= 100 ng recombinant CaMKIIδ, lane 2= murine embryonic fibroblast, lane 3= adult cardiac fibroblast (CF, $\sim 10^4$ cells), lane 4= 20 μ g mouse WH and, lanes 5-8 = 10-40 μ g solubilised mouse WH. Panel B. Typical immunoblot probed with custom made anti-CaMKIIδ antibody (Eurogentec). Samples tested include: (i) lane 1 and 2= $\sim 10^4$ – 10^6 myocytes and lanes 3-6= 10-40 μ g mouse WH, (ii) lane 1= $\sim 10^4$ CF and lane 2= 20 μ g mouse WH. Pre-stained protein markers were included in all immunoblots to determine the molecular weight of stained proteins.

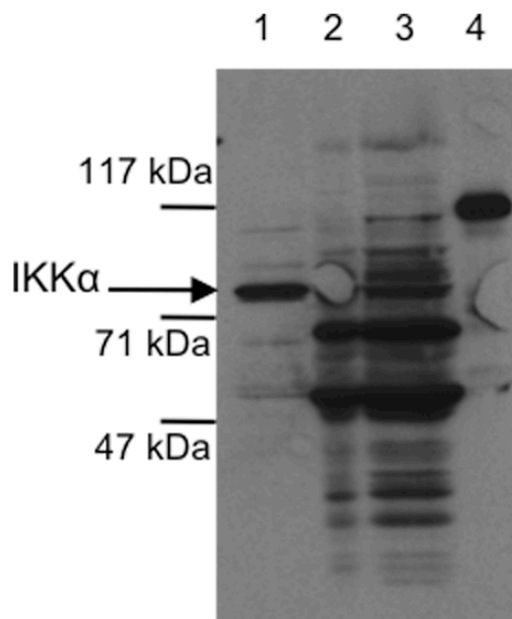
3.3.2 *IKK α*

To enable detection (and future quantification, see Chapter 5) of *IKK α* expression in WH and isolated CF and myocytes, an antibody that specifically detects *IKK α* in mouse heart was required. Three different *IKK α* antibodies from different companies were tested simultaneously on a variety of preparations. Commercially available *IKK α* antibodies tested included, i) Santa Cruz rabbit polyclonal (U.S.A., Cat. # sc-7218) diluted 1:5000-1:10000, ii) Santa Cruz rabbit polyclonal (U.S.A., Cat. # sc-7182) diluted 1: 5000-1:10000 and, iii) Calbiochem mouse monoclonal (U.K., Cat. # OP133) diluted 1:500. Both Santa Cruz *IKK α* antibodies were highly non-specific however the antibody produced by Calbiochem specifically detected *IKK α* with very little background, as illustrated in Figure 3.5. Diluting the Calbiochem antibody to 1:500 in TBST buffer and 5% non-fat dry milk, as described in Chapter 2 Section 2.15, enhanced the *IKK α* signal and reduced non-specific binding, therefore this antibody was used for all subsequent immunoblot experiments.

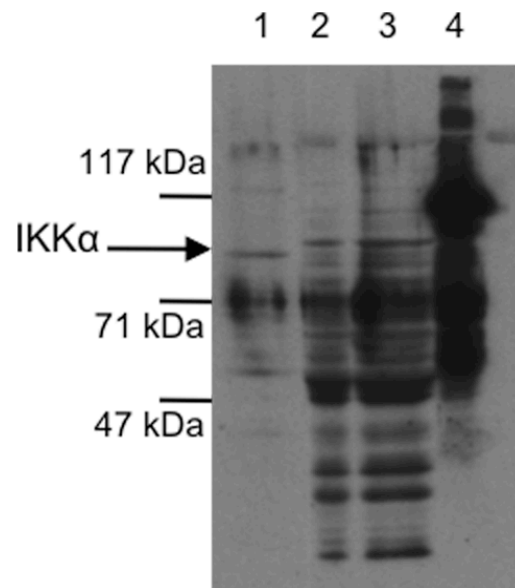
3.3.3 *IKK β*

Five *IKK β* antibodies from different companies were tested on mouse preparations in order to acquire an antibody that specifically detected *IKK β* with very little background. Commercially available *IKK β* antibodies tested included, i) Santa Cruz goat polyclonal (U.S.A., Cat. # sc-7329) diluted 1:5000-1:10000, ii) Santa Cruz rabbit polyclonal (U.S.A., Cat. # sc-7607) diluted 1:5000-1:10000, iii) Abcam (U.K., Cat. # sc-7607) diluted 1:1000-1:5000, iv) Imgenex mouse monoclonal (U.S.A., Cat. # IMG-129A) diluted 1:1000 and, v) Calbiochem mouse monoclonal (U.K., Cat. # OP134) diluted 1:500. All antibodies tested either did not detect anything or were highly non-specific for *IKK β* , with typical immunoblots shown in Figure 3.6. As illustrated in Figure 3.6C, *IKK β* is highly expressed in mouse CF and WH, however the anti-*IKK β* antibody (Calbiochem) used for this immunoblot proved inconsistent for subsequent immunoblotting despite antibody concentrations and buffer conditions remaining constant.

A.



B.



C.

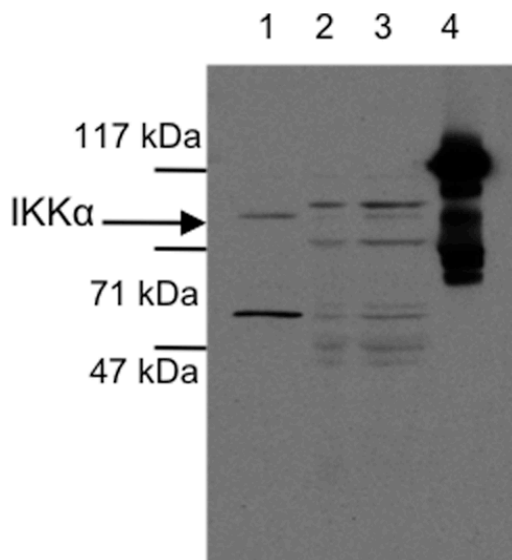


Figure 3.5 Specificity of commercially available anti-IKK α antibodies.

Mouse cardiac fibroblast ($\sim 10^4$ cells, lane 1), 20 μ g mouse whole homogenates (WH; lane 2), 30 μ g solubilised mouse WH (lane 3) and 10 ng recombinant GST-tagged IKK α (lane 4) were analysed by SDS-PAGE and membranes probed with either A- anti-IKK α at 1: 5,000 (Santa Cruz, Cat. # sc-7218), B- anti-IKK α at 1:5,000 (Santa Cruz, Cat. # sc-7182) or C. anti-IKK α (Calbiochem, Cat. # OP133) at 1: 500. Pre-stained protein markers were included in all immunoblots to determine the molecular weight of stained proteins.

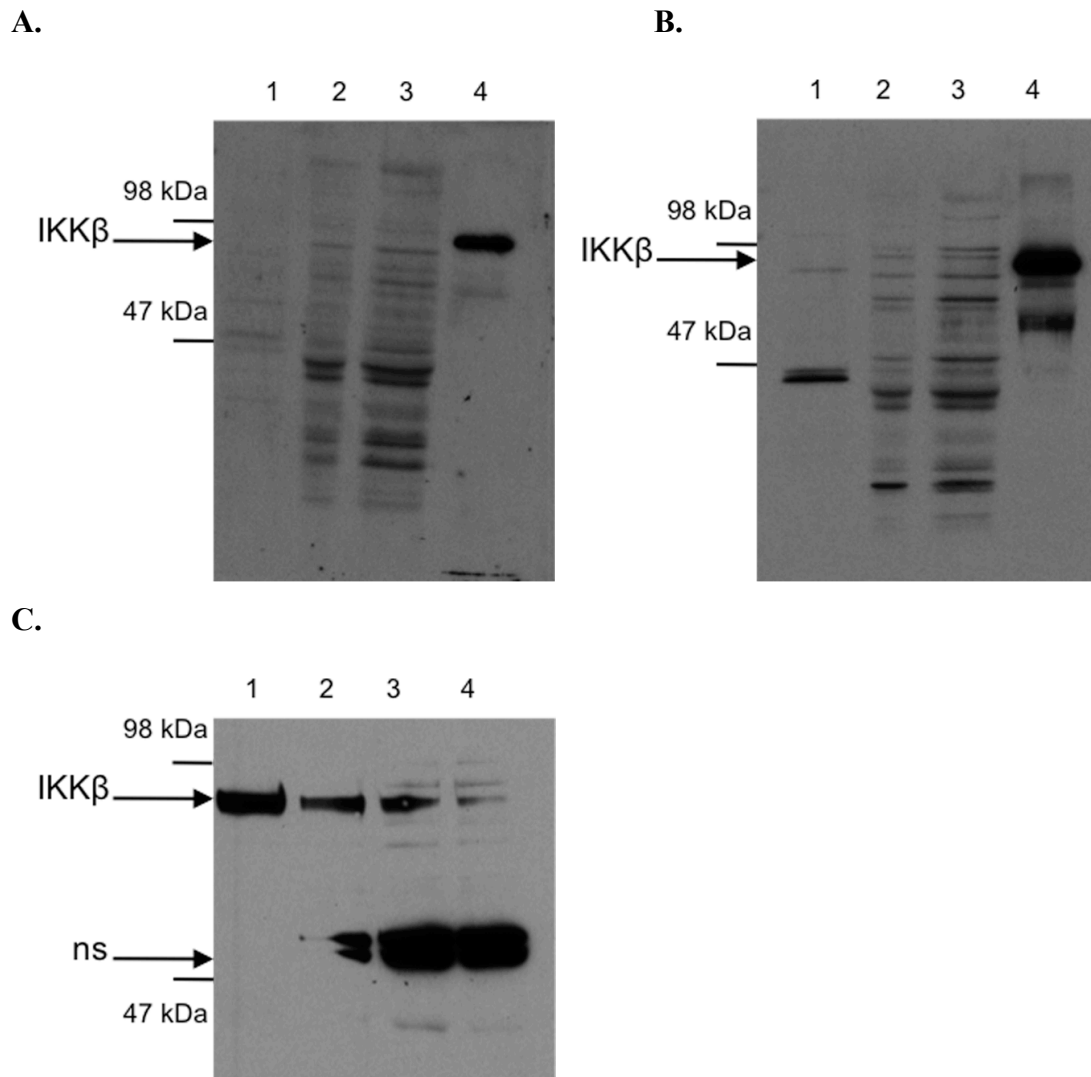


Figure 3.6 Specificity of commercially available anti-IKK β antibodies.

Panels A. and B. Mouse cardiac fibroblast (lane 1, $\sim 10^4$ cells), 20 μ g whole heart homogenate (lane 2), 30 μ g solubilised whole homogenate (lane 3) and 10 ng recombinant His-tagged IKK β were analysed by SDS-PAGE and membranes probed with either A- anti-IKK β at 1: 5000 (Santa Cruz, Cat. # sc-7329) or B- anti-IKK β at 1:5000 (Santa Cruz, Cat. # sc-7607). Panel C. 10 ng recombinant His tagged IKK β (lane 1), mouse cardiac fibroblast (lane 2, $\sim 10^4$ cells), 40 and 10 μ g whole heart homogenate, respectively (lanes 3 and 4). Membrane was probed with anti-IKK β at 1: 500 (Calbiochem, Cat. # OP134). Pre-stained protein markers were included in all immunoblots to determine the molecular weight of stained proteins. ns= non-specific.

3.3.4 *IKK γ*

An antibody with high specificity for IKK γ was required for protein interaction experiments, as mentioned previously. Commercially available IKK γ antibodies tested included, i) Santa Cruz rabbit polyclonal (Cat. # sc-8330) diluted 1:5000 and ii) Imgenex mouse monoclonal (Cat. # IMG-324A) diluted 1:1000. Both antibodies were able to detect IKK γ in a range of mouse heart preparations with high specificity, with a typical immunoblot shown in Figure 3.7.

3.3.5 *I κ B α*

As described in Chapter 1, the NF- κ B complex is sequestered to the cytosol due to association with the inhibitory subunit I κ B α . Degradation of the I κ B α subunit is required for NF- κ B activation and therefore I κ B α degradation can be used as a marker of activation of NF- κ B signaling. In order to determine whether adult CF can be used to investigate the functional effect of selective CaMKII δ inhibition on NF- κ B activity, an antibody that specifically detects I κ B α degradation with very little background was required. Two I κ B α antibodies produced by Cell Signalling Technology were tested (rabbit polyclonal Cat. # 9242 and mouse monoclonal Cat. # 4814). As illustrated in Figure 3.8, the mouse monoclonal I κ B α antibody detected I κ B α with high specificity, and was therefore used in all subsequent experiments at a concentration of 1:1000.

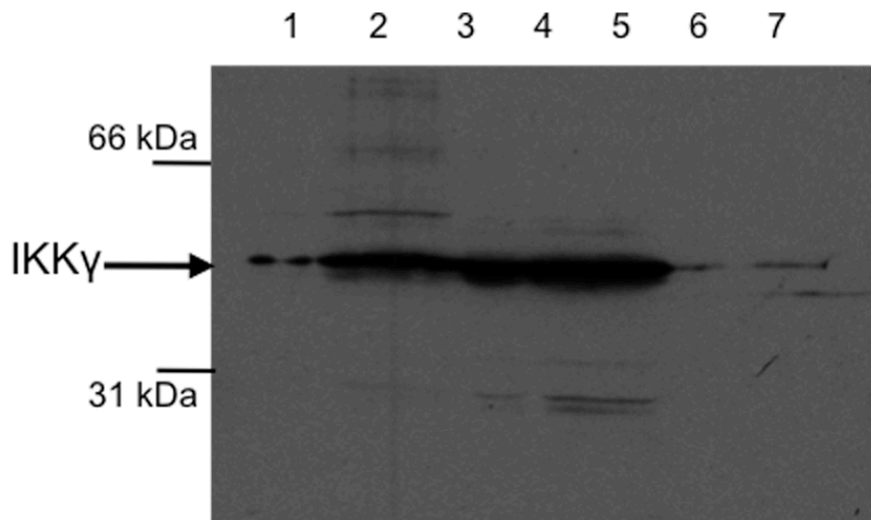


Figure 3.7 Specificity of commercially available anti-IKK γ antibodies.

10 and 20 μ g mouse whole homogenates (WH; lanes 1 and 2), 10, 20 and 40 μ g solubilised mouse WH (lanes 3-5) and $\sim 10^4 - 10^6$ cardiac fibroblasts (CFs; lanes 6 and 7) were analysed by SDS-PAGE and membranes probed with anti-IKK γ at 1: 500 (Imgenex, Cat. # IMG-324A). Pre-stained protein markers were included to determine the molecular weight of stained proteins.

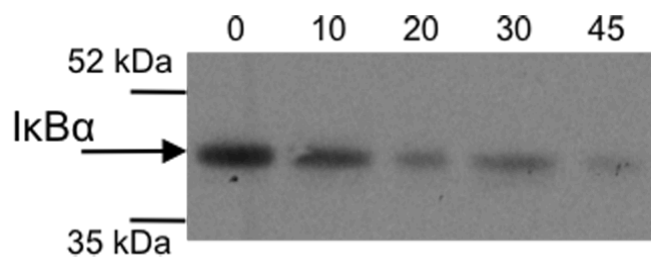


Figure 3.8 Specificity of commercially available anti-IκBα antibodies.

Adult CFs were treated with 5 $\mu\text{g/ml}$ LPS over a variable time course from 0 – 45 min. Reactions were stopped with Laemmli sample buffer and IκBα degradation was assessed by immunoblotting with anti-IκBα at 1:1000 (Cell Signalling Technology, Cat. # 4814). Pre-stained protein markers were included to determine the molecular weight of stained proteins.

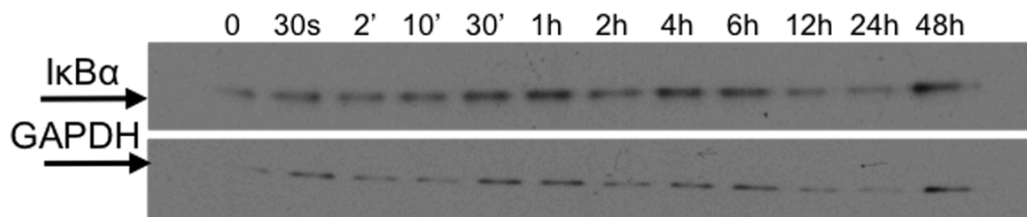
3.4 A functional role for CaMKII in NF- κ B signalling – effect of CaMKII inhibition on I κ B α degradation in stimulated cardiac fibroblasts

In order to establish whether CaMKII plays a role in the regulation of cardiac NF- κ B signalling, the effect of CaMKII inhibition upon agonist-induced I κ B α degradation was assessed using CFs. It was first essential to ensure that I κ B α degradation could be achieved via agonist stimulation of CF. It was also essential that the agonist of choice for this study resulted in marked degradation of I κ B α so that any potential reversal of degradation could be easily observed. Initially Ang II (0.1-1 μ M) and ET-1 (0.1-1 μ M) were tested, however limited I κ B α degradation was observed with these agonists (Figure 3.9A and B, respectively). Studies therefore used LPS as it is known to be a potent inducer of NF- κ B activation in neonatal mouse myocytes (Hall et al., 2005, Singh et al., 2009a).

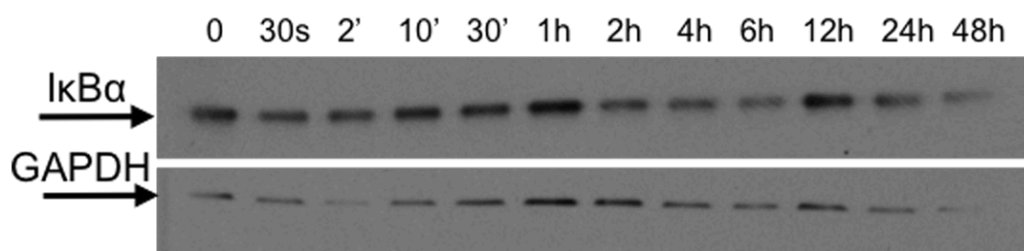
CF (p1) stimulated with 5 μ g/ml LPS resulted in significant I κ B α degradation over the time course tested. A representative time-course for degradation of I κ B α and therefore corresponding activation of NF- κ B signalling in the presence of LPS is shown in Figure 3.9C). Potential involvement of CaMKII in modulation of this pathway was explored by using the CaMKII peptide inhibitor autocamtide-2 inhibitory peptide (AIP). AIP was used at a final concentration of 5 μ M which has previously been shown to result in 95-100% inhibition of CaMKII activity in rabbit cardiac preparations (Currie et al., 2004). When cells were pre-treated for 1 h with AIP, I κ B α degradation in response to LPS was significantly inhibited (Figure 3.10A and B) and this was sustained at 30 minutes and 40 minutes of stimulation before the response returned to control levels after 60-120 minutes. In some cell preparations inhibition of I κ B α degradation by AIP was still evident after 60 minutes, such as in the sample immunoblot shown in Figure 3.10A.

For the first time this data highlights the potential role for CaMKII in regulating agonist-induced I κ B α degradation and corresponding activation of NF- κ B signalling in CFs.

A.



B.



C.

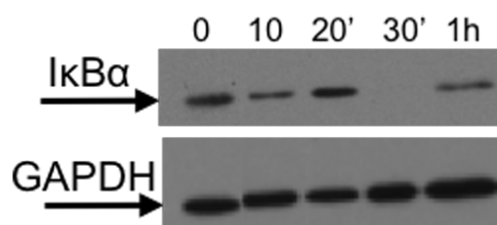
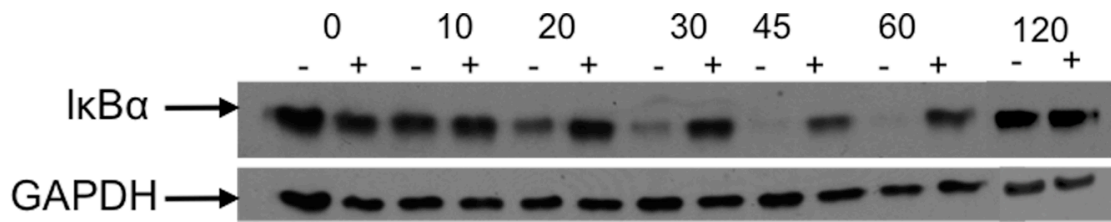


Figure 3.9 Agonist-induced IκBα degradation in adult cardiac fibroblasts.

Representative immunoblots of cardiac fibroblasts (CFs) exposed to 1 μM Ang-II (A), 1 μM ET-1 (B) or 5 μg/ml LPs (C) for the indicated periods of time. Reactions were stopped with Laemmli sample buffer and IκBα degradation was assessed by immunoblotting, used GAPDH as an internal loading control. Pre-stained protein markers were included to determine the molecular weight of stained proteins (data not shown).

A.



B.

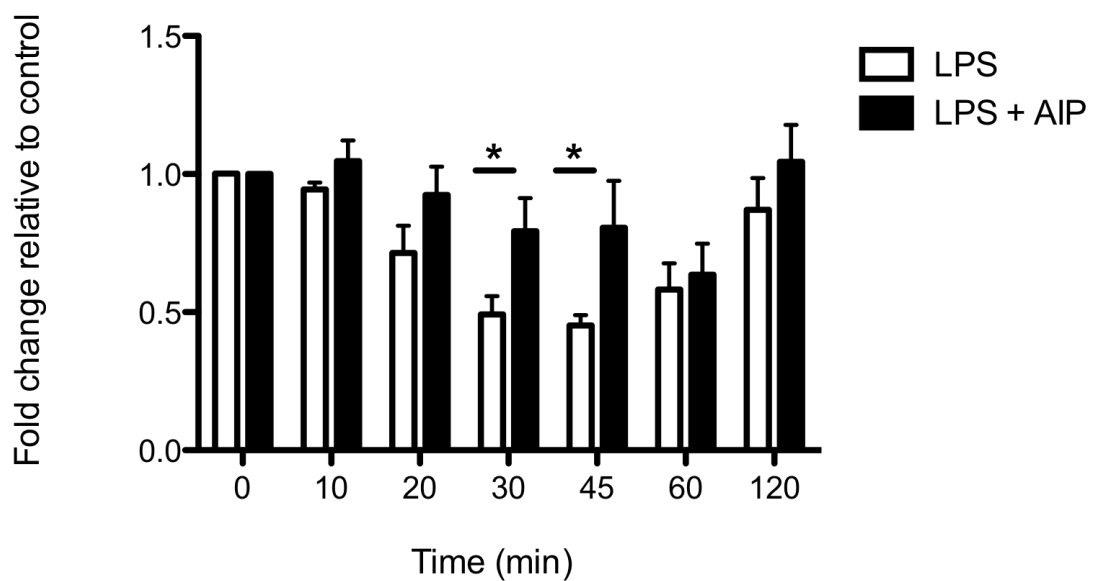


Figure 3.10 LPS-induced IκBα degradation in cardiac fibroblasts is reversed following CaMKII inhibition.

Cardiac fibroblasts (CFs) were exposed to LPS (5 μg/ml) for the indicated periods of time. Stimulations were performed in the presence and absence of pre-treatment with AIP (5 μM) and reactions stopped with Laemmli sample buffer. IκBα degradation was assessed by immunoblotting and quantified against an internal loading control, GAPDH. A representative immunoblot is shown (A). Densitometric analysis of immunoblots was performed (B), with data from 4 independent experiments expressed as means ± s.e.m. *p < 0.05 from the non-inhibited control reaction.

3.5 Investigation of CaMKII δ interaction with specific components of the NF- κ B signalling pathway using immunoprecipitation

Having established that CaMKII plays a functional role in activation of NF- κ B signalling, investigation of how this functional interaction may occur was important. Potential protein targets within the NF- κ B signalling pathway for CaMKII were examined using immunoprecipitation. Initial studies examining the potential for CaMKII δ -NF- κ B protein interaction focused on co-immunoprecipitation. Whole cardiac homogenates were used initially due to the high total protein concentration in these preparations, with further studies examining potential CaMKII δ -NF- κ B in cellular preparations (CFs and myocytes).

3.5.1 Introduction to immunoprecipitation

Immunoprecipitation uses a specific antibody to separate and identify one protein from a total protein preparation, for example isolating CaMKII δ from WH preparations. If the targeted protein is bound to other proteins as part of a complex, then these will also be ‘pulled-out’ by the antibody, for example using an antibody specific for IKK γ to immunoprecipitate the entire IKK complex, or to elucidate whether it is part of a larger complex of proteins. In this way it is possible to ‘pull-out’ of solution the known protein and anything else that is bound to it. Immunoblotting unknown components of the complex can then be performed to identify binding partners; a process referred to as co- immunoprecipitation.

3.5.1.1 Factors that determine the success of immunoprecipitating a protein

3.5.1.1.1 Lysis buffer composition

The key aim of these experiments was to immunoprecipitate intact protein complexes (i.e. CaMKII δ and components of NF- κ B signalling). This is only feasible if the proteins interact with each other with high affinity and the protein-protein interactions are intact during the immunoprecipitation process. Prior to formation of

antigen-antibody complexes, the antigen must first be extracted from the tissue or cell sample with minimal effect on its structural integrity so that it is in a form that is recognisable by the antibody. It is vital that the lysis buffer will leave proteins in their native conformation, thus the composition of the lysis buffer is crucial, particularly the type of detergent used. In general, non-ionic (e.g. Triton X-100, NP-40, Brij 35) detergents are relatively mild and tend to preserve non-covalent protein-protein interactions. Ionic detergents (e.g. SDS, sodium deoxycholate) are generally harsher agents that tend to denature protein-protein interactions and so may adversely affect the ability of the antibody to recognise and bind to its target antigen.

3.5.1.1.2 Precipitation of immune complexes

Protein A or G (bacterial proteins from *Staphylococcus aureus* and Group G Streptococci, respectively) coupled to insoluble resin such as sepharose beads are commonly used to capture antigen-antibody complexes. The affinity of Protein A or G for an antibody depends on the species and subclass of the immunoglobulin (IgG). Generally Protein G has greater affinity for polyclonal IgG and binds a broader range of IgG from eukaryotic species as well as binding more subclasses of IgG than Protein A. When using mouse or rabbit antibodies, as is the case in these experiments, Protein G coupled to sepharose beads is reportedly the best solid-phase support to use for immunoprecipitation. For SDS-PAGE analysis, loading buffer is used to elute the antigen-antibody complexes from the Protein G beads. As the loading buffer is a harsh elutant it will also elute any non-covalently bound antibody and antibody fragments, which will appear on the subsequent immunoblots.

3.5.1.1.3 Method for immunoprecipitation

There are two general methods for immunoprecipitation, (i) direct capture and (ii) indirect capture. The direct capture method involves affinity capturing the selected antibody onto Protein A/G sepharose beads. The immobilised antibody is then incubated with the protein mixture and used for capture and enrichment of the protein of interest. The indirect method involves incubation of the antibody of choice with the protein mixture, and after some time (~12 h) this is followed by incubation

with Protein A/G sepharose beads. Any antigen-antibody complexes present will bind to the sepharose beads.

3.5.2 Immunoprecipitation using a variety of mouse heart preparations

Immunoprecipitation experiments were unsuccessful in isolating IKK α , β or γ , or CaMKII δ , possibly due to the non-specific nature of some of the currently available antibodies against components of NF- κ B signalling and CaMKII δ , as described above.

Initial experiments focused on isolating IKK γ from a variety of preparations including WH, CFs and myocytes. The rationale for doing this is because IKK γ exists in a complex with IKK α and IKK β (Ghosh and Karin, 2002), so if IKK γ is successfully immunoprecipitated essentially the whole complex will have been immunoprecipitated. Immunoblotting precipitates for CaMKII δ (co-immunoprecipitation) would provide information on whether CaMKII δ interacts with the IKKs at the level of the IKK complex.

As highlighted in Table 3.1, many different combinations of conditions were tested on a range of preparations, however most results were negative (i.e. IKK γ could not be precipitated) or only a small proportion of IKK γ could be isolated. Results were also compromised by the presence of non-specific binding in the negative control preparation, as highlighted by the immunoblot presented in Figure 3.11 (lane 3). Non-specific binding is more likely to occur with WH preparations as they contain a vast array of different proteins. Using solubilised cell preparations with fewer proteins can help to avoid this non-specific binding. However, when isolated CF preparations were examined in these experiments the overall protein concentrations were too low to allow precipitation of IKK γ . Isolated myocytes were also examined and although protein concentrations were higher, experiments still yielded negative results, as highlighted in Table 3.1. In co-immunoprecipitation experiments immunoblotting IKK γ precipitates for CaMKII δ , it was too difficult to determine whether CaMKII δ co-immunoprecipitated with IKK γ due to the similar migration pattern of CaMKII δ (~56 kDa) and the heavy chain of the antibody (~50 kDa). This occurred because both the antibody used for immunoprecipitation and for

immunoblotting were of rabbit origin. To get around this issue, one species of antibody should be used for the immunoprecipitation procedure (e.g. rabbit) and a different species used for immunoblotting (e.g. mouse). As specific anti-CaMKII δ mouse monoclonal antibodies were unavailable for immunoblotting, immunoprecipitation experiments using a mouse monoclonal anti-IKK γ were conducted, however results were negative.

For these reasons, further experiments were designed to immunoprecipitate the catalytically active components of the IKK complex, with experiments focusing on IKK α as initial attempts to immunoprecipitate IKK β failed, possibly due to the highly non-specific nature of commercially available IKK β antibodies, as discussed in Section 3.3.2. Immunoprecipitation of IKK α was examined using a variety of preparations and immunoprecipitation protocol conditions (e.g. different lysis buffer compositions and direct capture versus indirect capture method), as described in Chapter 2, Section 1.16. Findings were similar to those for IKK γ . IKK α could either not be precipitated or only a very small proportion of IKK α was isolated with results compromised by the presence of non-specific binding in the negative control sample.

Further experiments were designed to immunoprecipitate CaMKII δ using the custom made anti-CaMKII δ antibody. Several different immunoprecipitation protocols and conditions (e.g. Protein G-sepharose beads versus Protein A-sepharose beads) were tested, including a protocol published previously (Huke and Bers, 2007) that used exactly the same CaMKII δ antibody. Results were similar to those for the IKK proteins, with many attempts to isolate CaMKII δ resulting in negative results. Analysis of precipitated CaMKII δ was also hindered due to the similar migration pattern of CaMKII δ and the heavy chain of the antibody and, due to the lack of specific CaMKII δ antibodies of an alternate species, this issue could not be resolved.

Antibody	Preparation	Protocol	Result
IP: Santa Cruz Cat. # sc-8330 IB: Imgenex Cat. # IMG-324A	CF	Protocol 3, direct and indirect capture tested (MacKenzie et al., 2007)	Negative
IP: Santa Cruz Cat. # sc-8330 IB: Imgenex Cat. # IMG-324A	Myocytes	Protocol 3 (MacKenzie et al., 2007)	Negative
IP: Santa Cruz Cat. # sc-8330 IB: Imgenex Cat. # IMG-324A	WH	Protocol 1 (Currie et al., 2004)	Negative
IP: Santa Cruz Cat. # sc-8330 IB: Imgenex Cat. # IMG-324A	WH	Protocol 3, direct and indirect capture tested (MacKenzie et al., 2007)	<ul style="list-style-type: none"> - Positive but signal very weak. - Non-specific binding. - Unable to co-IP for CaMKII due to low signal. - CaMKII kinase assay did not work due to low recovery of IKKγ.

Table 3.1 Immunoprecipitation of IKK γ from a variety of mouse heart preparations.

In all experiments shown, anti-IKK γ antibody produced by Santa Cruz was used for the immunoprecipitation procedure (IP) and anti-IKK γ antibody produced by Imgenex was used for immunoblotting (IB) to verify that IKK γ was precipitated from a variety of solubilised heart preparations including cardiac fibroblasts (CFs), myocytes and solubilised whole heart homogenate (WH).

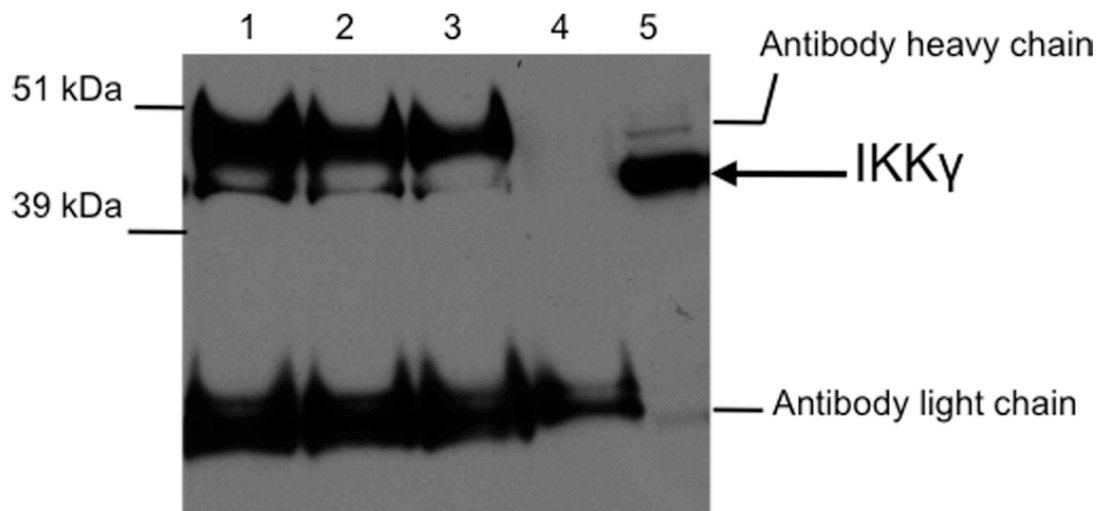


Figure 3.11 Immunoprecipitation of IKK γ from solubilised whole heart tissue.

A rabbit polyclonal anti-IKK γ antibody was used for the immunoprecipitation procedure and a mouse monoclonal anti-IKK γ antibody (Imgenex, Cat. # IMG-324A) was used for immunoblotting to verify that IKK γ was precipitated from solubilised whole heart preparations. Lane 1= 1 mg solubilised heart supernatant (s/n) + antibody, lane 2= 0.5 mg solubilised s/n + antibody, lane 3= 0.5 mg solubilised s/n – antibody (negative control), lane 4= no preparation (just solubilisation buffer) + antibody (negative control), lane 5 = 20 μ g solubilised s/n not subjected to IP (positive control). Pre-stained protein markers were included in all immunoblots to determine the molecular weight of stained proteins.

3.6 Investigation of CaMKII δ phosphorylation of specific components of the NF- κ B signalling pathway

As the commercially available antibodies against the IKK proteins proved inconsistent for immunoprecipitation analysis, the use of recombinant or purified proteins was employed to explore the potential for interaction between CaMKII and selected components of NF- κ B signalling. To assess whether CaMKII δ interacts with and phosphorylates specific IKK components of the NF- κ B signalling pathway, CaMKII δ (30 ng) was incubated with either IKK α or IKK β (each at 100 ng) in the presence of 50 μ M ATP/5 μ Ci 32 P-ATP. Subsequent phosphorylation was monitored by incorporation of radioactive phosphate.

Incubation of CaMKII δ with IKK α and β in the presence of [32 P]-ATP resulted in phosphorylation of all of these protein components, as illustrated in Figure 3.12 (lanes 1, 3 and 4, respectively). It is important to note that both CaMKII δ and the IKKs are capable of autophosphorylation therefore the intensity of phospho-signal could reflect differences in CaMKII-mediated phosphorylation (in the case of CaMKII δ (autophosphorylation) and the IKKs) and/or could show evidence for IKK autophosphorylation (in the case of the IKKs). To explore this possibility further, these reactions were repeated, but in the presence of the CaMKII inhibitor peptide AIP (5 μ M). It was reasoned that AIP would inhibit CaMKII-mediated phosphorylation of both CaMKII δ and the IKKs but will not affect autophosphorylation of IKKs, so any decrease in signal intensity following AIP treatment would only be due to CaMKII-mediated effects.

As anticipated, inclusion of AIP markedly reduced any autophosphorylation of CaMKII δ (Figure 3.12, lane 2). Interestingly the addition of AIP also significantly inhibited the phosphorylation of IKK β but not that of IKK α (Figure 3.12, lanes 6 and 5, respectively). It was also apparent that incubation of IKK α or IKK β with AIP in the absence of CaMKII δ had no effect on IKK autophosphorylation (data not shown). These data suggest that the phosphorylation signal associated with IKK α is due primarily to autophosphorylation but phosphorylation associated with IKK β is at least partly due to CaMKII δ -mediated phosphorylation. This highlights the possibility that CaMKII δ preferentially associates with and phosphorylates IKK β and this could be a possible target substrate for CaMKII δ in modulation of NF- κ B signalling.

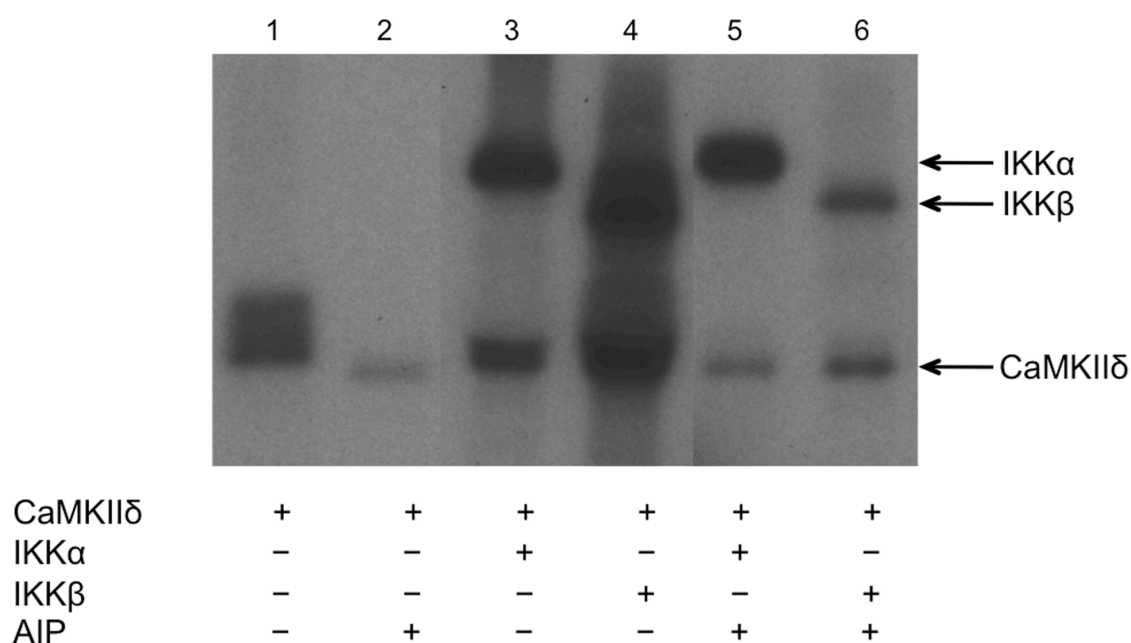


Figure 3.12 CaMKIIδ shows preferential phosphorylation of IKKβ over IKKα. CaMKIIδ (30 ng) was incubated with either IKKα (100 ng) or IKKβ (100 ng) at 30 °C for 30 minutes in the presence of 50 μM ATP/5 μCi ³²P-ATP and in the presence or absence of autocamide II related inhibitory peptide (AIP; 5 μM final concentration). All reaction mixtures contained 40 μg/ml calmodulin and 1.5 mM CaCl₂. Equivalent loads of sample were subjected to electrophoresis and incorporation of phosphate into CaMKIIδ and IKKs was detected using autoradiography.

3.7 Surface Plasmon Resonance

Surface Plasmon Resonance (SPR) studies were performed to assess the potential for direct protein-protein interactions between CaMKII δ and individual components of the IKK complex (IKK α , β and γ), using recombinant purified proteins. Although it appears more likely that direct CaMKII modulation of the active kinase component of the IKK complex (i.e. IKK α and IKK β) would affect NF- κ B signalling, IKK γ was included in these experiments to obtain a thorough analysis of the IKK complex. Although only a scaffolding protein, the possibility exists that CaMKII δ may bind to IKK γ , leading to conformational (and potentially functional) changes in the IKK complex.

3.7.1 Ligand immobilisation

In these studies the method for protein immobilisation to a sensor chip surface was direct immobilisation via amine coupling. This process involves activation of the carboxy groups of the carboxymethylated dextran matrix on the sensor chip surface with a mixture of 0.2 M EDC and 0.05 NHS to form succinimidyl esters, as described in Chapter 2, Section 1.18.2. These ester groups spontaneously react with any primary amine or other nucleophilic groups present on the ligand thus linking the ligand covalently to the dextran matrix. Excess succinimidyl esters are then deactivated using ethanolamine.

CaMKII δ was the protein chosen for immobilisation onto the sensor chip surface, because the (i) the running buffer used (Chapter 2, Section 2.18.2) and (ii) the immobilisation conditions including buffers, pH and temperature have all been previously optimised for this protein (Brocke et al., 1999, Verzili et al., 2000, Anthony et al., 2007). More importantly however, it is recommended that the immobilised protein should be the protein with the lower molecular weight, with the higher molecular weight protein used as the analyte. The rationale behind this is that greater mass of the higher molecular weight protein would be bound to the ligand on the chip surface at any given concentration of analyte, resulting in increased sensitivity in detection of protein-protein interaction (Beattie et al., 2008).

In order to immobilise CaMKII δ onto a sensor chip it is essential that the pH of the acetate buffer is one or two points below the isoelectric point (pI) of the protein. Therefore CaMKII δ with a pI value of 6.1 was diluted in pH 4.5 acetate buffer for immobilisation, as characterised previously (Anthony et al., 2007). As mentioned in Chapter 2, Section 2.18.2, Biacore systems have pairs of flow cells with serial flow direction. By immobilising the experimental protein on to one flow cell and either a control protein or no protein on to the other flow cell, an experimental sample can be directly compared with a control sample. In these experiments, CaMKII δ was immobilised onto flow cell 2 (Fc 2) of a CM5 sensor chip surface to a density of 7-8 pg/mm² of protein. As illustrated in Figure 3.13, protein immobilisation is represented by a gradual increase in RUs from the start of injection of CaMKII δ to the end of the injection. As an internal negative control to take into account any non-specific binding that may occur at the sensor chip surface, bovine serum albumin (BSA) was immobilised to the same density as CaMKII δ onto Fc 1. All results shown in the sensorgrams were thus subjected to a parallel subtraction between Fc 1 and Fc 2.

3.7.2 Determination of CaMKII δ Immobilisation and Reactivity

Before studying the interaction of CaMKII δ with members of the NF- κ B pathway, it was essential to determine whether (i) CaMKII δ was indeed immobilised onto the sensor chip and, (ii) CaMKII δ was active and functionally capable of protein binding. To assess these factors initial interaction experiments were performed using calmodulin as a positive control analyte. Calmodulin is a 16.7 kDa Ca²⁺ binding protein that is involved as a co-factor in the activation of CaMKII δ . If CaMKII δ is indeed immobilised onto the sensor chip and is active, then calmodulin should interact with high affinity. For these experiments, it was determined that approximately 7-8 pg/mm² of immobilised CaMKII δ would provide sufficient ligand for observation of an interaction with calmodulin. As expected and illustrated in Figure 3.14, the sensorgram shows the concentration-dependent (0.0125- 0.20 μ M) manner of calmodulin binding with CaMKII δ , demonstrating that there is a clear interaction between these proteins. These data suggest that CaMKII δ is immobilised correctly and is functionally capable of protein binding.

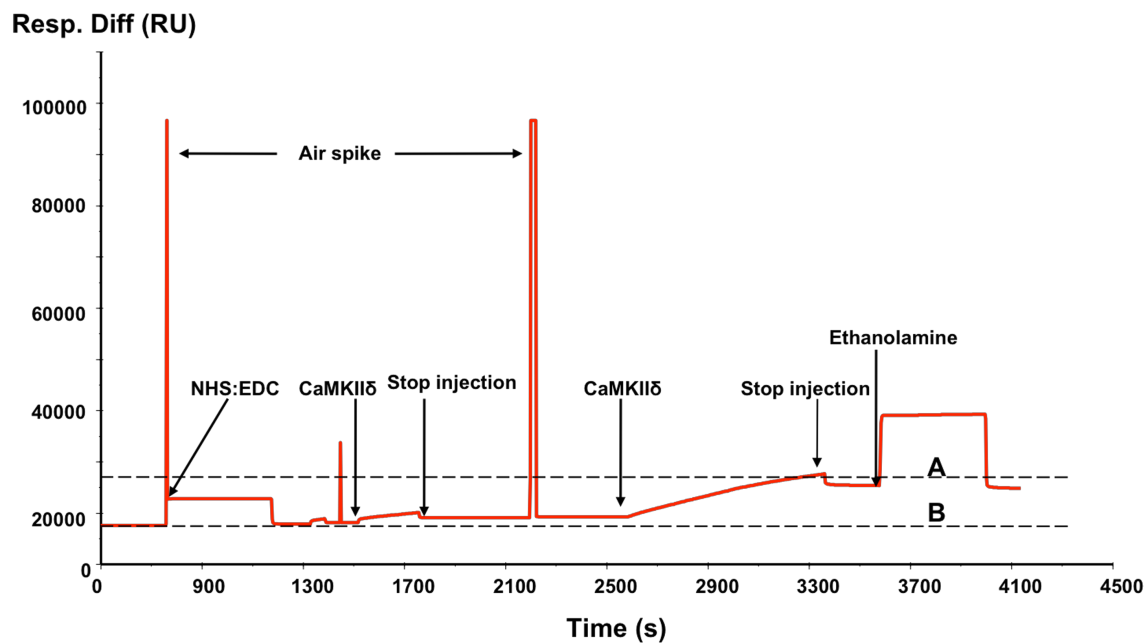


Figure 3.13 Immobilisation profile of CaMKII δ .

Typical sensorgram (Fc 2) depicting immobilisation of CaMKII δ onto a CM5 sensor chip to a density of approximately 7 - 8 $\mu\text{g}/\text{mm}^2$ protein. Firstly the chip is activated with an injection of 1:1 NHS: EDC solution, followed by CaMKII δ injection. CaMKII δ injection can be stopped and started again in order to achieve the optimum amount of protein immobilisation, as shown in the sensorgram where immobilisation was performed in two stages. The final step is deactivation of the chip surface with injection of 1 M ethanolamine pH 8.5. The difference between lines A and B represents the amount of ligand immobilised.

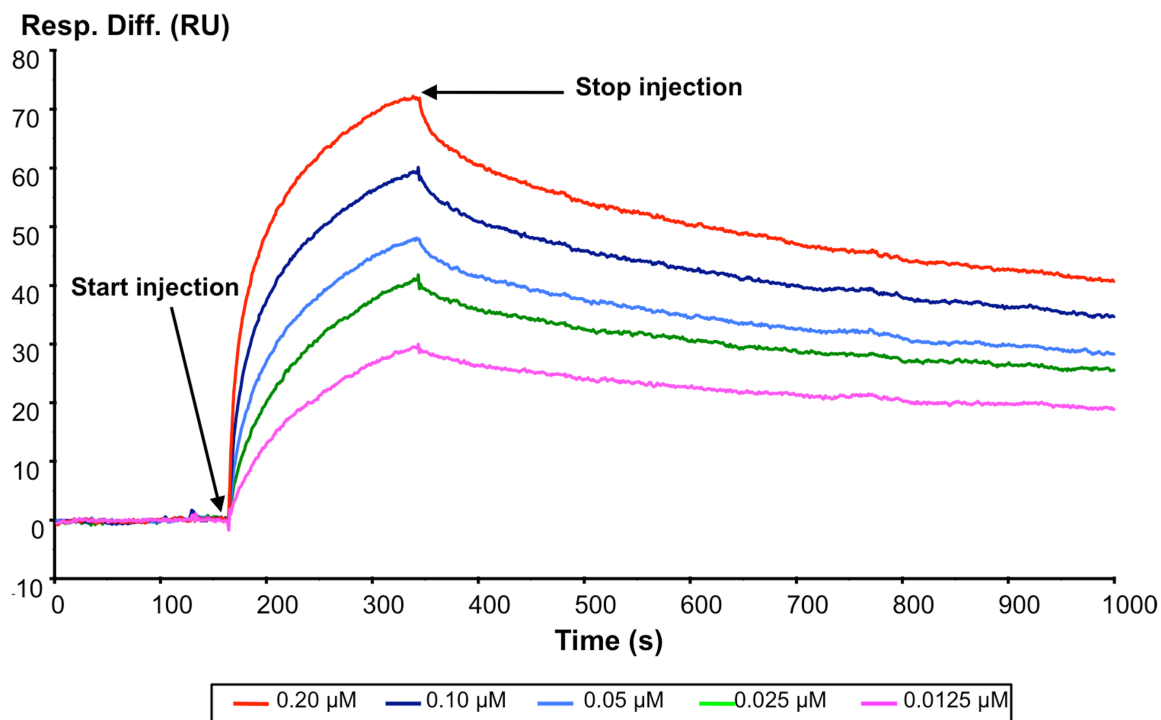


Figure 3.14 Calmodulin interaction with CaMKII δ .

Overlaid sensorgrams (Fc 2-1) depicting calmodulin interaction with immobilised CaMKII δ . Calmodulin in increasing concentrations was injected sequentially to achieve association with CaMKII δ . Surface generation was performed after each injection (traces not shown). The data has been parallel subtracted between Fc 2 and Fc 1 to take into account any non-specific binding that may be present. Data is representative of $n = 2$ independent experiments, with each point performed in duplicate.

3.8 Investigation of CaMKII δ interaction with IKKs using surface plasmon resonance

Having established that CaMKII δ is immobilised and functionally capable of protein-protein interactions, similar experiments investigating CaMKII δ interaction with IKK γ , IKK α , and IKK β were conducted. Recombinant IKK γ , IKK α and IKK β were prepared in similar concentrations (0.0125- 0.20 μ M) to calmodulin and tested for binding to 7-8 pg/mm^2 of immobilised CaMKII δ . Since no data on a potential IKK $\gamma/\alpha/\beta$ - CaMKII δ interaction was available for comparison, this range of analyte concentrations were chosen as SPR analyses investigating other interactions with proteins of the NF- κ B signalling pathway, including I κ B α and NF- κ B p65, were conducted at the nanomolar range (Bergqvist et al., 2006, Bergqvist et al., 2008, Psarra et al., 2009).

As illustrated in Figure 3.15 and Figure 3.16, recombinant IKK γ and IKK α , respectively, did not interact with immobilised CaMKII δ . IKK γ at higher concentrations (0.1 and 0.2 μ M) actually showed a negative change in the response, which probably reflects differential refractive index changes at Fc 1 and Fc 2. It is important to note that this effect was only observed for the two highest concentrations of the analyte. These were the least diluted preparations and any carryover of trace amounts of substance in the freeze-dried preparation of IKK γ will manifest itself at this stage. In contrast, IKK β was capable of interacting directly with CaMKII δ in a concentration-dependent manner, as illustrated in Figure 3.17. Under these conditions the interactions were of high affinity, with the addition of 0.0125 μ M IKK β giving a response difference of \sim 10 RU while 0.2 μ M IKK β resulted in a response difference of \sim 170 RU. This response was much greater than that observed for the equivalent concentrations of calmodulin and reflects a strong capacity for direct interaction between the two proteins (CaMKII δ and IKK β).

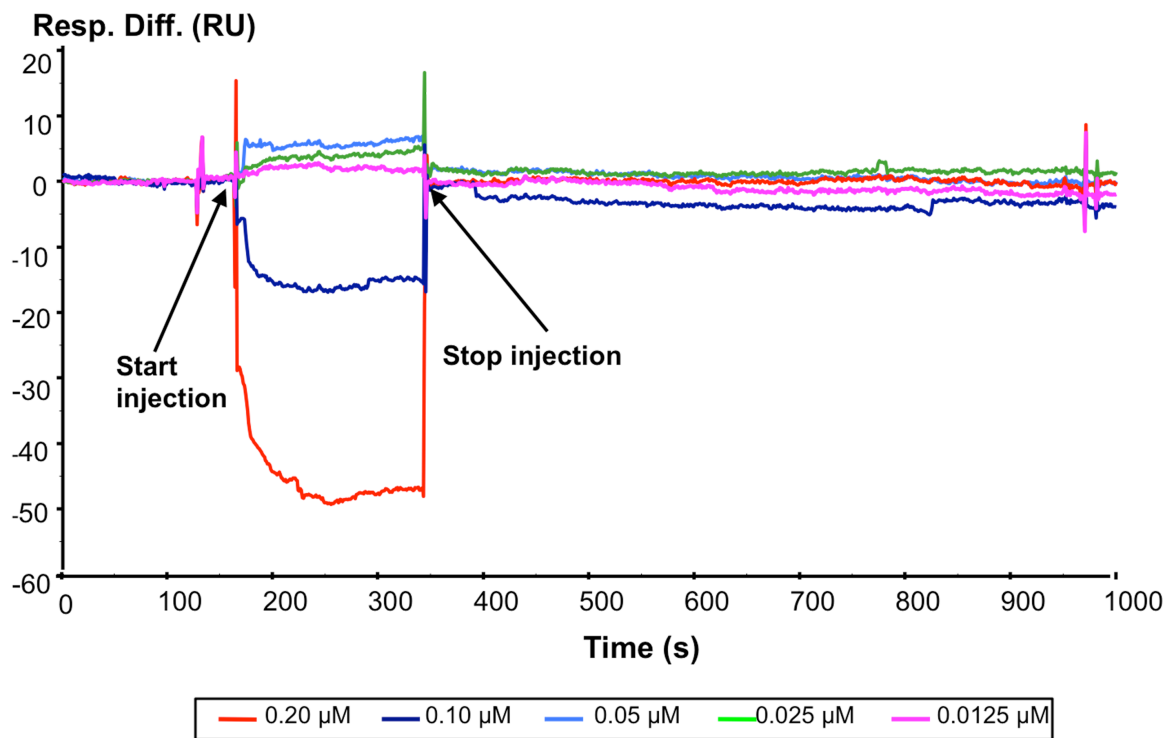


Figure 3.15 IKK γ does not interact with CaMKII δ .

Overlaid sensorgrams (Fc 2-1) depicting IKK γ interaction with immobilised CaMKII δ . IKK γ (0.0125-0.20 μ M) was injected in succession to achieve association with CaMKII δ over 60 seconds following which, the injection was terminated and protein dissociation monitored. The data has been parallel subtracted between Fc 2 and Fc 1 to take into account any non-specific binding that may be present. Data is from one experiment with each point performed in duplicate.

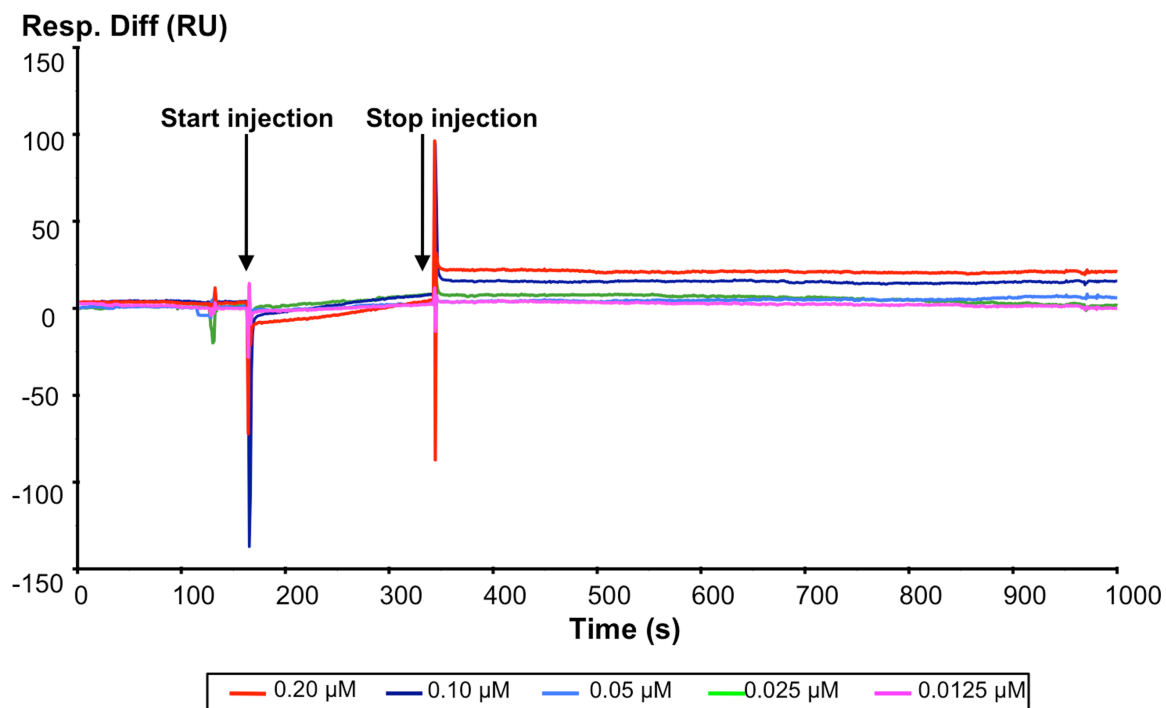


Figure 3.16 IKK α does not interact with CaMKII δ .

Overlaid sensorgrams (Fc 2-1) depicting IKK α interaction with immobilised CaMKII δ . IKK α (0.0125-0.20 μ M) was injected in succession to achieve association with CaMKII δ over 60 seconds following which, the injection was terminated and protein dissociation monitored. The data has been parallel subtracted between Fc 2 and Fc 1 to take into account any non-specific binding that may be present. Data is from one experiment with each point performed in duplicate.

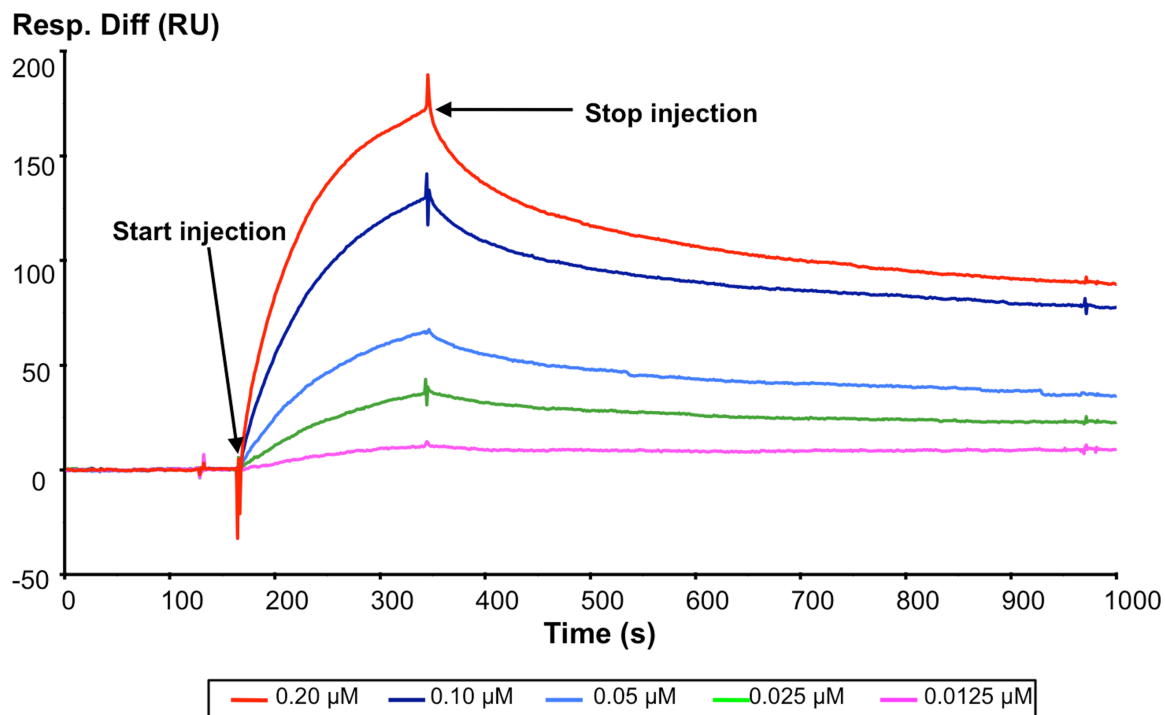


Figure 3.17 IKK β interaction with CaMKII δ .

Overlaid sensorgrams (Fc 2-1) depicting IKK β interaction with immobilised CaMKII δ . IKK β (0.0125-0.20 μ M) was injected in succession to achieve association with CaMKII δ over 60 seconds following which, the injection was terminated and protein dissociation monitored. Surface generation was performed after each injection (traces not shown). The data has been parallel subtracted between Fc 2 and Fc 1 to take into account any non-specific binding that may be present. Data is from one experiment representative of one other separate experiment, with each point performed in duplicate.

3.8.1 Assessment of conditions for CaMKII δ -IKK β interaction

To verify that the observed IKK β interaction with immobilised CaMKII δ was a real interaction between the two proteins of interest and did not occur via the His-tag of recombinant IKK β , further analysis was performed in the presence of 100 mM imidazole. Imidazole is an analogue of histidine traditionally used to modulate non-specific binding when purifying His-tagged proteins with affinity gels. If IKK β is interacting with CaMKII δ via its His-tag, then treatment with imidazole should displace bound IKK β from the sensor chip, causing a dramatic decrease in the observed response at any given concentration of analyte. The sensorgram depicted in Figure 3.18 indicates that treatment with imidazole had no significant effect on IKK β binding to the CaMKII δ sensor chip (~10 RU for 0.0125 μ M IKK β to ~140 RU for 0.2 μ M IKK β). Addition of IKK β under these conditions resulted in a similar concentration-dependent binding profile when compared with binding in the absence of imidazole (Figure 3.17). These data suggest that CaMKII δ is interacting with IKK β at a site distinct from the His-tag.

In view of the fact that both CaMKII δ and IKK β have kinase activity and are capable of autophosphorylation, it is possible that phosphorylation events may be involved in mediating CaMKII δ -IKK interactions. For this reason, experiments were repeated to determine the effect of adding 1 mM ATP to the running buffer. Addition of ATP had little effect on the IKK β -CaMKII δ profile observed in previous experiments, as depicted in the sensorgram in Figure 3.19. There was some reduction in absolute response (~170 RU (-ATP) cf. ~ 120 RU (+ATP) at 0.2 μ M), binding was still observed and this still occurred in a concentration-dependent manner, suggesting addition of ATP and possible subsequent phosphorylation does not prohibit interaction.

Finally, the possibility that the interaction may be Ca²⁺-dependent was examined. Removal of Ca²⁺ from the running buffer had no effect on the CaMKII δ -IKK β interaction (Figure 3.20) with concentration-dependent increases in binding occurring as before, with a maximum response of ~160RU for 0.2 μ M IKK β .

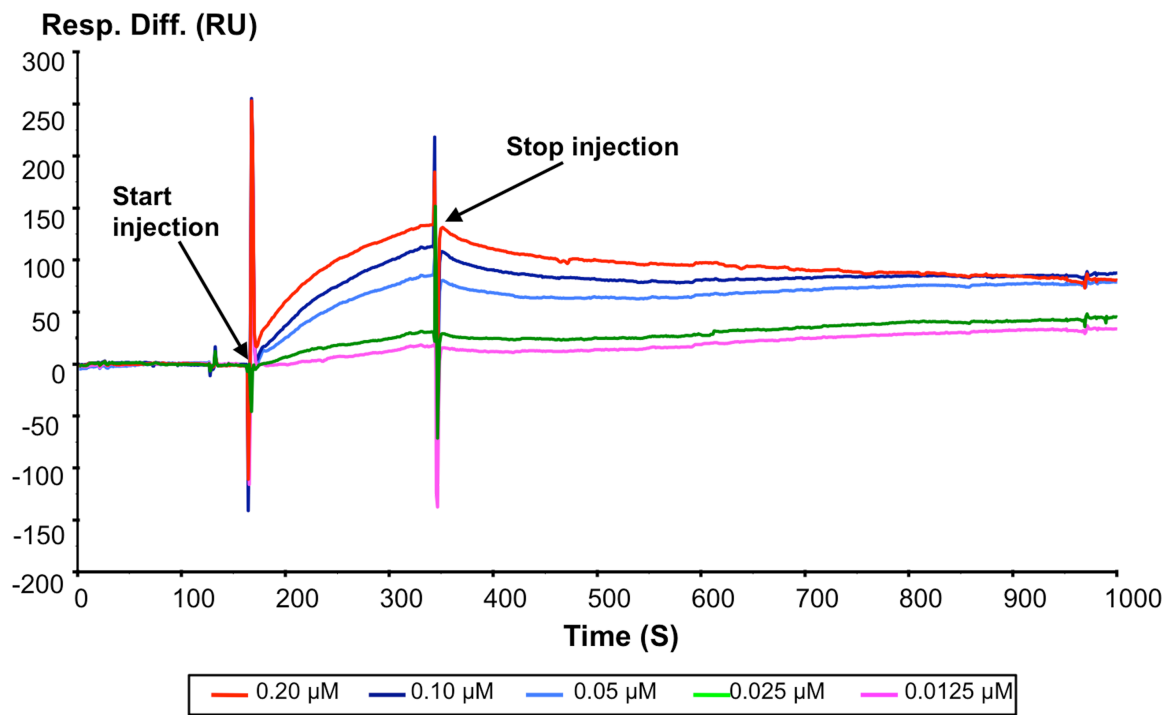


Figure 3.18 IKK β interaction with CaMKII δ in the presence of imidazole.

Overlaid sensorgrams (Fc 2-1) depicting IKK β (0.0125-0.20 μ M) interaction with immobilised CaMKII δ in the presence of 100 nM imidazole. The data has been parallel subtracted between Fc 2 and Fc 1 to take into account any non-specific binding that may be present. Data is from one experiment with each point performed in duplicate.

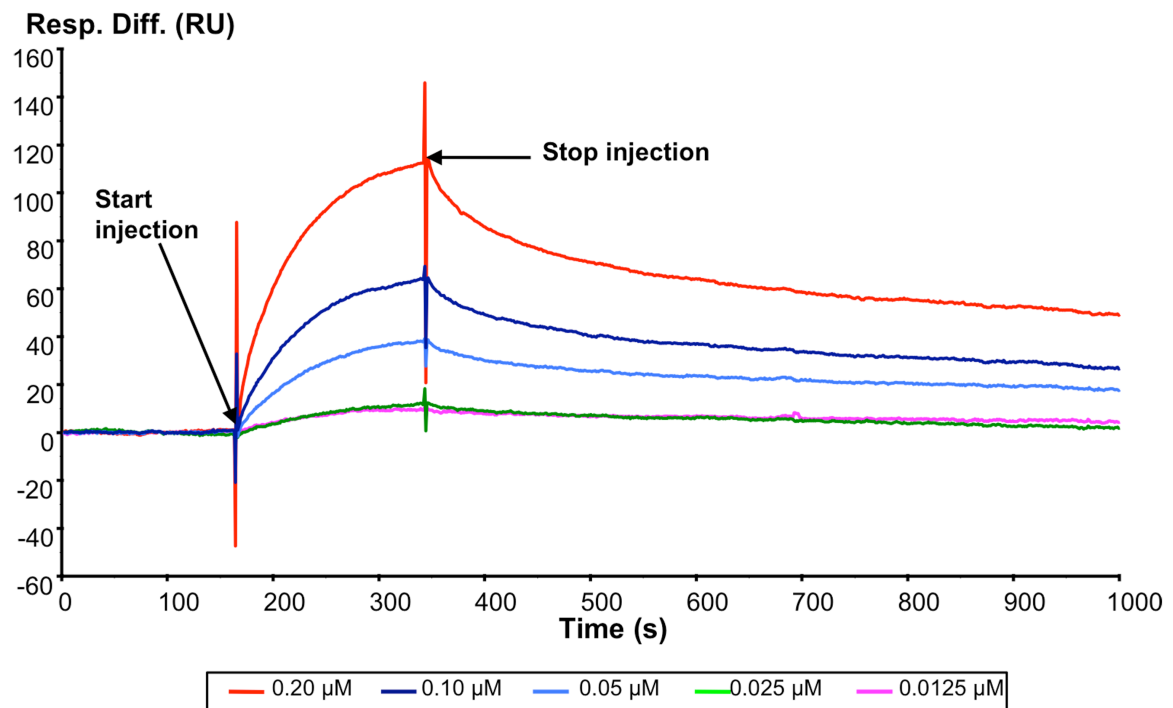


Figure 3.19 IKK β interaction with CaMKII δ in the presence of ATP.

Overlaid sensorgrams (Fc 2-1) depicting IKK β (0.0125-0.20 μM) interaction with immobilised CaMKII δ in the presence of 1 mM ATP. The data has been parallel subtracted between Fc 2 and Fc 1 to take into account any non-specific binding that may be present. Data is from one experiment with each point performed in duplicate.

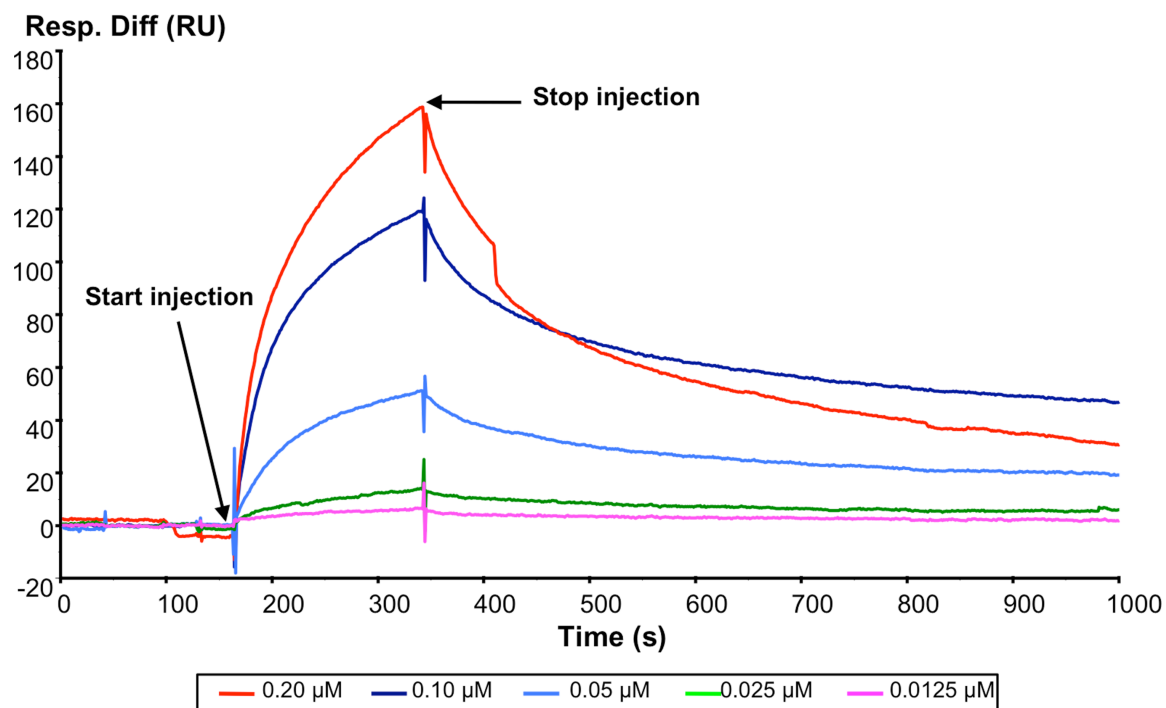


Figure 3.20 IKK β interaction with CaMKII δ in the absence of Ca $^{2+}$.

Overlaid sensorgrams (Fc 2-1) depicting IKK β (0.0125-0.20 μ M) interaction with immobilised CaMKII δ in running buffer lacking 1.5 mM Ca $^{2+}$. The data has been parallel subtracted between Fc 2 and Fc 1 to take into account any non-specific binding that may be present. Data is from one experiment with each point performed in duplicate.

3.9 Discussion

The aim of this chapter of the study was to explore the potential for modulation of the NF- κ B signalling pathway by CaMKII δ , possibly via direct protein interactions. Although some studies have suggested a link between CaMKII δ and NF- κ B signalling, there is only limited evidence for a link in the heart and the potential for direct protein-protein interactions between CaMKII δ and NF- κ B signalling have never previously been examined.

As mentioned in Chapter 1, CFs play a key role in the synthesis and degradation of the ECM (Camelliti et al., 2005) as well as secreting many growth factors and pro-inflammatory cytokines that act to modulate myocyte growth (Manabe et al., 2002). CFs have not been well studied, however there is growing evidence suggesting that CFs contribute to contractile and non-contractile function in normal and diseased heart (Vasquez et al., 2010, Chen et al., 2010). There is also evidence that they play a role in acute and chronic inflammation in the heart, releasing cytokines (Zeydel et al., 1991, Eghbali, 1992) and, importantly, CXC chemokines, which act to enhance neutrophil recruitment and amplify the acute inflammatory response in the heart (Lafontant et al., 2006). As mentioned in Chapter 1, NF- κ B signalling may modulate cardiac inflammation and fibrosis (Reddy et al., 2008), although information on activation of this pathway in CFs is limited. Targeting NF- κ B signalling in the heart has proved beneficial in recovery of normal cardiac function (Gupta et al., 2005, Gupta et al., 2008), however the mechanisms underlying cardiac NF- κ B activation have yet to be fully characterised. To date, research assessing alterations in NF- κ B activity (and CaMKII δ) following cardiac insult/stress has focused predominately on changes in myocytes and has overlooked these alterations in CF.

3.9.1 Characterisation of adult cardiac fibroblasts

Although the expression of CaMKII δ is well characterised in myocytes (Zhang et al., 2004) and has been detected in vascular smooth muscle fibroblasts (House and Singer, 2008) as well as L-fibroblasts (Szabo et al., 2007), it is only recently that CaMKII δ has been shown to be expressed in neonatal CF (Zhang et al., 2010c)

although to date it has not been reported whether adult CFs express CaMKII δ . Similarly the expression of NF- κ B proteins is well documented in myocytes (Das et al., 2008) and fibroblasts derived from various tissue types (Vardar-Sengul et al., 2009, Batsi et al., 2009, Ahmed et al., 2009), but as yet has not been examined in adult CFs.

Adult CFs were isolated from mouse and were confirmed to be CFs based on their morphology (Figure 3.3A) and staining patterns (see below). CFs differentiate into a myo-CF phenotype over time when kept in culture, with cells displaying an intermediate phenotype between CFs and smooth muscle cells, therefore expressing contractile proteins such as α -SMA (Brown et al., 2005b). For this reason, CFs were passaged only once and kept in culture for no longer than 2 weeks. Immunofluorescence staining for anti-vimentin and anti- α -SMA confirmed that the isolated cells were indeed CFs with no contamination from smooth muscle cells (Figure 3.3B, C, D). Some literature has suggested that anti-vimentin is not a specific marker for CFs as it labels other cell types such as endothelial cells and neurones. The DDR2 is reportedly a more specific marker for CF, with no expression detected in myocytes, endothelial cells, or smooth muscle cells (Goldsmith et al., 2004) however the specificity of DDR2 has also been debated, with leukocytes and tumours expressing DDR2 (Camelliti et al., 2005). Thus, it is evident from the literature that there is no truly specific marker for CFs, however given the characteristic morphological differences between cell types and the combination of analysis used in this study (assessment of cell morphology and immunofluorescent staining for anti- α -SMA) anti-vimentin can be used reliably to show that cultures consist predominately of CFs.

3.9.2 Functional role for CaMKII δ in NF- κ B signalling in adult cardiac fibroblasts

The present study has shown that adult mouse CFs highly express CaMKII δ and key components of NF- κ B signalling, including the IKK complex, which to our knowledge, has not previously been examined specifically in adult CFs (Figures 3.4-3.7). Initial experiments using these cells examined the potential for interaction

between CaMKII and NF- κ B signalling by measuring degradation of I κ B α as a marker for activation of the NF- κ B pathway.

I κ B α degradation was assessed in the presence and absence of AIP as an inhibitor of CaMKII and using a strong agonist of NF- κ B activation (LPS). For the first time this study demonstrates that selective inhibition of CaMKII (using AIP pre-treatment) prevents I κ B α degradation and subsequent NF- κ B activation in adult CF. CaMKII modulation of this pro-inflammatory signalling could result from interaction at one or several points in the NF- κ B signalling cascade (Figure 3.1) i.e. CaMKII could potentially interact with and phosphorylate components within the NF- κ B signalling pathway which would lead to activation.

Before the use of LPS, initial studies examined the use of more physiologically relevant agonists, Ang II and ET-1, to activate NF- κ B signalling in CF. Even when tested at 1 μ M, degradation of I κ B α was subtle (Figure 3.9). Results are disparate with respect to Ang II induced NF- κ B activation in the heart with some studies suggesting that Ang II induces NF- κ B activity in cardiac cells (Rouet-Benzineb et al., 2000), however others suggest that only chronic Ang II infusion *in vivo* activates NF- κ B signalling (Chen et al., 2004, Sárman et al., 2007, Freund et al., 2005). Others have shown similar results to those presented here, where Ang II did not induce I κ B α degradation in neonatal CFs (Sano et al., 2001). Literature on ET-1 induced NF- κ B signalling in the heart is limited, however a study has suggested that ET-1, acting via the ETA receptor, increases I κ B α degradation and NF- κ B:DNA binding in macrophages (Mangelus et al., 2001). Therefore the reason as to why ET-1 was unable to promote I κ B α degradation in this study may relate to reportedly higher expression levels of ETB than ETA in CFs (Porter and Turner, 2009).

Although LPS may not be considered a physiologically relevant agonist in the heart, toll-like receptor (TLR) signalling has been shown to mediate LV remodelling and cardiac dysfunction following MI (Timmers et al., 2008). Other studies have shown that the hypertrophic response to pressure overload is attenuated in TLR-4 deficient mice (Ha et al., 2005b) or by pharmacological inhibition of TLR-4 signalling (Ehrentraut et al., 2011). CaMKII may also be involved in TLR-4 signalling (Liu et al., 2008), supporting the use of LPS in this study.

3.9.3 Analysis of the CaMKII-NF- κ B interaction

Initial experiments investigating potential CaMKII δ -NF- κ B interactions at the level of the IKK complex using immunoprecipitation of native proteins from solubilised WH and solubilised cell extracts (CFs and myocytes) were unsuccessful. This was possibly due to the poor quality and specificity of some of the commercially available antibodies (Figures 3.4-3.7) leading to low and inconsistent recovery (Figure 3.11). During optimisation of the IP procedure, three different published protocols (Currie et al., 2004, MacKenzie et al., 2007, Huke and Bers, 2007) were assessed using different buffer compositions, different commercially available antibodies and different sepharose beads, however immunoprecipitation analysis of a potential CaMKII δ -IKK interactions were not possible.

To get around the issue of the low specificity of commercially available antibodies for the IKK proteins, other methods for immunoprecipitation can be used, such as overexpressing tagged proteins of interest in cells (e.g. haemagglutinin (HA) tagged CaMKII δ) and then immunoblotting for that tag. If cells are simultaneously transfected with two different proteins with different tags, immunoblotting for the alternate tag would provide basic information on whether these proteins interact *in vitro*, however it would not give information on endogenous interactions within CFs. These experiments were out of the time-scale of the present study as to date adult CFs have not been used for transfection studies, and this procedure would need optimisation which can take considerable time. Although other cell lines could be used such as human embryonic kidney-293 (HEK-293) cells, and techniques such as Fluorescence Resonance Energy Transfer (FRET) applied, to give information on whether two proteins interact *in vivo*, these studies were not feasible for the present study.

3.9.3.1 CaMKII δ selectively phosphorylates and directly interacts with IKK β

Having established that CaMKII δ plays a functional role in NF- κ B modulation and due to the aforementioned issues with IP analysis, autoradiography of purified proteins was performed to identify a specific target or targets for CaMKII activity within the pathway. Analysis of IKK phosphorylation by CaMKII δ was performed in

the presence and absence of a selective CaMKII inhibitor, AIP. These data provided initial evidence that IKK β may be a substrate for CaMKII as only the phosphorylation signal associated with IKK β (and not IKK α) was significantly reduced in the presence of AIP (Figure 3.12).

In light of this interesting result, SPR analysis was used to further investigate whether CaMKII δ could potentially interact with the IKK proteins. As mentioned, SPR is a relatively novel technique used to investigate biomolecular interactions. Although this technique employs recombinant proteins, its main advantages for studying protein-protein interactions, in comparison to other techniques such as co-IP, is that it provides information on association/dissociation of proteins and direct protein-protein interaction can be viewed and analysed in real time.

From these experiments it is clear that CaMKII δ selectively interacted with IKK β but did not interact with IKK γ or IKK α (Figures 3.17-3.19). The kinetics of IKK β binding were rapid with a slower dissociation rate, similar to that observed with calmodulin (Figure 3.14). Importantly, the extent of binding of IKK β to CaMKII δ was greater than that observed for calmodulin binding to CaMKII δ (~160 RU c.f. ~70RU for 0.2 μ M IKK β and 0.2 μ M calmodulin, respectively). This is the first evidence for a direct, selective and high affinity interaction between CaMKII δ and IKK β .

This is an important novel finding as there is currently no literature documenting a direct interaction between these proteins, however as mentioned previously, some studies have suggested that CaMKII δ is a mediator of IKK activation (Hughes et al., 2001). As demonstrated in Figure 3.2, IKK α and IKK β have very similar structures (~50% sequence identity), but as discussed in Chapter 1, have relatively distinct substrates and functions. These distinct functions arise from the two NF- κ B pathways, the canonical pathway and the non-canonical pathway, but also via the emergence of cellular activities out with NF- κ B signalling (see Chapter 1, Section 1.9). Previous work has demonstrated the prevalence of IKK β in (i) induction of NF- κ B activity and (ii) modulation of cardiac function. A series of studies have illustrated that the canonical pathway is activated in response to pro-inflammatory stimuli and is dependent on IKK γ and IKK β induced phosphorylation and degradation of I κ B inhibitory subunits, thus liberating the prototypical NF- κ B p50:p65 heterodimer (Hu et al., 1999, Takeda et al., 1999, Li et al., 1999a, Delhase et al.,

1999, Bonizzi and Karin, 2004). Importantly, neither IKK nor NF- κ B can be activated by agonist stimulation in IKK β -deficient cells and disruption of the IKK β locus is lethal (Tanaka et al., 1999). In contrast, IKK α disruption does not abolish activation of IKK or NF- κ B (Li et al., 1999b), suggesting that IKK β plays a more important role in canonical NF- κ B activation than IKK α . Other studies have shown that IKK α is absolutely required for activation of the non-canonical pathway (Israel, 2010).

In the heart, inhibition of I κ B phosphorylation has been shown to reduce reperfusion injury (Onai et al., 2004) and specific targeting and inhibition of IKK β has provided both acute and delayed cardioprotection (Moss et al., 2007, Moss et al., 2008). This has highlighted IKK β as a potential therapeutic target that could be used to modulate inflammation and cardiac damage following injury. The possibility that CaMKII δ may modulate cardiac NF- κ B pro-inflammatory signalling via interaction with IKK β indicates an important link that could be used for more selective modulation of this inflammatory route.

The IKK β -CaMKII δ interaction does not appear to be ATP or Ca²⁺-dependent because when experiments were repeated in the presence of ATP or the absence of Ca²⁺; IKK β still bound to CaMKII δ in a concentration dependent manner (Figures 3.22 and 3.23, respectively). Further analysis of the IKK β -CaMKII δ interaction revealed that binding was not via the His-tag of the IKK β protein but at some other distinct site (Figure 3.18). While it is beyond the scope and time frame of this study, determination of the stoichiometry of the IKK β -CaMKII δ interaction using the SPR technique in combination with mapping the specific site(s) of interaction should prove informative on whether CaMKII may phosphorylate unique sites on IKK β . This information could form the basis for disruptive intervention strategies in cardiac disease where both CaMKII δ and NF- κ B signalling are significantly elevated. The possibility of targeting the IKK β -CaMKII δ interaction to modulate cardiac function therapeutically could improve on previous suggestions of targeting CaMKII δ and NF- κ B individually (Anderson, 2005, Purcell and Molkentin, 2003, Cook et al., 2003). However, as the interpretation of the specifics of the IKK β -CaMKII δ interaction is based solely upon data obtained from recombinant or purified proteins, examination of this interaction in heart preparations either *in vitro* or *in vivo* will need to be addressed in future work.

Although the present study has not specifically examined myocytes, the probability that this interaction exists in both contractile and non-contractile cells of the heart suggests there is broad scope for therapeutic application. Activation of NF- κ B in both myocytes and CFs will induce gene programs that promote inflammation and this could potentially be halted across cell types via targeting the CaMKII δ -NF- κ B interaction.

3.10 Conclusions

In summary, data presented in this study show novel evidence for the existence of an interaction between CaMKII δ and the NF- κ B signalling pathway and for the first time, highlight the potential for CaMKII modulation of NF- κ B signalling in adult CFs. This study demonstrates CaMKII δ selectively phosphorylates and directly interacts with IKK β . Following the demonstration of CaMKII δ -IKK β interaction, it is then important to understand if NF- κ B activity is increased during cardiac disease in parallel with enhanced CaMKII activity. Data presented in the next chapters demonstrate the development and characterisation of an animal model of hypertrophy and examines alterations in CF function, NF- κ B and CaMKII activity following hypertrophy.

**Chapter 4: Development and
characterisation of a minimally
invasive aortic banding mouse
model of pressure-overload
mediated cardiac hypertrophy**

4.1 Introduction

To allow assessment of alterations in CaMKII δ and NF- κ B expression, phosphorylation and activity following hypertrophy, a key objective of this project was to establish and characterise a mouse model of cardiac hypertrophy using transverse aortic constriction. In the context of this project, future studies could then be performed to (i) assess changes in both signalling molecules following hypertrophy, (ii) assess CF function and, (iii) determine whether CaMKII δ – NF- κ B interaction may be altered in diseased hearts.

Animal models of cardiac disease have proved invaluable for assessing cardiac function *in vivo* and relating dysfunction to altered cellular parameters. Stenosis of the aorta by placement of a constricting band around the aorta, at the level of the ascending (Liao et al., 2002a), abdominal (Hara et al., 2002) or the transverse aorta (Rockman et al., 1991), is the most common animal model for studying left ventricular hypertrophy. Transverse aortic constriction (TAC), the most commonly used method, was pioneered in mouse by Rockman and colleagues (Rockman et al., 1991). Although a popular technique, the TAC model is technically challenging and time consuming as it is an invasive procedure requiring the thorax to be entered between the second and third left intercostal space, thus necessitating tracheal intubation and mechanical ventilation (Hu et al., 2003, Rockman et al., 1991). Such invasive procedures can lead to inflammatory reactions within the chest which may complicate the analyses of cardiac function (Hu et al., 2003). Similarly, banding of the abdominal aorta to induce pressure-overload can also cause problems as the extent of hypertrophy and likelihood of progressing to heart failure is increased when the band is placed closer to the heart (Nakamura et al., 2001). Thus, banding the thoracic aorta using a minimally invasive technique is preferable.

For these reasons, minimally invasive transverse aortic banding (MTAB) was the method chosen to induce pressure-overload hypertrophy. This experimental technique is reported to produce LV pressure-overload which leads to the development of cardiac hypertrophy analogous to the myocardial remodelling induced by naturally high blood pressure (Colomer et al., 2003) and aortic stenosis in humans (Tarnavski et al., 2004). By using the MTAB model to band the aortic arch the

pleural space is not entered, thus the procedure can be performed rapidly and with fewer complications leading to lower mortality and increased reproducibility.

As mentioned previously, the MTAB studies were performed in mice. In the past, the rat has commonly been used for cardiovascular research due to its larger size (~10 times bigger than mouse) (Tarnavski et al., 2004). Indeed the TAC procedure was first described in rat, however with the increasing availability of microdissecting microscopes and microsurgical instruments, and with the extensive characterisation of the mouse genome, cardiovascular research is increasingly using the mouse. The process is still technically difficult, with few laboratories documenting successful development of the MTAB model, however once suitable anaesthesia and surgical technique are established, there are huge benefits to using this approach. MTAB performed in mouse requires microsurgical skills and specialised equipment for surgery and phenotyping. The sheer challenge of MTAB surgery using mouse is emphasised by Figure 4.1, which puts the scale of the mouse heart into perspective. The aim of the work presented in this chapter is to detail the establishment and characterisation of a minimally invasive method (MTAB) for producing cardiac hypertrophy in mouse, with low mortality and good reproducibility to allow further investigations into CaMKII δ and NF- κ B signalling in the diseased heart.

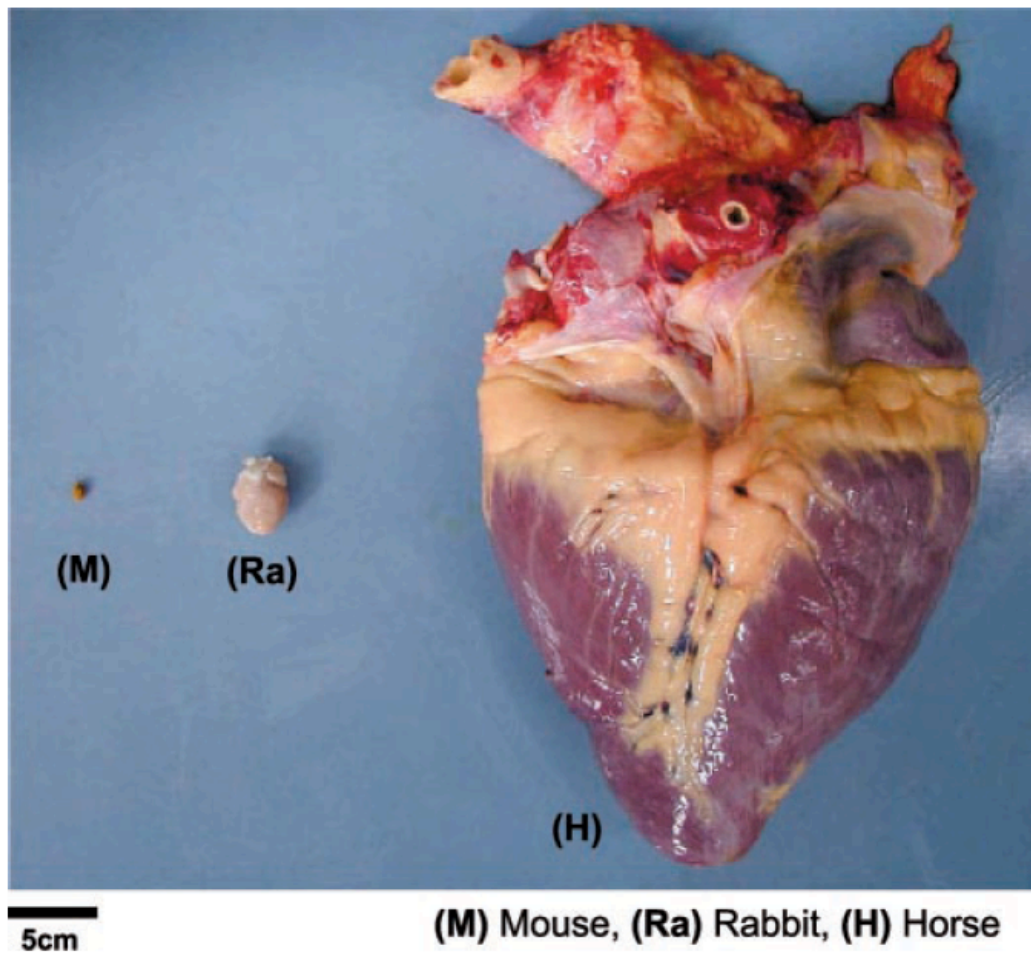


Figure 4.1 Comparison of the dimensions of the intact heart between different species.

Typical photograph of hearts from mouse (M), rabbit (Ra) and horse (H), demonstrating the sheer difference in size of organ between mammalian species, thus illustrating the challenges of mouse surgery.

Figure adapted from Loughrey et al., 2004).

4.2 Assessment of growth rate of in-house bred C57BL/6J animals

In order for the animals to survive the MTAB procedure and recover quickly from anaesthetic exposure, mice need to be healthy and at least 20-30 g in weight. This is particularly pertinent since animals will inevitably lose some weight post-surgery (~2 g; data not shown). In large studies like this one it is important to take into consideration the time it takes for an animal to reach critical weight for surgery, and the costs associated. As illustrated in Figure 4.2, in-house bred C57BL/6J male mice grow much faster and overall put on more weight than female animals. Thus, for these reasons all experiments used adult C57BL/6J male animals weighing between 25-30 g (10-16 weeks old). Other reasons for using only male animals, for example the effects of estrogen on cardiovascular function, will be addressed in the Discussion Section 4.10.

4.3 Assessment of anaesthesia

During initial characterisation of the MTAB procedure, various types of anaesthetic regimes were tested. Initially various combinations of commonly used injectable sedatives, anti-anxiety and anti-convulsant agents were used in correlation with published work (Hu et al., 2003) and with our collaborators (Dr. Nils Teucher, University of Goettingen, Germany). As summarised in Table 4.1, these agents proved unsuitable due to inappropriate dosing and/or respiratory depression, with many animals dying before the MTAB procedure began. The main limiting factor in using inhalation anaesthesia was the development of a cone mask small enough to hold the mouse snout securely in place during the surgical procedure. As illustrated in Figure 4.3, rigid tubing with a small metal bar placed length-wise across the lumen was used to hook the animal's front teeth under when lying in the supine position. As illustrated, this allowed continuous flow of gas anaesthesia through the inner tubing whilst the animal was held securely in place (Figure 4.3B). Subsequently, inhalation anaesthesia using a combination of isoflurane and oxygen proved most suitable due to the ability of fine control of the level of anaesthesia, with survival rates of ~75-80% as illustrated in Table 4.1.

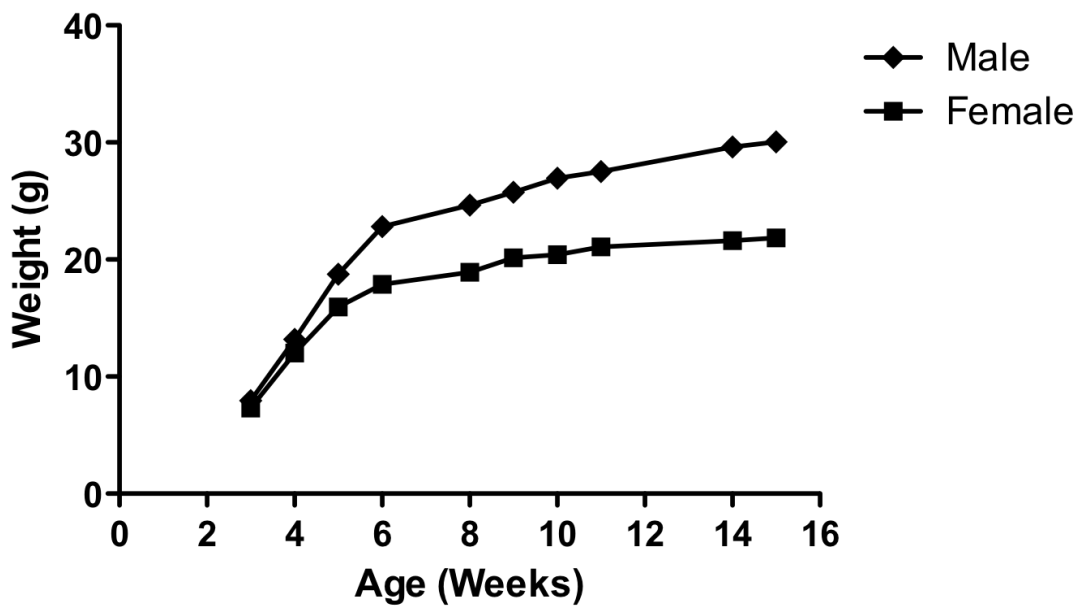


Figure 4.2 Growth curve of in-house bred C57BL/6J mice.

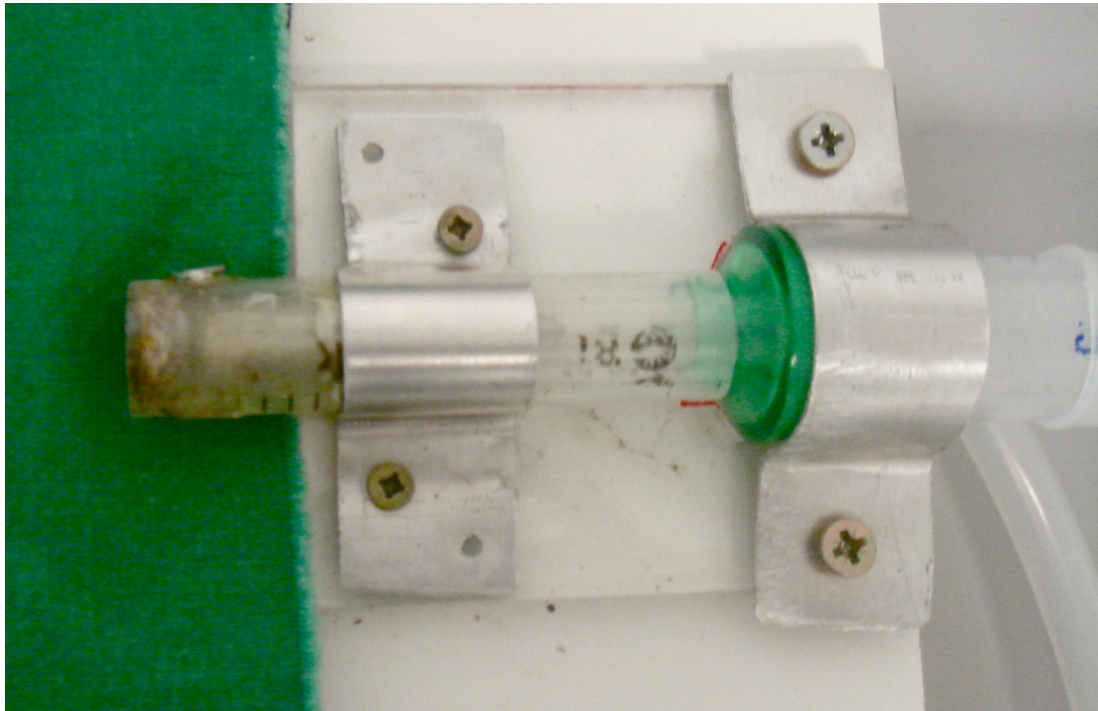
Male or female mice were group housed in conditions of a 12-hour light-dark cycle with ad-lib feeding (Rat and Mouse Chow; Special Diet Services) and water. Cages measured 43.5 cm x 27 cm x 12 cm, with 15 animals per cage. Values are means \pm s.e.m, n=15 per group.

Anaesthetic	Comments	Mortality
Ketamine/Xylazine (100mg/kg/10mg/kg)	<ul style="list-style-type: none"> • Various dosing regimes tested. • Tested plus/minus oxygen. • Animals regularly needed top-ups. 	<ul style="list-style-type: none"> • Animals died before surgery began or early during procedure.
S-Ketamine/Xylazine (100mg/kg/10mg/kg)	<ul style="list-style-type: none"> • Animals often needed topped up with isoflurane during surgery. • Anaesthesia often too light. 	<ul style="list-style-type: none"> • Animals died before surgery began or early during procedure.
Ketamine/Xylazine/Acepromazine (100mg/kg/10mg/kg /3mg/kg)	<ul style="list-style-type: none"> • Breathing irregular early during procedure. 	<ul style="list-style-type: none"> • Animals died before surgery complete.
Hypnorm/Midazolam (1:1 mix at 0.1 ml/10 g)	<ul style="list-style-type: none"> • Breathing irregular. 	<ul style="list-style-type: none"> • Animals died before surgery began.
Isoflurane/Oxygen (3% Isoflurane/100% Oxygen at 2 l/min)	<ul style="list-style-type: none"> • Animals were maintained with 1-2% Isoflurane in 100% Oxygen at 1 -1.5 l/min. 	<ul style="list-style-type: none"> • Currently ~20-25% with all mortality during procedure & not post-surgery.

Table 4.1 Summary of anaesthesia tested during optimisation of the MTAB procedure.

Various combinations of injectable anaesthesia were tested during the development of the MTAB model. Inhalation anaesthesia using Isoflurane in 100% oxygen proved the most effective.

A.



B.

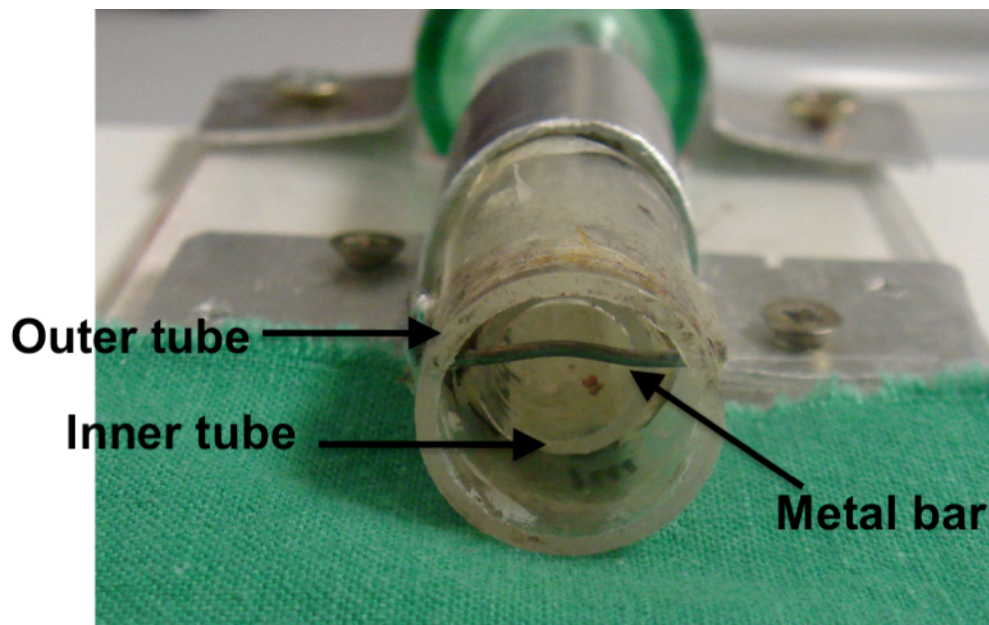


Figure 4.3 Design of the inhalation anaesthesia cone mask.

Panel A. Design of the cone mask used to deliver continuous gas anaesthesia during surgery/echocardiography. Panel B. Close-up image of the cone mask lumen with a metal bar placed lengthwise, used to securely hold the mouse snout in place. The inner tube delivers Isoflurane/100% oxygen, whilst the outer tube scavenges excess anaesthesia.

4.4 Minimally invasive transverse aortic banding (MTAB)

As outlined in Chapter 2: Section 1.2, the surgical techniques employed were an adaptation of an MTAB protocol described previously (Hu et al., 2003). Briefly, a small incision was made at the level of the suprasternal notch, the trachea was located (Figure 4.4A) and a small longitudinal cut was made down and through the sternum. As this surgical model is minimally invasive, during initial optimisation of the surgical technique only a small section (1-2 mm) of the skin and sternum were cut to allow visualisation of the aortic arch. This lead however to cutting too far down the sternum or to excessive retraction of the rib cage, both of which resulted in breathing difficulties and subsequently increased mortalities. Therefore, to avoid unnecessary and potentially damaging retracting of the rib cage, a larger longitudinal cut was made down the skin to aid localisation of the aortic arch.

Once the thymus was located (Figure 4.4B) and retracted to expose the aortic arch, a 5-0 silk suture was snared with a bent and blunted 25 G needle that was passed under the arch, as illustrated by Figure 4.4C. The suture was then tied between the origin of the right innominate and left common carotid arteries using a blunt 27 G needle to control the tightness of the constriction, as illustrated in Figure 4.4D-F and Figure 4.5. After ligation of the arch, the skin was sutured and the mice were allowed to recover until fully awake. Sham-operated animals went through the same procedure except the aortic arch was not tied. Animals were left for 48 h, 1 week or 4 weeks to allow cardiac remodelling to occur.

The whole surgical procedure, from the moment the animal was put under anaesthesia until it was fully recovered, was adapted and perfected so that it would take no more than 15-20 minutes. Perioperative and post-operative mortality rates were low (15-20% and <5%, respectively) and were commonly caused by haemorrhage.

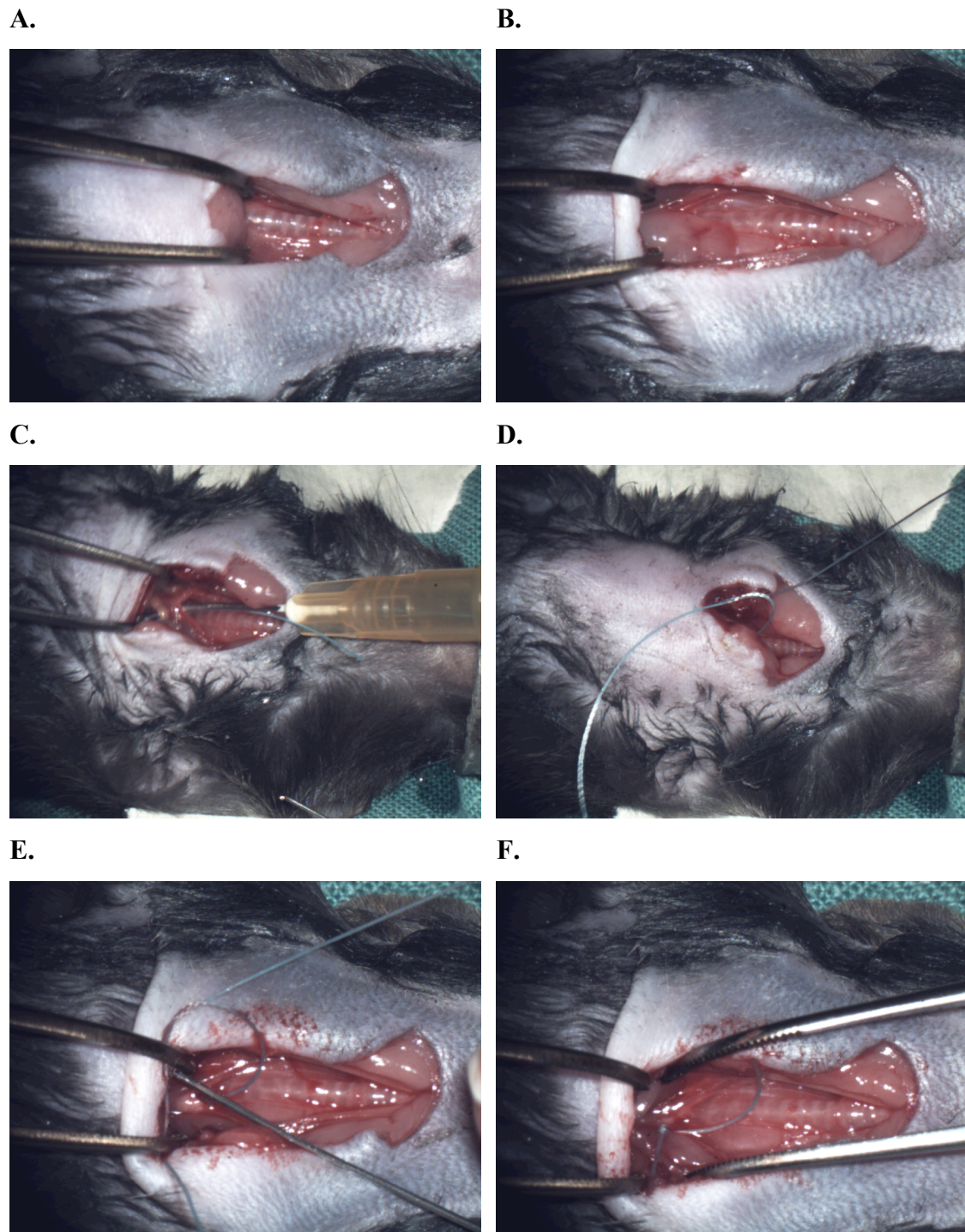


Figure 4.4 Representative images of MTAB mouse surgery.

Images depict key steps in the MTAB procedure. The trachea is located and the pre-tracheal muscle divided (A) before a mini-sternotomy to reveal the thymus (B). The thymus is retracted and a suture snared with a wire is passed under the arch (C) and a loose knot is tied (D). The suture is tied tightly using a bent 27 G needle to control the tightness of the constriction (E & F). After ligation of the arch, the skin is sutured and the mice allowed to recover until fully awake.

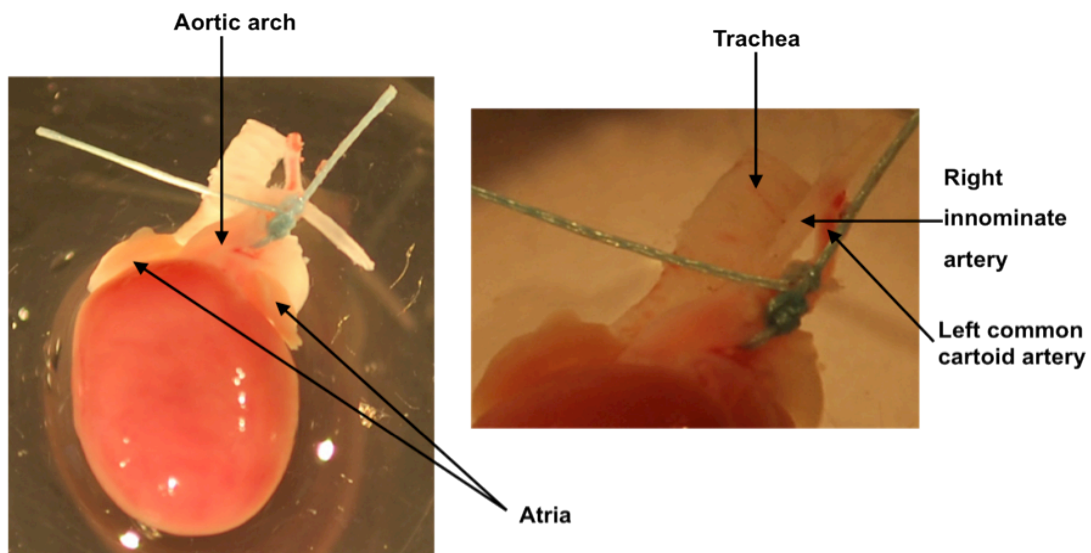


Figure 4.5 Suture detail around the transverse aortic arch.

Typical photograph of a mouse heart with the transverse aortic arch banded with a 5-0 silk suture between the origin of the right innominate and left common carotid arteries.

4.5 Assessment of mean arterial pressure (MAP) at 1 week in sham and MTAB animals

To determine whether the band placed around the transverse aortic arch was in fact producing pressure-overload, mean arterial blood pressure (MAP) was measured 1 week after MTAB or sham surgery. Although a number of experiments were performed measuring MAP through an arterial cannula placed in the right carotid artery (as described in Chapter 2: Section 2.4), these were compromised due to the lack of appropriate equipment. A full study was conducted by our collaborator, Dr. David Grieve (Queens University, Belfast), who to the best of our knowledge is the only other group using the MTAB model in the U.K. Measurements were performed on anaesthetised animals (as described in Chapter 2, Section 1.2) by cannulating the right carotid artery with a high-fidelity 1.2-F pressure-volume catheter (SciSense Inc.). Firstly, aortic pressure was measured before advancing the catheter into the LV for recording of steady-state function using a PowerLab system (ADI Instruments).

As shown in Table 4.2, systolic blood pressure (SBP) was markedly increased in MTAB animals compared to sham (110 ± 6.3 cf. 78 ± 2.6 , $p < 0.001$), as was MAP (MTAB 75 ± 3.3 mmHg cf. sham 60 ± 2.6 mmHg, $p < 0.01$). In addition LV pressure was increased in banded mice as evidenced by a marked increase in maximum LV pressure (LVP_{\max}) and an increase in LV end-diastolic pressure (LVED) with values of MTAB 106 ± 3.6 mmHg cf. sham 91 ± 4.8 mmHg ($p < 0.05$), and MTAB 12.7 ± 1.0 mmHg cf. sham 6.7 ± 0.81 mmHg ($p < 0.001$), respectively (Table 4.2). The first derivative of LV, $LVdP/dt_{\max}$ was decreased and $LVdP/dt_{\min}$ was increased suggesting decreased contractility and lusitropy of the LV in MTAB animals compared to sham (MTAB 6394 ± 484 mmHgs⁻¹ cf. sham 8604 ± 434 mmHgs⁻¹, and MTAB -5607 ± 375 mmHgs⁻¹ cf. sham -7608 ± 394 mmHgs⁻¹, respectively, $p < 0.01$; Table 4.2). The LV relaxation time constant, τ , was increased in MTAB animals suggesting that diastole is increased in these animals (MTAB 7.8 ± 0.6 ms cf. sham 6.3 ± 0.4 ms, $p < 0.05$, Table 4.2). Importantly, heart rates were not different between sham-operated and MTAB animals (sham 571 ± 27 bpm and MTAB 571 ± 27 bpm, $p > 0.05$, Table 4.2). Together these data demonstrate that banding the aortic arch in MTAB mice increases LV pressure, promoting systolic dysfunction and diastolic dysfunction.

	Sham (n=7)	MTAB (n=7)
Heart rate (bpm)	571 ± 27	571 ± 27
Systolic blood pressure	78 ± 2.6	110 ± 6.3****
Diastolic blood pressure	51 ± 2.7	59 ± 3.4
Mean arterial pressure (mmHg)	60 ± 2.6	75 ± 3.3**
LVP _{max} (mmHg)	91 ± 4.8	106 ± 3.6*
LVP _{min} (mmHg)	2.2 ± 0.8	6.2 ± 1.8
LVEDP (mmHg)	6.7 ± 0.81	12.7±1.0****
LVdP/dt _{max} (mmHg s ⁻¹)	8604 ± 435	6394 ± 484**
LVdP/dt _{min} (mmHg s ⁻¹)	-7608 ± 394	-5607 ± 375**
τ (ms)	6.3 ± 0.4	7.8 ± 0.6*

Table 4.2 Haemodynamic parameters in MTAB and sham-operated mice (data courtesy of Dr. Grieve, Queens University Belfast).

Measurements were taken 1 week post-sham or MTAB surgery. Abbreviations: LVP_{max}, maximum LV pressure; LVP_{min}, minimum LV pressure; LVEDP, LV end-diastolic pressure. Statistical significance was determined from unpaired Student's t-tests. Data are means ± s.e.m, with number of animals in parentheses. *P<0.05, **P<0.01, ***P<0.001.

4.6 Echocardiographic assessment of left ventricular function

Transthoracic echocardiography was used to functionally assess the effect on, cardiac contractility and the degree of hypertrophy induced by, the MTAB procedure. Typically echocardiography was performed on a lightly anaesthetised animal placed supine or in the left lateral decubitus position, with the linear or phase array probe angled in a clockwise manner to obtain an image of the parasternal long axis. The transducer was angled so that the aortic valve, mitral valve and left ventricle were in the long axis. From this, the parasternal short axis view can be obtained by angling the probe 90° with respect to the parasternal long axis of the LV. M-mode images can then be recorded at the level of the papillary muscle. Caution was taken not to apply excessive pressure on the chest as this could potentially cause deformation of the heart and bradycardia, leading to inaccurate measurements. Once the reproducibility of the method was established, cardiac contractility was assessed during systole and diastole. Left ventricular (LV) wall dimensions including anterior and posterior wall measurements, LV end systolic dimension (LVESD), LV end diastolic dimension (LVEDD) and % fractional shortening (FS) were assessed from M-mode traces from both sham and MTAB mice. Examples of short-axis views and M-mode traces from sham-operated and banded animals are shown in Figure 4.6.

After 2 weeks aortic banding LVESD and anterior wall thicknesses (AW) in both systole and diastole were not different between sham and MTAB animals, as illustrated in Figure 4.7A and Table 4.3. However, posterior wall thickness (PW) was increased during diastole (MTAB 1.57 ± 0.24 mm cf. sham 0.94 ± 0.08 mm, $p < 0.05$) and LVEDD was markedly decreased (MTAB 3.09 ± 0.16 mm cf. sham 3.80 ± 0.15 mm, $p < 0.01$), suggesting anatomical remodelling of the LV and diastolic dysfunction. Similar results were observed after 4 weeks aortic banding with increased PW measurements during diastole (MTAB 1.39 ± 0.20 mm cf. sham 0.91 ± 0.09 mm, $p < 0.05$) and decreased LVEDD in MTAB animals (3.26 ± 0.21 mm cf. sham 3.87 ± 0.13 mm, respectively, $p < 0.05$; Figure 4.7B and Table 4.3). Together these data suggest that anatomical remodelling of the heart begins from as early as 2 weeks post-aortic banding and is maintained at 4 weeks post- aortic banding.

In correlation with the observed LV remodelling, LV function as assessed by fractional shortening (% FS) was markedly decreased in MTAB animals 2 weeks

post-surgery (MTAB 28.0 ± 1.3 % cf. sham 44.2 ± 3.1 %, $p < 0.001$), as illustrated in Figure 4.8 and Table 4.3. This decreased fractional shortening was sustained at 4 weeks post-surgery (MTAB 24.3 ± 2.5 cf. sham 43.6 ± 1.7 , $p < 0.001$, Figure 4.8 and Table 4.3). Together these data suggest that LV contractility is compromised in banded animals from as early as 2 weeks post-surgery, and is sustained at 4 weeks post-surgery.

4.7 Post-mortem assessment of hypertrophy after 4 weeks sham or MTAB surgery

Heart weight to body weight ratios (HW/BW) were analysed to further determine the degree of hypertrophy induced by ligation of the transverse aortic arch. As illustrated in Figure 4.9 and Table 4.3, HW/BW ratios were significantly increased in MTAB 4 weeks post-surgery (MTAB 9.13 ± 0.56 cf. sham 4.59 ± 0.04 , $p < 0.001$). During the progression of HF due to LV failure, the LV can no longer efficiently pump blood out to the body's tissue as fast as it returns from the lungs and so there is a build up of blood in the vessels and the lungs. The activation of neurohumoral responses such as the renin-angiotensin system and vasopressin aim to compensate for the failing heart by increasing arterial vasoconstriction, venous constriction and blood volume, however these mechanisms can also aggravate HF by increasing ventricular afterload and preload (Klabunde, 2005). This ultimately forces some of the fluid in the blood into the lungs, causing pulmonary oedema. Right-sided heart failure can also lead to oedema in other tissues, namely the liver and kidneys. Lung and liver weights were therefore assessed for evidence of systemic congestion. As shown in Table 4.3, there was no difference in lung weight to body ratios (LuW/BW) and liver weight to body weight ratios (Li/BW) between MTAB and sham animals (9.58 ± 0.95 cf. 7.71 ± 0.44 , respectively, $p > 0.05$). Taken together, these results suggest that aortic banding for 4 weeks promotes compensated hypertrophy of heart.

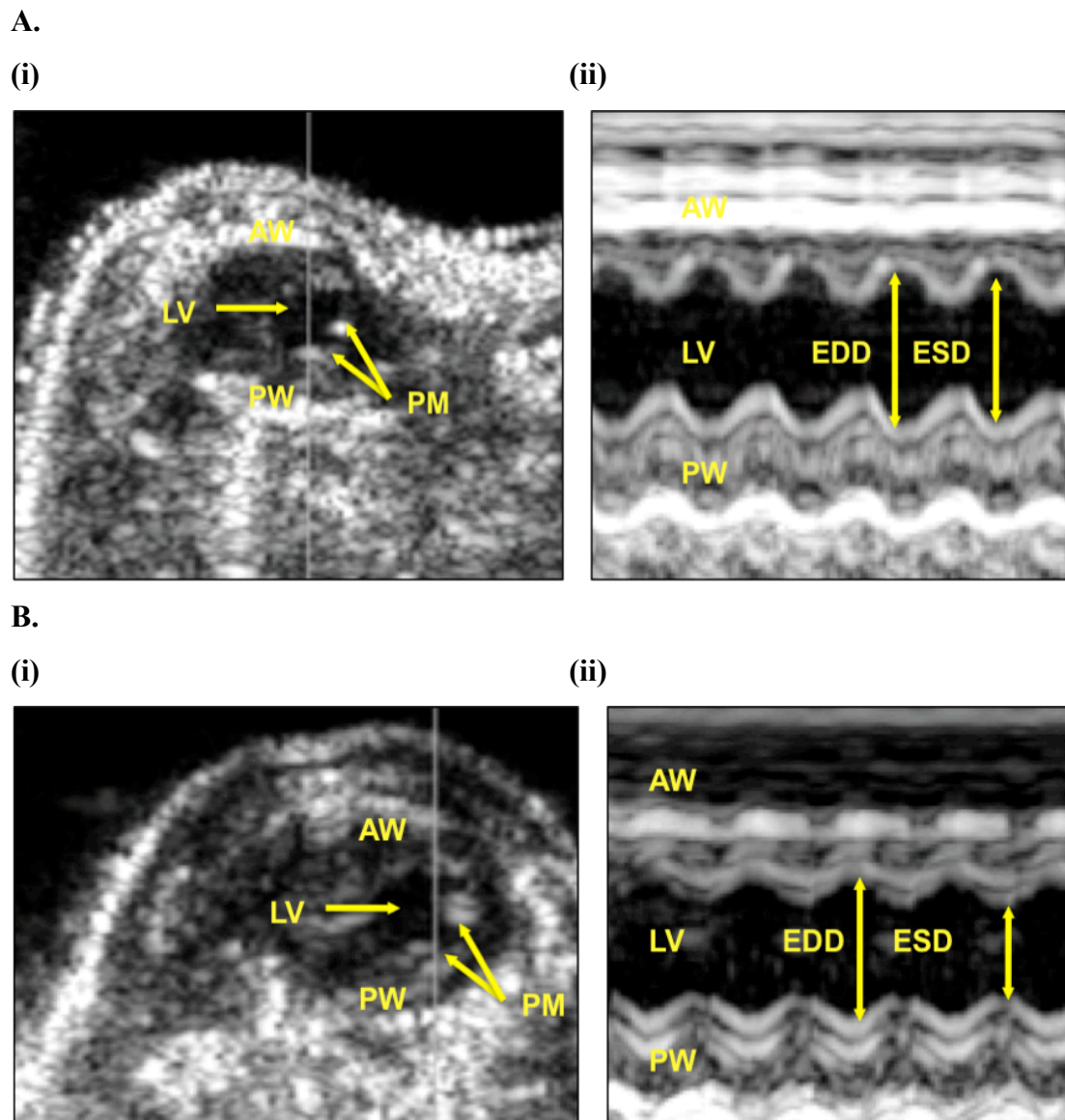
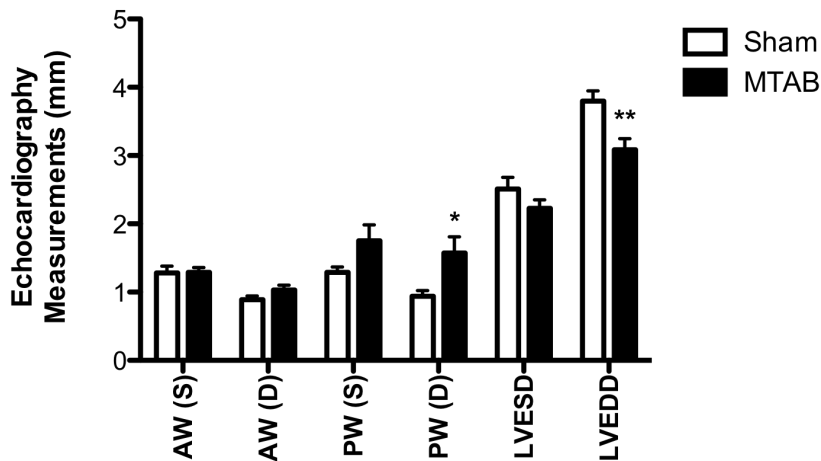


Figure 4.6 Representative echocardiography of Sham and MTAB animals.

Two-dimensional images of a typical left parasternal transverse section showing the short-axis (i), and M-mode traces (ii) from sham (A) and MTAB (B) mice 4 weeks post-surgery. Headed arrows indicate, AW, anterior wall of left ventricle; PW, posterior wall of left ventricle; PM, papillary muscle; LV, left ventricle; ESD, end-systolic diameter; EDD, end-diastolic diameter. Each parameter was measured from M-mode traces and averaged from three cardiac cycles.

A.



B.

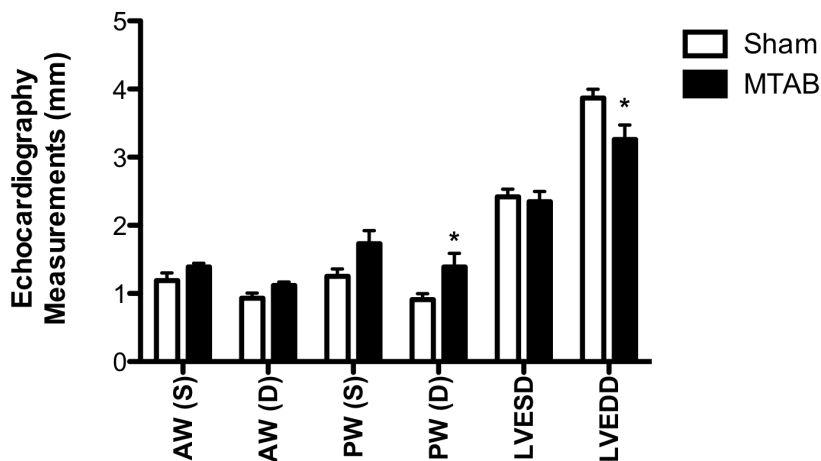


Figure 4.7 Echocardiography wall measurements after two and four weeks aortic banding.

Anterior wall (AW) and posterior wall thicknesses (PW) were measured during systole (S) and diastole (D) to determine the effect of 2 weeks (A) or 4 weeks (B) MTAB on anatomical remodelling of the heart. Left ventricular end-diastolic dimensions (LVEDD) and left ventricular end-systolic dimensions (LVESD) were also assessed. Individual values are summarised in Table 4.3. Statistical significance was determined from unpaired Student's t-tests. Data are means \pm s.e.m, n =10 for both groups, * $p < 0.05$, ** $p < 0.01$.

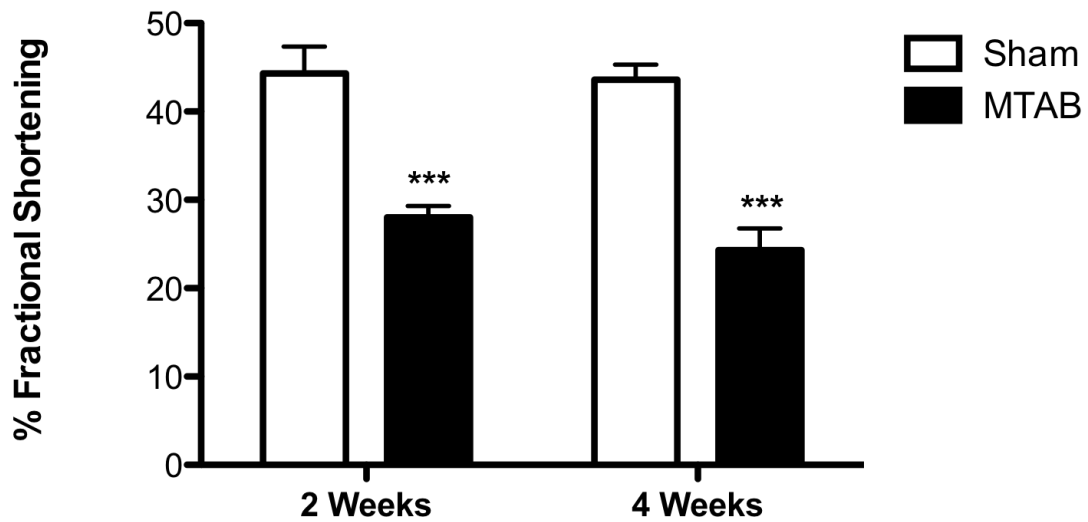
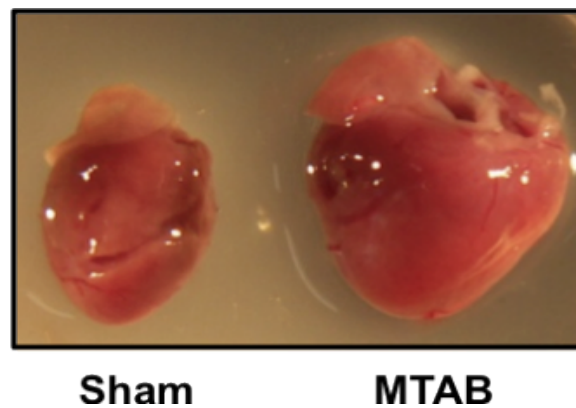


Figure 4.8 % Fractional Shortening after 2 and 4 weeks aortic banding.

MTAB after 2 weeks significantly depressed LV contractility and this was maintained after 4 weeks aortic constriction. Individual values are summarised in Table 4.3. Fractional shortening was calculated by, $\%FS = ((LVESD - LVEDD) / LVEDD) \times 100\%$. Statistical significance was determined from unpaired Student's t-tests. Data are means \pm s.e.m, n= 10 for all groups, *** p < 0.001.

A.



B.

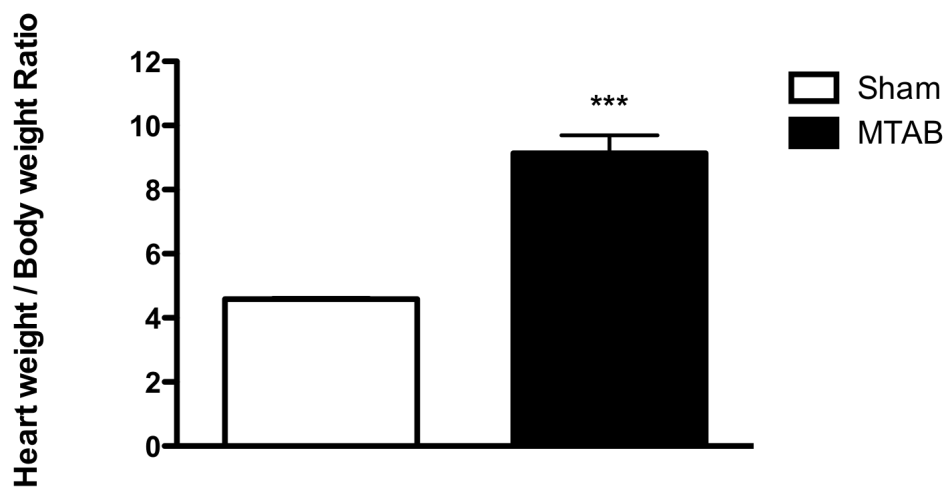


Figure 4.9 Heart weight to body weight measurements from sham and MTAB animals.

Panel A. Photograph depicting a typical increase in size of the heart following MTAB surgery. Panel B. Heart weight to body weight ratios were significantly increased in MTAB animals after 4 weeks banding. Statistical significance was determined from unpaired Student's t-tests. Data are means \pm s.e.m, n=10 for all groups, *** p < 0.001.

	2 weeks post-surgery		4 weeks post-surgery	
	Sham	MTAB	Sham	MTAB
Heart rate (bpm)	386 ± 19.4	402 ± 15.4	391 ± 12.6	372 ± 49.9
AW (S), mm	1.28 ± 0.10	1.29 ± 0.07	1.19 ± 1.11	1.40 ± 0.05
AW (D), mm	0.89 ± 0.05	1.03 ± 0.07	0.93 ± 0.08	1.12 ± 0.05
PW (S), mm	1.29 ± 0.08	1.75 ± 0.24	1.25 ± 0.11	1.73 ± 0.19
PW (D), mm	0.94 ± 0.08	1.57 ± 0.24*	0.91 ± 0.09	1.39 ± 0.20*
LVESD, mm	2.51 ± 0.17	2.23 ± 0.13	2.42 ± 0.11	2.35 ± 0.15
LVEDD, mm	3.80 ± 0.15	3.09 ± 0.16**	3.87 ± 0.13	3.26 ± 0.21*
FS (%)	44.2 ± 3.1	28.0 ± 1.3***	43.6 ± 1.7	24.3 ± 2.5***
HW/BW (mg/g)			4.59 ± 0.04	9.13 ± 0.56***
LuW/BW (mg/g)			7.71 ± 0.44	9.58 ± 0.95
LiW/BW (mg/g)			32.7 ± 1.6	33.5 ± 1.6

Table 4.3 Summary of echocardiographic and post-mortem measurements in sham-operated and MTAB mice.

Abbreviations: bpm, beats per minute; AW, anterior wall thickness during systole (S) and diastole (D); PW, posterior wall thickness during systole (S) and diastole (D); LVESD, left ventricular end-systolic dimension; LVEDD, left ventricular end-diastolic dimension; HW/BW, heart weight to body weight ratio; LuW/BW, lung weight to body weight ratio; LiW/BW, liver weight to body weight ratio. Values are means ± s.e.m. Statistical significance was determined from unpaired Student's t-tests. * p < 0.05, ** p < 0.01, *** p < 0.001.

4.8 Assessment of cardiac fibrosis at 4 weeks in sham and MTAB animals

Cardiac fibrosis is an important feature of maladaptive hypertrophy, characterised by increased collagen deposition and other ECM components. Although the ECM provides an essential structural network for transmitting force generation into organised systolic contraction of the heart, excessive ECM remodelling, collagen deposition and the associated increased production of growth and tissue differentiation factors during myocardial stress promotes myocardial stiffening, cell apoptosis and the recruitment of inflammatory cells (Creemers and Pinto, 2011). Together these factors contribute to deterioration of cardiac function.

Global cardiac fibrosis, assessed by picro-sirius red staining of total collagen, was significantly increased in MTAB animals 4 weeks after surgery (MTAB $5.9 \pm 1.6\%$ cf. sham $0.55 \pm 0.2\%$, $p < 0.05$), as illustrated in Figure 4.10. Values represent picro-sirius red stained area expressed as a percentage of the total area of interest. These data suggest that increased deposition of collagen, used as a marker for cardiac fibrosis, is a key feature of the remodelling heart.

4.9 Assessment of cardiac remodelling and cytokine expression 48 h, 1 week and 4 weeks after sham and MTAB surgery

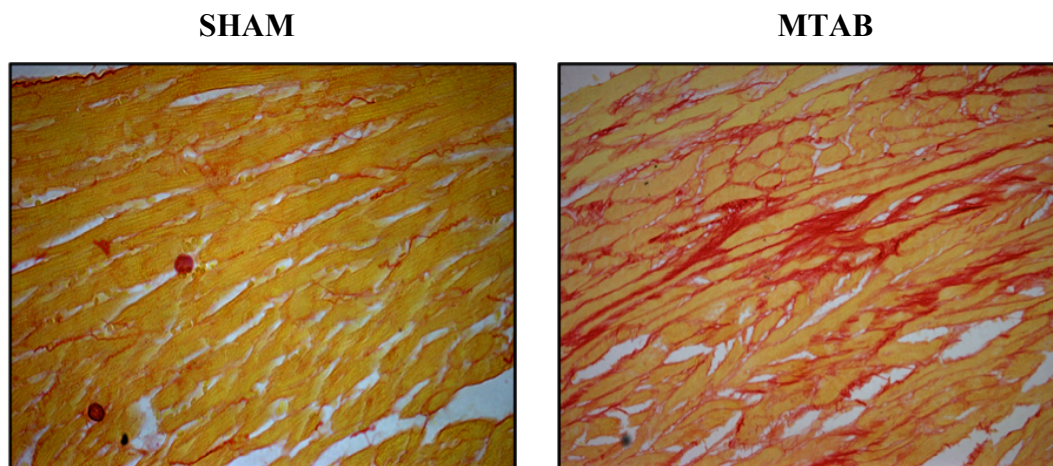
Pressure overload is accompanied by various molecular and cellular changes, including hypertrophy and acute/chronic inflammatory responses. Pro-inflammatory mediators, particularly cytokines such as IL-6 and TNF α , play a key role in promoting inflammation following tissue trauma, with increased expression correlating with decreased cardiac function (Torre-Amione et al., 1996). To determine whether cytokines play a role in this model of pressure-overload hypertrophy, production of IL-6 and TNF- α was quantified in whole ventricular tissue homogenates 48 h (to assess acute responses) and, 1 week and 4 weeks (to assess chronic responses) following aortic banding using ELISA as described in Chapter 2, Section 2.21. It is important to note that sham surgery may promote some localised inflammation, especially at early time points following surgery. However if cytokine signalling plays a role in myocardial remodelling then MTAB hearts should display significantly higher levels of cytokine production even at early time points (48 h), and this may be

sustained over time. In order to correlate cytokine production at 48 h with hypertrophic changes, echocardiography was performed in mice 48 h post-surgery.

Data presented in Table 4.4 demonstrates that after 48 h aortic banding there was an increase in PW thickness during diastole in MTAB animals compared to sham animals (1.47 ± 0.03 cf. 0.97 ± 0.12 , respectively, $p < 0.05$). However, LVESD, LVEDD, AW thickness in systole and diastole, and PW thickness during systole were not different between sham and MTAB animals at 48 h following surgery (Table 4.4). As expected, these data suggest that at this early time point following aortic banding the LV has not had time to undergo anatomical remodelling. In contrast, LV contractility of MTAB animals was prominently decreased 48 h after aortic banding (%FS, MTAB $25.9 \pm 1.40\%$ cf. sham $43.0 \pm 1.40\%$, $p < 0.01$), suggesting that LV function is compromised at this early time point.

Expression levels of total IL-6 were not different between MTAB and sham animals after 48 h or 1 week aortic banding (48 h, MTAB 44.8 ± 19.8 pg/mg total protein cf. sham 110.6 ± 39.5 pg/mg total protein; 1 week, MTAB 88.7 ± 9.50 pg/mg total protein cf. sham 110.9 ± 12.2 pg/mg total protein, $p > 0.05$; Table 4.5). Similarly, total levels of TNF- α were not different between MTAB and sham animals after 48 h or 1 week aortic banding (48 h, MTAB 42.8 ± 17.6 pg/mg total protein cf. sham 96.1 ± 31.4 pg/mg total protein; 1 week, MTAB 75.8 ± 10.5 pg/mg total protein cf. sham 86.9 ± 11.5 pg/mg total protein, $p > 0.05$; Table 4.5). IL-6 and TNF- α production from 4 week banded hearts is currently being assessed. Post-mortem analysis of heart weights, spleen weights, lung weights and liver weights normalised to body weights were not different between sham and MTAB animals after 48 h, 1 week or 4 weeks aortic constriction (Table 4.5). The absolute numbers of animals assessed in this study were very low ($n=3$) and so these results may be attributable to the inherent variability with this model of hypertrophy. This will be discussed in detail in Section 4.10. NF- κ B activity is another marker of pro-inflammatory status following MTAB and therefore will be assessed and discussed in Chapter 5. In addition, haemodynamic stress can lead to recruitment of inflammatory cells into the myocardium, and so leukocyte infiltration is currently being assessed 4 weeks post-surgery.

A.



B.

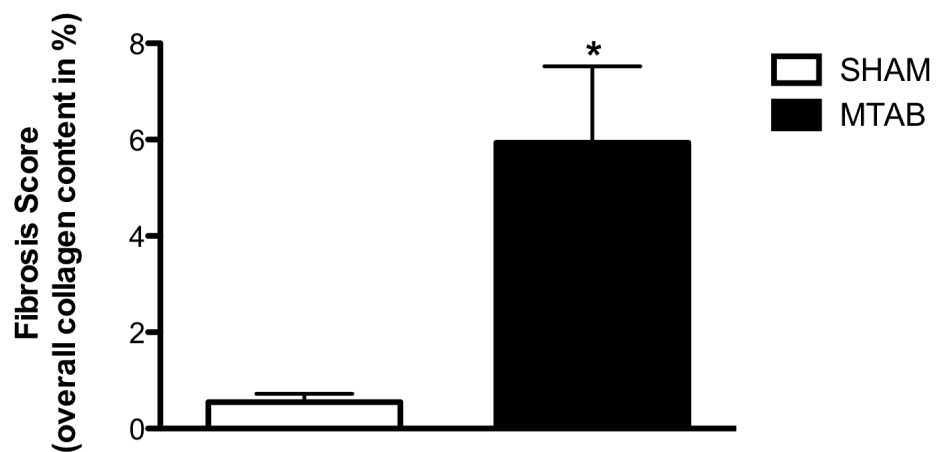


Figure 4.10 Picro-sirius red collagen quantification of sham-operated and MTAB heart sections.

Interstitial myocardial fibrosis, as assessed by picro-sirius red stained collagen, was markedly increased in MTAB compared to sham animals. Values represent stained area expressed as a percentage of the total area of interest. Statistical significance was determined from unpaired Student's t-tests. Data are means \pm s.e.m, $n \geq 4$, * $p < 0.05$.

	48 hours post-surgery	
	Sham	MTAB
AW (S), mm	1.37 ± 0.09	1.40 ± 0.20
AW (D), mm	0.87 ± 0.07	1.07 ± 0.27
PW (S), mm	1.63 ± 0.15	1.63 ± 0.22
PW (D), mm	0.97 ± 0.12	1.47 ± 0.03*
LVESD, mm	2.17 ± 0.12	2.60 ± 0.20
LVEDD, mm	3.80 ± 0.12	3.50 ± 0.20
Fractional shortening (%)	43.0 ± 2.23	25.9 ± 1.40**

Table 4.4 Summary of echocardiographic measurements in sham-operated and MTAB mice 48 hours post-surgery.

Abbreviations: AW, anterior wall thickness during systole (S) and diastole (D); PW, posterior wall thickness during systole (S) and diastole (D); LVESD, left ventricular end-systolic dimension; LVEDD, left ventricular end-diastolic dimension. Values are means ± s.e.m, n=3 for all groups. Statistical significance was determined from unpaired Student's t-tests. * p < 0.05, ** p < 0.01.

	48 hours post-surgery		1 week post-surgery		4 weeks post-surgery	
	Sham	MTAB	Sham	MTAB	Sham	MTAB
HW/BW (mg/g)	6.59 ± 0.37	6.28 ± 0.47	6.29 ± 0.45	6.28 ± 0.53	6.46 ± 0.34	8.03 ± 1.00
SW/BW (mg/g)	3.00 ± 0.37	3.53 ± 0.25	3.26 ± 0.08	3.64 ± 0.26	3.07 ± 0.10	3.56 ± 0.16
LuW/BW (mg/g)	6.87 ± 0.24	6.86 ± 0.32	6.35 ± 0.27	6.37 ± 0.20	6.06 ± 0.32	6.42 ± 0.14
LiW/BW (mg/g)	31.6 ± 1.60	30.4 ± 1.66	30.7 ± 2.72	31.2 ± 1.46	26.9 ± 0.48	29.5 ± 1.12
IL-6 (pg/mg total protein)	110.6 ± 39.5	44.8 ± 19.8	110.9 ± 12.2	88.7 ± 9.50		
TNF- α (pg/mg total protein)	96.1 ± 31.4	42.8 ± 17.6	86.9 ± 11.5	75.8 ± 10.5		

Table 4.5 Summary of post-mortem and cytokine measurements in sham and MTAB mice 48 hours, 1 week and 4 weeks post-surgery.

Abbreviations: HW/BW, heart weight to body weight ratio; SW, spleen weight; LuW, lung weight; LiW, liver weight, IL-6, interleukin-6; TNF α , tumour necrosis factor α . Statistical significance was determined from unpaired Student's t-tests. Data represent means \pm s.e.m from n=3 independent experiments.

4.10 Discussion

In this study we have successfully established and characterised a minimally invasive method for producing *in vivo* LV hypertrophy by banding the transverse aorta in mouse (MTAB), with low morbidity (<5%) and mortality (10-15%).

4.10.1 Characterising the MTAB protocol

The MTAB procedure used in this study was based on a previously published protocol (Hu et al., 2003), however a substantial amount of time was spent establishing and characterising the model to ensure that the technique was reproducible with minimal variations between animals; this was crucial for future work using the model. Only very limited literature exists on the MTAB model and we have for the first time identified important variables in the protocol that can improve the success rate of the surgery. Two key variables identified are (i) anaesthetic regime and, (ii) experimental equipment used.

4.10.1.1 Anaesthesia

During initial characterisation of the surgical procedure, various combinations of injectable anaesthetic agents were tested but proved unsuitable Table 4.1. The anaesthetic agents tested are commonly used for mouse surgery or are alternatives to drugs not currently licensed for use in the U.K. The first combination of anaesthesia tested was a mixture of ketamine, an NMDA receptor antagonist, and xylazine, an α_2 -adrenergic receptor agonist, and has been used previously for TAC surgery (Toischer et al., 2010). Ketamine produces 'dissociative' anaesthesia in which there is marked sensory loss, analgesia, amnesia and paralysis of movement without loss of consciousness. For this reason it is often used in conjunction with xylazine to produce and maintain sedation. However, even with the more active enantiomer of ketamine, S-ketamine, additional doses of anaesthesia were regularly required during the procedure. The amount of top up required varied between animals and the level of anaesthesia was unpredictable, with all animals experiencing respiratory

depression. This highlights the lack of control for the operator, which is a severe limitation when using injectable anaesthesia regimes. A combination of ketamine, xylazine and acepromazine (a phenothiazine derivative used in animals for sedation) also proved unsuitable. With all three of the above mentioned combinations of anaesthesia, animals died early during the procedure or even before it began, possibly due to bradycardia and hypotension caused by xylazine (Hart et al., 2001). The final injectable combination tested of hypnorm (fentanyl fluanisone), a commonly used neuroleptanalgesic, and the benzodiazepine hypnovel (midazolam), has previously been shown to maintain heart rate (HR) and MAP within physiological limits during mouse cardiac surgery (Jong et al., 2002). However, in this study the animals exhibited respiratory depression and subsequent arrest before surgery began. To our knowledge, this comparison of anaesthetic regimes has not previously been documented and is a critical factor in determining success of surgery (Martin et al., 2011, manuscript in preparation). Inhalation anaesthesia has benefits over injectable delivery due to an improved ability to control dosing. Once a suitable cone mask was designed for mouse (Figure 4.3), inhalation anaesthesia using a mixture of isoflurane and oxygen proved most suitable with survival rates of 80-85%.

In this study, anaesthesia was required not only for surgery but also for echocardiography. Since contractility was being assessed in anaesthetised animals, the effects of this administration had to be considered. Generally anaesthesia depresses cardiac function to varying extents (Connelly and Coronado, 1994, Hart et al., 2001, Szczesny et al., 2004, Ishizaka et al., 2004), so when using non-invasive echocardiography to assess the hemodynamic parameters in mice following surgery it is important that the anaesthetic regimen does not cause severe adverse effects on cardiac function. Several studies have shown that inhalation anaesthesia, such as halothane, is superior to injectables such as ketamine/xylazine as the latter reduces heart rate, LV FS and cardiac output (Chaves et al., 2001, Roth et al., 2002). Echocardiographic studies in mice have proved isoflurane to be the most suitable anaesthetic as MAP, HR and %FS remain stable during observations lasting several hours (Roth et al., 2002, Szczesny et al., 2004, Constantinides et al., 2011). Due to its low solubility in blood and fat, induction of and recovery from isoflurane anaesthesia is fast and due to its lack of metabolism, isoflurane is the ideal anaesthetic to use when repeated measures are necessary, as is the case in these investigations. Nevertheless, other studies have shown that the timing of measurements after the

onset of anaesthesia is crucial for preserved LV systolic and diastolic functions (Roth et al., 2002, Schaefer et al., 2005). For this reason, all echocardiographic measurements in these studies were taken within 10-15 minutes of the animal being administered anaesthesia.

4.10.1.2 Animals and sex-specific differences

These studies specifically used in-house bred C57BL/6J male mice as opposed to female animals. One reason for this, as illustrated in Figure 4.2, is due to the difference in overall size of male and female animals. It was found that the heavier male animals tended to survive better under anaesthesia and recover more quickly from the surgical procedure compared to female animals. Thus, the animals in these studies were used at a particular weight (~ 25- 30g) rather than age, however at this weight animals were 8+ weeks and considered adults. Another important reason for using male animals in these studies was due to gender related differences in molecular remodelling in response to pressure overload. Studies have revealed that male animals generally exhibited more pronounced hypertrophy than females, with depressed contractile function, higher mRNA expression of hypertrophic markers such as ANF and β -MHC and dysfunctional Ca^{2+} handling (Weinberg et al., 1999). Other research has shown that females have attenuated structural remodelling in myocardial infarction, compared with males who generally have a higher rate of cardiac rupture, higher degree of inflammation and overall poorer LV function (Cavasin et al., 2004).

These sex-differences have largely been attributed to 17β -estradiol (E2) signalling via oestrogen receptors (ER) α and β (Skavdahl et al., 2005). ER α and ER β are members of the nuclear hormone receptor super-family of ligand activated transcription factors that have been found to mediate the effects of E2 on the cardiovascular system, such as decreasing the development of atherosclerosis, preventing apoptosis in cardiac myocytes in heart failure and attenuating the response to pressure overload (Pedram et al., 2005, Skavdahl et al., 2005, Patten et al., 2008). Although both receptors are up-regulated in human myocardial pressure overload (Nordmeyer et al., 2004) and have been shown to play a role in the protection observed in female hearts (Wang et al., 2006, Jazbutyte et al., 2008), studies have

suggested that ER β plays a predominant role, eliciting different actions in males and females (Fliegner et al., 2010). The action of E2 on ER β appears to be related in part to increased extracellular matrix (ECM) protein turnover in males compared to females (Witt et al., 2008). This was confirmed using an ER $\beta^{-/-}$ mouse to illustrate that ER β promotes fibrosis in males but inhibits fibrosis in female hearts (Fliegner et al., 2010). A recent study highlighted similar results in female human aortic stenosis patients who displayed less fibrosis and faster regression of LV hypertrophy after valve replacement compared to their male counterparts, attributed to an increase in collagen I, collagen III and matrix metalloproteinase-2 (MMP-2) in male patients (Petrov et al., 2010). These observations were later confirmed by studying rat cardiac fibrosis, whereby E2 down regulated these proteins in fibroblasts derived from females but not from males (Petrov et al., 2010). More importantly however, E2 has been found to suppress CaMKII signalling in the heart, whereby CaMKII δ and phosphorylated CaMKII were up-regulated in the hearts of ovariectomised rats and were restored to normal by oestrogen replacement (Ma et al., 2009). In addition, cardiac contractility, Ca²⁺ transients and apoptosis were greater in ovariectomised rats upon ischaemia/reperfusion, and CaMKII inhibition (by KN-93) reversed these responses (Ma et al., 2009). Recent research has also shown that NF- κ B signalling inhibits the expression of ER α in a cardiomyocyte cell line (AC16) (Mahmoodzadeh et al., 2009). Given the nature of the current project and to ensure that there were no conflicting results due to the effects of E2 on the cardiovascular system, only male animals were used in these studies and all subsequent investigations.

4.10.1.3 Post-surgery remodelling period

In characterising the MTAB model, an important consideration in addition to sex was that of the post-surgical period for remodelling. Consultation of the literature was therefore important to ensure that cardiac hypertrophy was evident.

Literature has documented that at 7 days and 2 weeks after TAC surgery an increase in LV systolic pressure, increase in LV mass, and increase in LV wall thickness is observed (Colomer et al., 2003, Hu et al., 2003), however 4 weeks post-surgery is expected to produce greater hypertrophy with more pronounced changes in the expression of various proteins (Liao et al., 2002b) and decreased %FS (Mandl et

al., 2011). On the other hand, if banded animals are left for around 7–12 weeks, pressure overload induced remodelling will become de-compensatory and will eventually lead to HF (Lygate, 2006, Mandl et al., 2011).

As cardiac remodelling is a very dynamic and progressive process, it is important to consider more than one time point in order to determine how long after the banding procedure remodelling of the heart begins. As the heart responds to a stress or insult, the changes are numerous and it is essential that animal models reflect this complexity. In addition, recent literature has shown that hypertrophy differs in a time-dependent manner between different strains of mice (Barrick et al., 2007). In this study, structural remodelling following surgery was assessed at 4 weeks following MTAB or sham surgery to ensure that substantial remodelling could easily be observed, without the progression to HF. LV function was assessed using echocardiography at 2 weeks in addition to assessment at 4 weeks following surgery to determine the time-scale of structural remodelling in this particular model of cardiac hypertrophy.

4.10.2 In-vivo and post-mortem analysis of model

4.10.2.1 Pressure measurements

To ensure that the band placed around the transverse aorta was in fact producing an increase in pressure, MAP was assessed 1 week after banding. Our initial experiments using limited numbers of animals (n=3) and with limited equipment revealed no difference in MAP pressure between sham-operated and MTAB animals. Nevertheless after 4 weeks aortic banding, there was a substantial increase in HW/BW ratios in MTAB animals with no increase in LuW/BW or LiW/BW ratios (Figure 4.9 and Table 4.2), clearly indicating that the animals are undergoing hypertrophy due to constriction of the aorta (Liao et al., 2002b, Gao et al., 2005).

A possible explanation for these observations in MAP is likely due to the very small cohort of animals examined (n=3). As cardiac remodelling is such a dynamic process it is often difficult to determine exactly what stage of the disease process animals have progressed to after a certain period of banding and of course, this is different between animals due to inherent variability in response to pressure-overload (Mohammed et al., 2011). In addition, small differences in the tightness of the

constriction around the aortic arch can impact on the extent of remodelling and hypertrophy. Research has also suggested that ~25% of mice can gradually internalize the banding suture through the aortic wall, thus allowing blood flow both through the band and around the band, resulting in a drop in pressure and partial regression of hypertrophy (Lygate et al., 2006). This clearly highlights the requirement for large experimental group sizes. Unfortunately in the time frame of this study it was not possible to assess MAP in a greater number of animals.

Another possible reason for the observed MAP data could be due to the methodology used to measure the extent of pressure-overload. Although assessment of MAP has been used previously to determine the effectiveness of the TAC procedure (Liao et al., 2002b), direct measurement of LV pressure using a specialised micromanometer-tipped catheter inserted through the right carotid artery and into the LV may yield more reliable data (Hu et al., 2003). Unfortunately the equipment necessary to allow such measurements was not available in our laboratory nor was the expertise to perform such experiments. Nevertheless, LV pressure-measurements were performed on MTAB and sham-operated animals (with exactly the same protocol followed for surgery) by our collaborator Dr. David Grieve (Queens University, Belfast; manuscript in preparation Martin et al., 2011). These data suggest that the band placed around the transverse aorta was producing pressure-overload as a number of haemodynamic parameters such as SBP and LVEDP were increased in MTAB compared to sham mice and LV contractility was impaired as evidenced by a decrease in $LVdP/dt_{max}$ and an increase in $LVdP/dt_{min}$ in MTAB animals (Table 4.2). These data correspond with other independent studies in mice (Niizeki et al., 2008).

4.10.2.2 Echocardiography

A few days following banding of the aortic arch, the heart strives to pump blood against the increased afterload created by the constriction, thus compromising LV function. In mouse TAC models, LV hypertrophy is thought to develop rapidly with systolic function improving towards normal values over the first 2 weeks following banding (Nakamura et al., 2001), possibly as a result of hypercontractility (Takaoka et al., 2002). As summarised in Figure 4.7 and Table 4.3, echocardiography

measurements of AW thickness during both systole and diastole were not different from sham-operated animals, however PW thickness was increased during diastole 2 and 4 weeks after MTAB. Banded animals also displayed an increase in heart mass compared to sham-operated animals (Figure 4.9 and Table 4.3) and diastolic dysfunction was apparent in MTAB animals as evidenced by a decrease in % FS and LVEDD (Figures 4.7 and 4.8, and Table 4.3). These data are in correspondence with a compensated concentric hypertrophic phenotype, whereby the PW thickens to reduce wall stress and afterload (Nakamura et al., 2001, Hu et al., 2003, Zhou et al., 2004). It is important to note that heart rates were not different between sham-operated and MTAB animals 2 or 4 weeks after aortic banding (Table 4.3) as measures of %FS can depend on HR.

LV ejection fraction (EF) can also be used as a measure of LV contractility. EF is the percentage of the LV diastolic volume that is ejected with systole and is commonly calculated from 2D M-mode echo traces by cubing LVEDD and LVESD to give measures of LVED volume (V) and LVESV, respectively (Solomon, 2006). EF is then calculated by the following equation: $EF = ((LVEDV - LVESV) / (LVEDV)) \times 100$. However, small errors in measurements of LVEDD or LVESD are multiplied to the third power, resulting in wide errors of EF calculated by this method. More importantly, this method assumes an ellipsoid shape for the LV and is therefore inaccurate when LV geometry is abnormal, such as with progressive cardiac dilatation in HF when the LV volume increases and becomes more spherical (Bellenger et al., 2000, Solomon, 2006). Teichholz et al. (1976) derived a regression formula to correct for these changes in LV geometry, $(LV \text{ volume} = (7.0/2.4 + D) \times D^3$, where D= EDD or ESD) but again this method is only recommended when LV geometry is relatively normal (Teichholz et al., 1976). A recent study has suggested that LV EF determined by Teichholz and volumetric cardiac magnetic resonance do not differ on average, however 29% of subjects were assigned to a different EF category (e.g. normal, impaired or severely impaired). A more accurate measure of EF calculated from 2D echocardiography is by Simpson's biplane method, which has been found to correlate with EF calculated from cardiovascular magnetic resonance imaging (Bellenger et al., 2000). This method is based on manual tracing of the endocardial border in end-diastole and end-systole, with volume quantified by assuming that the LV cavity is a stack of elliptical discs whose volumes are quantified and summated using automated software (Solomon, 2006). In clinical practice however this method is often not used

due to the time taken to perform the analysis as well as the dependence on good visualisation of the endocardial border (Bellenger et al., 2000). Simpson's biplane method was not available for this study and so %FS measurements taken directly from M-mode echocardiography images were a more reliable measure of LV contractility in this study. Although, it is important to note that there are limitations when measuring %FS, for example, it only reflects regional contractile behaviour and therefore is most accurate in healthy individuals or those with heart disease that uniformly involves the entire LV. Nevertheless, calculation of %FS is relatively easy to perform and is a more reliable method for assessment of LV function than calculation of % EF in this study.

4.10.2.3 Organ weight to body weights ratios

Hypertrophic growth of the myocardium was evident in MTAB mice after 4 weeks aortic banding, as HW/BW ratios were increased in MTAB compared to sham animals (Figure 4.9 and Table 4.3). After 48 h, 1 week or 4 weeks of aortic banding, animals do not appear to have progressed to HF as there was no pulmonary or liver hypertrophy or congestion evident in MTAB animals (LuW/BW and LiW/BW ratios were not different between sham and MTAB animals, Table 4.3 and Table 4.5).

SW/BW ratios were not different between MTAB and sham-operated animals after 48 h, 1 week or 4 weeks MTAB surgery (Table 4.5), suggesting that inflammatory cell responses were not increased in banded animals, as discussed in section 4.10.2.5.

4.10.2.4 Cardiac fibrosis

In the normal heart there is a small amount of collagen/fibrosis present in the interstitial and perivascular space, which is important to provide a structural network for transmitting force generated by myocytes. During the compensatory phase of cardiac hypertrophy, an increase in collagen may be beneficial as the collagen matrix grows to support the increased myocyte hypertrophy. Chronic pressure-overload however promotes excessive deposition of collagen that decreases myocardial compliance resulting in myocardial stiffness and impaired filling during diastole

(Creemers and Pinto, 2011). As expected, 4 weeks MTAB promoted significant fibrosis of the heart (as assessed by total collagen deposition; Figure 4.10) in correlation with published data in mouse (Sun et al., 2007). Research has demonstrated that the severity of fibrosis closely correlates with the extent of LV hypertrophy and impaired % EF in valvular aortic stenosis patients (Hein et al., 2003). Although not assessed in this study, remodelling of the ECM induced by TAC involves an increase in collagen I, collagen III and MMP-2 (Gao et al., 2005).

A critical step in the development of cardiac fibrosis is the 'activation' of fibroblasts to a myofibroblast phenotype where they adopt intermediate characteristics between fibroblasts and smooth muscle cells. These cells tend to show increased levels of collagen synthesis, migration and pro-inflammatory cytokine release (Creemers and Pinto, 2011). Cytokines have been shown to regulate ECM protein turnover (Siwik et al., 2000) and ultimately play a role in hypertrophy and ventricular function.

4.10.2.5 Inflammation

Two key cytokines involved in the progression of cardiac diseases are IL-6 and TNF- α . IL-6 is a pleiotropic cytokine responsible for various cellular processes such as cell growth, apoptosis, differentiation and survival (Banerjee et al., 2009). Currently, the role of IL-6 in fibrosis is unclear with reports that IL-6^{-/-} promotes ventricular dilatation, increases interstitial fibrosis and alters cardiac cell populations (decreased myocytes and increased fibroblasts) and their cell-cell interactions (Banerjee et al., 2009). On the other hand, infusion of IL-6 for 7 days in rat promoted concentric LV hypertrophy, increased ventricular stiffness and fibrosis (Melendez et al., 2010), and an anti-IL-6 receptor antibody proved successful in ameliorating LV remodelling and decreasing MMP-2 activity after myocardial infarction (Kobara et al., 2010). In addition, IL-6 has been shown to be involved in promoting myocyte hypertrophy and fibrosis during chronic allograft rejection, with inhibition of IL-6 neutralising these effects (Diaz et al., 2009). Thus, IL-6 levels may dictate the outcome at different stages of cardiac remodelling (Vistnes et al., 2010).

TNF- α is a proinflammatory cytokine released by all cardiac cells in response to stress to stimulate an inflammatory response (Sato et al., 2003). Both circulating and

cardiac TNF- α levels have been reported to be elevated in dilated cardiomyopathy, myocardial infarction, and LV pressure-overload (Sato et al., 1999, Kassiri et al., 2005, Deswal et al., 2001). Increased TNF- α expression following aortic banding is associated with increased infiltration of inflammatory cells (lymphocytes and macrophages), cardiac hypertrophy, impaired LV function and increased expression of MMP-9; all of which were attenuated in a TNF- $\alpha^{-/-}$ mouse model (Sun et al., 2007). TNF- α is thought to induce ECM remodelling via upregulation of the angiotensin type 1 receptor (AT₁R) in cardiac fibroblasts (Peng et al., 2002, Gurantz et al., 2005) and through local induction of specific MMP's (Bradham et al., 2002).

In this MTAB model IL-6 and TNF- α expression were measured from whole ventricular heart homogenates after 48 h and 1 week banding to assess inflammation. Assessment of cytokine production after 4 weeks MTAB is currently on going. These specific times points were chosen to assess acute (48 h and 1 week) and chronic (4 weeks) inflammatory changes following banding. As summarised in Table 4.5, no differences between the expression levels of either cytokine at either time point in MTAB compared to sham-operated animals were observed, despite observing impaired contractility at 48 h (decreased %FS, Table 4.5). There may be a number of reasons for this unexpected result including, (i) the time points observed, (ii) the methodology used to assess cytokine expression and (iii), the total number of animals examined.

Literature has suggested that ~3 days after aortic banding, acute inflammatory changes including neutrophil/macrophage infiltrations are observed (Higashiyama et al., 2007) and IL-6 and IL-1 β expression are increased after 1 week (Song et al., 2010). Conversely, other research has suggested that cytokines are transiently expressed after aortic banding, with IL-6 and TNF- α mRNA maximal at 6 hours but returning to baseline within 3-7 days (Baumgarten et al., 2002, Ying et al., 2009). Therefore, it is possible in our studies that we missed these changes in cytokine production/expression. This is in line with other studies, suggesting that there is no increase in circulating cytokine levels after 1 week of aortic banding (Vistnes et al., 2010). It is important to note that these studies assessed mRNA cytokine levels as opposed to total protein levels, as was the case in this study. It is possible that the mRNA levels of cytokines do not correspond with an increase in protein expression, thus assessment of IL-6 and TNF- α mRNA at 48 h, 1 week and 4 weeks following banding via reverse-transcriptase polymerase chain reaction (RT-PCR) techniques are

on going. Similarly, it has been noted that cytokine receptor expression may increase following banding (Baumgarten et al., 2002) and HF (Deswal et al., 2001) and therefore it would be important to assess cytokine receptor expression in this MTAB model. In addition, when assessing cardiac inflammation it may be important to look at a wide range of cytokines (such as IL-1 β), growth factors (such as TGF- β) and proteins (such as C-reactive protein) as they have all been found to be upregulated in a variety of cardiac diseases and act to promote inflammation (Gurantz et al., 2005, Szabo-Fresnais et al., 2010, Turner et al., 2007, Honsho et al., 2009, Teekakirikul et al., 2010, Nagai et al., 2011, Zhang et al., 2010a). In this particular study it is also important to take into consideration the low numbers of samples assessed (n=3) and the inherent variability between animal responses to pressure-overload, as mentioned previously.

Other experimental factors should be taken into consideration, for example, the handling and storage of the heart samples before analysis of cytokine production. Storage conditions, anticoagulant and repeated freeze-thaw cycles have all been shown to impact on the detected levels of cytokines, including IL-6 and TNF- α (Riches et al., 1992, Thavasu et al., 1992, Flower et al., 2000, Jackman et al., 2011). Although all samples were handled in essentially the same way (as described in Chapter 2: Section 2.21), the amount of time samples were stored at -80C did vary and this may have an impact on the level of cytokine detected. Heparin was used when euthanizing the mice to prevent blood clotting in the heart, however heparin has been shown to interfere with antigen-antibody binding (Cannon et al., 1993), and thus the use of heparin should be avoided in subsequent experiments.

When assessing inflammation and inflammatory signalling following MTAB, it may also be important to assess infiltrating immune cells and mast cell activation as they release various cytokines and proteases involved in remodelling of the ECM (Higashiyama et al., 2007, Levick et al., 2009). Both immune cells and mast cells have been implicated in human-dilated cardiomyopathy and LV hypertrophy (Janicki et al., 2006, Levick et al., 2011), with mast cells playing a key role in the progression of LV hypertrophy to HF (Hara et al., 2002). Preliminary data from Dr Grieve's laboratory suggest that leukocyte infiltration is increased in MTAB compared to sham-operated animals 4 weeks post-surgery (data not shown). More experiments are required to confirm this as well as assessment of leukocyte infiltration at 48 h and 1 week following banding.

4.11 Conclusions

In summary, we have successfully established and characterised a minimally invasive method for producing pressure-overload induced left ventricular hypertrophy by banding the aorta in mouse. Substantial time has been invested to ensure high reproducibility and low morbidity and mortality. Echocardiography, haemodynamic and post-mortem measurements suggest that the MTAB model produces rapid and reproducible cardiac hypertrophy. The minimally invasive technique is a useful refinement of previous TAC models and should greatly facilitate the study of the pathophysiology and treatment of pressure-overload cardiac hypertrophy.

**Chapter 5: Alterations in
CaMKII and NF- κ B signalling
following cardiac hypertrophy**

5.1 Introduction

Having established that CaMKII δ modulates NF- κ B activity in adult CFs and that CaMKII δ directly interacts with IKK β , it was important to explore whether either or both signalling systems were altered following cardiac hypertrophy. Given the focus of the project on CFs compared with cardiac myocytes, the role of CaMKII δ in CF function following cardiac hypertrophy was also explored.

As mentioned previously, chronic pressure overload not only leads to hypertrophic growth of the myocardium but can also result in increased cardiac fibrosis and stiffness of the myocardium which contributes to the contractile dysfunction associated with compensated hypertrophy (Vasquez et al., 2011). Fibrosis results from a combination of increased CF proliferation and collagen deposition (Diez et al., 2007). Another important feature of the diseased heart is the accompanying inflammation that ensues following cardiac insult. There is increasing evidence that inflammation contributes to the pathophysiology associated with many forms of progressive heart disease, including cardiac hypertrophy (Bayes-Genis, 2007, Smeets et al., 2008). As alluded to previously, myocardial inflammation results from the release of a number of factors from CFs, including growth factors, cytokines and chemokines, that act to induce hypertrophic growth of myocytes and potentiate the inflammatory response via recruitment of inflammatory cells to the site of injury. Using the MTAB model of pressure-overload mediated cardiac hypertrophy, it was important to determine whether adult CF function (specifically proliferation) is altered during hypertrophy in parallel with the observed increase in collagen deposition 4 weeks post-surgery (Chapter 4, Section 4.8).

The pro-inflammatory NF- κ B pathway is a key candidate for activation of inflammatory responses during cardiac hypertrophy (Li et al., 2004, Alter et al., 2006). As mentioned previously, in its inactive state, NF- κ B resides in the cytosol tethered to the inhibitory protein, I κ B α . Upon activation, it is released from this protein and translocates to the nucleus to promote transcription of a variety of pro-inflammatory genes. It is therefore possible to measure activation of this pro-inflammatory signalling pathway by measuring increased levels of NF- κ B in nuclear preparations using an electrophoretic mobility shift assay (EMSA), as described in

Chapter 2, Section 2.20. In this way, pro-inflammatory signalling can be assessed following 4 weeks MTAB surgery.

Experiments presented in the current chapter will assess alterations in CaMKII δ and NF- κ B protein expression and activities following cardiac hypertrophy. Changes in CF proliferation following cardiac hypertrophy will also be monitored, and the possible role of CaMKII in CF function will be investigated.

5.2 Altered CaMKII δ protein expression and activity in cardiac preparations following hypertrophy

Whole ventricular homogenates, obtained 4 weeks post-surgery from both sham-operated and MTAB hearts, were analysed for expression of CaMKII δ using a custom-made antibody against the C-terminus of the protein. Quantitative immunoblotting using densitometry analysis demonstrated that CaMKII δ expression (relative to GAPDH) was increased 1.8 fold in MTAB compared to sham animals (0.457 ± 0.057 cf. 0.251 ± 0.025 , respectively, $n=9$ for both groups, $p<0.01$, Figure 5.1A and B). As shown in Figure 5.1C and D, increased expression of CaMKII δ during cardiac hypertrophy correlated with an increase in HW/BW ratio (Spearman $r=0.735$, $p<0.01$) and a decline in % FS (Spearman $r=-0.490$, $p<0.05$), respectively.

Assessment of the activation state of CaMKII in WH was monitored by quantifying autophosphorylation at Thr 286 using a specific phospho-CaMKII δ antibody (Thermo Scientific). Immunoblotting revealed that the phosphorylation status of CaMKII δ was significantly increased ~ 2.7 fold in MTAB hearts (0.498 ± 0.085 cf. sham 0.185 ± 0.014 , $n=9$ for both groups, $p<0.01$, Figure 5.2A and B). This increase in autophosphorylation and therefore activity of CaMKII δ observed during cardiac hypertrophy strongly correlated with an increase in HW/BW ratio (Spearman $r=0.680$, $p<0.01$) and a decline in %FS (Spearman $r=-0.533$, $p<0.05$, Figure 5.2C and D, respectively).

Together these data provide evidence that the expression and activity of CaMKII δ is increased in hypertrophied hearts, and correlates with the extent of hypertrophy and decline in cardiac function.

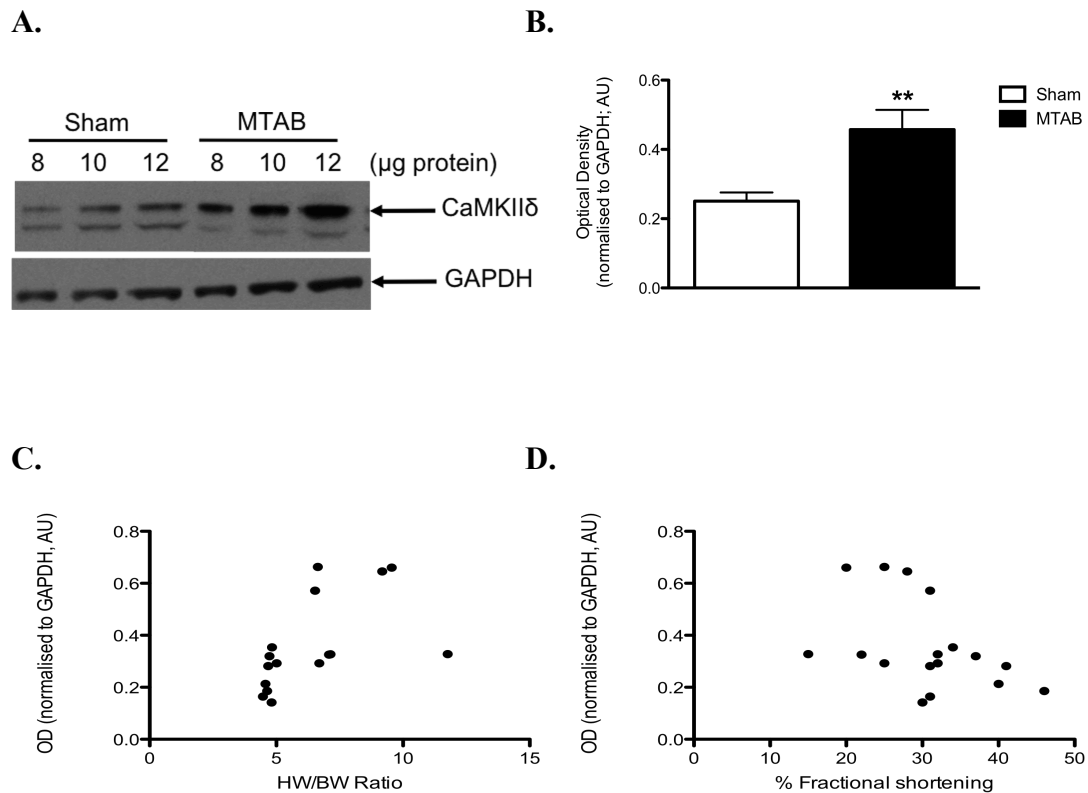


Figure 5.1 CaMKII δ expression in sham and MTAB whole heart homogenates

Panel A. A typical immunoblot of sham-operated and MTAB whole heart homogenates (8-12 μg) probed for CaMKII δ (upper panel) and GAPDH (lower panel). Panel B. Normalised densitometric analysis of immunoblots relative to GAPDH expression. Panel C. Correlation plot of heart weight/body weight (HW/BW) ratio versus normalised CaMKII δ protein expression. Panel D. Correlation plot of % fractional shortening versus normalised CaMKII δ protein expression. Data are means \pm S.E.M, $n \geq 9$ independent experiments, ** $p < 0.01$.

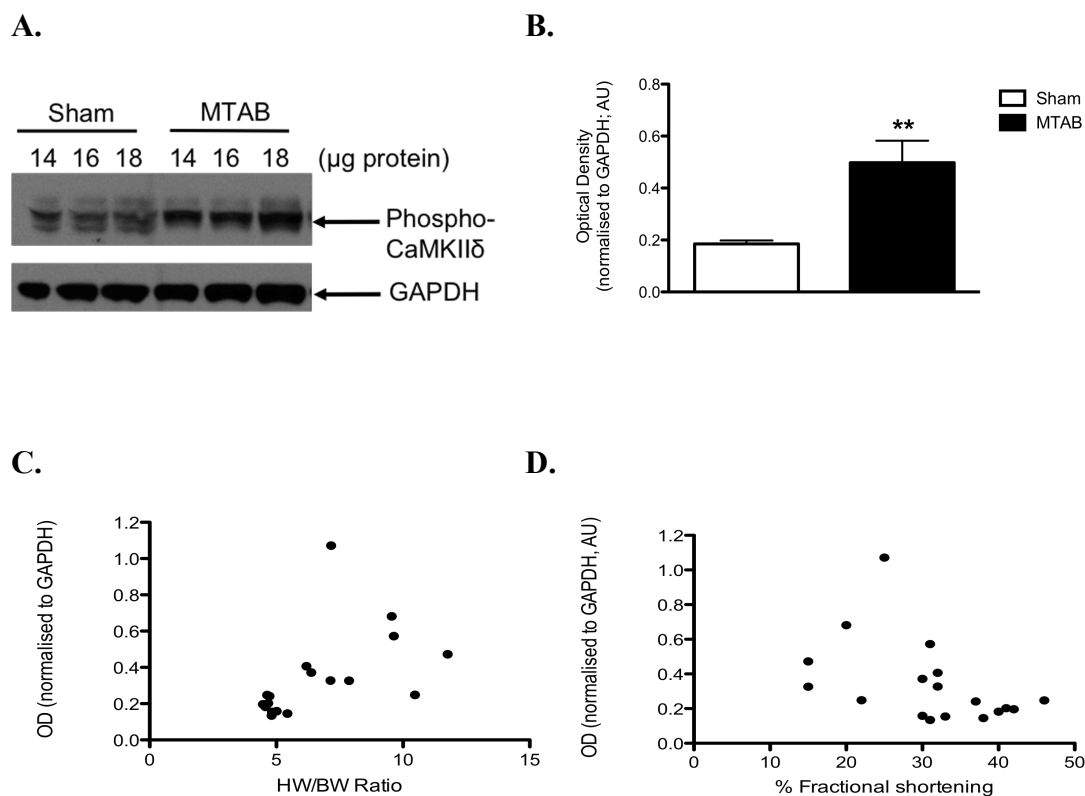


Figure 5.2 CaMKIIδ activity in sham and MTAB whole heart homogenates

Panel A. A typical immunoblot of sham-operated and MTAB whole heart homogenates (14-18 μg) probed for phospho-CaMKIIδ (Thr 286; upper panel) and GAPDH (lower panel). Panel B. Normalised densitometric analysis of immunoblots relative to GAPDH expression. Panel C. Correlation plot of heart weight/body weight (HW/BW) ratio versus normalised phospho-CaMKIIδ protein expression. Panel D. Correlation plot of % fractional shortening versus normalised phospho-CaMKIIδ protein expression. Data are means ± S.E.M, $n \geq 9$ independent experiments, ** $p < 0.01$.

5.3 *Pro-inflammatory signalling following cardiac hypertrophy*

Activation of pro-inflammatory NF- κ B signalling accompanying MTAB-mediated hypertrophy was then explored by assessing IKK α , IKK β and NF- κ B p65 expression in MTAB and sham-operated WH.

Quantitative immunoblotting using densitometry analysis demonstrated that IKK α expression (relative to GAPDH) was increased 1.5 fold in MTAB compared to sham animals (0.349 ± 0.036 cf. 0.229 ± 0.021 , $n=8$ and $n=7$, respectively, $p<0.05$, Figure 5.3A and B). Attempts to quantify IKK β expression were unsuccessful due to the highly non-specific nature of commercially available antibodies, as discussed in Chapter 3, Section 3.3.3. However, NF- κ B p65 expression was also significantly increased during cardiac hypertrophy, with a ~ 5.4 fold increase in protein expression in MTAB hearts compared to sham hearts (0.978 ± 0.291 cf. 0.182 ± 0.010 , respectively, $n=9$ for both groups, $p<0.05$, Figure 5.4C and D). Increased IKK α protein expression does not correlate with an increase in HW/BW ratio (Spearman $r=0.296$, $p=0.284$, Figure 5.3 panel C) and a decline in %FS (Spearman $r=-0.019$, $p=0.944$, Figure 5.3 panel D). However, NF- κ B p65 protein expression following cardiac hypertrophy correlated strongly with an increase in HW/BW ratio (Spearman $r=0.709$, $p<0.001$) and a decline in %FS (Spearman $r=-0.597$, $p<0.01$), as illustrated in Figures 5.3 and 5.4 panels C and D, respectively. Together these data suggest that NF- κ B signalling is altered following pressure overload.

Evidence for activation of NF- κ B following MTAB surgery was investigated using nuclear extracts prepared from ventricular tissue isolated from sham and MTAB hearts. Using an EMSA, nuclear extracts from MTAB and sham hearts were analysed for activity of NF- κ B, as described in Chapter 2, Section 2.20. Increased NF- κ B DNA binding was evident in extracts from MTAB tissue when compared with sham, and NF- κ B activity correlated with extent of hypertrophy (HW/BW ratio) and cardiac contractile dysfunction (decreased %FS; Figure 5.5A, respectively). Densitometric analysis showed a significant difference in the NF- κ B DNA binding activity between sham and MTAB tissue ($p<0.05$, Figure 5.5B). Taken together, these data provide support that pro-inflammatory signalling is elevated following MTAB surgery.

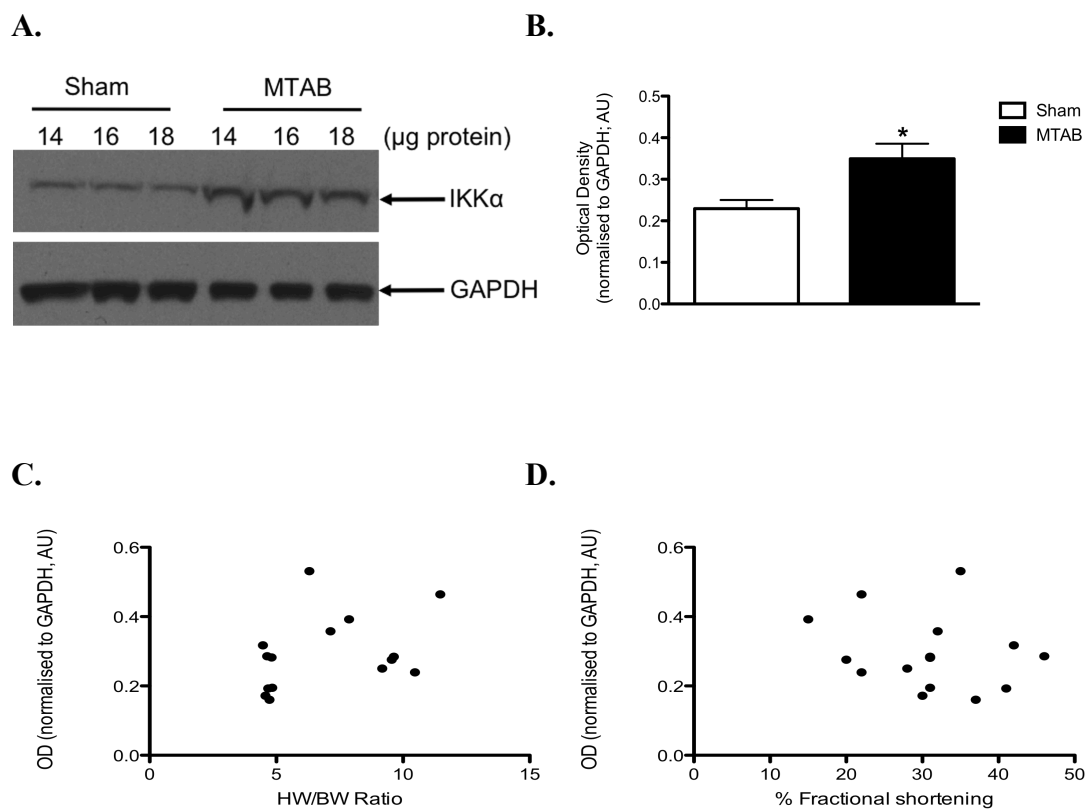


Figure 5.3 IKK α expression in sham and MTAB whole heart homogenates

Panel A. A typical immunoblot of sham-operated and MTAB whole heart homogenates (14-18 μ g) probed for IKK α (upper panel) and GAPDH (lower panel). Panel B. Normalised densitometric analysis of immunoblots relative to GAPDH expression. Panel C. Correlation plot of heart weight/body weight (HW/BW) ratio versus normalised IKK α protein expression. Panel D. Correlation plot of % fractional shortening versus normalised IKK α protein expression. Data are means \pm S.E.M, $n \geq 7$ independent experiments, * $p < 0.05$.

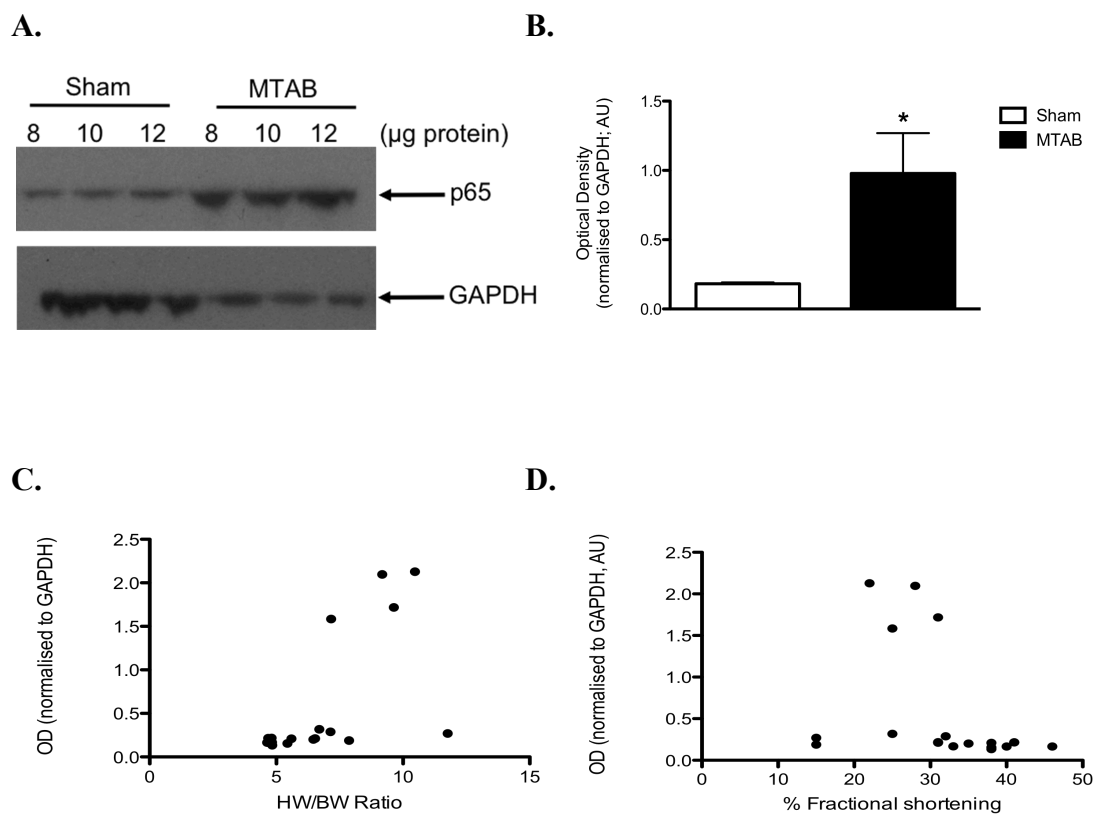
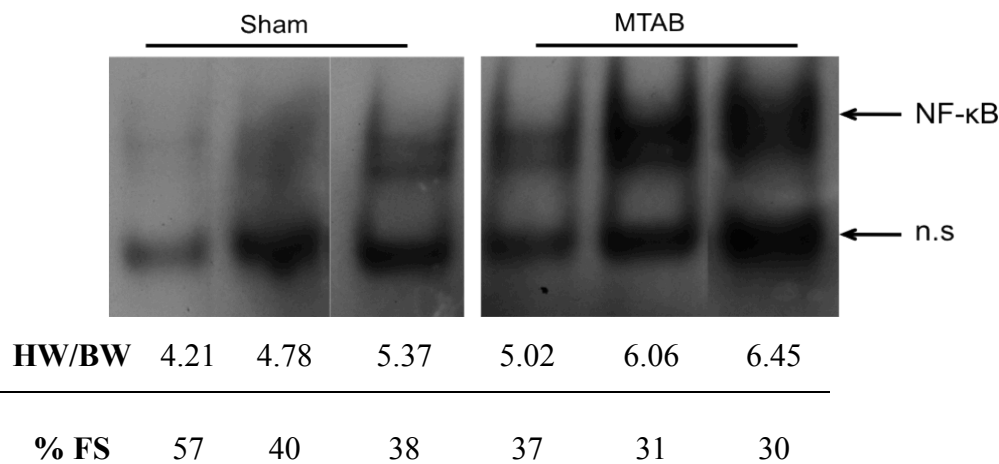


Figure 5.4 NF- κ B p65 expression in sham and MTAB whole heart homogenates
 Panel A. A typical immunoblot of sham-operated and MTAB whole heart homogenates (8-12 μg) probed for NF- κ B p65 (upper panel) and GAPDH (lower panel). Panel B. Normalised densitometric analysis of immunoblots relative to GAPDH expression. Panel C. Correlation plot of heart weight/body weight (HW/BW) ratio versus normalised NF- κ B p65 protein expression. Panel D. Correlation plot of % fractional shortening versus normalised NF- κ B p65 protein expression. Data are means \pm S.E.M, n=9 independent experiments, *p< 0.05.

A.



B.

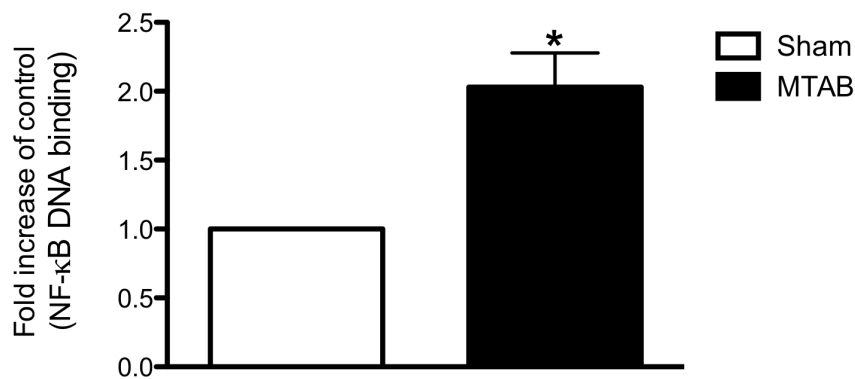


Figure 5.5 NF-κB activity in sham and MTAB whole heart nuclear extracts

Nuclear extracts (10 μg) from sham and MTAB hearts were prepared and incubated with ³²P-ATP-labelled NF-κB oligonucleotide probe to determine the binding activity using electrophoretic mobility gel shift assay (EMSA). Panel A. Autoradiogram of EMSA experiment, depicting NF-κB binding activity for n=3 sham and n=3 MTAB samples (upper panel) and values for heart weight to body weight ratios (HW/BW) and % fractional shortening (FS) for corresponding samples (lower panel). Panel B. Quantification of NF-κB DNA binding activity in sham and MTAB hearts. Densitometric signal was normalized to the control (sham) group and expressed as a percentage. Data are means ± S.E.M, *p<0.05, with statistical analysis performed on raw data.

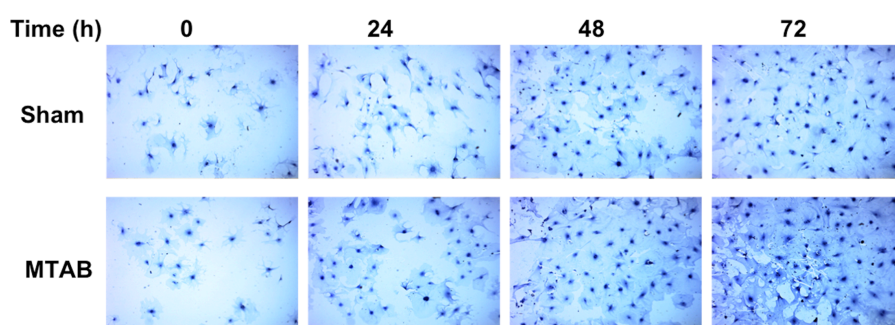
5.4 Cardiac fibroblast proliferation following cardiac hypertrophy and effect of CaMKII inhibition

Having established that collagen deposition was augmented following cardiac hypertrophy (Chapter 4, Section 4.8), experiments sought to establish a correlation with altered CF proliferation *in vitro*. To investigate whether CF proliferation rates were altered following hypertrophy, CFs were isolated from sham-operated and MTAB hearts 4 weeks after surgery. Both sets of cells were quiesced for 24 h prior to exposure to Ang II (1 μ M) for 0-72 h, as described in Chapter 2, Section 2.13. Representative images of CFs stained with haematoxylin are shown at each time point (Figure 5.6A). Results indicate that in response to Ang II, total CF cell number increased 1.4 fold over 72 h stimulation with a significant difference between sham-operated and MTAB cells evident after 48 h and 72 h (48 h; MTAB 59.6 ± 2.5 cells cf. sham 41.8 ± 2.3 cells, and 72h; MTAB 71.0 ± 7.2 cells cf. sham 50.9 ± 3.3 cells, respectively, $p < 0.001$; Figure 5.6B).

To determine whether CaMKII is involved in CF proliferation induced by Ang II, cells rendered quiescent by removal of growth support serum (for 24 h) were pre-treated with the CaMKII inhibitor, AIP (5 μ M), for 2 h followed by exposure to Ang II (1 μ M) for 0-72 h, as described above. As illustrated in Figure 5.7 and Figure 5.8, Ang II-induced CF proliferation was markedly reduced following pre-treatment with AIP in cells isolated from either sham-operated or MTAB hearts. Proliferation was significantly decreased at 24 h and this decrease was maintained at 48 h and 72 h in both sham (72 h; 50.9 ± 3.3 (untreated) cf. 29.8 ± 0.6 (AIP-treated), respectively) and MTAB cells (72 h; 71.0 ± 7.2 (untreated) cf. 37.5 ± 1.5 (AIP treated), respectively). This represented ~40% decrease in proliferation in sham cells and ~50% decrease in proliferation in MTAB cells following AIP treatment. Importantly, in cells isolated from both groups, AIP pre-treatment had no obvious effect on cell number at time zero (AIP-treated versus untreated cells, sham $p = 0.433$ and MTAB $p = 0.620$).

Taken together these findings demonstrate that i) adult CF proliferation is increased during cardiac hypertrophy and ii) CaMKII modulates CF proliferation in both the normal and hypertrophied heart.

A.



B.

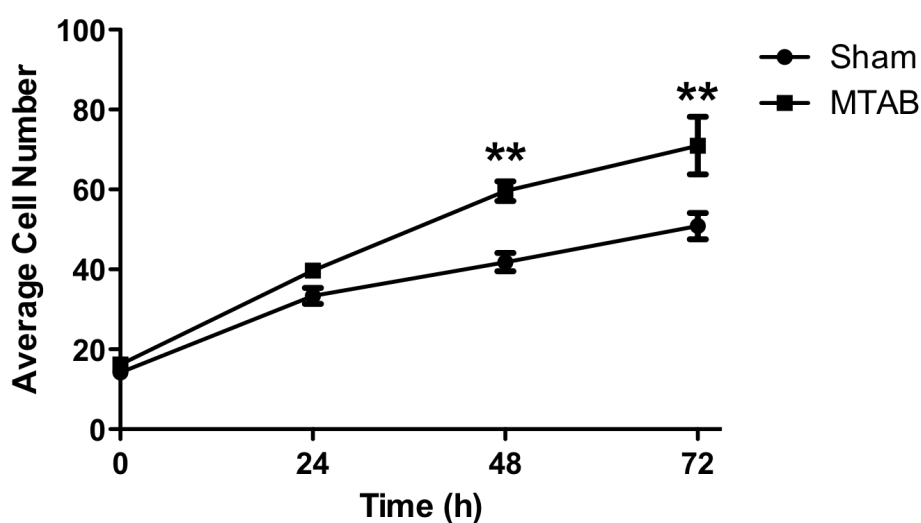
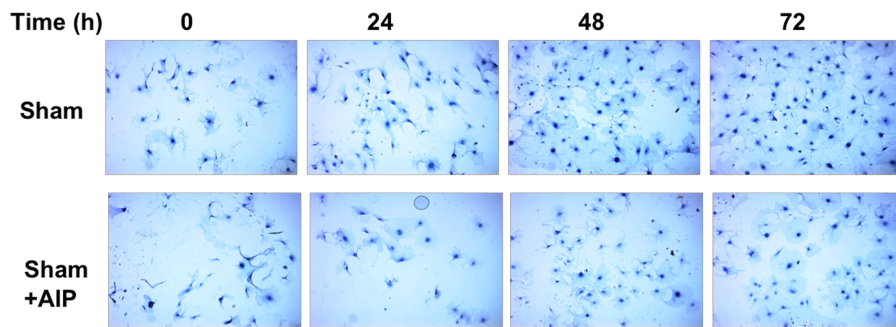


Figure 5.6 Proliferation of cardiac fibroblasts is increased in cells isolated from MTAB hearts compared with those isolated from sham-operated hearts

Cardiac fibroblasts (CFs) isolated from control and MTAB hearts and plated onto sterile cover slips, were exposed to Ang II (1 μ M) for 0-72 h before staining with haematoxylin and cell counting. Panel A. Representative images (20x objective) of cells from sham and MTAB hearts stained with haematoxylin at each time point. Data is from one experiment, typical of three others and each time point was performed in triplicate. Panel B. Mean cell numbers for sham and MTAB preparations counted as described in the methods section. Each data point represents mean \pm S.E.M., n=3, statistical significance was determined from two-way ANOVA with Bonferroni's post-hoc test, **p < 0.01.

A.



B.

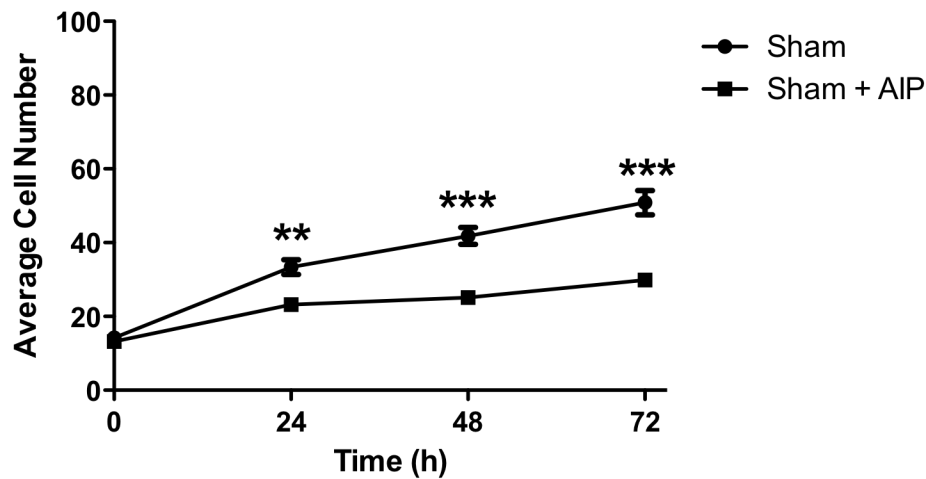
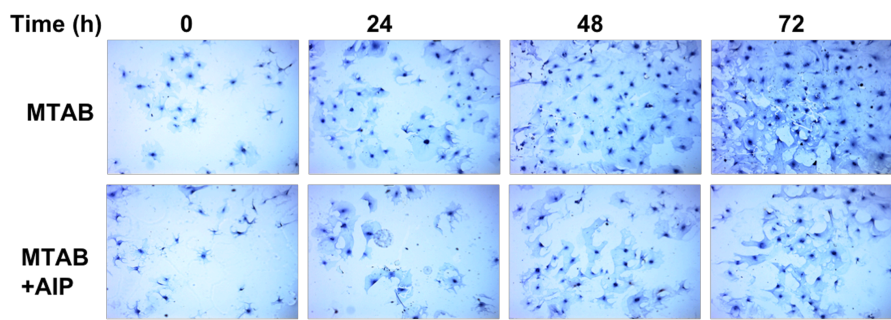


Figure 5.7 Proliferation of cardiac fibroblasts from sham-operated hearts is reduced following CaMKII inhibition

Panel A. Representative images of CF isolated from sham-operated hearts, at 0-72 h, stained with haematoxylin in the absence and presence of AIP pre-treatment, respectively. Panel B. Mean cell numbers taken over a period of 72 h stimulation from sham-operated preparations in the presence and absence of AIP. Each data point represents mean \pm S.E.M., $n=3$, statistical significance was determined from two-way ANOVA with Bonferroni's post-hoc test, ** $p < 0.01$, *** $p < 0.001$.

A.



B.

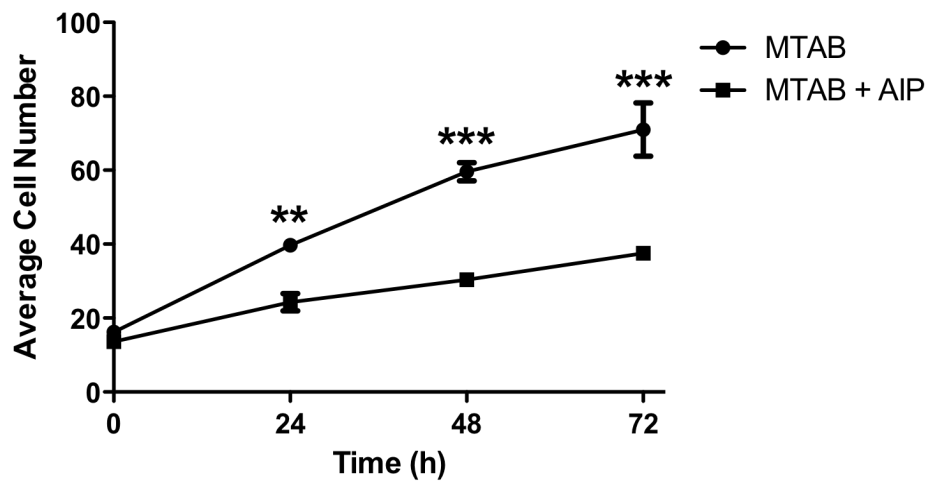


Figure 5.8 Proliferation of cardiac fibroblasts from sham-operated hearts is reduced following CaMKII inhibition

Panel A. Representative images of CF isolated from MTAB hearts, at 0-72 h, stained with haematoxylin in the absence and presence of AIP pre-treatment, respectively. Panel B. Mean cell numbers taken over a period of 72 h stimulation from MTAB preparations in the presence and absence of AIP. Each data point represents mean \pm S.E.M., $n=3$, statistical significance was determined from two-way ANOVA with Bonferroni's post-hoc test, ** $p < 0.01$, *** $p < 0.001$.

5.5 Discussion

The current study has provided evidence for the first time that CaMKII protein expression and activity are both upregulated in MTAB hearts, with activity levels correlating with the degree of hypertrophic growth of the myocardium and impaired cardiac contractile function (Figures 5.1 and 5.2). Importantly, increased expression of CaMKII δ is in line with other models of cardiac hypertrophy (Zhang et al., 2002b, Zhang et al., 2003b, Wang et al., 2008). A clear connection between increased levels and activity of CaMKII and the altered cardiac calcium handling and contractility that is characteristic of the diseased heart has been established in previous work (Sag et al., 2009, Dybkova et al., 2011) and this links directly with cardiac myocyte function. Importantly, data presented in this study provide novel evidence for CaMKII modulation of adult CF function, and that CF proliferation is altered following cardiac hypertrophy.

5.5.1 Altered NF- κ B expression and activity during cardiac hypertrophy

As mentioned in Chapter 1, NF- κ B signalling is a well-recognised pro-inflammatory marker and has previously been shown to be upregulated in cardiac disease (Alter et al., 2006, Kashiwase et al., 2005). Components of NF- κ B signalling, including IKK α and NF- κ B p65 were elevated following MTAB surgery (Figures 5.3 and 5.4). This is the first study to provide evidence for altered IKK α and NF- κ B p65 expression following MTAB-mediated hypertrophy. In addition, NF- κ B activation as assessed by NF- κ B DNA binding activity, was elevated ~2 fold in nuclear preparations from MTAB hearts when compared with sham-operated hearts (Figure 5.5A and B). Alterations in NF- κ B protein expression and activity correlated with the extent of hypertrophic growth of the myocardium and cardiac contractile dysfunction (Figures 5.4, panels C and D, and Figure 5.5A). These data provide evidence that pro-inflammatory signalling is elevated in the MTAB model of pressure-overload mediated cardiac hypertrophy. Importantly, this is the first time this has been demonstrated. Whether pro-inflammatory signalling is a cause or effect of the hypertrophic status in this study has not been established, however other studies have

shown that inhibition of NF- κ B signalling leads to regression of cardiac hypertrophy (Purcell et al., 2001, Li et al., 2004).

Altered protein expression and activity during cardiac hypertrophy may lead to potential alterations in CaMKII δ modulation of agonist-induced NF- κ B signalling. Assessment of the role of CaMKII in modulation of NF- κ B DNA binding activity in nuclear extracts prepared from CFs exposed to LPS were unsuccessful in the current study, possibly due to low protein recovery from cell lysates. Thus, future studies should address this, possibly via *in vivo* myocardial –specific CaMKII inhibition during the 4 weeks post-MTAB surgery. Supershift EMSA experiments will allow assessment of the particular NF- κ B signalling components involved in cardiac hypertrophy. Supershift assays are performed by incubating nuclear extracts with antibodies against the various nuclear components of NF- κ B signalling (e.g. p65, p50 and c-Rel). If the antibody binds to the NF- κ B:DNA complex, this produces a characteristic shift in mobility of the NF- κ B:DNA complex, thus allowing identification of the particular NF- κ B signalling components involved in cardiac hypertrophy. This will provide information on whether activation of NF- κ B is via the canonical or non-canonical signalling pathway. In addition, future studies should also be designed to examine the rate of regression of pressure-overload mediated cardiac hypertrophy following modulation of both CaMKII δ and NF- κ B signalling.

5.5.2 Altered CF function during cardiac hypertrophy and the role of CaMKII

This study has, for the first time, provided evidence that CaMKII plays a regulatory role that is specific to adult CF function. Data presented in this study shows that specific inhibition of CaMKII (using AIP) significantly reduced the CFs potential to proliferate *in vitro* (Figure 5.7 and 5.8). This is an important finding as increased CF proliferation is linked directly to increased collagen production and fibrosis in the diseased heart (Diez et al., 2007). This study also shows for the first time that CF proliferation was increased in cells that have been isolated from MTAB hearts (Figure 5.6). In the present study, Ang II was used to stimulate proliferation above basal rates in culture and this allowed a more rapid assessment of proliferative function. It is worth noting that higher basal rates of proliferation in cells isolated from MTAB hearts were observed, however this was over a longer time-scale (7-10

days) and future work should quantify this difference. The fact that both basal and agonist-stimulated responses are elevated in cells isolated from MTAB hearts clarifies that the hyperproliferative phenotype associated with the disease state is maintained in culture.

Until very recently, the possibility that CaMKII may modulate CF function remained largely ignored. A study using neonatal CFs suggested that CaMKII could play a role in proliferation (Zhang et al., 2010c) however this has never been examined in adult CFs nor has the potential role of CaMKII in hyperproliferative CFs from diseased hearts been addressed. Interestingly, other work in non-cardiac derived fibroblasts has highlighted a role for CaMKII δ in proliferation. In human fibroblasts derived and cultured from skin biopsies, CaMKII activation was shown to be central to insulin-mediated proliferation and inhibition of CaMKII resulted in inhibition of thymidine incorporation (Monaco et al., 2009). In a separate study, the role of CaMKII δ in balloon angioplasty-induced injury was examined in rat carotid arteries. In this model, there was evidence of significantly elevated expression of CaMKII δ along with increased vascular smooth muscle cell and fibroblast proliferation. Suppression of CaMKII δ using adenoviral siRNA infusion into the lumen of the carotid artery inhibited fibroblast proliferation following injury (House and Singer, 2008). Evidence is therefore emerging that CaMKII can modulate fibroblast function. The targets responsible for CaMKII-mediated effects on CF proliferation have yet to be identified however, it is likely that this involves fundamental regulation of CF signalling proteins and ion channels by CaMKII. Quantification of the expression and activity of CaMKII δ in CFs following MTAB surgery is the focus of future work.

5.6 Conclusions

In summary, data presented in this study show augmented CaMKII δ expression and activity during cardiac hypertrophy, with expression and activity correlating with the extent of observed hypertrophy and cardiac contractile dysfunction. In addition, this study for the first time has presented evidence for increased expression of components of NF- κ B signalling, namely IKK α and NF- κ B p65, following cardiac hypertrophy. Similarly to CaMKII δ , expression levels of individual components of NF- κ B signalling correlate with the extent of observed hypertrophy and cardiac

contractile dysfunction. NF- κ B activity was also elevated in MTAB hearts, suggesting that pro-inflammatory signalling is elevated following pressure-overload mediated hypertrophy. This study also provides novel data on altered CF function following cardiac hypertrophy and assigns a role to CaMKII in the regulation of adult CF function.

Chapter 6: General Discussion

It is already well established that CaMKII δ plays a pivotal role in modulation of myocardial contraction and relaxation in both the normal and diseased heart. Much less however, is known about other modes of regulation CaMKII δ may perform in the heart, particularly in relation to cardiac fibrosis and inflammation.

6.1 CaMKII δ - NF- κ B signalling interaction

Although previous work has suggested that CaMKII may modulate NF- κ B signalling (Kashiwase et al., 2005, Singh et al., 2009a), evidence for this existing in the heart is very limited and there is no indication of how this modulation may occur. Given the central importance of CaMKII δ in cardiac function and dysfunction, it is surprising that previous studies examining its potential role in mediating cardiac inflammation are so few. Despite strong evidence for altered pro-inflammatory NF- κ B signalling in cardiac dysfunction, details of the underlying regulatory mechanisms are limited.

In this study, it was shown that CaMKII is capable of modulating NF- κ B activation, and this observation supports previously published evidence from other systems (Hughes et al., 2001, Meffert et al., 2003). To date, there is only very limited evidence for the potential of a CaMKII-NF- κ B interaction in a cardiac setting (Singh et al., 2009a). Importantly, the present study provides new evidence of a link between CaMKII and NF- κ B in adult CFs. It is also the first time that a direct interaction between CaMKII δ and NF- κ B signalling at the level of IKK β has been shown. Evidence for this interaction has been obtained using two independent methods of investigation, namely autoradiography and SPR. Although a previous study has shown evidence for CaMKII modulation of IKK phosphorylation in T cells (Hughes et al., 2001), this is the first study to show evidence for selective CaMKII δ -mediated phosphorylation of IKK β and provide evidence for a direct protein-protein interaction between CaMKII δ and IKK β . The CaMKII δ – IKK β interaction was found not to be dependent on ATP, suggesting that the phosphorylation status of either CaMKII δ or IKK β does not affect the affinity of interaction. In addition, the CaMKII δ – IKK β interaction observed in this study was not altered by the presence or absence of Ca²⁺, suggesting that any interaction occurring during cardiac hypertrophy could be

independent of the impaired EC-coupling observed during cardiac disease (Sag et al., 2009).

Future research to further understand the interaction between CaMKII δ and IKK β should use more detailed SPR studies to evaluate the CaMKII δ – IKK β binding stoichiometry as well as to examine the binding kinetics of the interaction. Further examination of the site(s) of interaction should prove informative and will indicate whether CaMKII may phosphorylate unique sites on IKK β . This can be achieved using experimental techniques such as site-directed mutagenesis and/or peptide-array analysis. Immunoprecipitation analysis of the interaction in both solubilised CFs and whole cardiac homogenates was not possible during this study due to exceptionally faint and inconsistent recovery with the antibodies available. Interpretation of the specifics of the CaMKII δ – IKK β interaction was therefore based upon data obtained from purified proteins. This aspect of the study will need to be addressed in future work to determine whether (i) the CaMKII δ – IKK β interaction is evident in whole cardiac homogenates and whether it can be viewed at the cellular level (in adult CFs and myocytes) and, (ii) whether this interaction is altered during cardiac disease.

6.2 Characterisation of MTAB model

The MTAB surgical technique developed and characterised in this study provides a significant improvement over traditional aortic banding with a significantly shorter time for surgery and faster recovery rates. Very few laboratories worldwide have this model in place and therefore this has been a particular achievement in enhancing this project and future work of the group.

In this study, inhalation anaesthesia using isoflurane proved most suitable for MTAB surgery. Previous studies using this model have reported animal tolerance issues with injectable anaesthesia and notably, different anaesthetic regimes have been used between studies with little or no explanation regarding rationale (Hu et al., 2003, Toischer et al., 2010). This is the first study to monitor and report effects of alternative injectable and inhalation anaesthetic regimes in mice prior to and during MTAB surgery. The importance of this information cannot be overstated and it provides useful reference for future work using this model.

Cardiac dysfunction (both systolic and diastolic) and remodelling of the heart was evident as early as 1 week, with significant increases in both MABP and LVP following MTAB surgery. This was maintained at 2 weeks post-surgery and exacerbated at 4 weeks post-surgery, as evidenced by decreased % FS, remodelling and increased HW/BW ratios. Importantly, the extent of changes at 4 weeks were in line with those seen following traditional aortic banding (Niizeki et al., 2008), verifying the advantages of using the MTAB approach. These findings provide important information on the progression of cardiac remodelling following MTAB-mediated hypertrophy. Few studies using animal models study more than one time point during disease progression and this leads to considerable limitations in interpretation. Thus, a major strength of the current study is the information that has been attained at a number of time points following surgery. This information is important for future work using the MTAB model, particularly when assessing the potential of anti-hypertrophic inhibitors and the crucial timing of intervention.

As discussed in more detail below (Section 6.4), significant increases in CF proliferation and collagen production were observed following MTAB, providing evidence that fibrosis accompanies development of cardiac hypertrophy in this model. In addition, this study provides evidence for cardiac inflammation following MTAB, as discussed below (Section 6.3). Thus using the protocol outlined in this study, the MTAB procedure at 4 weeks post-surgery provides a reproducible model of cardiac hypertrophy with accompanying fibrosis and inflammation. It is therefore a useful platform for studying underlying regulatory mechanisms for these parameters as well as intervention strategies that may reverse development and/or progression of the condition.

6.3 CaMKII δ and pro-inflammatory signalling following cardiac hypertrophy

In this study, elevated protein expression and activity of CaMKII δ and components of the NF- κ B cascade correlated with progression of cardiac hypertrophy and decline in LV function. These data suggest the possibility that modulation of either or both of these pathways during cardiac disease could significantly reverse cardiac remodelling in response to haemodynamic stress. Future studies will examine this hypothesis using the MTAB model. Importantly, other markers of pro-

inflammatory signalling during cardiac hypertrophy should be assessed, for example quantification of inflammatory cell infiltration in response to haemodynamic stress as well as assessment of cytokine and chemokine expression.

As mentioned in Chapter 1, increased IKK β activity has been observed in human HF (Gupta and Sen, 2005). A previous study has demonstrated that inhibition of IKK β led to decreased myocardial remodelling associated with an animal model of HF, as well as reducing inflammatory cell infiltration and the expression of pro-inflammatory cytokines (Onai et al., 2007, Onai et al., 2004). In this particular study, IKK β expression following MTAB-mediated hypertrophy could not be quantified. As other components of NF- κ B signalling were upregulated during cardiac hypertrophy, including IKK α , it seems likely that IKK β expression will be upregulated in parallel. Nevertheless, future studies should examine IKK β expression following hypertrophy. This could be achieved using RT-PCR to avoid potential issues with antibodies as discussed in Chapter 3. Other important questions to address include, (i) whether inhibition of CaMKII δ *in vivo* decreases NF- κ B activity during MTAB-mediated hypertrophy and, (ii) whether CaMKII δ inhibition directly alters IKK β expression/activity.

6.4 Altered CF function following cardiac hypertrophy

As mentioned previously, another key feature that has been documented to accompany cardiac hypertrophy is cardiac fibrosis (Vasquez et al., 2011, Hedayat et al., 2010). Fibrosis is routinely found in association with cardiac hypertrophy and importantly, there is increasing data to suggest that pro-fibrotic pathways are activated early on in response to haemodynamic stress or sarcomere gene mutations, before hypertrophic remodelling is evident (Ho et al., 2010). Increased levels of myocardial fibrosis correlate with progression of hypertrophy and HF, therefore the extent of fibrosis is a useful marker of impaired cardiac function (Moreo et al., 2009). In the MTAB model, significant fibrosis was evident 4 weeks post-surgery, correlating with significant hypertrophy and impaired cardiac contractile function (decreased % FS). In addition, adult CF proliferation was significantly increased following cardiac hypertrophy. An increased proliferative capacity of CFs correlates strongly with development and progression of fibrosis. Thus, data presented in this

study highlight for the first time the potential of the MTAB model for studying dysfunction at the level of the CF as well as the cardiac myocyte and relating to changes *in vivo*.

An important novel finding observed in this study is that CaMKII can modulate adult CF proliferation. These data open up a whole new element in our understanding of the role of CaMKII in modulating cardiac function. There has been a somewhat blinkered view in our appreciation of the contribution that non-contractile cells may have towards regulating cardiac contractility through their proliferative, migratory and secretory actions. The recognition that CFs are an important component of contractile function and that CaMKII expressed in CFs modulates the proliferative response will have a pivotal role in changing this view. The potential for CFs to modulate cardiac myocyte function, and therefore indirectly regulate cardiac electrophysiology and ultimately contractility, should not be understated. A growing body of evidence has demonstrated the capacity for intercellular coupling between myocytes and CFs, and the possibility of electrical coupling has been highlighted (Vasquez et al., 2011). In isolated cell preparations, the absolute number of CFs has a strong influence on cardiac myocyte conduction with increased numbers, such as that seen in hyperproliferative conditions, creating an obstacle and reducing conduction velocity (Xie et al., 2009). In addition to physical changes in ECM production, increased numbers of CFs will result in increased growth factor secretion, which will ultimately influence hypertrophic growth. For these reasons, the concept of therapeutic targeting directed at the level of the CF is gaining appeal. This concept was strengthened recently with evidence showing CFs are essential for the adaptive response of the heart to stress following pressure overload. Findings from a mouse model of pressure overload-mediated hypertrophy showed that Klf5 deletion in CFs ameliorated cardiac hypertrophy and fibrosis when the same deletion in myocytes did not. This has provided the first evidence for a key role for CFs as mediators of hypertrophy (Takeda et al., 2010).

Future work using myocardial targeted CaMKII inhibition during cardiac hypertrophy and assessment of fibrosis will build upon the current data and will provide a crucial mechanistic understanding of how CaMKII signalling at a cellular level impacts on the remodelling process accompanying cardiac hypertrophy. It will be important to determine whether CaMKII δ and NF- κ B expression and activity are altered in CFs (and cardiac myocytes) following cardiac hypertrophy, in parallel with

the observed alterations in whole cardiac homogenates. If this is the case, modulation of the CaMKII δ –IKK β interaction specifically at a cellular level could be an attractive therapeutic target to prevent pro-inflammatory signalling associated with the remodelling heart.

6.5 CaMKII δ as a target for therapeutic intervention in cardiac hypertrophy

There is now extensive evidence in the literature that CaMKII δ plays an important and essential role in the development of cardiac disease. Accumulating evidence suggests that CaMKII δ is a multifunctional kinase, playing a crucial role in a number of processes including EC-coupling, cell growth, cell death and inflammation. Most of this evidence comes from studies using cardiac myocytes. Given the multiplicity of targets for CaMKII in myocytes, it seems likely that a similar range of protein targets exists in non-contractile cells, such as CFs. Both cell types (myocytes and CFs) play important roles in the remodelling process of the diseased heart, supporting the need to research CaMKII δ 's role in CF function, and its potential as a candidate for therapeutic intervention in cardiac disease.

The argument exists that more selective therapeutic strategies for the treatment of heart disease may be less damaging due to less non-specific and wider-ranging effects. Inhibition of CaMKII has previously been suggested as a therapeutic approach for the treatment of various cardiomyopathies. Global CaMKII inhibition however will not only eliminate the detrimental effects of elevated CaMKII during disease, it will also affect its key role in normal/healthy cardiac function. Selective targeting could be a valuable therapeutic approach in overcoming these problems. Findings from this study provide important novel information regarding the role of CaMKII δ in the heart. Targeting CaMKII δ specifically at the level of the CF could present a novel therapeutic approach to reduce or reverse cardiac fibrosis. In addition, targeting the novel protein-protein interaction between CaMKII δ and IKK β identified in this study, could be an approach used to target inflammation associated with cardiac disease. Experimental techniques such as peptide arrays coupled with mutagenesis studies could be used to map the CaMKII δ -IKK β interaction. Once the area of interaction has been elucidated, novel peptide inhibitors targeting this site of

interaction could be developed and tested for efficacy, initially *in vitro* using isolated adult CFs, and then *in vivo* using the MTAB model of pressure-overload hypertrophy.

Together, these strategies will improve upon current, but less selective cardiac therapies, and this may lead to important developments in the treatment and management of heart disease.

References

Agarwal A., Das K., Lerner N., Sathe S., Cicek M., Casey G. & Sizemore N. (2005) The AKT/IB kinase pathway promotes angiogenic/metastatic gene expression in colorectal cancer by activating nuclear factor-Kappa B and beta catenin. *Oncogene*, 24, 1021-1031.

Ago T., Yang Y., Zhai P. & Sadoshima J. (2010) Nifedipine inhibits cardiac hypertrophy and left ventricular dysfunction in response to pressure overload. *J Cardiovasc Transl Res*, 3, 304-313.

Ahmed S., Silverman M. D., Marotte H., Kwan K., Matuszczak N. & Koch A. E. (2009) Down-regulation of myeloid cell leukemia 1 by epigallocatechin-3-gallate sensitizes rheumatoid arthritis synovial fibroblasts to tumor necrosis factor alpha-induced apoptosis. *Arthritis Rheum*, 60, 1282-1293.

Ai X., Curran J. W., Shannon T. R., Bers D. M. & Pogwizd S. M. (2005) Ca²⁺/calmodulin-dependent protein kinase modulates cardiac ryanodine receptor phosphorylation and sarcoplasmic reticulum Ca²⁺ leak in heart failure. *Circ Res*, 97, 1314-1322.

Alter P., Rupp H. & Maisch B. (2006) Activated nuclear transcription factor-Kappa B in patients with myocarditis and dilated cardiomyopathy-relation to inflammation and cardiac function. *Biochem Biophys Res Commun*, 339, 180.

Anderson M. E. (2005) Calmodulin kinase signalling in heart: an intriguing candidate target for therapy of myocardial dysfunction and arrhythmias. *Pharmacol Ther*, 106, 39-55.

Anderson M. E. (2007) Multiple downstream proarrhythmic targets for calmodulin kinase II: Moving beyond an ion channel-centric focus. *Cardiovas Res*, 73, 657-666.

Anderson M. E., Brown J. H. & Bers D. M. (2011) CaMKII in myocardial hypertrophy and heart failure. *J Mol Cell Cardiol*, 51, 468-73.

Anest V., Hanson J. L., Cogswell P. C., Steinbrecher K. A., Strahl B. D. & Baldwin A. S. (2003) A nucleosomal function for I κ B kinase- α in NF- κ B-dependent gene expression. *Nature*, 423, 659-663.

Anthony D. F., Beattie J., Paul A. & Currie S. (2007) Interaction of calcium/calmodulin-dependent protein kinase II δ C with sorcin indirectly modulates ryanodine receptor function in cardiac myocytes. *J Mol Cell Cardiol*, 43, 492-503.

Antonsson A., Hughes K., Edin S. & Grundstrom T. (2003) Regulation of c-Rel nuclear localization by binding of Ca²⁺/calmodulin. *Mol Cell Biol*, 23, 1418-1427.

Asazuma-Nakamura Y., Dai P., Harada Y., Jiang Y., Hamaoka K. & Takamatsu T. (2009) Cx43 contributes to TGF- β signaling to regulate differentiation of cardiac fibroblasts into myofibroblasts. *Exp Cell Res*, 315, 1190-1199.

Ashida N., Senbanerjee S., Kodama S., Foo S. Y., Coggins M., Spencer J. A., Zamiri P., Shen D., Li L., Sciuto T., Dvorak A., Gerszten R. E., Lin C. P., Karin M. & Rosenzweig A. (2011) IKK β regulates essential functions of the vascular endothelium through kinase-dependent and -independent pathways. *Nat Commun*, 2, 1-9.

Backs J., Backs T., Bezprozvannaya S., McKinsey T. A. & Olson E. N. (2008) Histone deacetylase 5 acquires calcium/calmodulin-dependent kinase II responsiveness by oligomerization with histone deacetylase 4. *Mol Cell Biol* 28, 3437-3445.

Backs J., Backs T., Neef S., Kreusser M. M., Lehmann L. H., Patrick D. M., Grueter C. E., Qi X., Richardson J. A., Hill J. A., Katus H. A., Bassel-Duby R., Maier L. S. & Olson E. N. (2009) The delta isoform of CaM kinase II is required for pathological cardiac hypertrophy and remodeling after pressure overload. *Proc Natl Acad Sci*, 106, 2342-2347.

Backs J., Song K., Bezprozannaya S., Chang S. & Olson E. N. (2006) CaM kinase II selectively signals to histone deacetylase 4 during cardiomyocyte hypertrophy. *J Clin Invest*, 116, 1853-64.

Banerjee I., Fuseler J. W., Intwala A. R. & Baudino T. A. (2009) IL-6 loss causes ventricular dysfunction, fibrosis, reduced capillary density, and dramatically alters the cell populations of the developing and adult heart. *Am J Physiol Heart Circ Physiol*, 296, H1694-1704.

Bare D. J., Kettlun C. S., Liang M., Bers D. M. & Mignery G. A. (2005) Cardiac type 2 inositol 1,4,5-trisphosphate receptor: interaction and modulation by calcium/calmodulin-dependent protein kinase II *J Biol Chem*, 280, 15912-15920.

Barrick C. J., Rojas M., Schoonhoven R., Smyth S. S. & Threadgill D. W. (2007) Cardiac response to pressure overload in 129S1/SvImJ and C57BL/6J mice: temporal- and background-dependent development of concentric left ventricular hypertrophy. *Am J Physiol Heart Circ Physiol*, 292, H2119-2130.

Barry S. P., Davidson S. M. & Townsend P. A. (2008) Molecular regulation of cardiac hypertrophy. *Int J Biochem Cell Biol*, 40, 2023-2039.

Basak S. & Hoffmann A. (2008) Crosstalk via the NF- κ B signaling system. *Cytokine Growth Factor Rev*, 19, 187-197.

Batsi C., Markopoulou S., Vartholomatos G., Georgiou I., Kanavaros P., Gorgoulis V. G., Marcu K. B. & Kolettas E. (2009) Chronic NF- κ B activation delays RasV12-induced premature senescence of human fibroblasts by suppressing the DNA damage checkpoint response. *Mech Ageing Dev*, 130, 409-19.

Baudino T. A., Carver W., Giles W. & Borg T. K. (2006) Cardiac fibroblasts: friend or foe? *Am J Physiol Heart Circ Physiol*, 291, H1015-1026.

Baum J. & Duffy H. (2011) Fibroblasts and myofibroblasts: What are we talking about? *J Cardiovasc Pharmacol*, 57, 376-9.

Baumgarten G., Knuefermann P., Kalra D., Gao F., Taffet G. E., Michael L., Blackshear P. J., Carballo E., Sivasubramanian N. & Mann D. L. (2002) Load-dependent and -independent regulation of proinflammatory cytokine and cytokine receptor gene expression in the adult mammalian heart. *Circulation*, 105, 2192-2197.

Bayer K. U., Harbes K. & Schulman H. (1998) alphaKAP is an anchoring protein for a novel CaM kinase II isoform in skeletal muscle. *EMBO J*, 17, 5598-5605.

Bayes-Genis A. (2007) Hypertrophy and inflammation: too much for one heart? *Eur Heart J*, 28, 661-663.

Beattie J., Phillips K., Shand J., Szymanowska M., Flint D. & Allan G. (2008) Molecular interactions in the insulin-like growth factor (IGF) axis: a surface plasmon resonance (SPR) based biosensor study. *Mol Cell Biochem*, 307, 221-236.

Beg A. A., Sha W. C., Bronson R. T., Ghosh S. & Baltimore D. (1995) Embryonic lethality and liver degeneration in mice lacking the RelA component of NF- κ B. *Nature*, 376, 167-170.

Bellenger N. G., Burgess M. I., Ray S. G., Lahiri A., Coats A. J. S., Cleland J. G. F. & Pennell D. J. (2000) Comparison of left ventricular ejection fraction and volumes in heart failure by echocardiography, radionuclide ventriculography and cardiovascular magnetic resonance. Are they interchangeable? *Eur Heart J*, 21, 1387-1396.

Bergqvist S., Croy C. H., Kjaergaard M., Huxford T., Ghosh G. & Komives E. A. (2006) Thermodynamics reveal that helix four in the NLS of NF- κ B p65 anchors I κ B α , forming a very stable complex. *J Mol Bio*, 360, 421-434.

Bergqvist S., Ghosh G. & Komives E. A. (2008) The I κ B α /NF- κ B complex has two hot spots, one at either end of the interface. *Protein Sci*, 17, 2051-2058.

Bers D. (2006a) Cardiac ryanodine receptor phosphorylation: target sites and functional consequences. *Biochem J*, 15, 396(Pt 1): e1.

Bers D. M. (2002) Cardiac excitation-contraction coupling. *Nature*, 415, 198-205.

Bers D. M. (2006b) Altered cardiac myocyte calcium regulation in heart failure. *Physiology*, 21, 380-387.

Boknik P., Heinroth-Hoffmann I., Kirchhefer U., Knapp J., Linck B., Luss H., Muller T., Schmitz W., Brodde O.-E. & Neumann J. (2001) Enhanced protein phosphorylation in hypertensive hypertrophy. *Cardiovasc Res*, 51, 717-728.

Bonizzi G. & Karin M. (2004) The two NF- κ B activation pathways and their role in innate and adaptive immunity. *Trends Immunol*, 25, 280-288.

Bossuyt J., Helmstadter K., Wu X., Clements-Jewery H., Haworth R. S., Avkiran M., Martin J. L., Pogwizd S. M. & Bers D. M. (2008) Ca²⁺/calmodulin-dependent protein kinase II δ and protein kinase D overexpression reinforce the histone deacetylase 5 redistribution in heart failure. *Circ Res*, 102, 695-702.

Bradford M. M. (1976) A rapid and sensitive method for the quantitation of microgram quantities of protein utilizing the principle of protein-dye binding. *Anal Biochem*, 72, 248-254.

Bradham W. S., Moe G., Wendt K. A., Scott A. A., Konig A., Romanova M., Naik G. & Spinale F. G. (2002) TNF- α and myocardial matrix metalloproteinases in heart failure: relationship to LV remodeling. *Am J Physiol Heart Circ Physiol*, 282, H1288-1295.

Brocke L., Chiang L. W., Wagner P. D. & Schulman H. (1999) Functional implications of the subunit composition of neuronal CaM kinase II. *J Bio Chem*, 274, 22713-22722.

Brown M., McGuinness M., Wright T., Ren X., Wang Y., Boivin G. P., Hahn H., Feldman A. M. & Jones W. K. (2005a) Cardiac-specific blockade of NF- κ B in cardiac pathophysiology: differences between acute and chronic stimuli in vivo. *Am J Physiol Heart Circ Physiol*, 289, H466-476.

Brown R. D., Ambler S. K., Mitchell M. D. & Long C. S. (2005b) The cardiac fibroblast: Therapeutic target in myocardial remodeling and failure. *Annu Rev Pharmacol Toxicol*, 45, 657-687.

Brown R. D., Jones G. M., Laird R. E., Hudson P. & Long C. S. (2007) Cytokines regulate matrix metalloproteinases and migration in cardiac fibroblasts. *Biochem Biophys Res Commun*, 362, 200-205.

Bui N. T., Livolsi A., Peyron J.-F. & Prehn J. H. M. (2001) Activation of nuclear factor κ B and bcl-x survival gene expression by nerve growth factor requires tyrosine phosphorylation of I κ B α . *J Cell Biol*, 152, 753-764.

Bujak M. & Frangogiannis N. G. (2007) The role of TGF- β signaling in myocardial infarction and cardiac remodeling. *Cardiovasc Res*, 74, 184-195.

Camelliti P., Borg T. K. & Kohl P. (2005) Structural and functional characterisation of cardiac fibroblasts. *Cardiovasc Res*, 65, 40-51.

Camelliti P., Devlin G. P., Matthews K. G., Kohl P. & Green C. R. (2004a) Spatially and temporally distinct expression of fibroblast connexins after sheep ventricular infarction. *Cardiovasc Res*, 62, 415-425.

Camelliti P., Green C. R., LeGrice I. & Kohl P. (2004b) Fibroblast network in rabbit sinoatrial node. *Circ Res*, 94, 828-835.

Cannon J. G., Nerad J. L., Poutsika D. D. & Dinarello C. A. (1993) Measuring circulating cytokines. *J Appl Physiol*, 75, 1897-1902.

Cavasin M. A., Tao Z., Menon S. & Yang X.-P. (2004) Gender differences in cardiac function during early remodeling after acute myocardial infarction in mice. *Life Sci*, 75, 2181.

Celis R., Torre-Martinez G. & Torre-Amione G. (2008) Evidence for activation of immune system in heart failure: is there a role for anti-inflammatory therapy? *Curr Opin Cardiol*, 23, 254-260

Chaves A. A., Weinstein D. M. & Bauer J. A. (2001) Non-invasive echocardiographic studies in mice: Influence of anesthetic regimen. *Life Sci*, 69, 213-222.

Chen J.-B., Tao R., Sun H.-Y., Tse H.-F., Lau C.-P. & Li G.-R. (2010) Multiple Ca^{2+} signaling pathways regulate intracellular Ca^{2+} activity in human cardiac fibroblasts. *J Cell Physiol*, 223, 68-75.

Chen L. F. & Grenne W. C. (2004) Shaping the nuclear action of NF- κ B. *Mol Cell Biol*, 5, 392-401.

Chen Y., Arrigo A.-P. & Currie R. W. (2004) Heat shock treatment suppresses angiotensin II-induced activation of NF- κ B pathway and heart inflammation: a role for IKK depletion by heat shock? *Am J Physiol*, 287, H1104-H1114.

Chilton L., Giles W. R. & Smith G. L. (2007) Evidence of intercellular coupling between co-cultured adult rabbit ventricular myocytes and myofibroblasts. *J Physiol*, 583, 225-236.

Colbran R. J. (2004) Targeting of calcium/calmodulin-dependent protein kinase II. *Biochem J*, 378, 1-16.

Colomer J. M., Mao L., Rockman H. A. & Means A. R. (2003) Pressure overload selectively up-regulates Ca^{2+} /calmodulin-dependent protein kinase II in vivo. *Mol Endocrinol*, 17, 183-192.

Colomer J. M. & Means A. R. (2000) Chronic elevation of calmodulin in the ventricles of transgenic mice Increases the autonomous activity of calmodulin-dependent protein kinase II, which regulates atrial natriuretic factor gene expression. *Mol Endocrinol*, 14, 1125-36.

Connelly T. J. & Coronado R. (1994) Activation of the Ca^{2+} release channel of cardiac sarcoplasmic reticulum by volatile anesthetics. *Anesthesiology*, 81, 459-69.

Constantinides C., Mean R. & Janssen B. (2011) Effects of isoflurane anesthesia on the cardiovascular function of the C57BL/6 mouse. *ILAR J*, 52, 22-32.

Cook S. A., Novikov M. S., Ahn Y., Matsui T. & Rosenzweig A. (2003) A20 is dynamically regulated in the heart and inhibits the hypertrophic response. *Circulation*, 108, 664-667.

Coultrap S. J., Buard I., Kulbe J. R., Dell'Acqua M. L. & Bayer K. U. (2010) CaMKII Autonomy Is Substrate-dependent and Further Stimulated by Ca^{2+} /Calmodulin. *J Bio Chem*, 285, 17930-17937.

Cowling R. T., Gurantz D., Peng J., Dillmann W. H. & Greenberg B. H. (2002) Transcription Factor NF- κ B Is Necessary for Up-regulation of Type 1 Angiotensin II Receptor mRNA in Rat Cardiac Fibroblasts Treated with Tumor Necrosis Factor- α or Interleukin-1 β . *J Bio Chem*, 277, 5719-5724.

Crabos M., Roth M., Hahn A. W. & Erne P. (1994) Characterization of angiotensin II receptors in cultured adult rat cardiac fibroblasts. Coupling to signaling systems and gene expression. *J Clin Invest*, 93, 2372-2378.

Creemers E. E. & Pinto Y. M. (2011) Molecular mechanisms that control interstitial fibrosis in the pressure-overloaded heart. *Cardiovasc Res*, 89, 265-272.

Curran J., Hinton M. J., Rios E., Bers D. M. & Shannon T. R. (2007) β -Adrenergic enhancement of sarcoplasmic reticulum calcium leak in cardiac myocytes is mediated by calcium/calmodulin-dependent protein kinase. *Cir Res*, 100, 391-398.

Currie S. (2008) Cardiac ryanodine receptor phosphorylation by Ca^{2+} /calmodulin dependent protein kinase II: keeping the balance right. *Front Biosci*, 14, 5134-56.

Currie S., Elliott E. B., Smith G. L. & Loughrey C. M. (2011) Two candidates at the heart of dysfunction: The ryanodine receptor and calcium/calmodulin protein kinase II as potential targets for therapeutic intervention-An in vivo perspective. *Pharmacol Ther*, 131, 204-220.

Currie S., Loughrey C. M., Graig M.-A. & Smith G. L. (2004) Calcium/calmodulin-dependent protein kinase II delta associates with the ryanodine receptor complex and regulates channel function in rabbit heart. *Biochem J*, 377, 357-366.

Currie S. & Smith G. L. (1999a) Calcium/calmodulin-dependent protein kinase II activity is increased in sarcoplasmic reticulum from coronary artery ligated rabbit hearts. *FEBS Letters*, 459, 244-248.

Currie S. & Smith G. L. (1999b) Enhanced phosphorylation of phospholamban and downregulation of sarco/endoplasmic reticulum Ca^{2+} ATPase type 2 (SERCA 2) in cardiac sarcoplasmic reticulum from rabbits with heart failure. *Cardiovasc Res*, 41, 135-146.

Das B., Gupta S., Vasanji A., Xu Z., Misra S. & Sen S. (2008) Nuclear co-translocation of myotrophin and p65 stimulates myocyte growth: Regulation by myotrophin hairpin loops *J Biol Chem*, 283, 27947-27956.

del Monte F., Williams E., Lebeche D., Schmidt U., Rosenzweig A., Gwathmey J. K., Lewandowski E. D. & Hajjar R. J. (2001) Improvement in survival and cardiac metabolism after gene transfer of sarcoplasmic reticulum Ca^{2+} -ATPase in a rat model of heart failure. *Circulation*, 104, 1424-1429.

Delhase M., Hayakawa M., Chen Y. & Karin M. (1999) Positive and negative regulation of I κ B kinase activity through IKK β subunit phosphorylation. *Science*, 284, 309-313.

Deswal A., Petersen N. J., Feldman A. M., Young J. B., White B. G. & Mann D. L. (2001) Cytokines and cytokine receptors in advanced heart failure : An analysis of the cytokine database from the vesnarinone trial (VEST). *Circulation*, 103, 2055-2059.

Dhingra R., Shaw J., Aviv Y. & Kirshenbaum L. (2010) Dichotomous actions of NF- κ B signaling pathways in heart. *J Cardiovasc Transl Res*, 3, 344-354.

Diaz J. A., Booth A. J., Lu G., Wood S. C., Pinsky D. J. & Bishop D. K. (2009) Critical role for IL-6 in hypertrophy and fibrosis in chronic cardiac allograft rejection. *Am J Transplant*, 9, 1773-1783.

Diez J., Lopez B., Gonzalez A. & Querejeta R. (2007) The role of myocardial collagen network in hypertensive heart disease. *Curr Hyperten Rev*, 3, 1-7.

Dybkoval N., Sedej S., Napolitano C., Neef S., Rokita A. G., Hunlich M., Brown J. H., Kockskamper J., Priori S. G., Pieske B. & Maier L. S. (2011) Overexpression of CaMKII[delta]c in RyR2R4496C^{+/-} Knock-In Mice Leads to Altered Intracellular Ca²⁺ Handling and Increased Mortality. *Journal of the American College of Cardiology*, 57, 469-479.

Edman C. F. & Schulman H. (1994) Identification and characterization of δ]B-CaM kinase and δ C-CaM kinase from rat heart, two new multifunctional Ca²⁺/calmodulin-dependent protein kinase isoforms. *Biochim Biophys Acta*, 1221, 89-101.

Eghbali M. (1992) Cardiac fibroblasts: function, regulation of gene expression, and phenotypic modulation. *Basic Res Cardiol*, 87, 183-189.

Ehrentraut H., Weber C., Ehrentraut S., Schwederski M., Boehm O., Knuefermann P., Meyer R. & Baumgarten G. (2011) The toll-like receptor 4-antagonist eritoran reduces murine cardiac hypertrophy. *Eur J Heart Fail*, 13, 602-610.

El-Haou S., Balse E., Neyroud N., Dilanian G., Gavillet B., Abriel H., Coulombe A., Jeromin A. & Hatem S. N. (2009) Kv4 potassium channels form a tripartite complex with the anchoring protein SAP97 and CaMKII in cardiac myocytes. *Cir Res*, 104, 758-769.

Erickson J. R., He B. J., Grumbach I. M. & Anderson M. E. (2011) CaMKII in the cardiovascular system: sensing redox states. *Physiol Rev*, 91, 889-915.

Erickson J. R., Joiner M.-I. A., Guan X., Kutschke W., Yang J., Oddis C. V., Bartlett R. K., Lowe J. S., O'Donnell S. E., Aykin-Burns N., Zimmerman M. C., Zimmerman K., Ham A.-J. L., Weiss R. M., Spitz D. R., Shea M. A., Colbran R. J., Mohler P. J. & Anderson M. E. (2008) A dynamic pathway for calcium-independent activation of CaMKII by methionine oxidation. *Cell*, 133, 462-474.

Fielitz J., Kim M.-S., Shelton J. M., Qi X., Hill J. A., Richardson J. A., Bassel-Duby R. & Olson E. N. (2008) Requirement of protein kinase D1 for pathological cardiac remodeling. *Proc Natl Acad Sci*, 105, 3059-3063.

Fliegner D., Schubert C., Penkalla A., Witt H., Kararigas G., Dworatzek E., Staub E., Martus P., Noppinger P. R., Kintscher U., Gustafsson J.-A. & Regitz-Zagrosek V. (2010) Female sex and estrogen receptor- β attenuate cardiac remodeling and apoptosis in pressure overload. *Am J Physiol Regul Integr Comp Physiol*, 298, R1597-1606.

Flower L., Ahuja R. H., Humphries S. E. & Mohamed-Ali V. (2000) Effects of sample handling on the stability of IL-6, TNF-alpha and leptin. *Cytokine*, 12, 1712-1716.

Frangogiannis N. G. (2008) The immune system and cardiac repair. *Pharmacol Res*, 58, 88-111.

Frantz S., Fraccarollo D., Wagner H., Behr T. M., Jung P., Angermann C. E., Ertl G. & Bauersachs J. (2003) Sustained activation of nuclear factor kappa B and activator protein 1 in chronic heart failure. *Cardiovas Res*, 57, 749-756.

Frantz S., Hu K., Bayer B., Gerondakis S., Strotmann J., Adamek A., Ertl G. & Bauersachs J. (2006) Absence of NF- κ B subunit p50 improves heart failure after myocardial infarction. *FASEB J.*, 20, 1918-1920.

Fredj S., Bescond J., Louault C., Delwail A., Lecron J.-c. & Potreau D. (2005a) Role of interleukin-6 in cardiomyocyte/cardiac fibroblast interactions during myocyte hypertrophy and fibroblast proliferation. *J Cell Physiol*, 204, 428-436.

Fredj S., Bescond J., Louault C. & Potreau D. (2005b) Interactions between cardiac cells enhance cardiomyocyte hypertrophy and increase fibroblast proliferation. *J Cell Physiol*, 202, 891-899.

Freund C., Schmidt-Ullrich R., Baurand A., Dunger S., Schneider W., Loser P., El-Jamali A., Dietz R., Scheidereit C. & Bergmann M. W. (2005) Requirement of nuclear factor- κ B in angiotensin II- and isoproterenol-induced cardiac hypertrophy in vivo. *Circulation*, 111, 2319-2325.

Frey N., McKinsey T. A. & Olson E. N. (2000) Decoding calcium signals involved in cardiac growth and function. *Nat Med*, 6, 1221.

Frey N. & Olson E. N. (2003) Cardiac hypertrophy: The good, the bad, and the ugly. *An Rev Physiol*, 65, 45-79.

Gamble C., McIntosh K., Scott R., Ho K. H., Plevin R. & Paul A. (2011) Inhibitory kappa B kinases as targets for pharmacological regulation. *Br J Pharmacol*, doi: 10.1111/j.1476-5381.2011.01608.x.

Gao X.-M., Kiriazis H., Moore X.-L., Feng X.-H., Sheppard K., Dart A. & Du X.-J. (2005) Regression of pressure overload-induced left ventricular hypertrophy in mice. *Am J Physiol Heart Circ Physiol*, 288, H2702-2707.

Gaudesius G., Miragoli M., Thomas S. P. & Rohr S. (2003) Coupling of cardiac electrical activity over extended distances by fibroblasts of cardiac origin. *Circ Res*, 93, 421-428.

Ghosh S. & Karin M. (2002) Missing pieces in the NF- κ B puzzle. *Cell*, 109, S81-S96.

Goldsmith E. C., Hoffman A., Morales M. O., Potts J. D., Price R. L., McFadden A., Rice M. & Borg T. K. (2004) Organization of fibroblasts in the heart. *Dev Dyn*, 230, 787-794.

Grabellus F., Levkau B., Sokoll A., Welp H., Schmid C., Deng M. C., Takeda A., Breithardt G. & Baba H. A. (2002) Reversible activation of nuclear factor- κ B in human end-stage heart failure after left ventricular mechanical support. *Cardiovasc Res*, 53, 124-130.

Gray M. O., Long C. S., Kalinyak J. E., Li H.-T. & Karliner J. S. (1998) Angiotensin II stimulates cardiac myocyte hypertrophy via paracrine release of TGF- β 1 and endothelin-1 from fibroblasts. *Cardiovasc Res*, 40, 352-363.

Grimm M., El-Armouche A., Zhang R., Anderson M. E. & Eschenhagen T. (2007) Reduced contractile response to [alpha]1-adrenergic stimulation in atria from mice with chronic cardiac calmodulin kinase II inhibition. *J Mol Cell Cardiol*, 42, 643.

Grueter C. E., Abiria S. A., Dzhura I., Wu Y., Ham A.-J. L., Mohler P. J., Anderson M. E. & Colbran R. J. (2006) L-type Ca²⁺ channel facilitation mediated by phosphorylation of the beta- subunit by CaMKII. *Mol Cell*, 23, 641-650.

Gupta S. & Sen S. (2005) Role of the NF-κB signaling cascade and NF-κB-targeted genes in failing human hearts *J Mol Med*, 83, 1432-1440.

Gupta S., Young D., Maitra R. K., Gupta A., Popovic Z. B., Yong S. L., Mahajan A., Wang Q. & Sen S. (2008) Prevention of cardiac hypertrophy and heart failure by silencing of NF-κB. *J Mol Bio*, 375, 637.

Gupta S., Young D. & Sen S. (2005) Inhibition of NF-κB induces regression of cardiac hypertrophy, independent of blood pressure control, in spontaneously hypertensive rats. *Am J Physiol Heart Circ Physiol*, 289, H20-29.

Gurantz D., Cowling R. T., Varki N., Frikovsky E., Moore C. D. & Greenberg B. H. (2005) IL-1[beta] and TNF-[alpha] upregulate angiotensin II type 1 (AT1) receptors on cardiac fibroblasts and are associated with increased AT1 density in the post-MI heart. *J Mol Cell Cardiol*, 38, 505-515.

Ha T., Li Y., Gao X., McMullen J. R., Shioi T., Izumo S., Kelley J. L., Zhao A., Haddad G. E., Williams D. L., Browder I. W., Kao R. L. & Li C. (2005a) Attenuation of cardiac hypertrophy by inhibiting both mTOR and NF[κappa]B activation in vivo. *Free Radic Bio Med*, 39, 1570.

Ha T., Li Y., Hua F., Ma J., Gao X., Kelley J., Zhao A., Haddad G. E., Williams D. L., William Browder I., Kao R. L. & Li C. (2005b) Reduced cardiac hypertrophy in toll-like receptor 4-deficient mice following pressure overload. *Cardiovasc Res*, 68, 224-234.

Hagemann D., Bohlender J., Hoch B., Krause E.-G. & Karczewski P. (2001) Expression of Ca²⁺/calmodulin-dependent protein kinase II delta-subunit isoforms in rats with hypertensive cardiac hypertrophy. *Mol Cell Biochem*, 220, 69-76.

Hall G., Hasday J. D. & Rogers T. B. (2006) Regulating the regulator: NF- κ B signaling in heart. *J Mol Cell Cardiol*, 41, 580.

Hall G., Singh I. S., Hester L., Hasday J. D. & Rogers T. B. (2005) Inhibitor- κ B kinase- β regulates LPS-induced TNF- α production in cardiac myocytes through modulation of NF- κ B p65 subunit phosphorylation. *Am J Physiol Heart Circ Physiol*, 289, H2103-2111.

Hamid T., Guo S. Z., Kingery J. R., Xiang X., Dawn B. & Prabhu S. D. (2010) Cardiomyocyte NF- κ B p65 promotes adverse remodeling, apoptosis, and endoplasmic reticulum stress in heart failure. *Cardiovasc Res*.

Hara M., Ono K., Hwang M.-W., Iwasaki A., Okada M., Nakatani K., Sasayama S. & Matsumori A. (2002) Evidence for a role of mast cells in the evolution to congestive heart failure. *J Exp Med*, 195, 375-381.

Hart C. Y. T., Burnett J. C. & Redfield M. M. (2001) Effects of avertin versus xylazine-ketamine anesthesia on cardiac function in normal mice. *Am J Physiol* 281, H1938-H1945.

Hasenfuss G. (1998) Animal models of human cardiovascular disease, heart failure and hypertrophy. *Cardiovasc Res*, 39, 60-76.

Hayden M. & Ghosh S. (2004) Signaling to NF- κ B. *Genes Dev*, 18, 2195-224.

Hayden M. S. & Ghosh S. (2008) Shared Principles in NF- κ B Signaling. *Cell*, 132, 344-362.

Hedayat M., Mahmoudi M., Rose N. & Rezaei N. (2010) Proinflammatory cytokines in heart failure: double-edged swords. *Heart Fail Rev*, 15, 543-562.

Hein S., Arnon E., Kostin S., Schonburg M., Elsasser A., Polyakova V., Bauer E. P., Klovekorn W.-P. & Schaper J. (2003) Progression from compensated hypertrophy to failure in the pressure-overloaded human heart: Structural deterioration and compensatory mechanisms. *Circulation*, 107, 984-991.

Hempel P., Hoch B., Bartel S. & Karczewski P. (2002) Hypertrophic phenotype of cardiac calcium/calmodulin-dependent protein kinase II is reversed by angiotensin converting enzyme inhibition. *Basic Res Cardiol*, 97, 96-101.

Higashiyama H., Sugai M., Inoue H., Mizuyachi K., Kushida H., Asano S. & Kinoshita M. (2007) Histopathological study of time course changes in inter-renal aortic banding-induced left ventricular hypertrophy of mice. *Int J Exp Pathol*, 88, 31-38.

Higuchi Y., Otsu K., Nishida K., Hirotsu S., Nakayama H., Yamaguchi O., Matsumura Y., Ueno H., Tada M. & Hori M. (2002) Involvement of reactive oxygen species-mediated NF- κ B activation in TNF- α -induced cardiomyocyte hypertrophy. *J Mol Cell Cardiol*, 34, 233-240.

Hikoso S., Yamaguchi O., Nakano Y., Takeda T., Omiya S., Mizote I., Taneike M., Oka T., Tamai T., Oyabu J., Uno Y., Matsumura Y., Nishida K., Suzuki K., Kogo M., Hori M. & Otsu K. (2009) The I κ B kinase β /nuclear factor κ B signaling pathway protects the heart from hemodynamic stress mediated by the regulation of manganese superoxide dismutase expression. *Circ Res*, 105, 70-79.

Hirotsu S., Otsu K., Nishida K., Higuchi Y., Morita T., Nakayama H., Yamaguchi O., Mano T., Matsumura Y., Ueno H., Tada M. & Hori M. (2002) Involvement of nuclear factor- κ B and apoptosis signal-regulating kinase 1 in G-protein-coupled receptor agonist-induced cardiomyocyte hypertrophy. *Circulation*, 105, 509-515.

Ho C. Y., Lopez B., Coelho-Filho O. R., Lakdawala N. K., Cirino A. L., Jarolim P., Kwong R., Gonzalez A., Colan S. D., Seidman J. G., Diez J. & Seidman C. E. (2010)

Myocardial fibrosis as an early manifestation of hypertrophic cardiomyopathy. *N Engl J Med*, 363, 552-563.

Hoberg J. E., Yeung F. & Mayo M. W. (2004) SMRT derepression by the I κ B kinase α : A prerequisite to NF- κ B transcription and survival. *Mol Cell*, 16, 245-255.

Hoch B., Meyer R., Hetzer R., Krause E.-G. & Karczewski P. (1999) Identification and expression of δ -isoforms of the multifunctional Ca²⁺/calmodulin-dependent protein kinase in failing and nonfailing human myocardium. *Circ Res*, 84, 713-721.

Honsho S., Nishikawa S., Amano K., Zen K., Adachi Y., Kishita E., Matsui A., Katsume A., Yamaguchi S., Nishikawa K., Isoda K., Riches D. W. H., Matoba S., Okigaki M. & Matsubara H. (2009) Pressure-mediated hypertrophy and mechanical stretch induces IL-1 release and subsequent IGF-1 generation to maintain compensative hypertrophy by affecting Akt and JNK pathways. *Circ Res*, 105, 1149-1158.

House S. J. & Singer H. A. (2008) CaMKII- δ isoform regulation of neointima formation after vascular injury. *Arterioscler Thromb Vasc Biol*, 28, 441-447.

Howe C. J., LaHair M. M., Maxwell J. A., Lee J. T., Robinson P. J., Rodriguez-Mora O., McCubrey J. A. & Franklin R. A. (2002) Participation of the calcium/calmodulin-dependent kinases in hydrogen peroxide-induced I κ B phosphorylation in human T lymphocytes. *J Bio Chem*, 277, 30469-30476.

Hu P., Zhang D., Swenson L., Chakrabarti G., Abel E. D. & Litwin S. E. (2003) Minimally invasive aortic banding in mice: effects of altered cardiomyocyte insulin signaling during pressure overload. *Am J Physiol Heart Circ Physiol*, 285, H1261-1269.

Hu W.-H., Pendergast J. S., Mo X.-M., Brambilla R., Bracchi-Ricard V., Li F., Walters W. M., Blits B., He L., Schaal S. M. & Bethea J. R. (2005) NIBP, a Novel NIK and IKK β -binding Protein That Enhances NF- κ B Activation. *J. Biol. Chem.*, 280, 29233-29241.

Hu Y., Baud V., Delhase M., Zhang P., Deerinck T., Ellisman M., Johnson R. & Karin M. (1999) Abnormal morphogenesis but intact IKK activation in mice lacking the IKK α subunit of I κ B kinase. *Science*, 284, 316-320.

Huang H., Tang Q.-Z., Wang A.-B., Chen M., Yan L., Liu C., Jiang H., Yang Q., Bian Z.-Y., Bai X., Zhu L.-H., Wang L. & Li H. (2010a) Tumor suppressor A20 protects against cardiac hypertrophy and fibrosis by blocking transforming growth factor- β -activated kinase 1-dependent signaling. *Hypertension*, 56, 232-239.

Huang R. Y. à., Laing J. G., Kanter E. M., Berthoud V. M., Bao M., Rohrs H. W., Townsend R. R. & Yamada K. A. (2010b) Identification of CaMKII phosphorylation sites in connexin43 by high-resolution mass spectrometry. *J Proteome Res*, null-null.

Hudmon A. & Schulman H. (2002) Structure-function of the multifunctional Ca²⁺/calmodulin-dependent protein kinase II. *Biochem J.*, 364, 593-611.

Hudson M. P., Armstrong P. W., Ruzyllo W., Brum J., Cusmano L., Krzeski P., Lyon R., Quinones M., Theroux P., Sydlowski D., Kim H. E., Garcia M. J., Jaber W. A. & Weaver W. D. (2006) Effects of selective matrix metalloproteinase inhibitor (PG-116800) to prevent ventricular remodeling after myocardial infarction: results of the PREMIER (Prevention of Myocardial Infarction Early Remodeling) Trial. *J Am Coll Cardiol*, 48, 15-20.

Hughes K., Antonsson Å. & Grundström T. (1998) Calmodulin dependence of NF[κ]B activation. *FEBS Letters*, 441, 132.

Hughes K., Edin S., Antonsson A. & Grundstrom T. (2001) Calmodulin-dependent kinase II mediates T cell receptor/CD3- and phorbol ester-induced activation of I κ B kinase. *J Biol Chem*, 276, 36008-36013.

Huke S. & Bers D. M. (2007) Temporal dissociation of frequency-dependent acceleration of relaxation and protein phosphorylation by CaMKII. *J Mol Cell Cardiol*, 42, 590-599.

Huke S., DeSantiago J., Kaetzel M. A., Mishra S., Brown J. H., Dedman J. R. & Bers D. M. (2010) SR-targeted CaMKII inhibition improves SR Ca²⁺ handling, but accelerates cardiac remodeling in mice overexpressing CaMKII[delta]C. *J Mol Cell Cardiol*, 50, 230-8.

Ikeuchi M., Tsutsui H., Shiomi T., Matsusaka H., Matsushima S., Wen J., Kubota T. & Takeshita A. (2004) Inhibition of TGF-β signaling exacerbates early cardiac dysfunction but prevents late remodeling after infarction. *Cardiovasc Res*, 64, 526-535.

Ishiguro K., Green T., Rapley J., Wachtel H., Giallourakis C., Landry A., Cao Z., Lu N., Takafumi A., Goto H., Daly M. J. & Xavier R. J. (2006) Ca²⁺/Calmodulin-Dependent Protein Kinase II Is a Modulator of CARMA1-Mediated NF-κB Activation. *Mol. Cell. Biol.*, 26, 5497-5508.

Ishizaka S., Sievers R. E., Zhu B.-Q., Rodrigo M. C., Joho S., Foster E., Simpson P. C. & Grossman W. (2004) New technique for measurement of left ventricular pressure in conscious mice. *Am J Physiol Heart Circ Physiol*, 286, H1208-1215.

Israel A. (2010) The IKK complex, a central regulator of NF-κB activation. *Cold Spring Harb Perspect Biol*, 2, a000158.

Jackman R. P., Utter G. H., Heitman J. W., Hirschhorn D. F., Law J. P., Geftter N., Busch M. P. & Norris P. J. (2011) Effects of blood sample age at time of separation on measured cytokine concentrations in human plasma. *Clin. Vaccine Immunol.*, 18, 318-326.

Jang M. K., Goo Y. H., Sohn Y. C., Kim Y. S., Lee S.-K., Kang H., Cheong J. & Lee J. W. (2001) Ca²⁺/Calmodulin-dependent Protein Kinase IV Stimulates Nuclear Factor-kappa B Transactivation via Phosphorylation of the p65 Subunit. *J. Biol. Chem.*, 276, 20005-20010.

Janicki J. S., Brower G. L., Gardner J. D., Forman M. F., Stewart J. A., Murray D. B. & Chancey A. L. (2006) Cardiac mast cell regulation of matrix metalloproteinase-

related ventricular remodeling in chronic pressure or volume overload. *Cardiovasc Res*, 69, 657-665.

Jaski B. E., Jessup M. L., Mancini D. M., Cappola T. P., Pauly D. F., Greenberg B., Borow K., Dittrich H., Zsebo K. M. & Hajjar R. J. (2009) Calcium upregulation by percutaneous administration of gene therapy in cardiac disease (CUPID Trial), a first-in-human Phase 1/2 clinical trial. *J Cardiac Fail*, 15, 171-181.

Jazbutyte V., Arias-Loza P. A., Hu K., Widder J., Govindaraj V., von Poser-Klein C., Bauersachs J., Fritzscheier K.-H., Hegele-Hartung C., Neyses L., Ertl G. & Pelzer T. (2008) Ligand-dependent activation of ER β lowers blood pressure and attenuates cardiac hypertrophy in ovariectomized spontaneously hypertensive rats. *Cardiovasc Res*, 77, 774-781.

Jong W., Zuurbier C., De Winter R., Van Den Heuvel D., Reitsma P., Ten Cate H. & Ince C. (2002) Fentanyl-fluanisone-midazolam combination results in more stable hemodynamics than does urethane alpha-chloralose and 2,2,2-tribromoethanol in mice. *Contemp Top Lab Anim Sci*, 41, 28-32.

Kashiwase K., Higuchi Y., Hirotani S., Yamaguchi O., Hikoso S., Takeda T., Watanabe T., Taniike M., Nakai A., Tsujimoto I., Matsumura Y., Ueno H., Nishida K., Hori M. & Otsu K. (2005) CaMKII activates ASK1 and NF- κ B to induce cardiomyocyte hypertrophy. *Biochem Biophys Res Commun*, 327, 136.

Kassiri Z., Oudit G. Y., Sanchez O., Dawood F., Mohammed F. F., Nuttall R. K., Edwards D. R., Liu P. P., Backx P. H. & Khokha R. (2005) Combination of tumor necrosis factor- α ablation and matrix metalloproteinase inhibition prevents heart failure after pressure overload in tissue inhibitor of metalloproteinase-3 knock-out mice. *Circ Res*, 97, 380-390.

Kawano S., Kubota T., Monden Y., Kawamura N., Tsutsui H., Takeshita A. & Sunagawa K. (2005) Blockade of NF- κ B ameliorates myocardial hypertrophy in response to chronic infusion of angiotensin II. *Cardiovasc Res*, 67, 689-698.

Kirchhefer U., Schmitz W., Scholz H. & Neumann J. (1999) Activity of cAMP-dependent protein kinase and Ca²⁺/calmodulin-dependent protein kinase in failing and nonfailing human hearts. *Cardiovasc Res*, 42, 254-261.

Klabunde R. E. (2005) *Cardiovascular Physiology Concepts*, Lippincott Williams & Wilkins.

Klocke R., Tian W., Kuhlmann M. T. & Nikol S. (2007) Surgical animal models of heart failure related to coronary heart disease. *Cardiovasc Res*, 74, 29-38.

Kobara M., Noda K., Kitamura M., Okamoto A., Shiraishi T., Toba H., Matsubara H. & Nakata T. (2010) Antibody against interleukin-6 receptor attenuates left ventricular remodelling after myocardial infarction in mice. *Cardiovasc Res*, 87, 424-430.

Kohl P. (2003) Heterogeneous cell coupling in the heart: an electrophysiological role for fibroblasts. *Circ Res*, 93, 381-383.

Kohl P., Kamkin A., Kiseleva I. & Noble D. (1994) Mechanosensitive fibroblasts in the sino-atrial node region of rat heart: interaction with cardiomyocytes and possible role. *Exp Physiol*, 79, 943-956.

Kratsios P., Huth M., Temmerman L., Salimova E., Al Banchaabouchi M., Sgoifo A., Manghi M., Suzuki K., Rosenthal N. & Mourkioti F. (2010) Antioxidant amelioration of dilated cardiomyopathy caused by conditional deletion of NEMO/IKK{gamma} in cardiomyocytes. *Circ Res*, 106, 133-144.

Krum H. & Teerlink J. R. (2011) Medical therapy for chronic heart failure. *The Lancet*, 378, 713-721.

Kushnir A., Shan J., Betzenhauser M. J., Reiken S. & Marks A. R. (2010) Role of CaMKIIδ phosphorylation of the cardiac ryanodine receptor in the force frequency relationship and heart failure. *Proc Natl Acad Sci*, 107, 10274-10279.

Kuwahara F., Kai H., Tokuda K., Kai M., Takeshita A., Egashira K. & Imaizumi T. (2002) Transforming growth factor-β function blocking prevents myocardial

fibrosis and diastolic dysfunction in pressure-overloaded rats. *Circulation*, 106, 130-135.

Lafontant P. J., Burns A. R., Donnachie E., Haudek S. B., Smith C. W. & Entman M. L. (2006) Oncostatin M differentially regulates CXC chemokines in mouse cardiac fibroblasts. *Am J Physiol Cell Physiol*, 291, C18-26.

LaFramboise W. A., Scalise D., Stoodley P., Graner S. R., Guthrie R. D., Magovern J. A. & Becich M. J. (2007) Cardiac fibroblasts influence cardiomyocyte phenotype in vitro. *Am J Physiol Cell Physiol*, 292, C1799-1808.

Leask A. (2010) Potential therapeutic targets for cardiac fibrosis: TGF- β , angiotensin, endothelin, CCN2, and PDGF, partners in fibroblast activation. *Cir Res*, 106, 1675-1680.

Lemon D. D., Horn T. R., Cavaasin M. A., Jeong M. Y., Haubold K. W., Long C. S., Irwin D. C., McCune S. A., Chung E., Leinwand L. A. & McKinsey T. A. (2011) Cardiac HDAC6 catalytic activity is induced in response to chronic hypertension. *J Mol Cell Cardiol*, 51, 41-50.

Leuschner F., Katus H. A. & Kaya Z. (2009) Autoimmune myocarditis: Past, present and future. *J Autoimmun*, 33, 282-289.

Levick S. P., McLarty J. L., Murray D. B., Freeman R. M., Carver W. E. & Brower G. L. (2009) Cardiac mast cells mediate left ventricular fibrosis in the hypertensive rat heart. *Hypertension*, 53, 1041-1047.

Levick S. P., Melendez G. C., Plante E., McLarty J. L., Brower G. L. & Janicki J. S. (2011) Cardiac mast cells: the centrepiece in adverse myocardial remodelling. *Cardiovasc Res*, 89, 12-19.

Li B., Dedman J. R. & Kaetzel M. A. (2006) Nuclear Ca²⁺/calmodulin-dependent protein kinase II in the murine heart. *Biochim Biophys Acta*, 1763, 1275.

Li H.-L., Zhuo M.-L., Wang D., Wang A.-B., Cai H., Sun L.-H., Yang Q., Huang Y., Wei Y.-S., Liu P. P., Liu D.-P. & Liang C.-C. (2007) Targeted cardiac overexpression of A20 improves left ventricular performance and reduces compensatory hypertrophy after myocardial infarction. *Circulation*, 115, 1885-1894.

Li Q., Antwerp D. V., Mercurio F., Lee K.-F. & Verma I. M. (1999a) Severe liver degeneration in mice lacking the I κ B kinase 2 gene. *Science*, 284, 321-325.

Li Y., Ha T., Gao X., Kelley J., Williams D. L., Browder I. W., Kao R. L. & Li C. (2004) NF- κ B activation is required for the development of cardiac hypertrophy in vivo. *Am J Physiol Heart Circ Physiol*, 287, H1712-1720.

Li Z.-W., Chu W., Hu Y., Delhase M., Deerinck T., Ellisman M., Johnson R. & Karin M. (1999b) The IKK β subunit of I κ B kinase (IKK) is essential for nuclear factor κ B activation and prevention of apoptosis. *J Exp Med*, 189, 1839-1845.

Liao R., Jain M., Cui L., D'Agostino J., Aiello F., Luptak I., Ngoy S., Mortensen R. M. & Tian R. (2002a) Cardiac-specific overexpression of GLUT1 prevents the development of heart failure attributable to pressure overload in mice. *Circulation*, 106, 2125-2131.

Liao Y., Ishikura F., Beppu S., Asakura M., Takashima S., Asanuma H., Sanada S., Kim J., Ogita H., Kuzuya T., Node K., Kitakaze M. & Hori M. (2002b) Echocardiographic assessment of LV hypertrophy and function in aortic-banded mice: necropsy validation. *Am J Physiol*, 282, H1703-H1708.

Lilienbaum A. & Israel A. (2003) From Calcium to NF- κ B Signaling Pathways in Neurons. *Mol. Cell. Biol.*, 23, 2680-2698.

Ling H., Zhang T., Pereira L., Means C. K., Cheng H., Gu Y., Dalton N. D., Peterson K. L., Chen J., Bers D. & Brown J. H. (2009) Requirement for Ca²⁺/calmodulin-dependent kinase II in the transition from pressure overload-induced cardiac hypertrophy to heart failure in mice. *J Clin Invest*.

Ling L., Cao Z. & Goeddel D. V. (1998) NF- κ B-inducing kinase activates IKK- α by phosphorylation of Ser-176. *Proc Natl Acad Sci*, 95, 3792-3797.

Little G. H., Bai Y., Williams T. & Poizat C. (2007) Nuclear calcium/calmodulin-dependent protein kinase II $\{\delta\}$ preferentially transmits signals to histone deacetylase 4 in cardiac cells. *J Biol Chem*, 282, 7219-7231.

Little G. H., Saw A., Bai Y., Dow J., Marjoram P., Simkhovich B., Leeka J., Kedes L., Kloner R. A. & Poizat C. (2009) Critical role of nuclear calcium/calmodulin-dependent protein kinase II δ B in cardiomyocyte survival in cardiomyopathy. *J Biol Chem*, 284, 24857-24868.

Liu X., Yao M., Li N., Wang C., Zheng Y. & Cao X. (2008) CaMKII promotes TLR-triggered proinflammatory cytokine and type I interferon production by directly binding and activating TAK1 and IRF3 in macrophages. *Blood*, 112, 4961-4970.

Lokuta A. J., Rogers T. B., Lederer W. J. & Valdivia H. H. (1995) Modulation of cardiac ryanodine receptors of swine and rabbit by a phosphorylation-dephosphorylation mechanism. *J Physiol*, 487, 609-622.

Lompre A.-M., Hajjar R. J., Harding S. E., Kranias E. G., Lohse M. J. & Marks A. R. (2010) Ca²⁺ cycling and new therapeutic approaches for heart failure. *Circulation*, 121, 822-830.

Loughrey C. M., Smith G. L. & MacEachern K. E. (2004) Comparison of Ca²⁺ release and uptake characteristics of the sarcoplasmic reticulum in isolated horse and rabbit cardiomyocytes. *Am J Physiol Heart Circ Physiol*, 287, H1149-1159.

Lu Y.-M., Shioda N., Han F., Moriguchi S., Kasahara J., Shirasaki Y., Qin Z.-H. & Fukunaga K. (2007) Imbalance between CaM kinase II and calcineurin activities impairs caffeine-induced calcium release in hypertrophic cardiomyocytes. *Biochem Pharmacol*, 74, 1727.

Lucas J. A., Zhang Y., Li P., Gong K., Miller A. P., Hassan E., Hage F., Xing D., Wells B., Oparil S. & Chen Y.-F. (2010) Inhibition of transforming growth factor-

{beta} signaling induces left ventricular dilation and dysfunction in the pressure-overloaded heart. *Am J Physiol Heart Circ Physiol*, 298, H424-432.

Lygate C. (2006) Surgical models of hypertrophy and heart failure: Myocardial infarction and transverse aortic constriction. *Drug Discovery Today: Disease Models*, 3, 283-290.

Lygate C., Schneider J., Hulbert K., ten Hove M., Sebag-Montefiore L., Cassidy P., Clarke K. & Neubauer S. (2006) Serial high resolution 3D-MRI after aortic banding in mice: band internalization is a source of variability in the hypertrophic response. *Basic Res Cardiol*, 101, 8-16.

Ma Y., Cheng W., Wu S. & Wong T. (2009) Oestrogen confers cardioprotection by suppressing Ca^{2+} /calmodulin-dependent protein kinase II. *Br J Pharmacol*, 157, 705-715.

MacKenzie C. J., Ritchie E., Paul A. & Plevin R. (2007) IKK[alpha] and IKK[beta] function in TNF[alpha]-stimulated adhesion molecule expression in human aortic smooth muscle cells. *Cell Signal*, 19, 75-80.

Mahmoodzadeh S., Fritschka S., Dworatzek E., Pham T. H., Becher E., Kuehne A., Davidson M. M. & Regitz-Zagrosek V. (2009) Nuclear factor- κ B regulates estrogen receptor- α transcription in the human heart. *J Biol Chem*, 284, 24705-24714.

Maier L. S. (2011) CaMKII regulation of voltage-gated sodium channels and cell excitability. *Heart Rhythm*, 8, 474-477.

Maier L. S. & Bers D. M. (2002) Calcium, calmodulin and calcium-calmodulin kinase II: Heartbeat to heartbeat and beyond. *J Mol Cell Cardiol*, 34, 919-939.

Maier L. S. & Bers D. M. (2007) Role of Ca^{2+} /calmodulin-dependent protein kinase (CaMK) in excitation-contraction coupling in the heart. *Cardiovasc Res*, 73, 631-640.

Maier L. S., Zhang T., Chen L., DeSantiago J., Brown J. H. & Bers D. M. (2003) Transgenic CaMKII Δ C overexpression uniquely alters cardiac myocyte Ca^{2+}

handling: Reduced SR Ca²⁺ load and activated SR Ca²⁺ release. *Circ Res*, 92, 904-911.

Maltsev V. A., Reznikov V., Undrovinas N. A., Sabbah H. N. & Undrovinas A. (2008) Modulation of late sodium current by Ca²⁺, calmodulin, and CaMKII in normal and failing dog cardiomyocytes: similarities and differences. *Am J Physiol*, 294, H1597-H1608.

Manabe I., Shindo T. & Nagai R. (2002) Gene expression in fibroblasts and fibrosis: Involvement in cardiac hypertrophy. *Circ Res*, 91, 1103-1113.

Mandl A., Huong Pham L., Toth K., Zambetti G. & Erhardt P. (2011) Puma deletion delays cardiac dysfunction in murine heart failure models through attenuation of apoptosis: Clinical perspective. *Circulation*, 124, 31-39.

Mangelus M., Galron R., Naor Z. & Sokolovsky M. (2001) Involvement of nuclear factor-KappaB in endothelin-A-receptor-induced proliferation and inhibition of apoptosis. *Cell Mol Neurobiol*, 21, 657-674.

Mangmool S., Shukla A. K. & Rockman H. A. (2010) β -Arrestin-dependent activation of Ca²⁺/calmodulin kinase II after β_1 -adrenergic receptor stimulation. *J Cell Bio*, 189, 573-587.

Mann D. L., McMurray J. J. V., Packer M., Swedberg K., Borer J. S., Colucci W. S., Djian J., Drexler H., Feldman A., Kober L., Krum H., Liu P., Nieminen M., Tavazzi L., van Veldhuisen D. J., Waldenström A., Warren M., Westheim A., Zannad F. & Fleming T. (2004) Targeted anticytokine therapy in patients with chronic heart failure. *Circulation*, 109, 1594-1602.

Massa P. E., Li X., Hanidu A., Siamas J., Pariali M., Pareja J., Savitt A. G., Catron K. M., Li J. & Marcu K. B. (2005) Gene expression profiling in conjunction with physiological rescues of IKK α -null cells with wild type or mutant IKK α reveals distinct classes of IKK α /NF- κ B-dependent genes. *J Biol Chem*, 280, 14057-14069.

Mattiazzi A., Mundina-Weilenmann C., Guoxiang C., Vittone L. & Kranias E. (2005) Role of phospholamban phosphorylation on Thr17 in cardiac physiological and pathological conditions. *Cardiovasc Res*, 68, 366-375.

Maulik N., Goswami S., Galang N. & Das D. K. (1999) Differential regulation of Bcl-2, AP-1 and NF-[kappa]B on cardiomyocyte apoptosis during myocardial ischemic stress adaptation. *FEBS Letters*, 443, 331.

McMurray J. & Pfeffer M. A. (2002a) New therapeutic options in congestive heart failure: Part I. *Circulation*, 105, 2099-2106.

McMurray J. & Pfeffer M. A. (2002b) New therapeutic options in congestive heart failure: Part II. *Circulation*, 105, 2223-2228.

McSpadden L. C., Kirkton R. D. & Bursac N. (2009) Electrotonic loading of anisotropic cardiac monolayers by unexcitable cells depends on connexin type and expression level. *American Journal of Physiology - Cell Physiology*, 297, C339-C351.

Meffert M. K., Chang J. M., Wiltgen B. J., Fanselow M. S. & Baltimore D. (2003) NF-[kappa]B functions in synaptic signaling and behavior. *Nat Neurosci*, 6, 1072.

Melendez G. C., McLarty J. L., Levick S. P., Du Y., Janicki J. S. & Brower G. L. (2010) Interleukin 6 mediates myocardial fibrosis, concentric hypertrophy, and diastolic dysfunction in rats. *Hypertension*, 56, 225-231.

Mills G. D., Kubo H., Harris D. M., Berretta R. M., Piacentino V., III & Houser S. R. (2006) Phosphorylation of phospholamban at threonine-17 reduces cardiac adrenergic contractile responsiveness in chronic pressure overload-induced hypertrophy. *Am J Physiol Heart Circ Physiol*, 291, H61-70.

Miragoli M., Salvarani N. & Rohr S. (2007) Myofibroblasts induce ectopic activity in cardiac tissue. *Circ Res*, 101, 755-758.

Misra A., Haudek S. B., Knuefermann P., Vallejo J. G., Chen Z. J., Michael L. H., Sivasubramanian N., Olson E. N., Entman M. L. & Mann D. L. (2003) Nuclear

factor- κ B protects the adult cardiac myocyte against ischemia-induced apoptosis in a murine model of acute myocardial infarction. *Circulation*, 108, 3075-3078.

Mohammed S. F., Storlie J. R., Oehler E. A., Bowen L. A., Korinek J., Lam C. S. P., Simari R. D., Burnett Jr J. C. & Redfield M. M. (2011) Variable phenotype in murine transverse aortic constriction. *Cardiovasc Pathol*, In Press, Corrected Proof.

Monaco S., Illario M., Rusciano M. R., Gragnaniello G., Di Spigna G., Leggiero E., Pastore L., Fenzi G., Rossi G. & Vitale M. (2009) Insulin stimulates fibroblast proliferation through calcium-calmodulin-dependent kinase II. *Cell Cycle*, 8, 2024-2030.

Moreo A., Ambrosio G., De Chiara B., Pu M., Tran T., Mauri F. & Raman S. V. (2009) Influence of myocardial fibrosis on left ventricular diastolic function: noninvasive assessment by cardiac magnetic resonance and echo. *Cir Cardiovas Imaging*, 2, 437-443.

Morgan E. N., Boyle E. M., Jr., Yun W., Griscavage-Ennis J. M., Farr A. L., Canty T. G., Jr., Pohlman T. H. & Verrier E. D. (1999) An essential role for NF- κ B in the cardioadaptive response to ischemia. *Ann Thorac Surg*, 68, 377-382.

Mork H. K., Sjaastad I., Sande J. r. B., Periasamy M., Sejersted O. M. & Louch W. E. (2007) Increased cardiomyocyte function and Ca^{2+} transients in mice during early congestive heart failure. *J Mol Cell Cardiol*, 43, 177-186.

Moss N. C., Stansfield W. E., Willis M. S., Tang R.-H. & Selzman C. H. (2007) IKKbeta inhibition attenuates myocardial injury and dysfunction following acute ischemia-reperfusion injury. *Am J Physiol Heart Circ Physiol*, 293, H2248-2253.

Moss N. C., Tang R.-H., Willis M., Stansfield W. E., Baldwin A. S. & Selzman C. H. (2008) Inhibitory kappa B kinase-[beta] is a target for specific nuclear factor kappa B-mediated delayed cardioprotection. *J Thorac Cardiovasc Surg*, 136, 1274.

Mustapha S., Kirshner A., De Moissac D. & Kirshenbaum L. A. (2000) A direct requirement of nuclear factor-kappa B for suppression of apoptosis in ventricular myocytes. *Am J Physiol Heart Circ Physiol*, 279, H939-945.

Nagai T., Anzai T., Kaneko H., Mano Y., Anzai A., Maekawa Y., Takahashi T., Meguro T., Yoshikawa T. & Fukuda K. (2011) C-reactive protein overexpression exacerbates pressure overload-induced cardiac remodeling through enhanced inflammatory response. *Hypertension*, 57, 208-215.

Nakamura A., Rokosh D. G., Paccanaro M., Yee R. R., Simpson P. C., Grossman W. & Foster E. (2001) LV systolic performance improves with development of hypertrophy after transverse aortic constriction in mice. *Am J Physiol*, 281, H1104-H1112.

Nian M., Lee P., Khaper N. & Liu P. (2004) Inflammatory cytokines and postmyocardial infarction remodeling. *Cir Res*, 94, 1543-1553.

Niizeki T., Takeishi Y., Kitahara T., Arimoto T., Ishino M., Bilim O., Suzuki S., Sasaki T., Nakajima O., Walsh R. A., Goto K. & Kubota I. (2008) Diacylglycerol kinase- ϵ restores cardiac dysfunction under chronic pressure overload: a new specific regulator of G α_q signaling cascade. *Am J Physiol*, 295, H245-H255.

Nishida M., Onohara N., Sato Y., Suda R., Ogushi M., Tanabe S., Inoue R., Mori Y. & Kurose H. (2007) G $\alpha_{12/13}$ -mediated up-regulation of TRPC6 negatively regulates endothelin-1-induced cardiac myofibroblast formation and collagen synthesis through nuclear factor of activated T cells activation. *J Biol Chem*, 282, 23117-23128.

Nordmeyer J., Eder S., Mahmoodzadeh S., Martus P., Fielitz J., Bass J., Bethke N., Zurbrugg H. R., Pregla R., Hetzer R. & Regitz-Zagrosek V. (2004) Upregulation of myocardial estrogen receptors in human aortic stenosis. *Circulation*, 110, 3270-3275.

Ogawa T., Linz W., Stevenson M., Bruneau B. G., Kuroski de Bold M. L., Chen J. H., Eid H., Scholkens B. A. & de Bold A. J. (1996) Evidence for load-dependent and

load-independent determinants of cardiac natriuretic peptide production. *Circulation*, 93, 2059-2067.

Olson E. N. & Williams R. S. (2000) Calcineurin signalling and muscle remodelling. *Cell*, 101, 689-692.

Onai Y., Suzuki J.-i., Kakuta T., Maejima Y., Haraguchi G., Fukasawa H., Muto S., Itai A. & Isobe M. (2004) Inhibition of I κ B phosphorylation in cardiomyocytes attenuates myocardial ischemia/reperfusion injury. *Cardiovasc Res*, 63, 51-59.

Onai Y., Suzuki J.-i., Maejima Y., Haraguchi G., Muto S., Itai A. & Isobe M. (2007) Inhibition of NF- κ B improves left ventricular remodeling and cardiac dysfunction after myocardial infarction. *Am J Physiol Heart Circ Physiol*, 292, H530-538.

Ottaviano F. & Yee K. O. (2011) Communication signals between cardiac fibroblasts and cardiac myocytes. *J Cardiovasc Pharmacol*, 57 513-21.

Papageorgiou A.-P. & Heymans S. (2011) Interactions between the extracellular matrix and inflammation during viral myocarditis. *Immunobiology*, Epub ahead of print.

Patten R. D. & Hall-Porter M. R. (2009) Small animal models of heart failure. *Circulation*, 120, 138-144.

Patten R. D., Pourati I., Aronovitz M. J., Alsheikh-Ali A., Eder S., Force T., Mendelsohn M. E. & Karas R. H. (2008) 17 beta-estradiol differentially affects left ventricular and cardiomyocyte hypertrophy following myocardial infarction and pressure overload. *J Card Fail*, 14, 245-253.

Pedram A., Razandi M., Aitkenhead M. & Levin E. R. (2005) Estrogen inhibits cardiomyocyte hypertrophy in vitro: Antagonism of calcineurin-related hypertrophy through induction of MCIP1 *J Biol Chem*, 280, 26339-26348.

- Pedrotty D. M., Klinger R. Y., Kirkton R. D. & Bursac N. (2009) Cardiac fibroblast paracrine factors alter impulse conduction and ion channel expression of neonatal rat cardiomyocytes. *Cardiovasc Res*, 83, 688-697.
- Peng J., Gurantz D., Tran V., Cowling R. T. & Greenberg B. H. (2002) Tumor necrosis factor-(alpha)-induced AT1 receptor upregulation enhances angiotensin II-mediated cardiac fibroblast responses that favor fibrosis. *Circ Res*, 91, 1119-1126.
- Peng W., Zhang Y., Zheng M., Cheng H., Zhu W., Cao C.-M. & Xiao R.-P. (2010) Cardioprotection by CaMKII- δ B is mediated by phosphorylation of heat shock factor 1 and subsequent expression of inducible heat shock protein 70. *Circ Res*, 106, 102-110.
- Perrelli M. G., Pagliaro P. & Penna C. (2011) Ischemia/reperfusion injury and cardioprotective mechanisms: Role of mitochondria and reactive oxygen species. *World J Cardiology*, 3, 186-200.
- Petrov G., Regitz-Zagrosek V., Lehmkuhl E., Krabatsch T., Dunkel A., Dandel M., Dworatzek E., Mahmoodzadeh S., Schubert C., Becher E., Hampl H. & Hetzer R. (2010) Regression of myocardial hypertrophy after aortic valve replacement. *Circulation*, 122, S23-S28.
- Pfeffer M., Pfeffer J., Fishbein M., Fletcher P., Spadaro J., Kloner R. & Braunwald E. (1979) Myocardial infarct size and ventricular function in rats. *Cir Res*, 44, 503-512.
- Piacentini L., Gray M., Honbo N. Y., Chentoufi J., Bergman M. & Karliner J. S. (2000) Endothelin-1 stimulates cardiac fibroblast proliferation through activation of protein kinase C. *J Mol Cell Cardiol*, 32, 565-576.
- Porter K. E. & Turner N. A. (2009) Cardiac fibroblasts: At the heart of myocardial remodeling. *Pharmacol Ther*, 123, 255-278.
- Poyet J.-L., Srinivasula S. M., Lin J.-h., Fernandes-Alnemri T., Yamaoka S., Tschlis P. N. & Alnemri E. S. (2000) Activation of the I κ B Kinases by RIP via IKK γ /NEMO-mediated Oligomerization. *J Biol Chem*, 275, 37966-37977.

Prajapati S., Yamamoto Y., Gaynor R. B. & Tu Z. (2006) IKK α Regulates the Mitotic Phase of the Cell Cycle by Modulating Aurora A Phosphorylation. *Cell Cycle*, 5, 2371-2380.

Prasad A. M., Ma H., Sumbilla C., Lee D. I., Klein M. G. & Inesi G. (2007) Phenylephrine hypertrophy, Ca²⁺-ATPase (SERCA2), and Ca²⁺ signaling in neonatal rat cardiac myocytes. *Am J Physiol*, 292, C2269-C2275.

Psarra A. M., Hermann S., Panayotou G. & Spyrou G. (2009) Interaction of mitochondrial thioredoxin with glucocorticoid receptor and NF- κ B modulates glucocorticoid receptor and NF- κ B signalling in HEK-293 cells. *Biochem J*, 422, 521-531.

Purcell N. H. & Molkenin J. D. (2003) Is nuclear factor kappa-B an attractive therapeutic target for treating cardiac hypertrophy? *Circulation*, 108, 638-640.

Purcell N. H., Tang G., Yu C., Mercurio F., DiDonato J. A. & Lin A. (2001) Activation of NF- κ B is required for hypertrophic growth of primary rat neonatal ventricular cardiomyocytes. *Proc Natl Acad Sci*, 98, 6668-6673.

Ramirez M. T., Zhao X.-L., Schulman H. & Brown J. H. (1997) The nuclear delta B isoform of Ca²⁺/calmodulin-dependent protein kinase II regulates atrial natriuretic factor gene expression in ventricular myocytes. *J Biol Chem*, 272, 31203-31208.

Rang H. P., Dale M. M., Ritter J. M. & Moore P. K. (2003) Chapter 17: The heart. *Pharmacology*. Elsevier Churchill Livingstone.

Reddy L. G., Jones L. R., Pace R. C. & Stokes D. L. (1996) Purified, reconstituted cardiac Ca²⁺-ATPase is regulated by phospholamban but not by direct phosphorylation with Ca²⁺/calmodulin-dependent protein kinase. *J Biol Chem*, 271, 14964-14970.

Reddy V. S., Harskamp R. E., van Ginkel M. W., Calhoon J., Baisden C. E., Kim I.-S., Valente A. J. & Chandrasekar B. (2008) Interleukin-18 stimulates fibronectin

expression in primary human cardiac fibroblasts via PI3K-Akt-dependent NF- κ B activation. *J Cell Physiol*, 215, 697-707.

Regula K. M., Ens K. & Kirshenbaum L. A. (2002) IKKbeta is required for Bcl-2-mediated NF-kappa B activation in ventricular myocytes. *J Biol Chem*, 277, 38676-38682.

Riches P., Gooding R., Millar B. C. & Rowbottom A. W. (1992) Influence of collection and separation of blood samples on plasma IL-1, IL-6 and TNF-[alpha] concentrations. *J Immunol Methods*, 153, 125-131.

Robbins J. (2004) Genetic modification of the heart: exploring necessity and sufficiency in the past 10 years. *J Mol Cell Cardiol*, 36, 643-652.

Rockman H. A., Ross R. S., Harris A. N., Knowlton K. U., Steinhilber M. E., Field L. J., Ross J. & Chien K. R. (1991) Segregation of atrial-specific and inducible expression of an atrial natriuretic factor transgene in an in vivo murine model of cardiac hypertrophy. *Proc Natl Acad Sci*, 88, 8277-8281.

Rohr S. (2009) Myofibroblasts in diseased hearts: New players in cardiac arrhythmias? *Heart Rhythm*, 6, 848-856.

Roth D. M., Swaney J. S., Dalton N. D., Gilpin E. A. & Ross J., Jr. (2002) Impact of anesthesia on cardiac function during echocardiography in mice. *Am J Physiol Heart Circ Physiol*, 282, H2134-2140.

Rouet-Benzineb P., Gontero B., Dreyfus P. & Lafuma C. (2000) Angiotensin II induces nuclear factor- [kappa] B activation in cultured neonatal rat cardiomyocytes through protein kinase C signaling pathway. *J Mol Cell Cardiol*, 32, 1767-1778.

Sag C. M., Wadsack D. P., Khabbazzadeh S., Abesser M., Grefe C., Neumann K., Opiela M.-K., Backs J., Olson E. N., Heller Brown J., Neef S., Maier S. K. G. & Maier L. S. (2009) CaMKII contributes to cardiac arrhythmogenesis in heart failure. *Cir Heart Fail*, 2, 664-75.

Saito T., Fukuzawa J., Osaki J., Sakuragi H., Yao N., Haneda T., Fujino T., Wakamiya N., Kikuchi K. & Hasebe N. (2003) Roles of calcineurin and calcium/calmodulin-dependent protein kinase II in pressure overload-induced cardiac hypertrophy. *J Mol Cell Cardiol*, 35, 1153.

Sakurai H., Chiba H., Miyoshi H., Sugita T. & Toriumi W. (1999) I κ B kinases phosphorylate NF- κ B p65 subunit on serine 536 in the transactivation domain. *J Biol Chem*, 274, 30353-30356.

Sangeetha M., Pillai M. S., Philip L., Lakatta E. G. & Shivakumar K. (2011) NF- κ B inhibition compromises cardiac fibroblast viability under hypoxia. *Exp Cell Res*, 317, 899-909.

Sano M., Fukuda K., Kodama H., Pan J., Saito M., Matsuzaki J., Takahashi T., Makino S., Kato T. & Ogawa S. (2000) Interleukin-6 family of cytokines mediate angiotensin II-induced cardiac hypertrophy in rodent cardiomyocytes. *J Biol Chem*, 275, 29717-29723.

Sano M., Fukuda K., Sato T., Kawaguchi H., Suematsu M., Matsuda S., Koyasu S., Matsui H., Yamauchi-Takahara K., Harada M., Saito Y. & Ogawa S. (2001) ERK and p38 MAPK, but not NF- κ B, are critically involved in reactive oxygen species-mediated induction of IL-6 by angiotensin II in cardiac fibroblasts. *Circ Res*, 89, 661-669.

Santiago J.-J., Dangerfield A. L., Rattan S. G., Bathe K. L., Cunnington R. H., Raizman J. E., Bedosky K. M., Freed D. H., Kardami E. & Dixon I. M. C. (2010) Cardiac fibroblast to myofibroblast differentiation in vivo and in vitro: Expression of focal adhesion components in neonatal and adult rat ventricular myofibroblasts. *Dev Dyn*, 239, 1573-1584.

Sármán B., Skoumal R., Leskinen H., Rysä J., Ilves M., Soini Y., Tuukkanen J., Pikkarainen S., Lakó-Futó Z., Sármán B., Papp L., deChâtel R., Tóth M., Ruskoaho H. & Szokodi I. (2007) Nuclear factor- κ B signaling contributes to severe, but not

moderate, angiotensin II-induced left ventricular remodeling. *J Hypertens*, 29, 1927-39.

Sato H., Watanabe A., Tanaka T., Koitabashi N., Arai M., Kurabayashi M. & Yokoyama T. (2003) Regulation of the human tumor necrosis factor- α promoter by angiotensin II and lipopolysaccharide in cardiac fibroblasts: different cis-acting promoter sequences and transcriptional factors. *J Mol Cell Cardiol*, 35, 1197-1205.

Satoh M., Nakamura M., Saitoh H., Satoh H., Maesawa C., Segawa I., Tashiro A. & Hiramori K. (1999) Tumor necrosis factor- α -converting enzyme and tumor necrosis factor- α in human dilated cardiomyopathy. *Circulation*, 99, 3260-3265.

Schaefer A., Meyer G. P., Brand B., Hilfiker-Kleiner D., Drexler H. & Klein G. (2005) Effects of anesthesia on diastolic function in mice assessed by echocardiography. *Echocardiography*, 22, 665-670.

Schmidt C., Peng B., Li Z., Sclabas G. M., Fujioka S., Niu J., Schmidt-Supprian M., Evans D. B., Abbruzzese J. L. & Chiao P. J. (2003) Mechanisms of proinflammatory cytokine-induced biphasic NF- κ B activation. *Mol Cell*, 12, 1287-1300.

Schott P., Jacobshagen C., K^hler J. r., Seidler T., Asif A. R., Dihazi H., Hasenfuss G. & Maier L. S. (2011) Proteome changes in CaMKII δ C-overexpressing cardiac myocytes. *Cardiovasc Pathol*, 19, e241-e250.

Schwabe R. F. & Sakurai H. (2005) IKK β phosphorylates p65 at S468 in transactivation domain 2. *FASEB J.*, 9 1758-60.

Sen R. & Baltimore D. (1986) Multiple nuclear factors interact with the immunoglobulin enhancer sequences. *Cell*, 46, 705-716.

Shah A. M. & Mann D. L. (2011) In search of new therapeutic targets and strategies for heart failure: recent advances in basic science. *The Lancet*, 378, 704-712.

Singh M. & Anderson M. (2011) Is CaMKII a link between inflammation and hypertrophy in heart? *J Mol Med*, 89 537-43.

Singh M., Kapoun A., Higgins L., Kutschke W., Thurman J., Zhang R., Singh M., Yang J., Guan X., Lowe J., Weiss R., Zimmermann K., Yull F., Blackwell T., Mohler P. & Anderson M. (2009a) Ca^{2+} /calmodulin-dependent kinase II triggers cell membrane injury by inducing complement factor B gene expression in the mouse heart *J Clin Invest*, 119, 986-996.

Singh P., Salih M. & Tuana B. (2009b) Alpha-kinase anchoring protein alphaKAP interacts with SERCA2A to spatially position calcium/calmodulin-dependent protein kinase II and modulate phospholamban phosphorylation. *J Biol Chem*, 284, 28212-28221.

Siwik D. A., Chang D. L.-F. & Colucci W. S. (2000) Interleukin-1 β and tumor necrosis factor- α decrease collagen synthesis and increase matrix metalloproteinase activity in cardiac fibroblasts in vitro. *Circ Res*, 86, 1259-1265.

Skavdahl M., Steenbergen C., Clark J., Myers P., Demianenko T., Mao L., Rockman H. A., Korach K. S. & Murphy E. (2005) Estrogen receptor- β mediates male-female differences in the development of pressure overload hypertrophy. *Am J Physiol Heart Circ Physiol*, 288, H469-476.

Skelding K. & Rostas J. (2009) Regulation of CaMKII in vivo: The importance of targeting and the intracellular microenvironment. *Neurochem Res*, 34, 1792-1804.

Skelding K. A., Suzuki T., Gordon S., Xue J., Verrills N. M., Dickson P. W. & Rostas J. A. P. (2010) Regulation of CaMKII by phospho-Thr253 or phospho-Thr286 sensitive targeting alters cellular function. *Cell Signal*, 22, 759-769.

Smeets P. J. H., Teunissen B. E. J., Planavila A., de Vogel-van den Bosch H., Willemsen P. H. M., van der Vusse G. J. & van Bilsen M. (2008) Inflammatory pathways are activated during cardiomyocyte hypertrophy and attenuated by peroxisome proliferator-activated receptors PPAR α and PPAR δ . *J Biol Chem*, 283, 29109-29118.

Solomon S. D. (2006) Chapter 5: Ventricular systolic function. *Essential Echocardiography: A Practical Handbook with DVD*. 2 ed., Humana Press.

Solt L. A., Madge L. A. & May M. J. (2009) NEMO-binding domains of both IKK α and IKK β regulate I κ B kinase complex assembly and classical NF- κ B activation. *J Biol Chem*, 284, 27596-27608.

Song X., Kusakari Y., Xiao C.-Y., Kinsella S. D., Rosenberg M. A., Scherrer-Crosbie M., Hara K., Rosenzweig A. & Matsui T. (2010) mTOR attenuates the inflammatory response in cardiomyocytes and prevents cardiac dysfunction in pathological hypertrophy. *Am J Physiol*, 299, C1256-C1266.

Sossalla S., Fluschnik N., Schotola H., Ort K. R., Neef S., Schulte T., Wittkopper K., Renner A., Schmitto J. D., Gummert J., El-Armouche A., Hasenfuss G. & Maier L. S. (2010) Inhibition of elevated Ca²⁺/calmodulin-dependent protein kinase II improves contractility in human failing myocardium. *Circ Res*, 107 1150-61.

Stansfield W. E., Rojas M., Corn D., Willis M., Patterson C., Smyth S. S. & Selzman C. H. (2007) Characterization of a model to independently study regression of ventricular hypertrophy. *J Surg Res*, 142, 387-393.

Sun M., Chen M., Dawood F., Zurawska U., Li J. Y., Parker T., Kassiri Z., Kirshenbaum L. A., Arnold M., Khokha R. & Liu P. P. (2007) Tumor necrosis factor- α mediates cardiac remodeling and ventricular dysfunction after pressure overload state. *Circulation*, 115, 1398-1407.

Szabo E., Papp S. & Opas M. (2007) Differential calreticulin expression affects focal contacts via the calmodulin/CaMK II pathway. *J Cell Physiol*, 213, 269-277.

Szabo-Fresnais N., Lefebvre F., Germain A., Fischmeister R. & PomÈrance M. (2010) A new regulation of IL-6 production in adult cardiomyocytes by [beta]-adrenergic and IL-1[beta] receptors and induction of cellular hypertrophy by IL-6 trans-signalling. *Cell Signal*, 22, 1143-1152.

Szczesny G., Veihelmann A., Massberg S., Nolte D. & Messmer K. (2004) Long-term anaesthesia using inhalatory isoflurane in different strains of mice--the haemodynamic effects. *Lab Anim*, 38, 64-69.

Takahashi N., Calderone A., Izzo N. J., Maki T. M., Marsh J. D. & Colucci W. S. (1994) Hypertrophic stimuli induce transforming growth factor-beta 1 expression in rat ventricular myocytes. *J Clin Invest*, 94, 1470-1476.

Takaoka H., Esposito G., Mao L., Suga H. & Rockman H. A. (2002) Heart size-independent analysis of myocardial function in murine pressure overload hypertrophy. *Am J Physiol*, 282, H2190-H2197.

Takeda K., Takeuchi O., Tsujimura T., Itami S., Adachi O., Kawai T., Sanjo H., Yoshikawa K., Terada N. & Akira S. (1999) Limb and skin abnormalities in mice lacking IKK. *Science*, 284, 313-316.

Takeda N., Manabe I., Uchino Y., Eguchi K., Matsumoto S., Nishimura S., Shindo T., Sano M., Otsu K., Snider P., Conway S. J. & Nagai R. (2010) Cardiac fibroblasts are essential for the adaptive response of the murine heart to pressure overload. *J Clin Invest*, 120, 254-265.

Tanaka M., Fuentes M. E., Yamaguchi K., Durnin M. H., Dalrymple S. A., Hardy K. L. & Goeddel D. V. (1999) Embryonic lethality, liver degeneration, and impaired NF- κ B activation in IKK- β -deficient mice. *Immunity*, 10, 421-429.

Tarnavski O., McMullen J., Schinke M., Nie Q., Kong S. & Izumo S. (2004) Mouse cardiac surgery: comprehensive techniques for the generation of mouse models of human diseases and their application for genomic studies. *Physiol Genomics* 16, 349-60.

Teekakirikul P., Eminaga S., Toka O., Alcalai R., Wang L., Wakimoto H., Naylor M., Konno T., Gorham J. M., Wolf C. M., Kim J. B., Schmitt J. P., Molkenkin J. D., Norris R. A., Tager A. M., Hoffman S. R., Markwald R. R., Seidman C. E. & Seidman J. G. (2010) Cardiac fibrosis in mice with hypertrophic cardiomyopathy is

mediated by non-myocyte proliferation and requires TGF- β . *J Clin Invest*, 120, 3520-3529.

Teichholz L. E., Kreulen T., Herman M. V. & Gorlin R. (1976) Problems in echocardiographic volume determinations: Echocardiographic-angiographic correlations in the presence or absence of asynergy. *Am J Cardiol*, 37, 7-11.

Thavasu P. W., Longhurst S., Joel S. P., Slevin M. L. & Balkwill F. R. (1992) Measuring cytokine levels in blood: Importance of anticoagulants, processing, and storage conditions. *J Immunol Methods*, 153, 115-124.

Thompson S. A., Copeland C. R., Reich D. H. & Tung L. (2011) Mechanical coupling between myofibroblasts and cardiomyocytes slows electric conduction in fibrotic cell monolayers. *Circulation*, 123, 2083-2093.

Timmers L., Sluijter J. P. G., van Keulen J. K., Hofer I. E., Nederhoff M. G. J., Goumans M.-J., Doevendans P. A., van Echteld C. J. A., Joles J. A., Quax P. H., Piek J. J., Pasterkamp G. & de Kleijn D. P. V. (2008) Toll-like receptor 4 mediates maladaptive left ventricular remodeling and impairs cardiac function after myocardial infarction. *Circ Res*, 102, 257-264.

Timmers L., van Keulen J. K., Hofer I. E., Meijs M. F. L., van Middelaar B., den Ouden K., van Echteld C. J. A., Pasterkamp G. & de Kleijn D. P. V. (2009) Targeted deletion of nuclear factor κ B p50 enhances cardiac remodeling and dysfunction following myocardial infarction. *Circ Res*, 104, 699-706.

Toischer K., Rokita A. G., Unsold B., Zhu W., Kararigas G., Sossalla S., Reuter S. P., Becker A., Teucher N., Seidler T., Grebe C., Preuss L., Gupta S. N., Schmidt K., Lehnart S. E., Kruger M., Linke W. A., Backs J., Regitz-Zagrosek V., Schafer K., Field L. J., Maier L. S. & Hasenfuss G. (2010) Differential cardiac remodeling in preload versus afterload. *Cir*, 122, 993-1003.

Tomasek J., Gabbiani G., Hinz B., Chaponnier C. & Brown R. (2002) Myofibroblasts and mechano-regulation of connective tissue remodelling. *Nat Rev Mol Cell Biol*, 3.

Torre-Amione G., Kapadia S., Benedict C., Oral H., Young J. B. & Mann D. L. (1996) Proinflammatory cytokine levels in patients with depressed left ventricular ejection fraction: A report from the studies of left ventricular dysfunction (SOLVD). *J Am Coll Cardiol*, 27, 1201-1206.

Toyofuku T., Curotto Kurzydowski K., Narayanan N. & MacLennan D. H. (1994) Identification of Ser 38 as the site in cardiac sarcoplasmic reticulum Ca(2+)-ATPase that is phosphorylated by Ca²⁺/calmodulin-dependent protein kinase. *J Biol Chem*, 269, 26492-26496.

Turner N. A., Mughal R. S., Warburton P., O'Regan D. J., Ball S. G. & Porter K. E. (2007) Mechanism of TNF α -induced IL-1 α , IL-1 β and IL-6 expression in human cardiac fibroblasts: Effects of statins and thiazolidinediones. *Cardiovasc Res*, 76, 81-90.

Valen G., Yan Z. & Hansson G. K. (2001a) Nuclear factor kappa-B and the heart. *J Am Coll Cardiol* 38, 307-314.

Valen G., Yan Z. & Hansson G. K. (2001b) Nuclear factor kappa-B and the heart. *Journal of the American College of Cardiology*, 38, 307-314.

Van der Heiden K., Cuhlmann S., Luong L. A., Zakkar M. & Evans P. C. (2010) Role of nuclear factor κ B in cardiovascular health and disease. *Clin Sci*, 118, 593-605.

Van Huffel S., Delaei F., Heyninck K., De Valck D. & Beyaert R. (2001) Identification of a novel A20-binding inhibitor of nuclear factor-kappa B activation termed ABIN-2. *J Biol Chem*, 276, 30216-30223.

van Wamel A. J. E. T., Ruwhof C., van der Valk-Kokshoorn L. J. M., Schrier P. I. & van der Laarse A. (2002) Stretch-induced paracrine hypertrophic stimuli increase TGF- β 1 expression in cardiomyocytes. *Mol Cell Biochem* 236, 147-153.

Vander A., Sherman J. & Luciano D. (1998) Chapter 14: Circulation, Section C: The heart. *Human Physiology: The Mechanisms of Body Function*.

Vardar-Sengul S., Arora S., Haluk Baylas H. & Mercola D. (2009) Expression profile of human gingival fibroblasts induced by interleukin-1 β reveals central role of nuclear factor-kappa B in stabilizing human gingival fibroblasts during inflammation. *J Periodontology*, 80, 833-849.

Vasquez C., Benamer N. & Morley G. E. (2011) The cardiac fibroblast: Functional and electrophysiological considerations in healthy and diseased hearts. *J Cardiovasc Pharmacol*.

Vasquez C., Mohandas P., Louie K. L., Benamer N., Bapat A. C. & Morley G. E. (2010) Enhanced fibroblast-myocyte interactions in response to cardiac injury. *Circ Res*, 107, 1011-1020.

Vermeulen L., De Wilde G., Notebaert S., Berghe W. V. & Haegeman G. (2002) Regulation of the transcriptional activity of the nuclear factor-kappaB p65 subunit. *Biochem Pharmacol*, 64, 963-970.

Verzili D., Zamparelli C., Mattei B., Noegel A. A. & Chiancone E. (2000) The sorcin-annexin VII calcium-dependent interaction requires the sorcin N-terminal domain. *FEBS Letters*, 471, 197-200.

Villarreal F., Kim N., Ungab G., Printz M. & Dillmann W. (1993) Identification of functional angiotensin II receptors on rat cardiac fibroblasts. *Circulation*, 88, 2849-2861.

Vistnes M., Waehre A., Nygard S., Sjaastad I., Andersson K. B., Husberg C. & Christensen G. (2010) Circulating cytokine levels in mice with heart failure are etiology dependent. *J Appl Physiol*, 108, 1357-1364.

Wagner S., Dybkova N., Rasenack E. C. L., Jacobshagen C., Fabritz L., Kirchhof P., Maier S. K. G., Zhang T., Hasenfuss G., Brown J. H., Bers D. M. & Maier L. S. (2006) Ca²⁺/calmodulin-dependent protein kinase II regulates cardiac Na⁺ channels. *J Clin Invest*, 116, 3127-3138.

Wagner S., Hacker E., Grandi E., Weber S. L., Dybkova N., Sossalla S., Sowa T., Fabritz L., Kirchhof P., Bers D. M. & Maier L. S. (2009) Ca^{2+} /calmodulin kinase II differentially modulates potassium currents. *Circ Arrhythm Electrophysiol*, 2, 285-294.

Wang J., Chen H., Seth A. & McCulloch C. A. (2003) Mechanical force regulation of myofibroblast differentiation in cardiac fibroblasts. *Am J Physiol Heart Circ Physiol*, 285, H1871-1881.

Wang M., Crisostomo P., Wairiuko G. M. & Meldrum D. R. (2006) Estrogen receptor- α mediates acute myocardial protection in females. *Am J Physiol*, 290, H2204-H2209.

Wang Y., Tandan S., Cheng J., Yang C., Nguyen L., Sugianto J., Johnstone J. L., Sun Y. & Hill J. A. (2008) Ca^{2+} /Calmodulin-dependent protein kinase II-dependent remodeling of Ca^{2+} current in pressure overload heart failure. *J Biol Chem*, 283, 25524-25532.

Wang Z., Nolan B., Kutschke W. & Hill J. A. (2001) Na^+ - Ca^{2+} Exchanger Remodeling in Pressure Overload Cardiac Hypertrophy. *J Biol Chem*, 276, 17706-17711.

Wehrens X. H. T., Lehnart S. E., Reiken S. R. & Marks A. R. (2004) Ca^{2+} /calmodulin-dependent protein kinase II phosphorylation regulates the cardiac ryanodine receptor. *Circ Res*, 94, e61-e70.

Wehrens X. H. T. & Marks A. R. (2004) Novel therapeutic approaches for heart failure by normalizing calcium cycling. *Nat Rev Drug Discov*, 3, 565-574.

Weinberg E., O., Thienelt C. D., Katz Sarah E., Bartunek J., Tajima M., Rohrbach S., Douglas P., S. Douglas & Lorell B., H. (1999) Gender differences in molecular remodeling in pressure overload hypertrophy. *J Am Coll Cardiol*, 34, 264.

Wertz I. E., O'Rourke K. M., Zhou H., Eby M., Aravind L., Seshagiri S., Wu P., Wiesmann C., Baker R., Boone D. L., Ma A., Koonin E. V. & Dixit V. M. (2004) De-

ubiquitination and ubiquitin ligase domains of A20 downregulate NF- κ B signalling. *Nature*, 430, 694-699.

Witt H., Schubert C., Jaekel J., Fliegner D., Penkalla A., Tiemann K., Stypmann J., Roepcke S., Brokat S., Mahmoodzadeh S., Brozova E., Davidson M. M., Noppinger P. R., Grohé C. & Regitz-Zagrosek V. (2008) Sex-specific pathways in early cardiac response to pressure overload in mice. *J Mol Med*, 86, 1013-1024.

Wong S. C. Y., Fukuchi M., Melnyk P., Rodger I. & Giaid A. (1998) Induction of cyclooxygenase-2 and activation of nuclear factor- κ B in myocardium of patients with congestive heart failure. *Circulation*, 98, 100-103.

Wu S., Yin R., Ernest R., Li Y., Zhelyabovska O., Luo J., Yang Y. & Yang Q. (2009) Liver X receptors are negative regulators of cardiac hypertrophy via suppressing NF- κ B signalling. *Cardiovasc Res*, 84, 119-126.

Wu X., Zhang T., Bossuyt J., Li X., McKinsey T. A., Dedman J. R., Olson E. N., Chen J., Brown J. H. & Bers D. M. (2006) Local InsP3-dependent perinuclear Ca²⁺ signaling in cardiac myocyte excitation-transcription coupling. *J Clin Invest*, 116, 675-682.

Wu Y., Temple J., Zhang R., Dzhura I., Zhang W., Trimble R., Roden D. M., Passier R., Olson E. N., Colbran R. J. & Anderson M. E. (2002) Calmodulin kinase II and arrhythmias in a mouse model of cardiac hypertrophy. *Circulation*, 106, 1288-1293.

Xiao G., Fong A. & Sun S.-C. (2004) Induction of p100 processing by NF- κ B-inducing kinase involves docking I κ B kinase α (IKK α) to p100 and IKK α -mediated phosphorylation. *J Biol Chem*, 279, 30099-30105.

Xie Y., Garfinkel A., Weiss J. N. & Qu Z. (2009) Cardiac alternans induced by fibroblast-myocyte coupling: mechanistic insights from computational models. *Am J Physiol*, 297, H775-H784.

- Xiong Z., Sun G., Zhu C., Cheng B., Zhang C., Ma Y. & Dong Y. (2010) Artemisinin, an anti-malarial agent, inhibits rat cardiac hypertrophy via inhibition of NF- κ B signaling. *Eur J Pharmacol*, 649, 277-284.
- Xu A., Hawkins C. & Narayanan N. (1993) Phosphorylation and activation of the Ca²⁺-pumping ATPase of cardiac sarcoplasmic reticulum by Ca²⁺/calmodulin-dependent protein kinase. *J Biol Chem*, 268, 8394-7.
- Xu L., Lai D., Cheng J., Lim H. J., Keskanokwong T., Backs J., Olson E. N. & Wang Y. (2010) Alterations of L-type calcium current and cardiac function in CaMKII δ knockout mice. *Circ Res*, 107, 398-407.
- Yamamoto Y., Verma U. N., Prajapati S., Kwak Y.-T. & Gaynor R. B. (2003) Histone H3 phosphorylation by IKK- α is critical for cytokine-induced gene expression. *Nature*, 423, 655-659.
- Ying X., Keunsang L., Na L., Daniel C., Leonardo M. & Nikolaos F. (2009) Characterization of the inflammatory and fibrotic response in a mouse model of cardiac pressure overload. *Histochem Cell Biol*, 131, 471-481.
- Young D., Popovic Z. B., Jones W. K. & Gupta S. (2008) Blockade of NF- κ B using I κ B α dominant-negative mice ameliorates cardiac hypertrophy in myotrophin-overexpressed transgenic mice. *J mol Biol*, 381, 559-568.
- Yu C.-M., Tipoe G. L., Wing-Hon Lai K. & Lau C.-P. (2001) Effects of combination of angiotensin-converting enzyme inhibitor and angiotensin receptor antagonist on inflammatory cellular infiltration and myocardial interstitial fibrosis after acute myocardial infarction. *J Am Coll Cardiol*, 38, 1207-1215.
- Zannad F., Dousset B. & Alla F. (2001) Treatment of congestive heart failure: Interfering the aldosterone-cardiac extracellular matrix relationship. *Hypertension*, 38, 1227-1232.

Zelarayan L., Renger A., Noack C., Zafiriou M.-P., Gehrke C., van der Nagel R., Dietz R., de Windt L. & Bergmann M. W. (2009) NF- κ B activation is required for adaptive cardiac hypertrophy. *Cardiovasc Res*, cvp237.

Zeydel M., Puglia K., Eghbali M., Fant J., Seifert S. & Blumenfeld O. O. (1991) Properties of heart fibroblasts of adult rats in culture. *Cell Tissue Res*, 265, 353-359.

Zhang J., Ping P., Vondriska T. M., Tang X.-L., Wang G.-W., Cardwell E. M. & Bolli R. (2003a) Cardioprotection involves activation of NF- κ B via PKC-dependent tyrosine and serine phosphorylation of I κ B- α . *Am J Physiol Heart Circ Physiol*, 285, H1753-1758.

Zhang R., Khoo M. S. C., Wu Y., Yang Y., Grueter C. E., Ni G., Price E. E., Thiel W., Guatimosim S., Song L.-S., Madu E. C., Shah A. N., Vishnivetskaya T. A., Atkinson J. B., Gurevich V. V., Salama G., Lederer W. J., Colbran R. J. & Anderson M. E. (2005) Calmodulin kinase II inhibition protects against structural heart disease. *Nat Med*, 11, 409.

Zhang R., Zhang Y. Y., Huang X. R., Wu Y., Chung A. C. K., Wu E. X., Szalai A. J., Wong B. C. Y., Lau C.-P. & Lan H. Y. (2010a) C-reactive protein promotes cardiac fibrosis and inflammation in angiotensin II-induced hypertensive cardiac disease. *Hypertension*, 55, 953-960.

Zhang T. & Brown J. H. (2004) Role of calcium/calmodulin-dependent protein kinase II in cardiac hypertrophy and heart failure. *Cardiovasc Res*, 63, 476-486.

Zhang T., Guo T., Mishra S., Dalton N. D., Kranias E. G., Peterson K. L., Bers D. M. & Brown J. H. (2010b) Phospholamban ablation rescues sarcoplasmic reticulum Ca²⁺ handling but exacerbates cardiac dysfunction in CaMKII δ C transgenic mice. *Circ Res*, 106, 354-362.

Zhang T., Johnson E. N., Gu Y., Morissette M. R., Sah V. P., Gigena M. S., Belke D. B., Dillmann W. H., Rogers T. B., Schulman H., Ross J. & Brown J. H. (2002a) The Cardiac-specific Nuclear δ B Isoform of Ca²⁺/Calmodulin dependent Protein

Kinase II Induces Hypertrophy and Dilated Cardiomyopathy Associated with Increased Protein Phosphatase 2A Activity. *The journal of Biological Chemistry*, 277, 1261-1267.

Zhang T., Johnson E. N., Gu Y., Morissette M. R., Sah V. P., Gigena M. S., Belke D. D., Dillmann W. H., Rogers T. B., Schulman H., Ross J. & Brown J. H. (2002b) The cardiac-specific nuclear δ B isoform of Ca^{2+} /calmodulin-dependent protein kinase II induces hypertrophy and dilated cardiomyopathy associated with increased protein phosphatase 2A activity. *J Biol Chem*, 277, 1261-1267.

Zhang T., Kohlhaas M., Backs J., Mishra S., Phillips W., Dybkova N., Chang S., Ling H., Bers D. M., Maier L. S., Olson E. N. & Brown J. H. (2007) CaMKII $\{\delta\}$ isoforms differentially affect calcium handling but similarly regulate HDAC/MEF2 transcriptional responses. *J Biol Chem*, 282, 35078-35087.

Zhang T., Maier L. S., Dalton N. D., Miyamoto S., Ross J., Bers D. M. & Brown J. H. (2003b) The deltaC isoform of CaMKII is activated in cardiac hypertrophy and induces dilated cardiomyopathy and heart failure. *Cir Res*, 92, 912-919.

Zhang T., Miyamoto S. & Brown J. H. (2004) Cardiomyocyte calcium and calcium/calmodulin-dependent protein kinase II: Friends of foes? *Recent Prog Horm Res*, 59, 141-168.

Zhang W., Chen D.-Q., Qi F., Wang J., Xiao W.-Y. & Zhu W.-Z. (2010c) Inhibition of calcium-calmodulin-dependent kinase II suppresses cardiac fibroblast proliferation and extracellular matrix secretion. *J Cardiovasc Pharmacol*, 55, 96-105

Zhou B., Rao L., Peng Y., Wang Y., Li Y., Gao L., Chen Y., Xue H., Song Y., Liao M. & Zhang L. (2009) Functional polymorphism of the NFKB1 gene promoter is related to the risk of dilated cardiomyopathy. *BMC Medical Genetics*, 10, 47.

Zhou Y.-Q., Foster F. S., Nieman B. J., Davidson L., Chen X. J. & Henkelman R. M. (2004) Comprehensive transthoracic cardiac imaging in mice using ultrasound

biomicroscopy with anatomical confirmation by magnetic resonance imaging. *Physiol. Genomics*, 18, 232-244.

Zhu W., Woo A. Y. H., Yang D., Cheng H., Crow M. T. & Xiao R. P. (2007) Activation of CaMKII δ C is a common intermediate of diverse death stimuli-induced heart muscle cell apoptosis. *J Biol Chem*, 282, 10833-10839.